Comparative studies on elongation and termination of the three RNA polymerases from *S. cerevisiae in vitro*

DISSERTATION ZUR ERLANGUNG DES DOKTORGRADES DER NATURWISSENSCHAFTEN (DR. RER. NAT.) DER FAKULTÄT FÜR BIOLOGIE UND VORKLINISCHE MEDIZIN DER UNIVERSITÄT REGENSBURG

vorgelegt von

Philipp Merkl

aus Regensburg

im Jahr

2013

Das Promotionsgesuch wurde eingereicht am: 30. September 2013

Die Arbeit wurde angeleitet von: Prof. Dr. Herbert Tschochner

Prüfungsausschuss:

Vorsitzender: PD Dr. Joachim Griesenbeck

1. Prüfer: Prof. Dr. Herbert Tschochner
2. Prüfer: Prof. Dr. Thomas Moss (Université Laval, Québec, Kanada)
3. Prüfer: Prof. Dr. Klaus Grasser

Die vorliegende Arbeit wurde im Zeitraum von Oktober 2009 bis September 2013 am Lehrstuhl für Biochemie III des Instituts für Biochemie, Genetik und Mikrobiologie der Universität Regensburg unter Anleitung von Prof. Dr. Herbert Tschochner angefertigt.

Ich erkläre hiermit, dass ich diese Arbeit selbst verfasst und keine anderen als die angegebenen Quellen und Hilfsmittel verwendet habe.

Diese Arbeit war bisher noch nicht Bestandteil eines Prüfungsverfahrens.

Andere Promotionsversuche wurden nicht unternommen.

Regensburg, den

Philipp Merkl

Table of contents

CHAPTER I – SUMMARY

In *Saccharomyces cerevisiae* (hereafter called yeast), three RNA polymerases synthesize the nuclear transcriptome. During the transcriptional cycle, RNA polymerase I, II and III (Pol I, II and III) are recruited to their respective promoter, elongate the nascent transcript in the context of chromatin and finally terminate transcription. Whereas the initation step is quite well understood, our knowledge about elongation and termination is very limited. Therefore, we developed an *in vitro* transcription system in which elongation and termination of RNA Pol I can be analyzed independent of promoter-specific initiation. The same transcription system allowed comparison of the three RNA polymerases regarding their behaviour, if barriers are encountered during elongation. In summary, the following questions were addressed:

1) Several DNA cis elements and trans-acting factors are described to support RNA Pol I dependent transcription termination. Among the protein factors are the Reb1 homolog Ydr026c/Nsi1 which was recently found to be required for efficient Pol I termination *in vivo*, Reb1, which terminates transcription *in vitro* and the replication fork blocking protein Fob1. We further investigated the role of these factors in the termination process regarding *i)* the role of Nsi1 and other possible trans-acting factors and *ii)* the influence of mutations in Pol I subunits in transcription termination. We found that Nsi1 imposed an elongation barrier for Pol I. Furthermore, we could show that presence of the 35S rDNA terminator-proximal Reb1 binding site was sufficient for Nsi1-dependent Pol I pausing/termination *in vitro* which was further enhanced by the T-rich 1 element. In addition, our data suggest that Nsi1 and Fob1 exhibit a cooperative effect in Pol I transcription termination *in vitro*.

2) We further wanted to elucidate whether RNA Pol I, II and III deal differently with elongation obstacles in general. Thus, we comparatively analyzed Pol I, II and III transcription of templates complexed with the physiological elongation barriers Nsi1, Reb1 and Fob1 *in vitro*. Furthermore, the unphysiological bacterial strong DNA-binding proteins LexA and LacI as well as the mouse rDNA terminaton factor TTF-I were included in the analysis. We could show that Nsi1 and Reb1 were

specifically impairing Pol I transcription elongation. Contrary, LexA only imposed a road-block for Pol II. On the other hand, TTF-I was an elongation obstacle for all three RNA polymerases.

3) In all eukaryotic cells, gene transcription occurs in the context of chromatin. Chromatin is a complex assembly of DNA and DNA bound proteins, with histone molecules forming the abundant, basic unit of chromatin, the nucleosome. It is of great importance to understand how the different RNA polymerases cope with the chromatin template. It has been suggested, that actively transcribed Pol I and III genes are devoid of nucleosomes, whereas Pol II genes are nucleosomal. To analyze whether the RNA polymerases have intrinsic activities to deal differently with the nucleosomal templates, we comparatively investigated Pol I, II and III transcription elongation on templates complexed with nucleosomes *in vitro*. Many studies employing *in vitro* assays have already analyzed chromatin transcription by the different RNA Pols. However, it is hard to compare the individual results, since the respective *in vitro* systems used for analysis often differ significantly in many aspects, whereas side-by-side comparison of Pol I, II and III is possible in our system. Furthermore, we used RNA Pol I mutants to elucidate the contribution of certain subunits to transcribe through nucleosomal templates. We observed that Pol I and III were able to transcribe a nucleosomal template *in vitro*, whereas in agreement with the literature a single nucleosome imposed a very strong barrier for Pol II elongation. Additionally, we could demonstrate that subunit A49 significantly contributes to Pol I's ability to overcome the nucleosomal barrier.

CHAPTER II – INTRODUCTION

2.1 RNA polymerases – ubiquitous conserved enzymes

2.1.1 Outline

In 1869, nucleic acids were isolated by Friedrich Miescher for the first time. However, it took several decades to discover that the substance which was by then called nuclein was comprised of the two different nucleic acids DNA and RNA and to elucidate their chemical composition (reviewed in Allen 1941). Several ribonucleotide (rNTP) -consuming enzymatic activities like polynucleotide phosphorylase (GRUNBERG-MANAGO et al. 1955) or the CCA-adding enzyme (Preiss et al. 1961), were described in the following years. Nonetheless it remained unclear until 1959/1960 how RNA was synthesized. Simultaneously, Jerard Hurwitz (Hurwitz et al. 1960), Sam Weiss (Weiss & Gladstone 1959), Audrey Stevens (Stevens 1960) and James Bonner (Huang et al. 1960) reported RNA-synthesizing activities which marked the discovery of DNA-dependent RNA polymerases (RNAP). While Weiss obtained a fraction exhibiting polymerase activity from rat liver tissue, Bonner worked with a pea extract and Stevens and Hurwitz fractionated *E. coli* lysates. Contrary to the view back then emanating from the hypothesis of the existence of one RNA polymerase, the world of RNA polymerases has significantly changed until today and still continues to evolve. Today we know that every organism contains at least one RNA polymerase and a multitude of viruses carry the genetic information for one.

Chemically, DNA-dependent RNA polymerases are nucleotidyl transferases which catalyze polymerisation of rNTPs in 5'-3' direction. Thereby, phosphodiester bonds are formed by a nucleophilic attack of the 3'-OH group of the last nucleotide in the RNA chain on the α-phosphorus of the incoming rNTP. Unlike DNA polymerases, RNA polymerases do not need a primer. The sequence

of the synthesized RNA is determined by the DNA template and equal to the sequence of the coding DNA strand albeit thymine is replaced by uracil. Therefore, RNA synthesis by RNA polymerases was called transcription.

In vivo, the transcriptional cycle can be roughly dissected into the three main steps initiation, elongation and termination. Briefly, upon initiation the RNA polymerase is recruited to a specific recognition sequence upstream of the respective gene called promoter by initiation factors hence forming the closed complex. Unwinding of the transcription bubble marks the transition to the open complex state. Next, the first nucleotides are added. During elongation, the polymerase is released from the promoter and the RNA chain is further extended. Transcription termination is defined as polymerisation cessation and release of the transcript and the polymerase. The literature knows further subdivisions of these three steps, of which some are well-defined and constantly used and some depend on the view of the respective authors. Initiation is sometimes subdivided in the two steps pre-initiation complex (PIC) formation and actual recruitment of the polymerase including unwinding of the DNA helix. Promoter escape or clearance is defined as the point when the initiation factors break away from the polymerase and the RNAP has left the promoter behind. Sometimes this is referred to as a fourth step in the transcription cycle, albeit it is also seen as the first step of elongation. After promoter clearance, a phase of short transcript production and polymerase pausing and backtracking follows, known as the abortive transcription phase. RNA chain elongation itself is often termed as productive elongation.

2.1.2 T7 RNA polymerase

Within viral RNA polymerases, T7 RNA Pol, which was also used in this study, is the best characterized. It was discovered in 1970 upon infection of *E. coli* with T7 bacteriophages (Chamberlin et al. 1970). The T7 gene I is coding for this one-subunit polymerase with a molecular weight of 98kDa (Davanloo et al. 1984). In the T7 genome 17 T7 RNA Pol promoters were identified (Dunn & Studier 1983). They consist of 23 highly conserved base pairs (TAATACGACTCACTATAG*GGAGA, * marks the TSS) which are recognized by the polymerase with high specificity (Davanloo et al. 1984). Upon binding of the polymerase to the promoter, the closed complex is formed. Subsequently, the promoter DNA is bent by the polymerase at an angle of 40°-60° in the region from -2 to +1 referenced to the transcription start site (Újvári & Martin 2000) and the transcription bubble is opened. Promoter strand separation is driven by incorporation of nucleotide +2 (Stano et al. 2002).

Once a stable initiation complex has been formed upon incorporation of roughly 10nt, the polymerase switches to elongation mode and promoter clearance occurs (Liu & Martin 2002). Two termination signals for T7 RNA Pol were identified so far. (Dunn & Studier 1983) reported that the TΦ region in the late part of the T7 genome served as a transcription terminator. Upon transcription, the nascent RNA forms a hairpin structure which leads to termination in combination with a downstream T-rich region on the non-template strain. Furthermore it was demonstrated that the presence of a T-rich stretch alone leads to termination (Mead et al. 1986). Additionally, it was observed that T7 RNA Pol terminated at prokaryotic RNA polymerase terminators (Jeng et al. 1990). T7 RNA Pol shows homology to mitochondrial and chloroplast RNA polymerases in plants as well as to mitochondrial RNA polymerase in *S. cerevisiae* (Kelly et al. 1986). Based on studies indicating structural homologies, it was suggested that T7 RNA Pol is evolutionary related to DNA polymerases (Steitz et al. 1994).

2.1.3 Bacterial RNA polymerase

The bacterial RNA polymerase consists of 5 (core enzyme) or 6 (holoenzyme) subunits named with greek letters: $\alpha^{I}\alpha^{II}\beta\beta'\sigma\omega$ with a total molecular weight of roughly 470kDa (Ebright 2000). The x-ray structure of RNA polymerase from *T. aquaticus* was solved in 1999 and revealed a claw-like shaped enzyme with a central cleft of roughly 25Å diameter harboring the catalytical Mg^{2+} ion (Zhang et al. 1999). The catalytically active center is comprised of the two largest subunits β' and β which resemble the two pincers of the claw and the bottom of the cleft. α^{I} and α^{II} are located distal of the cleft and interact with β and β', respectively. Both α subunits contain an N-terminal domain (NTD) which is necessary for interactions with the β subunits and a C-terminal domain (CTD) which interacts with promoter DNA (Busby & Ebright 1994). The ω subunit is located at the β' CTD and stabilizes the association of β' with the $\alpha^{I}\alpha^{II}\beta$ subassembly (Minakhin et al. 2001). The σ-subunit binds to β' and is required for promoter-specific initiation. The core enzyme does not recognize promoters albeit it is catalytically active. Promoter recruitment requires presence of a σ-factor, of which 7 different coding sequences are found in the *E. coli* genome (Pérez-Rueda & Collado-Vides 2000). Usually, transcription is initiated by the housekeeping σ^{70} which was named after its molecular weight. Among others, specialized σ factors are activated upon nutrient depletion, transition to stationary phase, nitrogen shortage or heat shock (reviewed in Gruber & Gross 2003). A typical prokaryotic promoter recognized by σ^{70}-associated RNAP consists of the Pribnow box (5'-TATAAT-3') located at position -10

(compared to the TSS), the -35 region (5'-TTGACA-3') and the UP element located further upstream. However, not all promoters contain all elements and the actual sequences often differ from the consensus. Promoters identified by alternative sigma factors can differ to great extent. σ factors are involved in all aspects of transcription initiation including locating the RNA polymerase to the promoter, DNA melting, initiation of RNA synthesis and promoter escape (Borukhov & Severinov 2002). It has been believed for a long time that transition from initiation to elongation required the dissociation of the σ factor due to steric conflicts with the nascent RNA. Recently it was shown that in early stages of elongation σ can stay associated with the RNAP although the association to β' is altered (Kapanidis et al. 2005). Two kinds of transcription terminators are found in the *E. coli* genome (reviewed in Uptain et al. 1997; Richardson 1993). Factor-independent terminators are comprised of GC-rich inverted repeats followed by a T-rich stretch comparable to the T7 RNA Pol terminator. They induce RNAP pausing and destabilization of the RNA-DNA hybrid due to the weak A-T interactions and thus release of the nascent RNA. The factor-dependent terminators do not share sequence homology but require the presence of the termination factors Rho (ρ), Tau (τ) or nusA (Banerjee et al. 2006) with Rho accounting for 50% of the factor-dependent terminators. Rho was discovered and purified by (Roberts 1969). It is a helicase (Brennan et al. 1987), translocase and ATPase. The mechanism of Rho-dependent termination is well understood. While the polymerase is stalled at the Rho pausing site (Kassavetis & Chamberlin 1981), Rho recognizes the Rho utilization site on the nascent RNA which has a low G but high C content (Morgan et al. 1985). Then Rho translocates along the RNA towards the polymerase thereby hydrolyzing ATP. Upon arrival, Rho unwinds the RNA-DNA hybrid and thus causes release of the transcript (Richardson 2002; Richardson 2003).

2.1.4 Archaeal RNA polymerase

Investigation of archaeal transcription started with the purification of RNA polymerase from *Halobacterium cutirubrum* (Louis & Fitt 1971). Early on it was evident that archaeal transcription occurs homologously to that in eukarya (reviewed in Reeve et al. 1997). Archaea contain one 13-subunit RNAP which shares significant structural and mechanistic homology with the eukaryotic RNAPs but especially with Pol II (Huet et al. 1983; Prangishvilli et al. 1982). Recent publications revealing the x-ray structure of RNAP from *S. solfataricus* and *S. shibatae* confirmed this close relationship (Hirata et al. 2008; Korkhin et al. 2009) and the number of 13 subunits. Furthermore,

similarity of the Pol II and archaeal pre-initiation complexes (PIC) was demonstrated by x-ray crystallography (Kosa et al. 1997).

Archaea possess homologues of the eukaryotic transcription factors TATA-binding protein (TBP) (Rowlands et al. 1994), the basal transcription factor TFIIB (Ouzounis & Sander 1992) (TFB or aTFA), TFIIS (TFS) (Hausner et al. 2000) and TFIIEα (TFE) (Bell et al. 1998). Interestingly, archaeal transcription regulators are related to the ones found in bacteria (reviewed in Geiduschek & Ouhammouch 2005). Archaeal promoters consist of the TATA box (Hausner et al. 1991) and a purine-rich adjacent upstream sequence (TFB-responsive element, BRE). It was shown that archaeal RNAP, TFB and archaeal TBP are necessary and sufficient for promoter-dependent transcription *in vitro* (Hausner et al. 1996; Hethke et al. 1996). Upon initiation, both TBP and TFB bind to the promoter thus forming the PIC. Next, RNAP is recruited to the PIC (Hausner et al. 1996; Bell et al. 1999). Transition from closed to open complex occurs upon promoter opening which is mediated by the B-linker region of TFB (Kostrewa et al. 2009). After open complex formation, RNAP scans the DNA in cooperation with the B-reader domain of TFB to identify the TSS (Kostrewa et al. 2009). TFE was shown to be necessary for initiation on weak promoters by enhancement of TATA-box recognition (Bell et al. 2001) and described as part of the elongation complex (Grünberg et al. 2007). The knowledge about archaeal RNAP elongation is very limited. It was shown that upon transition from initiation to elongation, subunit H exhibits a conformational change (Grünberg et al. 2010). Furthermore, it was demonstrated that TFS stimulates the intrinsic RNA cleavage activity of RNAP thus showing similarity to its homolog TFIIS (Hausner et al. 2000; Grünberg et al. 2010). There are indications that TFS-mediated cleavage activity is important for transcription fidelity (Thomas et al. 1998), rescuing of stalled elongation complexes (Reines et al. 1993) and at pausing sites (Marr & Roberts 2000). However, TFS cleavage is apparently not linked to polymerase backtracking (Grünberg et al. 2010). Current knowledge suggests that termination of archaeal RNAP does not require additional factors. In contrast, arrest and termination are dependent on oligo dT stretches in the template DNA in analogy to RNA Pol III (Mūller et al. 1985; Thomm et al. 1993; Spitalny & Thomm 2008). Most recent studies revealed that the trigger loop in the RNAP active center plays a role in correct transcription termination, since its deletion or mutation lead to increased pausing and termination (Fouqueau et al. 2013). In summary, the archaeal transcription machinery exhibits similarities with eukaryotic RNA Pol II and III as well as with the bacterial transcription regulation thus indicating common ancestry.

2.2 Eukaryotic RNA polymerases

2.2.1 From one to five – an overview

It took almost a decade from the discovery of the RNA polymerase until it was demonstrated that eukaryotes contain three different RNAPs which were distinctly located in the nucleolus or the nucleoplasm (Roeder & Rutter 1969; Roeder & Rutter 1970). Today it is common knowledge that eukaryotic RNAPs have distinct targets. With trypanosomes being the only described exception (Günzl et al. 2003), Pol I solely synthesizes the 35S (47S in higher eukaryotes) rRNA precursor. Pol II transcribes mRNA precursors, microRNAs (miRNA) (Lee et al. 2004) and a fraction of the small nuclear RNAs (snRNA). Pol III synthesizes the 5S rRNA (Szymanski et al. 1998), tRNAs (Sprinzl et al. 1991) and other small noncoding RNAs including U3 and U6 snRNA and RNase P RNA (Gupta & Reddy 1991). More recent studies revealed that two additional RNAPs named RNA Pol IV and V exist in plants which are structurally related to Pol II (reviewed in Haag & Pikaard 2011). Both Pol IV and V are involved in RNA directed DNA methylation (RdDM) mediated by siRNAs (Herr et al. 2005; Onodera et al. 2005). The primary transcript(s) of Pol IV were not identified so far whereas Pol V-dependent RNAs were described *in vivo* (Wierzbicki et al. 2008). Enzymatic activity of Pol IV and V was not yet demonstrated *in vitro*. Furthermore, mitochondria and chloroplasts contain their own RNAPs (2.1.2).

The evolutionary background for the existence of up to five RNA polymerases in eukaryotes remains unclear. One key feature of eukaryotic RNAPs is their spatial separation in different nuclear sub-domains. However, it is evident that although all eukaryotic RNAPs are highly specialized, they share mechanistic and structural homologies.

2.2.2 Structure and subunit composition of yeast RNA Pol I, II and III

In yeast, RNA Pol I, II and III contain 14, 12 and 17 subunits, respectively. According to current nomenclature, the name of a subunit consists of a capital letter referring to the appearance in Pol I, II or three combined with a number indicating the molecular weight of the subunit in kDa. However,

also names in Rpxy format are used with x being a, b or c for the polymerase and y being the subunit number. An overview together with prokaryotic RNAPs is given in **Table 2-1**.

Eukaryotes			Archaea	Bacteria	subunit function	subunit location
Pol I	**Pol II**	**Pol III**				
A190	Rpb1	C160	A'+A''	β'	catalytic	core
A135	Rpb2	C128	B (B'+B'')	β	catalytic	core
AC40	Rpb3	AC40	D	α		core
AC19	Rpb11	AC19	L	α		core
ABC27	ABC27 (Rpb5)	ABC27	H	ω		core
ABC23	ABC23 (Rpb6)	ABC23	K			core
ABC14.5	ABC14.5 (Rpb8)	ABC14.5	-			core
ABC10a	ABC10a (Rpb10)	ABC10a	N			core
ABC10b	ABC10b (Rpb12)	ABC10b	P			core
A12.2	Rpb9	C11	X		RNA cleavage	core
A14	Rpb4	C17	F		initiation complex formation	stalk
A43	Rpb7	C25	E			stalk
A49	(Tfg1)	C37			initiation complex stabilization	Pol I/III specific subcomplex
A34.5	(Tfg2)	C53				
		C82				Pol III specific subcomplex
		C34				
		C31				

Table 2-1: Subunit composition of eukaryotic, archaeal and bacterial RNA polymerases. The table is adapted from (Vannini & Cramer 2012). Common subunits of Pol I, II and III are highlighted in blue, common subunits of Pol I and III are highlighted in green. Tfg1 and Tfg2 are not defined as Pol II subunits and thus given in brackets although they exhibit structural homology to A49/A34.5 and C53/C37.

By now, crystal structures of the 10-subunit core Pol II are available at a resolution of 2.8Å (Cramer et al. 2000; Cramer et al. 2001) and at 3.8Å for the complete Pol II (Armache et al. 2005). Pol I structure was extensively studied with cryo-EM and immuno EM (Schultz et al. 1993; Klinger et al. 1996; Bischler et al. 2002; De Carlo et al. 2003; Kuhn et al. 2007). Up to now, only one cryo-EM based structure of Pol III is available (Vannini et al. 2010). However, no crystal structures are published for either Pol I or Pol III to date apart from subcomplexes. Nonetheless, homology modeling of Pol I and III subunits into the cryo-EM structure by means of the Pol II crystal structure further consolidated analogies between the structures of the three polymerases (reviewed in Vannini & Cramer 2012). As

outlined in 2.1.3 and 2.1.4, crystal structures of bacterial and archaeal RNAP are available which share significant structural homology to their eukaryotic counterparts.

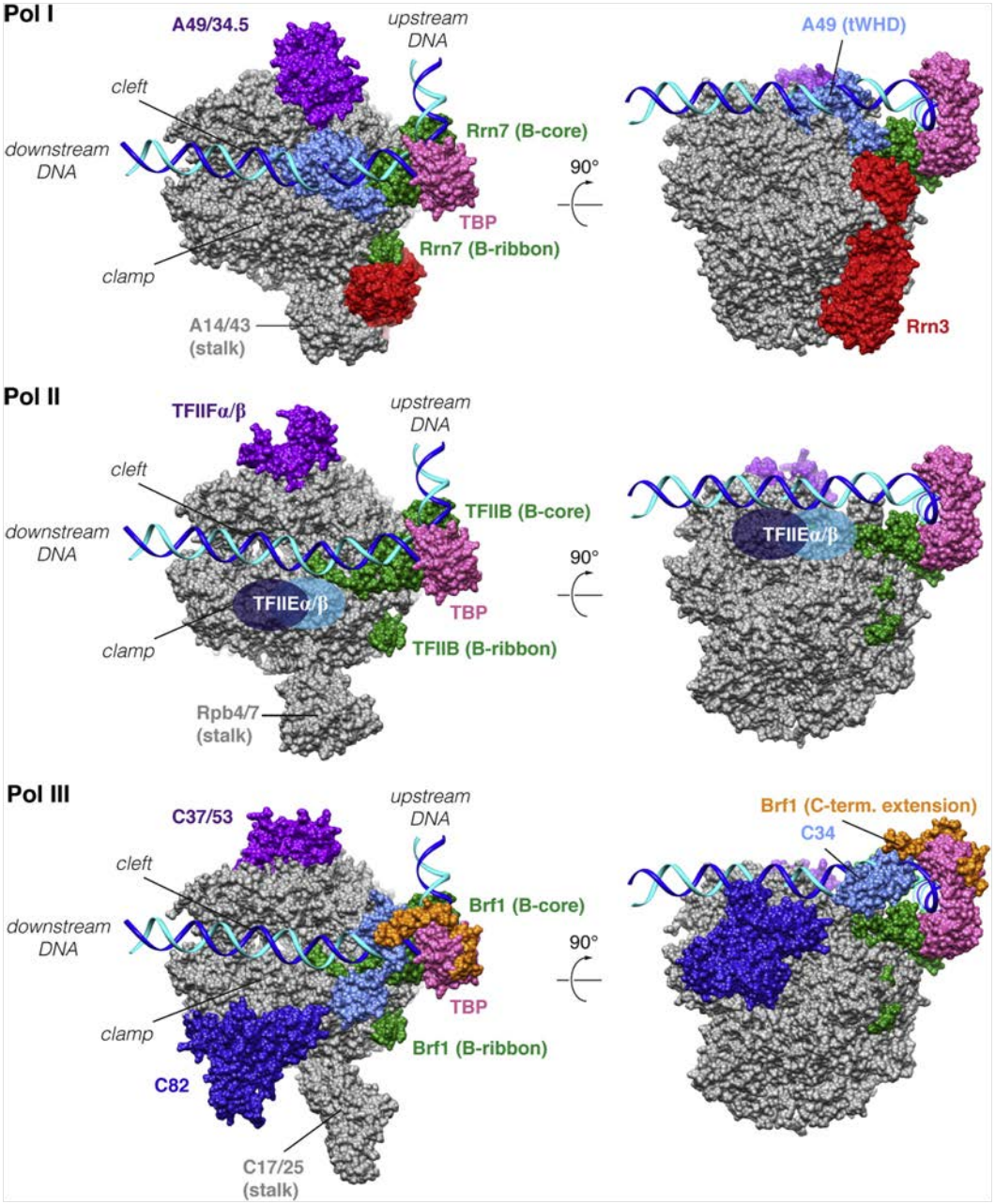

Fig. 2-1: Conserved core topology of transcription initiation complexes. Initiation complex models are based on a minimal Pol II initiation complex model containing closed promoter DNA, Pol II, TBP, and TFIIB (Kostrewa et al., 2009). The X-ray structure of the complete Pol II (Armache et al., 2005) and the Pol II-based homology models for the Pol I and Pol III core (Kuhn et al., 2007 and Jasiak et al., 2006) are represented as gray molecular surfaces. TBP and Rrn3 (Blattner et al., 2011) are shown as pink and red molecular surfaces, respectively. TFIIB, TFIIE, TFIIF, and related factors are depicted as molecular surfaces, (Chen et al., 2010, Vannini et al., 2010 and Blattner et al., 2011) (Patrick Cramer,unpublished data). The presumed location of TFIIE, based on crosslinking data, is indicated with semitransparent filled circles (Chen et al., 2007). The locations of C82 and C34 were determined by electron microscopy (Vannini et al., 2010), and the location of the A49 tandem WH domain was inferred by crosslinking (Patrick Cramer, unpublished data). For each of the three models, two orthogonal views are shown. Adapted from (Vannini & Cramer 2012)

Pol I, II and III share a homologous 10 subunit core (reviewed in Vannini & Cramer 2012). From the Pol II structure, it is evident that the two large subunits Rpb1 and Rpb2 form the central mass with a cleft between them harboring the catalytically active metal ion.The Rpb1-Rpb2 complex is anchored via a subassembly of Rpb3, Rpb10, Rpb11 and Rpb12. The core polymerase is completed by Rpb5, 6 and 9. In Pol I and III one subunit of the core is not only structurally related to the Pol II counterpart Rpb9 but also to the Pol II transcription factor TFIIS (Ruan et al. 2011). A protruding stalk is formed by heterodimeric complexes consisting of A43/A14 in Pol I, Rpb4/7 in Pol II and C25/C17 in Pol III (Armache et al. 2005; Peyroche et al. 2002; Jasiak et al. 2006; Hu et al. 2002). From this point, the three polymerases contain different numbers of subunits. However, subcomplexes of Pol I and III subunits exhibit partial structural homologies to general transcription factors of Pol II. The heterodimers A49 (N-terminal domain)/A34.5 and C53/C37 (Kassavetis et al. 2010; Landrieux et al. 2006) are related to the TFIIF subunits Tfg1 and Tfg2. Furthermore, C82 and C34 are proposed to be homologs to the TFIIE subunits TFIIEα and TFIIEβ (Wang & Roeder 1997). Structural similarities were also detected between the C-terminal domain of A49 and TFIIEβ. Structural homology studies can be extended beyond polymerase subunits to further transcription factors (reviewed in Vannini & Cramer 2012).

2.2.3 Cellular localization and spatial organization of the rRNA genes

The rDNA locus constitutes the nucleolus, a subcompartment of the nucleus in which RNA Pol I transcription takes place. On electron microscopic images the nucleolus can be morphologically dissected into three categories, which are called fibrillar centers (FC), dense fibrillar centers (DFC) and the granular component (GC) (Schwarzacher & Wachtler 1993). The rDNA is located in the FCs which are found close to the nuclear envelope. They are surrounded by the DFCs which are constituted of the Pol I transcripts (Cmarko et al. 2000) hence suggesting that Pol I transcription occurs at the interphase between FCs and DFCs. The granular components eventually contain maturing pre-ribosomes (Léger-Silvestre et al. 1999).

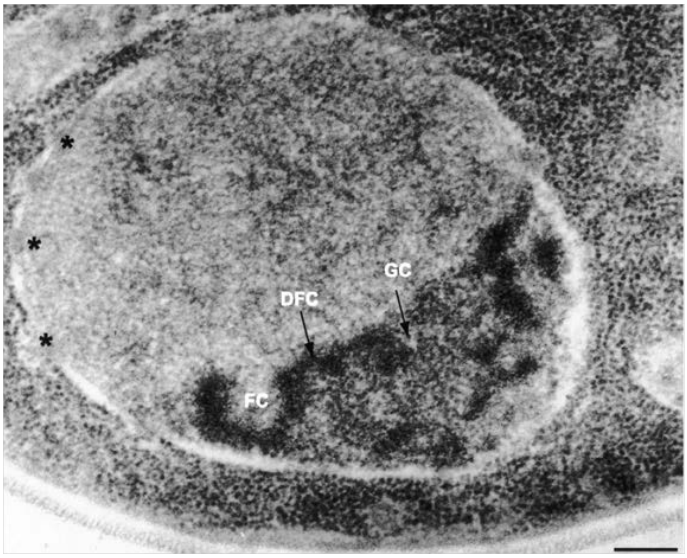

Fig. 2-2: The electron micrograph depicts the morphology of a yeast nucleus after cryofixation and freeze-substitution. The nucleus is seen to be outlined by a double envelope with pores (asterisks). In the nucleolus, three distinct morphological compartments are identified: the fibrillar centres (FC) are detected near the nuclear envelope, surrounded by a dense fibrillar component (DFC) that extends as a network throughout the nucleolar volume. A granular component (GC) is dispersed throughout the rest of the nucleolus. Bar represents 200nm. (from Léger-Silvestre et al., 1999)

2.2.4 The only yeast Pol I target *in vivo*: The rDNA locus

The rDNA locus in *S. cerevisiae* differs significantly from other genomic loci as it is present in an average of 150-200 copies per cell which are situated on the right arm of chromosome XII. This number is not fixed but variable due to recombination events in the cell. One rDNA copy was defined as the SmaI restriction fragment of the locus (Cramer et al. 1977; Cramer & Rownd 1980). The copies are arranged as repetitive tandem elements with a length of 9.1kb each in a head to tail conformation (Petes 1979). Each repeat harbours the Pol I-transcribed 35S rDNA gene and the 5S rDNA gene which is transcribed in the opposite direction by Pol III (Philippsen et al. 1978). Only about 50% of the rDNA copies are transcriptionally active and thus nucleosome depleted (open), whereas the other half is assembled into nucleosomes and transcriptionally inactive (closed) (Dammann et al. 1993). The 35S rDNA contains the sequences for the mature 18S, 5.8S and 25S rRNAs separated by the internal transcribed spacers 1 and 2 (ITS 1 & 2) (Kressler et al. 1999). Two external transcribed spacers (ETS 1 & 2) flank the 35S rDNA at the 5' and 3' end. Two rDNA regions were described to be involved in regulation of 35S rRNA transcription, the Pol I promoter (2.3.1) and the enhancer / terminator region (2.3.3). Originally declared as an enhancer for the next downstream 35S gene (Elion & Warner 1986), it was demonstrated to be dispensable for rDNA transcription *in vivo* (Wai et al. 2001) and implicated in Pol I termination (Lang et al. 1994; van der Sande et al. 1989). Several

other cis-regulatory elements are present in the two intergenic spacers (IGS1 & 2). Among those is an autonomous replication sequence (rARS) from which bi-directional replication of the locus is started during s-phase (Linskens & Huberman 1988). This enables the possibility of simultaneous transcription and replication. A replication fork barrier (RFB) is located at the 3' end of the terminator region which prevents collisions between the replication and the transcription machineries. The replication fork can progress through the RFB towards the 35S rDNA but not in the opposite direction (Brewer & Fangman 1988; Brewer et al. 1992; Kobayashi et al. 1992). The RFB provides a binding platform for the replication fork binding protein Fob1, which is required for RFB activity (Kobayashi & Horiuchi 1996). Recent studies revealed two binding sites for Fob1 named RFB1 and 3. A model of Fob1 binding proposes that the RFB is wrapped around Fob1 and thereby contacting both binding sites (Kobayashi 2003). Furthermore, Fob1 plays a role in expansion and compaction of the rDNA locus which is achieved by homologous recombination.

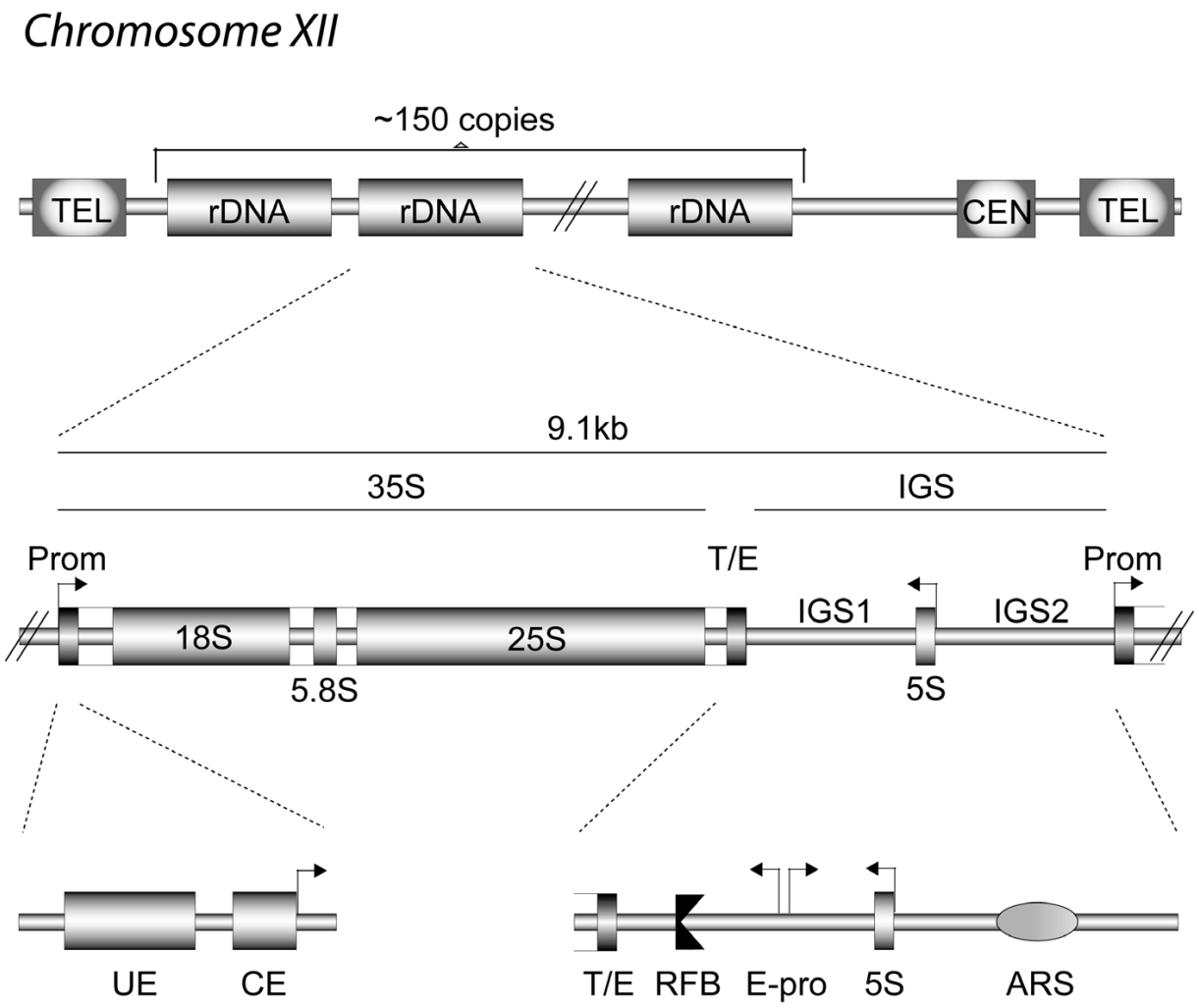

Figure 2-3: Schematic representation of the rRNA gene locus of *S. cerevisiae.* The position of the rDNA repeat cluster on chromosome XII with respect to the centromere (CEN) and telomeres (T) is shown. Each 9.1kb large rDNA repeat consists of the Pol I-transcribed 35S rRNA gene (precursor for the 18S, 5.8S and 25S rRNAs), the RNA Pol III-transcribed 5S rRNA gene and two intergenic spacer regions IGS1 and IGS2. Arrows mark transcription start sites and direction. The positions of

several DNA elements are indicated. The upstream element (UE) and core element (CE) constitute the Pol I promoter (P). Termination occurs at the terminator (T) which is located within a region called the enhancer (E). The autonomous replication sequence (ARS), the bidirectional Pol II promoter E-Pro and the replication fork barrier (RFB) are depicted. (modified from Goetze et al., 2010)

Recombination events require double strand breaks which are induced by pausing of the DNA replication machinery (Burkhalter & Sogo 2004; Kobayashi et al. 1998). Deletion of Fob1 leads to a 50% reduction of rDNA copies (Kobayashi et al. 1998). Another region required for repeat expansion (EXP) is located further downstream but in close proximity to the RFB (Kobayashi et al. 2001). It contains a bi-directional Pol II promoter (E-Pro) which marks the transcription start for non-coding RNAs (Ganley et al. 2005). It is suggested that these non-coding transcripts interfere with cohesin association to the rDNA locus during mitosis. Since cohesin association is believed to facilitate sister chromatid fixation and thus prevention of crossovers and dissimilar recombination events, cohesin loss may lead to changes in rDNA repeat number (Kobayashi & Ganley 2005; Kobayashi et al. 2004).

2.3 The transcriptional cycles of yeast RNA Pol I, II and III

Studies on eukaryotic transcription were carried out in many model organisms. As chapter 2.3 focuses on yeast RNA polymerases, mostly data from this organism are reviewed. However, in case of homologous factors in yeast and higher eukaryotes, also results obtained from such studies were included to support the yeast data or to provide ideas how respective homologous factors could function in yeast.

2.3.1 Transcription initiation

A) *Pol I*

The Pol I promoter is located upstream of the 35S rDNA gene and consists of the core element (CE) and the upstream element (UE). CE is located between position -28 and +8 with respect to the TSS whereas UE spans from -146 to -51 (Kulkens et al. 1991; Musters et al. 1989). It was demonstrated

that CE is essential for initiation and sufficient for a basal transcription level, whereas elevated levels of transcription require UE (Keener et al. 1998; Musters et al. 1989; Steffan et al. 1998). Upon transcription initiation, both CE and UE are recognized and bound by the respectively named core factor (CF) (Keys et al. 1994; Lalo et al. 1996) and upstream activating factor (UAF) (Keys et al. 1996). Together with TBP and Rrn3 they comprise the four described Pol I initiation factors. CF is a multiprotein complex consisting of the three subunits Rrn6, Rrn7 and Rrn11 (Keys et al. 1994; Lalo et al. 1996). UAF is comprised of the six proteins Rrn5, Rrn9, Rrn10, Uaf30 and the histones H3 and H4 (Keener et al. 1997; Keys et al. 1996; Siddiqi et al. 2001). Recruitment of UAF to UE is mediated by subunit Uaf30 (Steffan et al. 1998; Hontz et al. 2008; Goetze et al. 2010). UAF seems to function as a key player in rDNA transcription since its deletion results in reorganization of the promoter chromatin (Goetze et al. 2010). It was demonstrated that deletion of Rrn5, Rrn9 or Rrn11 prevents Pol I transcription of the 35S rDNA which is then performed by Pol II from a cyptic promoter situated in the UE (Vu et al. 1999). Additionally, in a *uaf30* Δ strain, the 35S rDNA is transcribed by Pol I and II. Furthermore, UAF plays a role in Sir2-mediated rDNA silencing since it could be shown that Uaf30 is required for Sir2 recruitment (Goetze et al. 2010; Bryk et al. 1997; Cesarini et al. 2010; Fritze et al. 1997; Smith & Boeke 1997). It was shown that TBP binds to UAF and CF *in vitro*, thus suggesting a bridging function (Steffan et al. 1996). The fourth initiation factor Rrn3 interacts directly with the Pol I subunit A43 independently of the template and with the CF subunit Rrn6 (Yamamoto et al. 1996; Peyroche et al. 2000). Only about 2% of the Pol I complexes are associated with Rrn3 *in vivo* and thus in an initiation-competent state (Milkereit & Tschochner 1998). Currently, two models for transcription initiation are under discussion. Since it was demonstrated that UAF stably associates with the UE (Vogelauer et al. 1998), it is accepted that PIC formation starts with binding of UAF. Next, TBP binds to UAF and stabilizes the CF-DNA interaction or recruits CF to the DNA to complete the PIC. However it remains unclear, whether UAF, CF and TBP remain stably associated with the promoter DNA (Keys et al. 1996) or whether CF and the Pol I-Rrn3 complex re-initiate to start a new transcription cycle (Aprikian et al. 2001; Bordi et al. 2001). Recent data further support the hierarchy of events suggested by Keys and co-workers (Goetze et al. 2010). In both models, finally Pol I-Rrn3 is recruited to the PIC. Interestingly Rrn3 is dispensable for Pol I recruitment but the resulting complex is not transcriptionally active (Aprikian et al. 2001). Furthermore, the two subunits A49 and A34.5 seem to exhibit an influence on Rrn3 recruitment to the promoter and its dissociation from the polymerase upon transition to elongation and are required for high Pol I loading rates (Beckouet et al. 2008; Albert et al. 2011).

B) *Pol II*

Due to the multiplicity of Pol II-transcribed genes, many variants of Pol II promoters exist. In general, the regulatory DNA elements can be divided into two fractions: The core promoter which is necessary for basal levels of transcription *in vitro* and PIC assembly (Smale & Kadonaga 2003) and upstream activating (UAS) or repressing sequences (URS) located 5' of the core promoter in yeast (Errede et al. 1984; Mellor 2006; Gray & Fassler 1996). A variety of functional sequence elements is known from metazoan Pol II core promoters of which the TATA element is the only clearly conserved one in yeast (Sugihara et al. 2011; Basehoar et al. 2004). Several general Pol II transcription factors exist in yeast, of which TBP, TFIIA, TFIIB and TFIIF are required for formation and stabilization of the PIC on the core promoter. However the designation of TFIIA as a general transcription factor is currently under discussion (Høiby et al. 2007). It is generally accepted that PIC formation is nucleated by recruitment of TBP to the core promoter. The TBP-TATA complex is then recognized by TFIIB. A further main function of TFIIB is to position Pol II correctly over the TSS (Kostrewa et al. 2009; Miller & Hahn 2006; Hahn 2004; Thomas & Chiang 2006). The TFIIB-TBP-TATA complex then serves as a platform which is recognized by the Pol II-TFIIF complex. It was demonstrated that TFIIF functions in stabilization of Pol II in the PIC, selection of the TSS and stabilization of the RNA-DNA hybrid in early steps of transcription (Hahn 2004; Thomas & Chiang 2006). Open complex formation requires the ATPase and helicase activity of TFIIH which is recruited by TFIIE (Revyakin et al. 2004; Schaeffer et al. 1993; Schaeffer et al. 1994; Flores et al. 1992).

Pol II transcription initiation in yeast is regulated to great extent by transcription coactivators as the multiprotein complexes SAGA, TFIID, Mediator, NuA4 and at least 169 transcription factors (Teixeira et al. 2006; reviewed in Hahn & Young 2011). Roughly 90% of yeast Pol II promoters are TFIID-dependent and it is speculated that TFIID recognition sites are present in the respective promoters (Shen et al. 2003; Huisinga & Pugh 2004). TFIID-dependent promoters were found to be normally constitutively active and did not contain the TATA element. TATA-containing promoters (19% of all yeast Pol II promoters) on the other hand are partially (50%) dependent on the transcription activator SAGA (Huisinga & Pugh 2004). TFIID is composed of TBP and several TBP activating factors (TAFs). TBP delivery by SAGA is controlled by its subunits Spt3, Spt8 and TAFIIS (Belotserkovskaya et al. 2000). Besides the core initiation mechanism, TFIID and SAGA are transcription coactivators necessary for initiation at gene-class specific promoters (Vannini & Cramer 2012). In these gene-specific pathways, either TFIID or SAGA contact the UAS via interaction of the activating factors and

hence help to recruit TBP to the core promoter (Kuras et al. 2000; Bryant & Ptashne 2003; Qiu et al. 2004; Li et al. 2000).

C) *Pol III*

Pol III promoters are fundamentally different from their Pol I and Pol II counterparts as some of their functional elements are located within the transcribed regions. Among others, there are two major sorts of Pol III promoters named type 1 and type 2 in yeast. Typically, tRNA genes contain type 2 promoters which are comprised of two cis elements called A and B boxes, which are located 12-20bp or 42-80bp downstream of the TSS, respectively (Dieci et al. 2002; Marck et al. 2006; Sharp et al. 1985; Pavesi et al. 1994). The type 1 promoter occurs at the 5S rRNA gene and is composed of the A box, an intermediate element and a C box (Challice & Segall 1989). Type 2 promoters are directly recognized by the transcription factor IIIC. Contrary, at type 1 promoters the C-box is first bound by TFIIIA which subsequently recruits TFIIIC. At both promoter types, the TBP-containing transcription factor IIIB (Hernandez 1993) is recruited next to a region located roughly 50bp upstream of the TSS (Geiduschek & Kassavetis 2001). In yeast and plants, TATA elements were identified in the region of TFIIIB recruitment, thus establishing them as promoter core elements (Dieci et al. 2000; Yukawa et al. 2000; Hamada et al. 2001). Once it was recruited, TFIIIB serves as a platform for Pol III association and thus PIC formation. In TATA-containing promoters, the TSS is located 28-30bp downstream of the 5' end of the TATA element (Joazeiro et al. 1996; Dieci et al. 2006).

2.3.2 Transcription elongation

A) *Pol I*

Until recently, elongation of Pol I was poorly studied and still our knowledge is very limited (reviewed in Schneider 2012). However, evidence is emanating linking the elongation step with overall control of the rRNA synthesis rate and rRNA processing (Schneider et al. 2007; V. Stefanovsky et al. 2006; Y. Zhang et al. 2010; Koš & Tollervey 2010; Osheim et al. 2004; Dragon et al. 2002). Recent studies suggested that the subunit A12.2 and the A49/A34.5 dimer were providing Pol I with an intrinsic ability to overcome elongation obstacles (Kuhn et al. 2007; Geiger et al. 2010). It was demonstrated

that Pol I is able to cleave the nascent transcript in an arrested elongation complex. This cleavage activity is promoted by subunit A12.2 (Kuhn et al. 2007) which allows Pol I to escape from an arrest on its own. Concerning A49 and A34.5, determination of crystal structures revealed that parts of subunit A49 and A34.5 are homologous to the Pol II elongation factor TFIIF subunits Tfg1 and 2 (Geiger et al. 2010). As TFIIF was (amongst other functions) characterized as an elongation factor for Pol II (Conaway et al. 2000; Dvir et al. 2001) *in vitro* and *in vivo*, a similar role for A49 and A34.5 was suggested. Both subunits are not essential, but absence or mutations lead to severe growth defects (Liljelund et al. 1992; Gadal et al. 1997). Polymerases lacking the dimer were shown to be less elongation competent than WT Pol I *in vitro* and this effect could be rescued by addition of recombinant A49 (Kuhn et al. 2007). Although not involved in clearing of barriers during elongation, it was reported that the aspartate residue 784 in subunit A135 was crucial for optimal elongation rates *in vivo* and *in vitro* (Schneider et al. 2007). D784 is located in the funnel and thus might play a role in NTP loading. When D784 is substituted for glycine, the Pol I elongation rate *in vitro* was shown to be reduced 10-fold compared to the WT (Schneider et al. 2007).

Apart from its intrinsic capabilities to deal with elongation barriers, several trans-acting elongation factors have been described for Pol I. Early on, it was demonstrated that the Spt4/Spt5 heterodimer influences Pol II transcription (Wada et al. 1998; Swanson & Winston 1992). In yeast, Spt4 and Spt5 can be co-purified with Pol I (Schneider et al. 2006). Whereas Spt5 is an essential gene, a Δ*spt4* mutant exhibits a Pol I elongation aberration (Schneider et al. 2006) manifesting itself in increased rRNA levels. Thus it was concluded that Spt4 and Spt5 are negative regulators of Pol I transcription elongation. Contrary to these observations, there is evidence that Spt4 and Spt5 positively influence Pol I elongation (Anderson et al. 2011). In a comparative approach, binding of Spt5 to Pol I and Pol II was assessed *in vitro* (Viktorovskaya et al. 2011). It was shown that recombinantly expressed domains of Spt5 interacted with Pol II and Pol I subunits A135, A49 and A34.5.

The Paf1 complex (Paf1C) is described as a positive trans-acting effector of Pol I transcription elongation (Mueller & Jaehning 2002; Squazzo et al. 2002; Zhang et al. 2009; A. P. P. Zhang et al. 2010). It is comprised of five subunits (Mueller & Jaehning 2002), of which none is essential in yeast. However, Δ*paf1* or Δ*ctr9* mutants exhibit severe growth defects due to decreased levels of rRNA synthesis and negative effects on rRNA processing (Zhang et al. 2009). Nonetheless, the polymerase density on the 35S rDNA is equal to a WT strain. Direct interaction of Paf1C with an RNAP has only been documented for Pol II (Krogan et al. 2002; Mueller et al. 2004; Squazzo et al. 2002), however it was demonstrated that Paf1C is associated with the rDNA. A positive influence of Paf1C on Pol I elongation rates was demonstrated *in vitro* (Y. Zhang et al. 2010) and thus proposed *in vivo*.

The HMG-box protein UBF was described as a Pol I transcription factor. It exists in mammalian cells and its function was addressed by many studies. Since it has a homolog in yeast called Hmo1 (Gadal et al. 2002), some UBF functions will be discussed here. UBF was first described as a Pol I transcription activator in human cells (Jantzen et al. 1990). It was assigned a role in the initiation step and several studies proposed mechanistic explanations (Bell et al. 1988; Tuan et al. 1999; Kihm et al. 1998; Kwon & Green 1994; Voit et al. 1992; McStay et al. 1991; Jantzen et al. 1990). However, recent publications have challenged this UBF function. In addition, it was demonstrated that UBF inhibits Pol I transcription *in vivo* and *in vitro* (V. Stefanovsky et al. 2006). However this negative effect was not due to decreased loading of Pol I onto the 45S rDNA and thus not an initiation defect. Hence, a role for UBF in elongation might be envisioned, which is supported by the fact that UBF is associated with the coding region of the 45S rDNA in mammals (O'Sullivan et al. 2002) and its homolog Hmo1 is associated with actively transcribed rDNA repeats in yeast (Merz et al. 2008). Two studies provided different explanations for the role of UBF. In (V. Y. Stefanovsky et al. 2006) it was suggested that association of UBF with the rDNA leads to a nucleosome-like structure which is influential on elongating Pol I. On the other hand, it was proposed that UBF increases the promoter clearance rate of Pol I *in vitro*. In yeast, it was demonstrated that Hmo1 is required for regulation of ribosomal protein transcription via the TOR pathway (Berger et al. 2007). Furthermore, it was shown that Hmo1 is stabilizing the nucleosome-free state of the 35S rDNA which may help to maintain a nucleosome-depleted chromatin environment for elongating Pol I (Wittner et al. 2011). Thus, there is significant evidence that UBF and Hmo1 play a crucial role in chromatin structure formation or maintenance, however the actual mechanism remains elusive.

B) *Pol II*

Besides its function in Pol II initiation, TFIIF stimulates Pol II elongation rates and decreases elongation pausing (Flores et al. 1989; Price et al. 1989; Bengal et al. 1991; Izban & Luse 1992; Tan et al. 1994). ChIP assays have documented that TFIIF is localized predominantly near the promoter region (Krogan et al. 2002; Pokholok et al. 2002). Mechanistically it was proposed that TFIIF recognizes paused elongation complexes, re-associates with them and alters Pol II conformation to a elongation-competent state (Zawel et al. 1995). However, TFIIF does not stay associated with elongating Pol II. Furthermore, TFIIF is directly interacting with the elongation factors Spt5 (Lindstrom et al. 2003), components of the Paf1C (Shi et al. 1997) and influences TFIIS-mediated RNA cleavage (Elmendorf et al. 2001; Zhang et al. 2003).

Upon transcriptional arrest triggered by polymerase pausing and subsequent backtracking, TFIIS enables further Pol II readthrough by promoting cleavage of the nascent RNA (Fish & Kane 2002; Conaway et al. 2003). In general, TFIIS reduces Pol II pausing and thus stimulates transcription elongation (Rappaport et al. 1987; Reinberg & Roeder 1987; Sluder et al. 1989; Bengal et al. 1991). It was demonstrated that TFIIS enhances the intrinsic RNA cleavage activity of Pol II (Rudd et al. 1994; Orlova et al. 1995) although the exact mechanism remains unknown. Recent structural studies of a Pol II-TFIIS complex revealed significant changes in Pol II conformation upon binding of TFIIS (Kettenberger et al. 2003). The structure supports the assumption that the nascent RNA and the DNA template are re-aligned correctly and Pol II conformation changes to an elongation mode.

Another factor influencing Pol II transcription elongation is the DSIF (DRB sensitivity inducing factor) complex. It was named after its ability to make an *in vitro* transcription reaction susceptible to DRB (5,6-dichloro-1-β-D-ribofuranosylbenzimidazole) (Wada et al. 1998). DSIF is a heterodimeric complex consisting of the human homologs of yeast Spt4 and 5. First designated as an inhibitory effector of Pol II transcription (Wada et al. 1998), DSIF was later described as an elongation stimulator (Yamaguchi et al. 1999). In vitro transcription studies revealed that hSpt4 alone has a stimulatory effect on elongation (Rondón et al. 2004). Furthermore, genetic and physical interactions of DSIF with TFIIS, Paf1C, Spt6 and Pol II were demonstrated (reviewed in Sims et al. 2004).

Like for Pol I, Paf1C was shown to positively effect Pol II elongation (Rondón et al. 2004). Additionally, Pol II transcription elongation depends on the phosphorylation state of the polymerase CTD (reviewed in Sims et al. 2004; Saunders et al. 2006). Apart from trans-acting factors which influence polymerase fidelity and processivity, elongation is also regulated at the chromatin template level (2.4).

Besides the discussed examples, a vast amount of Pol II elongation factors was identified in mammals (reviewed in Sims et al. 2004; Saunders et al. 2006). Among those are NELF, CSB, P-TEFb, ELL, the elongins and many others which are outside the scope of this study.

C) *Pol III*

Concerning trans-acting Pol III elongation factors, no data are available so far. The only exception is concerning how Pol III handles nucleosomal templates which will be discussed later. Nonetheless, the structural homology of Pol III subunits to Pol II transcription factors (2.2.2) led to the hypothesis that

Pol III is permanently associated with some of its transcription factors (Carter & Drouin 2010). In analogy to the Pol II situation, subunit C11, the partial structural homolog to TFIIS was reported to promote transcript cleavage during transcriptional arrest (Chédin et al. 1998).

2.3.3 Transcription termination

A) *Pol I (reviewed in Nemeth et al. 2013)*

In yeast, the intergenic spacer 1 (IGS1) of an rDNA repeat (2.2.4) harbors the Pol I termination region which was previously described as an enhancer for Pol I transcription (Elion & Warner 1986). In the early 1990s, a minimal model that supported Pol I transcription termination *in vitro* was established in the Reeder laboratory. The system was based on an initiation-independent approach using tailed templates (Dedrick & Chamberlin 1985; Kane & Chamberlin 1985). For efficient termination, purified Pol I, the DNA-binding protein Reb1 and a template containing the 11bp long Reb1 binding site (Reb1 BS) and the 10-15bp long T-rich stretch located 10-20bp upstream of the Reb1 BS were required (Lang et al. 1994; Lang & Reeder 1995; Reeder & Lang 1994). Mechanistically, it was proposed that Pol I is paused by Reb1 and in cooperation with the T-rich stretch destabilizes the elongation complex. Taken together this leads to transcript and polymerase release from the template. However, the termination efficiency *in vitro* was rather low (70%-20%). *In vivo*, the role of Reb1 is less well defined. It was demonstrated that Reb1 is also associated with a number of regulatory regions upstream of Pol II transcribed genes (Ju et al. 1990; Morrow et al. 1993; Pinskaya et al. 2009). Since Reb1 is an essential protein in yeast, only depletion studies could be carried out, of which none revealed significant influences on Pol I termination (Braglia et al. 2011; Kawauchi et al. 2008). Interestingly, Reb1 association to its binding site in the terminator region could not be observed *in vivo* above background levels (Kawauchi et al. 2008; Goetze et al. 2010; Reiter et al. 2012). Concerning the cis-elements, it was demonstrated that the Reb1 binding site and the T-rich stretch were required for efficient termination *in vivo* (Reeder et al. 1999). In a recent study, a homolog of Reb1 was shown to interact with the terminator-proximal Reb1 BS in vivo (Reiter et al. 2012). It contains three Myb-like DNA-binding domains as Reb1 and was named Nsi1 (NTS1 silencing protein) according to its described function in nucleolar Pol II silencing (Ha et al. 2012). Furthermore, Fob1, which is associated with the replication fork barrier (RFB) was shown to support Pol I termination (Braglia et al. 2011). Apart from that, further factors involved in co-transcriptional rRNA processing

were assigned roles in Pol I termination *in vivo*. Among those are the 5'-> 3' exonuclease Rat1, the RNase III-like endonuclease Rnt1, the helicase Sen1 and the polynucleotide kinase Grc3 (Elela et al. 1996; Braglia et al. 2011; Braglia et al. 2010; Kawauchi et al. 2008; El Hage et al. 2008). Additionally, nucleosome remodeling factors like Chd1, Isw1 and Isw2 were discussed as influential on Pol I termination (Jones et al. 2007).

Currently, two mechanisms of Pol I transcription termination are discussed. The first model originates from the *in vitro* analyses by the Reeder group as outlined above. A DNA-bound trans-acting factor induces polymerase pausing and cooperates with the upstream T-rich element thus promoting release of transcript and polymerase. This model is supported by a recent publication (Reiter et al. 2012) in which a novel *in vivo* system to assess transcription termination was established. In this approach, all rDNA repeats were modified such that the Pol I terminator region spanning from the T-rich element to the RFB (322bp) was inserted into the internal transcribed spacer 1 (ITS1) between 18S and 5.8S rDNA. This resulted in a reduced growth phenotype due to premature termination. It was demonstrated that Pol I occupancy was lower downstream of the ITS1. Efficient termination was dependent on presence of Nsi1 and further supported by the T-rich element.

On the other hand, it was proposed that co-transcriptional rRNA processing and 35S rRNA 3' end formation is directly linked to Pol I termination (Braglia et al. 2011; Kawauchi et al. 2008; El Hage et al. 2008). It was demonstrated that deletion of Rnt1, Rat1, Sen1 or Grc3 gives rise to Pol I transcripts which are extended into the IGS1. Mutations in Rat1 or Sen1 lead to enhanced Pol I occupancy downstream or the terminator region as assayed by ChIP. All the above factors were shown to be associated with the terminator region (Braglia et al. 2010; Braglia et al. 2011; Kawauchi et al. 2008; El Hage et al. 2008). In summary this led to a hypothesis similar to the described torpedo model for Pol II. In a first and well understood step, the RNaseIII-like endonuclease cleaves the nascent 35S rRNA at a stem-loop structure in the ETS2 (Elela et al. 1996; Allmang & Tollervey 1998; Henras et al. 2004; Kufel et al. 1999). It was proposed that the resulting 5' end is a target for the polynucleotide kinase Grc3, however the actual mechanism remains elusive. The phosphorylated 5' end then is recognized by the exonuclease Rat1 and subsequently degraded in cooperation with the helicase Sen1. When Rat1 reaches the elongating polymerase, it is proposed to act like a torpedo and disrupt the Pol I-RNA-DNA ternary complex. According to the model, the complexed Reb1 BS serves as a pausing or speed reducing element to allow Rat1 to catch up with the polymerase (Reeder et al. 1999; Braglia et al. 2011). Moreover, the Reb1 BS was proclaimed being part of a failsafe termination mechanism in case of deletion of Rnt1 or the Rnt1 cleavage site (Braglia et al. 2011). In this putative secondary way,

the RNA is cleaved at the T-rich stretch by an unknown endonuclease hence forming an alternative 5' RNA end recognized by Rat1 (Braglia et al. 2011).

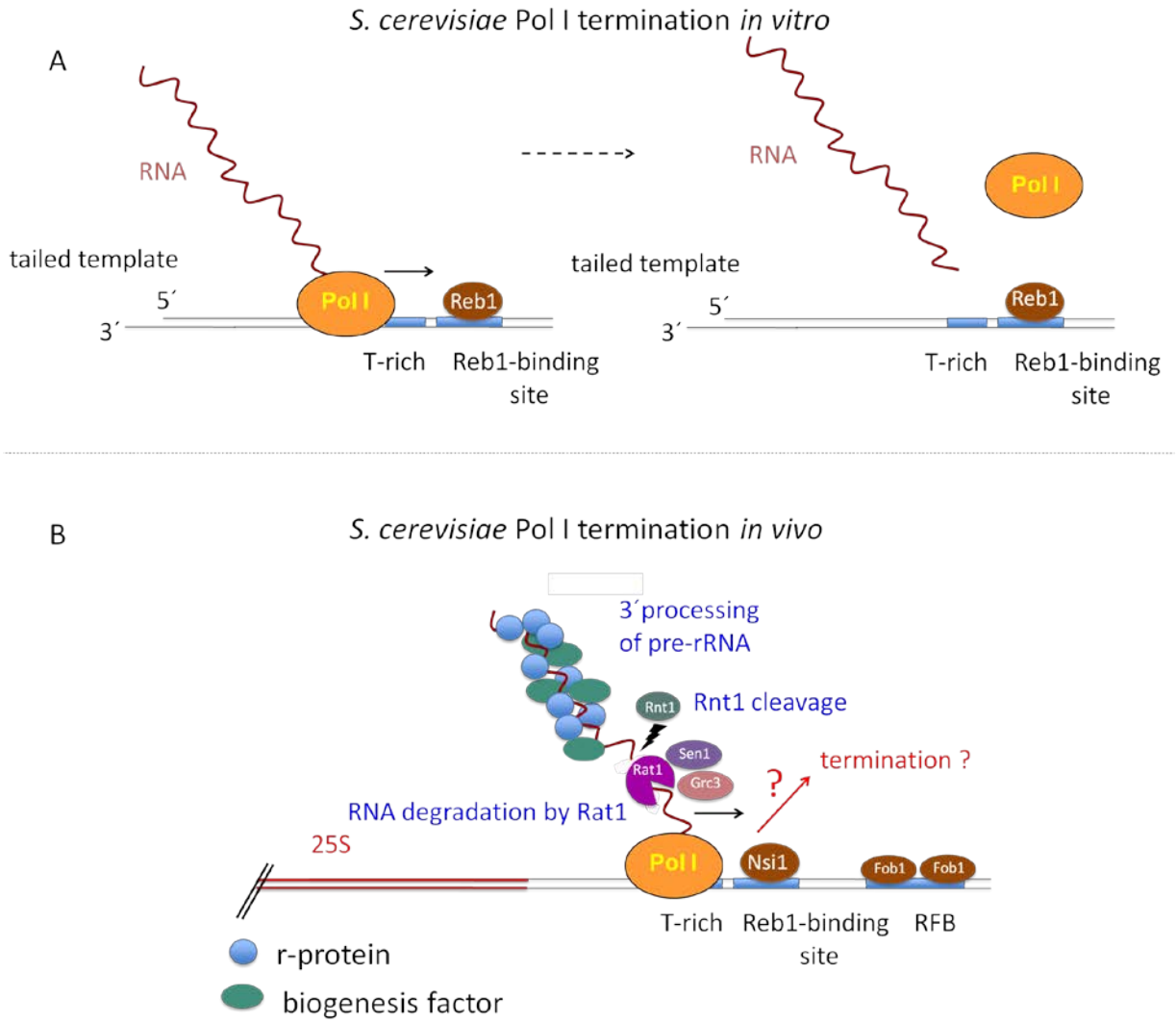

Fig. 2-4: Two models for yeast RNA Pol I termination. (A) Model of yeast Pol I termination *in vitro*. Transcription *in vitro* can be efficiently terminated by purified Pol I in the presence of purified DNA-bound Reb1, and a T-rich element upstream of the Reb1 binding site. A promoter-independent transcription assay is used. **(B)** Model of yeast Pol I termination *in vivo*. Pol I transcription termination *in vivo* is accompanied/supported by processing of the nascent transcript. Factors which were suggested to be involved in pre-rRNA processing and termination are the endo- and exonuclease Rnt1 and Rat1, the helicase Sen1 and the RNA/DNA kinase Grc3. Factors required for efficient termination which interact with cis elements of the termination region are the NTS1-silencing protein Nsi1 and the replication fork barrier binding protein Fob1. Possible mechanisms of termination and consequences of leaky termination are discussed in the text. Note: a reduced level of premature termination can be observed, if the termination element without the described co-transcriptional cleavage sites (Rnt1 and T1) is inserted within ITS1. (Németh et al. 2013)

However, many questions remain concerning which mechanism is happening *in vivo* or if elements of both models can be fit into one. Furthermore, none of the models provides a satisfying explanation for the apparent leakiness of Pol I termination. Both *in vitro* (70%) and *in vivo* (80%) termination

efficiencies below 100% were observed at the main terminator (T-rich and Reb1 BS) (Lang et al. 1994; Reeder et al. 1999). Studies using an artificial construct containing the promoter-proximal Reb1 BS which has a stronger affinity to Reb1 resulted in a minimal readthrough of 10% (Reeder et al. 1999). Those transcripts were further elongated until a second T-rich stretch (T2, also named a failsafe terminator) located roughly 250bp downstream of the 3' end of the 25S rDNA or until the RFB (~300bp downstream of 25S) (Reeder et al. 1999; El Hage et al. 2008; Prescott et al. 2004).

In mouse, the Pol I terminator region is also located in the 5' part of the IGS1 but differs significantly from its yeast counterpart. It contains 10 repetitions of the actual terminator element, of which each is a binding site for TTF-I (Gurney 1985; Grummt et al. 1985). A mouse terminator element was defined as an 18bp sequence containing a restriction site for SalI and thus named Sal box (Grummt, Rosenbauer, et al. 1986). TTF-I (transcription termination factor 1) can be roughly dissected in three functional parts (Evers et al. 1995; Evers & Grummt 1995). Whereas the N-terminal section inhibits DNA binding and is involved in TTF-I oligomerization, the C-terminal part harbours two Myb-like domains which mediate DNA binding activity. The central part is promoting transcription termination. Pol I termination occurs just upstream of the first terminator element (T_1) and is dependent on TTF-I (Gurney 1985; Grummt et al. 1985). Mutations in the terminator element which inhibit binding of TTF-I negatively influence transcription termination (Grummt, Kuhn, et al. 1986; Kermekchiev & Grummt 1987; Grummt, Rosenbauer, et al. 1986; Bartsch et al. 1988). Transcription termination by TTF-I depends on correct orientation of the terminator element (Smid et al. 1992; Kuhn et al. 1990; Grummt, Rosenbauer, et al. 1986). As in yeast, a T-rich stretch is located upstream of T_1, however it was shown not to be required for efficient termination (Kuhn et al. 1988). Mechanistically, it is suggested that Pol I is stopped when encountering a bent DNA structure due to TTF-I (Smid et al. 1992). The Pol I transcript release factor (PTRF) subsequently promotes the dissociation of the ternary complex via direct interaction with Pol I (Mason et al. 1997; Jansa et al. 1998; Jansa et al. 2001). There has been no evidence for a torpedo-like Pol I termination mechanism in higher eukaryotes. Furthermore, it is not clear, how 3' end formation of the 45S rRNA occurs and if it is linked to termination (Parker & Bond 1989; Miwa et al. 1987). It has been further suggested that oligomerization of TTF-I leads to bridging between terminator (T_1 – T_{10}) and promoter (T_0) and thus establishment of an rDNA loop at actively transcribed repeats (Sander & Grummt 1997; Denissov et al. 2011).

B) *Pol II*

For Pol II, a poly-A site (PAS) dependent and a Sen1 dependent pathway were described as the two major mechanisms of termination (reviewed in Kuehner et al. 2011; Mischo & Proudfoot 2013). It is proposed that termination at most protein-coding genes follows the poly-A way. This process is tightly coupled to 3' end formation of the nascent mRNA and can be dissected in two steps. After transcription of the poly-A site, Pol II is stalled and the nascent RNA is cleaved by an endonuclease. Next, the pre-mRNA gets polyadenylated and the downstream RNA is degraded (Logan et al. 1987; Whitelaw & Proudfoot 1986). Creation and processing of the 3' end of the pre-mRNA is highly complex and involves about 20 proteins in yeast (Mandel et al. 2008; Millevoi & Vagner 2010). Hereby, the Rpb1 CTD serves as an anchor for the recruitment of the first processing factors. It is suggested that factor binding leads to conformational changes which in turn trigger polymerase pausing. Subsequently, a paused state of Pol II is necessary for further association of processing factors and termination stimulation (Glover-Cutter et al. 2008). Two main effectors in this pathway are the multiprotein complexes cleavage and polyadenylation factor (CPF) and the cleavage factor (CF) which bind to the nascent RNA when the poly-A site (PAS) has been transcribed. In yeast, the PAS consists of an adenine-rich efficiency element, an A-rich positioning element and a U-rich element spanning the actual cleavage site (Guo & Sherman 1996; Bardwell et al. 1991; Dichtl & Keller 2001; Zaret & Sherman 1982; Valentini et al. 1999). Subcomponents of both CPF and CF interact with the Pol II CTD and subsequently promote cleavage of the nascent RNA. Nonetheless, it was proposed that efficient release of Pol II from the template requires Rat1 which recognizes the new 5' end and torpedoes Pol II as outlined for Pol I (Teixeira et al. 2004; Ghazal et al. 2009; Rondón et al. 2009; Nabavi & Nazar 2010). However, it was demonstrated that Rat1 –promoted degradation of the RNA was not sufficient by itself for polymerase release in vitro (Dengl & Cramer 2009).

For most non-coding RNAs transcribed by Pol II, 3' end formation occurs via endonuclease cleavage and/or via action of the exosome-TRAMP complex (Houseley & Tollervey 2009). The three main factors involved in this pathway are the helicase Sen1 and the RNA binding proteins Nrd1 and Nab3 (Kim et al. 1999; Steinmetz & Brow 1996; Steinmetz et al. 2001; Steinmetz et al. 2006). The exact mechanism remains unknown but it is proposed that interaction of the three factors with the Rpb1 CTD leads to conformational changes in Pol II which facilitate termination (Carroll et al. 2007). Instead of Rat1 which torpedoes the polymerase, the actual termination event is postulated to occur as Sen1 unwinds the RNA-DNA hybrid.

C) *Pol III*

RNA Pol III transcription is terminated after synthesis of a poly-U stretch, corresponding to a poly-T sequence on the non-template DNA strand (Matsuzaki et al. 1994; Bogenhagen & Brown 1981). It was proposed that no other trans-acting factors or RNA secondary structures were involved in Pol III termination. The actual mechanism remained unclear, however it was suggested that the weak A-U basepairing thermodynamically destabilizes the RNA-DNA hybrid and thus leads to RNA and DNA release (Yager & Von Hippel 1991). A very recent study challenged this hypothesis (Nielsen et al. 2013). Nielsen and co-workers demonstrated that transcription of an immobilized artificial template containing a poly-T stretch resulted in RNAs that remained associated with the elongation complex. They concluded that the T-stretch rather served as a pausing signal for Pol III than a release element. From this, the hypothesis was established that an RNA secondary structure like a hairpin in close proximity to the poly-T stretch was involved in transcript release in analogy to bacterial transcription termination. However, termination mechanisms like forward translocation (Santangelo & Roberts 2004) and RNA-DNA shearing could be excluded (Larson et al. 2008). It is proposed, that termination occurs via allosteric destruction of the Pol III elongation complex by the hairpin formation (Epshtein et al. 2007).

Pol III transcription termination is also influenced by polymerase subunits. For the TFIIF and A49/A34.5 – homolog C53/C37 a role in slowing down Pol III on the T-stretch of the SUP4 tRNA gene was reported (Landrieux et al. 2006). The TFIIS-like domain of subunit C11 promotes intrinsic RNA cleavage by Pol III that occurs during elongation pausing, proofreading, and termination (Rijal & Maraia 2013; Alic et al. 2007; Iben et al. 2011). In a recent study, two separate mechanisms for Pol III transcription termination were proposed, depending on the subunit composition of the enzyme (Arimbasseri & Maraia 2013). However, the actual mechanistic contribution of C53, C37 and C11 are still not sufficiently clarified.

2.4 Transcription of nucleosomal templates by Pol I, II and III

The natural template of RNA polymerases is not naked DNA but chromatin, a complex assembly of DNA, associated proteins and non-coding RNAs. The main structural unit of chromatin, most abundant component and first level of DNA compaction is the nucleosome. Core nucleosomes are comprised of two histones H2A, H2B, H3 and H4 each (Kornberg 1974; Kornberg & Thomas 1974). The nucleosomal proteins are arranged in two substructural complexes, a $(H3/H4)_2$ central tetramer surrounded by two H2A/H2B dimers. In yeast, 147bp of DNA are wrapped around the histone octamer in 1.65 turns. The DNA-histone complex is stabilized by hydrogen bonds, hydrophobic and ionic interactions. Chromatin structure is highly dynamic and its conformational changes are coupled to the cell cycle and processes like transcription. Concerning transcription, it is believed that the three RNA polymerases encounter different chromatin states at their target genes *in vivo*.

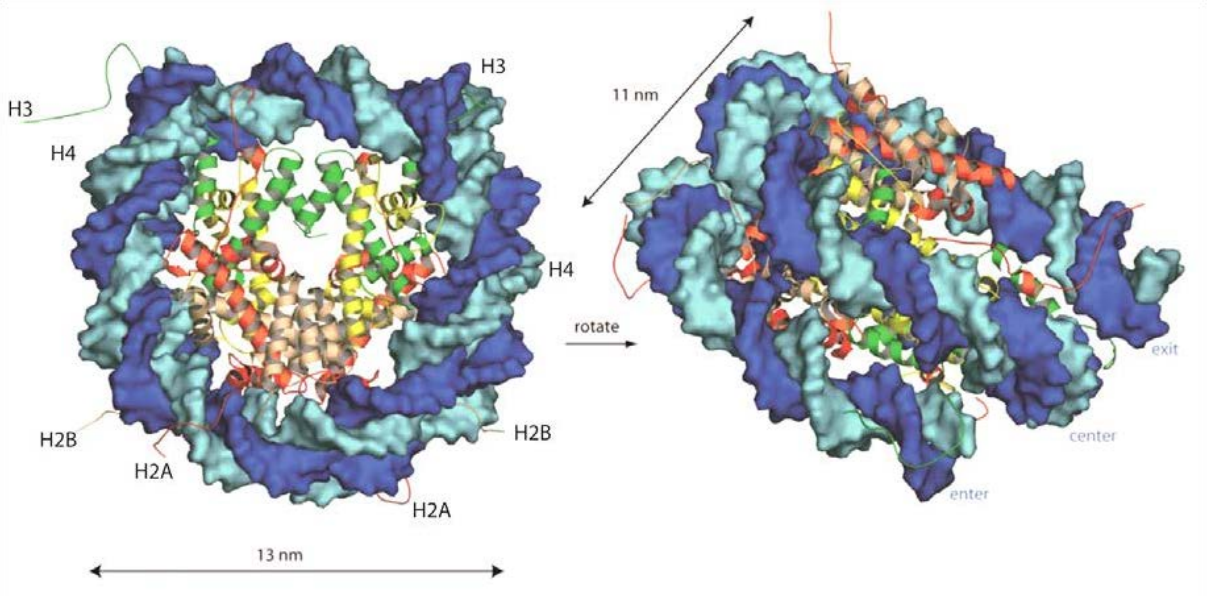

Fig. 2-5: The atomic structure of the nucleosome core particle. 147 bp of DNA (colored in different shades of blue) are wrapped around the histone octamer in 1.7 turns. The histone octamer is composed of two copies of each histone H2A (red), H2B (pink), H3 (green) and H4 (yellow) and forms the nucleosome core particle. Histone tails protrude from the nucleosome core particle (modified from Khorasanizadeh 2004)

A) *Pol I*

Early biochemical studies suggested that transcriptionally active rDNA repeats are associated with nucleosomes (Matsui & Busch 1977; Higashinakagawa et al. 1977; Weintraub & Groudine 1976). However, data obtained by EM analysis of chromatin Miller spreads (Miller & Beatty 1969) showed that transcribed rDNA repeats were depleted of nucleosomes. Furthermore, the mentioned study revealed the existence of two distinct chromatin states, with 50% of the repeats being transcriptionally active (open) and 50% being silenced (closed). It was demonstrated that transcriptional activity correlated with distinct chromatin states by psoralen photocrosslinking (Conconi et al. 1989). rDNA which was relatively resistant to psoralen crosslinking and representing the inactive state was shown to be associated with nucleosomes. Contrary, heavily psoralen crosslinked repeats were lacking nucleosomal arrays and associated with nascent RNA (Dammann et al. 1993). Combination of psoralen crosslinking with chromatin endogenous cleavage (ChEC) (Schmid et al. 2004) further revealed that open copies were minimally associated with histones (and thus putatively nucleosomes) but instead with Hmo1, whereas the opposite was true for closed copies (Merz et al. 2008). However, there is evidence for a dynamic nucleosomal arrangement in yeast (French et al. 2003). Active and inactive repeats in mammals can also be distinguished by different nucleosome positioning at the promoter (Längst et al. 1998), the DNA methylation pattern and the N-terminal histone tail modifications (Santoro et al. 2002; Németh et al. 2008). Little is known about how Pol I deals with a nucleosomal template. There are lines of evidence suggesting that chromatin transcription of mammalian Pol I requires the histone chaperones nucleolin and nucleophosmin (Angelov et al. 2006; Rickards et al. 2007; Okuwaki et al. 2001; Murano et al. 2008). Furthermore, it was demonstrated that nucleosome remodelers Chd1, Isw1 and Isw2 are associated with rDNA repeats (Jones et al. 2007). In a recent study, it was demonstrated that human Pol I was able to transcribe through a nucleosomal template *in vitro* with 10% efficiency compared to naked DNA (Birch et al. 2009). However, the histone chaperone FACT (facilitates chromatin transcription) was co-purified with the polymerase. *In vivo*, FACT is was suggested to be associated with active rDNA genes and downregulation of FACT expression leads to reduced cellular rDNA levels (Birch et al. 2009). Thus it was proposed that FACT helps Pol I to overcome nucleosomal barriers *in vivo*. Nonetheless, the exact mechanism of chromatin transcription by Pol I remains unclear as well as the general necessity for it in closed copy opening.

Futhermore, there is evidence that beyond Pol I transcription termination, TTF-I is also a key regulator regarding the epigenetic state of the rDNA locus in mouse and human (reviewed in

Grummt & Längst 2013). It was demonstrated that binding of TTF-I to a recognition site (T_0) upstream of the Pol I promoter moderates nucleosome remodeling which is necessary for efficient rDNA transcription (Längst et al. 1998; Längst et al. 1997). Activation of transcription by TTF-I occurs via recruitment of the ATPase CSB (Cockayne Syndrome protein B) which in turn serves as an anchor for the histone methyltransferase G9a (Yuan et al. 2007). Additionally, TTF-I functions in rDNA silencing. It was shown that T_0-bound TTF-I interacts with the NoRC (Nucleolar Remodeling Complex) subunit TIP5 (TTF-I interacting protein 5) (Németh et al. 2004). Subsequently, TIP5 directs DNA methyltransferases and histone deacetylases to the rDNA promoter and hence contributes to establishment of a heterochromatin state (Zhou et al. 2002; Santoro et al. 2002). It was suggested that NoRC function requires the association of TIP5 with a non-coding transcript named pRNA (promoter RNA) which is originating from a promoter situated in the IGS1 region (T_{sp}) (Mayer et al. 2006; Santoro et al. 2010). Recent studies proposed that the pRNA forms a transient triplex structure with the T_0 DNA which leads to dissociation of TTF-I and recruitment of the methyltransferase Dnmt3b (Schmitz et al. 2010). Methylation of a certain CpG residue by Dnmt3b in turn prevents initiation complex formation.

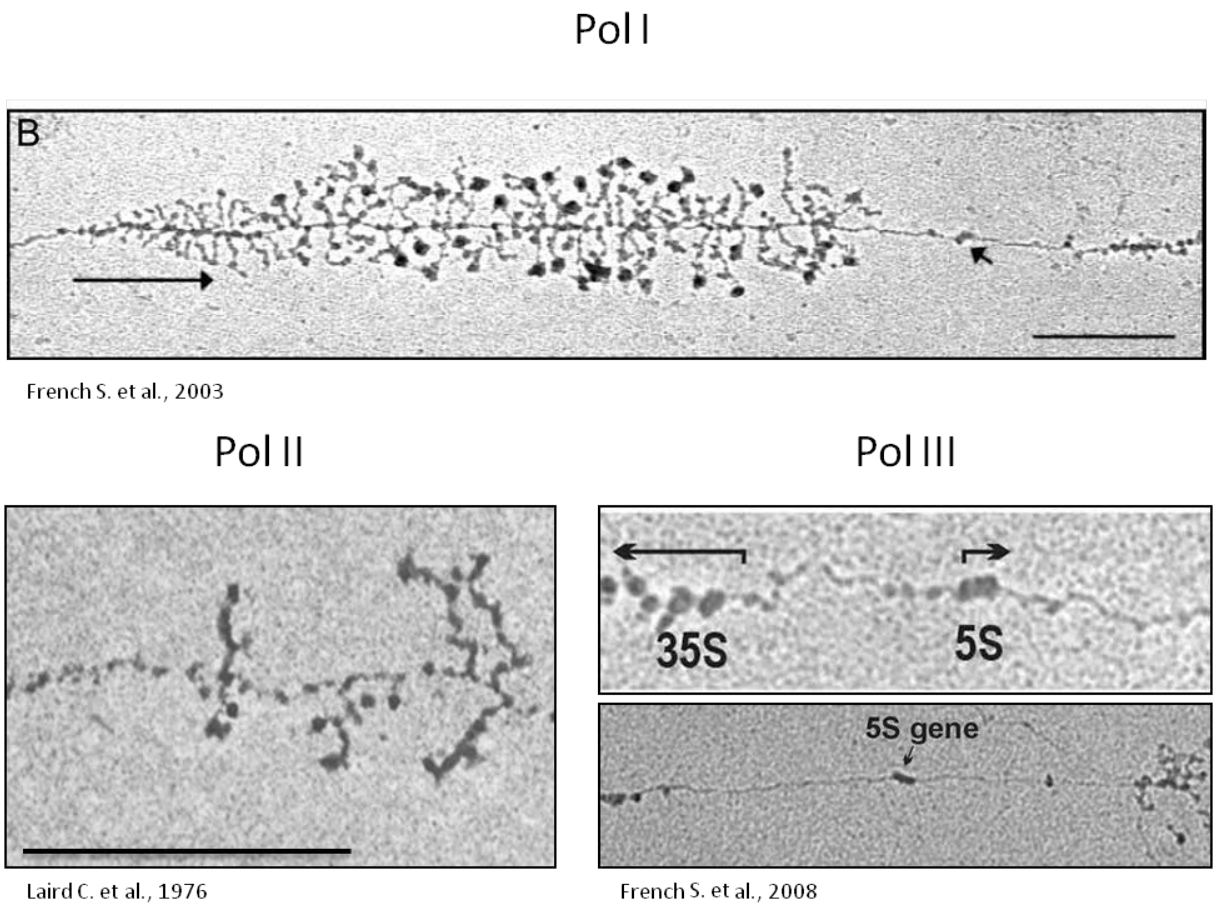

Fig. 2-6: Electron micrographs of actively transcribed Pol I, II and III genes. (Pol I) Representative electron micrograph of one rDNA repeat after chromatin spreading. The long arrow indicates direction of Pol I transcription of the 35S rRNA gene.

The short arrow indicates the structure frequently seen at the position of the 5S rRNA gene. Bar represents 400nm **(Pol II)** Spreaded embryonic chromatin of *D. melanogaster* with protruding nascent transcripts of a non-ribosomal gene. Small dots along the DNA represent nucleosomes. Bar represents 1µm. **(Pol III)** Identification of active *S. cerevisiae* 5S rRNA genes in rDNA intergenic spacers. Elongated dot represents Pol III complexes. (all adapted from French et al. 2003; French et al. 2008; Laird & Chooi 1976)

B) *Pol II*

Pol II transcription in the context of chromatin was addressed in genome-wide studies as well as single locus analyses. Genome-wide studies indicate that the average nucleosome density on the yeast chromosomes is relatively constant with a median spacing of 23bp (Yuan et al. 2005; Mavrich et al. 2008; Albert et al. 2007; Brogaard et al. 2012). However, it was demonstrated that the coding regions of nearly all Pol II target genes are occupied by nucleosomes, whereas regulatory regions of actively transcribed genes are often nucleosome-free (Yuan et al. 2005; Knezetic & Luse 1986; Izban & Luse 1991; Lorch et al. 1987). Apart from genome-wide studies, a few single gene loci were analyzed regarding their nucleosomal state, including PHO5, HIS3, CHA1, MFA2 and the centromere of chromosome III and the (Moreira & Holmberg 1998; Saunders et al. 1990; Teng et al. 2001). Both genome-wide approaches and single locus analyses revealed a consensus pattern of nucleosomal organization at promoter regions is observed in the *S. cerevisiae* genome. It is well established, that the region from -300bp to -150bp relative to the TSS can be occupied by a nucleosome (named -1) and hence regulate the accessibility of the promoter cis-elements. Transition from repressed to active state is proposed to be accompanied by histone tail modification and eventually nucleosome eviction. The next nucleosome downstream of the TSS (designated +1) is very tightly positioned (Mavrich et al. 2008) and often contains histone variants and histone tail modifications (Kouzarides 2007; Cosgrove & Wolberger 2005; Malik & Henikoff 2003). The following downstream nucleosomes exhibit less consensus spacing, histone variant incorporation and histone tail modifications with growing distance from the +1 nucleosome (Li et al. 2007; Lieb & Clarke 2005).

A nucleosome imposes a strong barrier for elongating Pol II *in vitro* (Kireeva et al. 2005) with its polymerase stalling potency being dependent on the strength of the actual histone-DNA interactions (Bondarenko et al. 2006). Single molecule transcription experiments using an optical trap confirmed the nucleosomal barrier to Pol II, which in this case was insuperable depending on the reaction conditions (Hodges et al. 2009). However, if respective nucleosome positioning sequences are inserted in the genome, transcription is not greatly affected (Gaykalova et al. 2011). This led to the

assumption that *in vivo* Pol II can overcome nucleosomal barriers with the help of additional effectors.

It was demonstrated that spontaneous release of the first 20bp which are wrapped around the nucleosome occurs with a frequency of roughly 250ms (Li et al. 2005). Furthermore, it is known that nucleosome disassembly occurs via eviction of an H2A/H2B dimer from the octamer (Gansen et al. 2009; Böhm et al. 2011). Taken together, this leads to the mechanistic hypothesis that Pol II can gain access to nucleosomal DNA and then Pol II traversal is facilitated by loss of a H2A/H2B dimer. This model is supported by publications reporting that Pol II can remove an H2A/H2B dimer from the nucleosome upon single round transcription *in vitro* (Bintu et al. 2011; Kireeva et al. 2002). It was further reported that loss of the H2A/H2B dimer favored Pol II traversal through the remaining histone hexamer (Bintu et al. 2011; Kireeva et al. 2002). In single molecule optical trap experiments it was determined that Pol II was able to elongate roughly 30bp into the wrapped DNA before it encountered the first barrier (Hodges et al. 2009). This barrier was due to the strong interactions between DNA and the H2A/H2B dimer.

Nonetheless, several trans-acting factors influence Pol II transcription of nucleosomal templates. Among those are chromatin remodelers which can translocate nucleosomes along the DNA, exchange or evict histones or evict the complete nucleosome from the DNA via ATP hydrolysis (Clapier & Cairns 2009; Hota & Bartholomew 2011). Chromatin remodelers are divided in the four subfamilies switch/sucrose nonfermentable (SWI/SNF), imitation switch (ISWI), chromodomain-helicase-DNA-binding protein (CHD) and inositol-requiring 80 (INO80). SWI/SNF were detected at Pol II gene promoters and open reading frames in yeast and it was suggested that they travel with the elongating polymerase (Schwabish & Struhl 2007; Shivaswamy & Iyer 2008). It is believed that SWI/SNF act by eviction of histone octamers and play a role in transcription activation upon change of environmental conditions (Lorch et al. 1999; Bruno et al. 2003; Dechassa et al. 2010). Both ISWI and the CHD family have been assigned a role in transcription elongation. It was shown that ISWI family members can exchange histones and lower the nucleosomal barrier to Pol II transcription *in vitro* (Bruno et al. 2003; Gaykalova et al. 2011). CHD-like factors were found to colocalize with Pol II *in vivo*. Furthermore, Chd1 interactions with the histone chaperone FACT and the Pol II elongation factors DSIF and Spt4/5 were demonstrated (Simic et al. 2003; Srinivasan et al. 2005). Both CHD and ISWI are reportedly sliding nucleosomes along the DNA hence forming ordered nucleosomal arrays. In yeast, ISWI facilitates nucleosome positioning on the edge of the 5’ and 3’ nucleosome-free regions (Lusser et al. 2005; Whitehouse et al. 2007; Gkikopoulos et al. 2011). Among other functions, INO80 family members promote exchange of H2A against its variant H2AZ and vice versa.

Not only chromatin remodelers are involved in transcription of nucleosomal DNA but also a multitude of histone chaperones. Unlike the remodelers, chaperones do not consume ATP but exhibit strong affinities to surfaces of the histone octamer and thus are able to disrupt nucleosomes or to promote histone exchange (Das et al. 2010). Disruption of an H2A/H2B dimer from the octamer upon passage of Pol II is facilitated by Nap1 and FACT. Thereby Nap1 cooperates with nucleosome remodeling factors like Chd1 and the RSC complex (Lorch et al. 2006; Walfridsson et al. 2007). It is proposed that Nap1 in general controls the H2A/H2B density on coding regions and hence influences Pol II transcription elongation (Andrews et al. 2008). The histone chaperone FACT promotes the elongation of Pol II on nucleosomal templates *in vitro* (Orphanides et al. 1998). *In vivo*, FACT is associated with elongating Pol II and physically interacts with Pol II elongation factors including Chd1, DSIF, Spt6, Paf1 and Nap1 (Saunders et al. 2003; Mason & Struhl 2003). FACT activity is stimulated by ubiquitinylation of lysine 123 in H2B (H2BK123) *in vitro* (Pavri et al. 2006). It remains unknown, whether Nap1 and FACT act cooperatively or separately and whether the main in vivo contribution to Pol II elongation comes from H2A/H2B dimer eviction or nucleosome reassembly upstream of the elongating polymerase (Schwabish & Struhl 2004; Rosario & Pemberton 2008). Asf1 (anti silencing factor 1) and Spt6 (suppressor of ty homolog 6) are chaperones of the H3/H4 tetramer. It was demonstrated that Asf1 is associated with Pol II transcribed genes and promotes loss and re-deposition of H3 (Schwabish & Struhl 2004). Spt6 is associated with Pol II (Andrulis et al. 2000) and facilitates chromatin transcription *in vivo* by enhancing Pol II's elongation rate (Ardehali et al. 2009). It is suggested that Spt6 plays a role in depositioning of H3 after polymerase readthrough since loss of Spt6 function results in a generally lowered H3 density at transcribed genes (Ivanovska et al. 2011). However, it cannot be judged by now whether the stimulatory effect of Spt6 on chromatin transcription by Pol II is promoted by re- or disassembly of H3 (Kaplan et al. 2003).

Obviously, histone post-translational modifications and use of non-canonical histones are involved in transcription regulation and nucleosome traversal of RNA polymerase (reviewed in Petesch & Lis 2012).

C) *Pol III*

Concerning Pol III, it is suggested that the respective actively transcribed genes are devoid of nucleosomes *in vivo* (Wittig & Wittig 1982; Morse et al. 1992) proposing that Pol III possesses the ability to transcribe a mono-nucleosomal template *in vitro* without additional factors (Studitsky et al. 1997). A recent study implicates action of FACT in Pol III transcription *in vivo* hence proclaiming FACT

a general chromatin transcription factor for all eukaryotic RNA polymerases (Birch et al. 2009). Additionally, several studies showed that chromatin remodeling and histone modifications were necessary for Pol III elongation through nucleosomal arrays *in vitro* (Englander et al. 1993; Ura et al. 1997; Tse et al. 1998; Ng et al. 2002; Arimbasseri & Bhargava 2008).

2.5 Objectives

A first main focus of this study was laid on transcription termination of Pol I. A recent publication from our group (Reiter et al. 2012) proposed Nsi1 as a novel Pol I termination factor *in vivo*. We wanted to take another approach and assess Pol I termination in an initiation-independent *in vitro* transcription system. It is still unclear how the actual mechanism of Pol I transcription termination works and none of the currently discussed models includes Nsi1. Since Nsi1 but not Reb1 was detected at the terminator-proximal Reb1 BS *in vivo*, we wanted to elucidate, if Nsi1 could fulfill Reb1 functions in an *in vitro* termination assay. We further wanted to investigate which terminator cis elements and trans-acting factors are necessary and sufficient for Pol I termination *in vitro* and to determine their respective influence. An additional task was to investigate possible cooperative effects in Pol I termination between the three main factors of interest Reb1, Nsi1 and Fob1. Furthermore, we sought to elucidate the contribution and/or necessity of Pol I subunits for termination *in vitro*. By inclusion of Pol I mutants in the analysis, we hoped to get further mechanistical insight in the termination event.

Second, we wanted to compare yeast Pol I, II and III regarding to their behaviour, if barriers are encountered during transcription in general. To determine polymerase-inherent differences and similarities during elongation, an *in vitro* approach independent of initiation was the first choice for reasons of comparability. The study includes physiological barriers like Reb1, Nsi1 and Fob1 as well as the strong DNA binding proteins LexA (A. P. P. Zhang et al. 2010; Butala et al. 2009; Butala et al. 2007), the Lac repressor (LacI)(Müller-Hill 1975) and the mouse Pol I termination factor TTF-I.

Finally, a side-by-side comparison of Pol I, II and III regarding their ability to transcribe nucleosomal templates was a major goal. Although transcription of nucleosomal templates was extensively studied (2.4), a comparative in vitro study including all three polymerases was never conducted. First we aimed at polymerase-inherent differences in the ability to transcribe chromatin templates. Next,

we wanted to determine whether polymerase subunits or respective homologous transcription factors influenced elongation on a nucleosomal template *in vitro*.

CHAPTER III – MATERIAL & METHODS

3.1 Material

3.1.1 Chemicals

All chemicals and solvents used in this work were purchased at the highest available purity from Sigma-Aldrich, Merck, Fluka, Roth, Serva or J.T.Baker, except agarose electrophoresis grade (Invitrogen), G418/Geneticin (Gibco), milk powder (Sukofin), Nonidet P-40 substitute (NP40) (USB Corporation), Tris ultrapure (USB Corporation). Restriction enzymes, chemicals and other enzymes needed for standard manipulation of DNA (3.2.1) were purchased from New England Biolabs.
Ingredients for growth media were purchased from BD Biosciences (Bacto Agar, Bacto Peptone, Bacto Tryptone and Bacto Yeast Extract). Water was always purified with an Elga Purelab Ultra device prior to use. If a certain supplier was crucial, this is indicated in the method description.

3.1.2 Media

Water for media preparation had a resistivity of 18.2MΩ. All media were autoclaved for 20min at 110°C and stored at 4°C. If antibiotics were to be added, this was done after the medium temperature fell below approximately 50°C. For casting of plates, 2% agar was added to the solution prior to autoclaving. For SF21 insect cell cultivation, SFII 900 SFM medium was purchased from Life Technologies.

medium	ingredients	concentration/percentage
lysogeny broth (LB) (Sambrook et al. 1989)	tryptone yeast extract NaCl (agar)	10g/l 5g/l 10g/l (20g/l)
LB_{Amp}	LB Ampicillin (agar)	 100µg/ml (20g/l)
$LB_{Amp\ Tetra\ Genta\ IPTG}$	LB ampicillin tetracycline genatmycin IPTG (agar)	 100µg/ml 10µg/ml 10µg/ml 0.5mM (20g/l)
$LB_{Amp\ Tetra\ Genta\ IPTG\ X\text{-}GAL}$	LB ampicillin tetracycline gentamycin IPTG X-GAL (agar)	 100µg/ml 10µg/ml 10µg/ml 0.5mM 50mg/ml (20g/l)
super optimal broth (SOB) (Hanahan 1983)	tryptone yeast extract NaCl KCl $MgCl_2$ (after autoclaving) $MgSO_4$ (after autoclaving)	20g/l 5g/l 0.6g/l 0.2g/l 10mM 10mM
YPD	yeast extract peptone glucose (agar)	10g/l 20g/l 20g/l (20g/l)
$YPD_{Geneticin}$	YPD geneticin	 400mg/l

YPG	yeast extract peptone galactose (agar)	10g/l 20g/l 20g/l (20g/l)

Table 3-1: Media.

3.1.3 Buffers

All buffers were prepared with purified water with a resistivity of 18.2MΩ. The pH values were adjusted with a standard pH meter at RT with 37% HCl or 10M NaOH if not indicated otherwise. Specifications provided as percentages are mass per volume (m/v) for solids and volume per volume (v/v) for fluids. Protease inhibitors, dithiothreitol (DTT) and β-mercaptoethanol were added freshly prior to use.

A) *General buffers*

buffer	ingredients	concentration/percentage
TE buffer	Tris/HCl, pH 8 EDTA	10mM 1mM
AE buffer	Tris/HCl, pH 9 EDTA	10mM 0.5mM
EB buffer	Tris/HCl, pH 8	10mM
5x TBE buffer	Tris/HCl boric acid EDTA	450mM 450mM 10mM
loading buffer AGE	Tris/HCl pH 8.0 EDTA bromophenol blue xylene cyanol glycerol	10mM 1mM 0.01% 0.01% 33.3%

10x oligo annealing buffer	Tris/HCl pH 7.5 NaCl EDTA	100mM 1M 10mM
4x upper Tris buffer	Tris/HCl, pH 6.8 SDS bromophenol blue	1.5M 0.4%
4x lower Tris buffer	Tris/HCl SDS	1.5M 0.4%
10x SDS PAGE electrophoresis buffer	Tris/HCl Glycine SDS	0.5M 1.9M 1%
loading buffer SDS PAGE	Tris/HCl, pH 6.8 Glycerol SDS β-mercaptoethanol Bromophenol blue	0.25M 40% 8.4% 0.57M
transfer buffer (Western blot)	Tris/HCl glycine methanol	25mM 192mM 20%
Ponceau staining solution	HOAc Ponceau S	5% 0.1%
10x PBS	NaCl KCl KH_2PO_4	1.37M 27mM 20mM
PBST	PBS Tween 20	1x 0.05%
TELit	LiOAc Tris/HCl pH 8 (HOAc) EDTA pH 8	100mM 10mM 1mM

LitSORB	LiOAc Tris/HCl pH 8 (HOAc) EDTA pH 8 Sorbitol sterile filtered	100mM 10mM 1mM 1M
LitPEG	LiOAc Tris/HCl pH 8 (HOAc) EDTA pH 8 polyethylene glycol 3350 sterile filtered	100mM 10mM 1mM 40%
Tfb 1	KOAc $MnCl_2$ KCl Glycerol pH 5.8 with HOAc sterile filtered	30mM 50mM 100mM 15%
Tfb 2	MOPS $CaCl_2$ KCl Glycerol pH 7 sterile filtered	10mM 75mM 10mM 15%
100x Protease inhibitors (PIs)	benzamidine phenylmethylsulfonylflouride (PMSF)	33mg/ml 17mg/ml
Solution I	Tris/HCl pH 8 EDTA RNase A	15mM 10mM 100µg/ml
Solution II	NaOH SDS	0.2M 1%

Table 3-2: General buffers.

B) *Solutions for Coomassie and silver staining*

buffer	ingredients	concentration/percentage
Coomassie staining solution	water methanol glacial acetic acid Coomassie blue	50% 40% 10%
destaining solution for protein polyacrylamide gel	water methanol glacial acetic acid	50% 40% 10%
fixation solution	MeOH HOAc formaldehyde	50% 12% 0.02%
washing solution	EtOH	50%
pre-treatment solution	$Na_2S_2O_3$	0.8mM
staining solution	$AgNO_3$ formaldehyde	0.2% 0.075%
developer	Na_2CO_3 formaldehyde pre-treatment solution	6% 0.05% 2.5%
stop solution	HOAc	1%

Table 3-3: Solutions for Coomassie and silver staining.

C) *Buffers for RNA polymerase/transcription factor IIF (TFIIF) purification*

buffer	ingredients	concentration/percentage
P1 KOAc	KOAc Hepes pH 7.8	200mM 20mM

	$MgCl_2$ glycerol PIs	1mM 20% 1x
P2 KOAc	KOAc Hepes pH 7.8 $MgCl_2$ glycerol NP40 (PIs)	200mM 20mM 1mM 20% 0.1% (1x)
P1 KCl 200/300/500	KCl Tris/HCl pH 8 MgAc glycerol PIs	200/300/500mM 20mM 5mM 20% 1x
P2 KCl 200/300/500	KCl Tris/HCl pH 8 MgAc glycerol NP40 (PIs)	200/300/500mM 20mM 5mM 20% 0.1% (1x)
C1	Hepes pH 8 NaCl $MgCl_2$ DTT $CaCl_2$ imidazole	20mM 50mM 10mM 2.5mM 2mM 1mM
C2	C1 NaCl	1x 50mM

Table 3-4: Buffers for RNA polymerase and TFIIF purification.

D) *Buffers for purification of recombinant proteins via the FLAG tag*

buffer	ingredients	concentration/percentage
TAP 100	NaCl Tris/HCl pH 7.5 $MgCl_2$ NP40 DTT PIs	100mM 50mM 5mM 0.15% 1mM 1x
TAP 300	NaCl Tris/HCl pH 7.5 $MgCl_2$ NP40 DTT PIs	300mM 50mM 5mM 0.15% 1mM 1x

Table 3-5: Buffers for FLAG tag purification.

E) *Buffers for purification of recombinant Reb1-His$_6$ and Hmo1-His$_6$*

buffer	ingredients	concentration/percentage
resuspension buffer 1	Tris/HCl pH 8 EDTA β-mercaptoethanol PIs	10mM 1mM 5mM 1x
resuspension buffer 2	Tris/HCl pH 7 EDTA β-mercaptoethanol PIs	10mM 1mM 5mM 1x
washing buffer 1	Tris/HCl pH 7 NaCl imidazole PIs	50mM 1M 2mM 1x
washing buffer 2	Tris/HCl pH 7	50mM

	NaCl imidazole PIs	1M 2mM 1x
elution buffer	Tris/HCl pH 8 NaCl imidazole	50mM 300mM 1x

Table 3-6: Buffers for purification of Hmo1-His_6 and Reb1-His_6.

F) *Buffers for purification of the recombinant A49-His_6/A34.5 dimer*

buffer	ingredients	concentration/percentage
buffer A	Tris pH 7.5 β-mercaptoethanol	50mM 5mM
buffer B	Tris pH 7.5 NaCl β-mercaptoethanol PIs	50mM 300mM 5mM 1x
buffer C	Tris pH 7.5 NaCl β-mercaptoethanol PIs	50mM 1M 5mM 1x
buffer D	Tris pH 7.5 NaCl imidazole β-mercaptoethanol PIs	50mM 300mM 10mM 5mM 1x
buffer E	Tris pH 7.5 NaCl imidazole β-mercaptoethanol	50mM 300mM 200mM 5mM

Table 3-7: Buffers for purification of the A49-His_6/A34.5 dimer.

G) Buffers for chromatin assembly

buffer	ingredients	concentration/percentage
high salt buffer	Tris pH 7.6 NaCl EDTA NP40 β-mercaptoethanol	10mM 2M 1mM 0.05% 1mM
20x low salt buffer	Tris pH 7.6 NaCl EDTA NP40 β-mercaptoethanol	200mM 1M 20mM 1% 20mM
6x loading buffer	Glycerol orange g	60%

Table 3-8: Solutions for chromatin assembly.

H) *Buffers for in vitro transcription*

buffer	ingredients	concentration/percentage
10x T7 RNA polymerase buffer	Tris/HCl pH 7.9 $MgCl_2$ spermidine DTT	400mM 60mM 20mM 100mM
10x new transcription buffer (NTB)	Hepes pH 8 $MgCl_2$ EDTA EGTA DTT	200mM 100mM 50mM 0.5mM 25mM

Proteinase K storage buffer	Tris/HCl pH 7.5 $CaCl_2$ glycerol	20mM 1mM 50%
Proteinase K buffer	NaCl Tris/HCl pH 7.5 EDTA SDS	300mM 10mM 5mM 0.6%
Proteinase K mix (20 reactions)	Proteinase K Proteinase K buffer	110µl 4.7ml
denaturing RNA loading buffer	formamide de-ionized TBE bromophenol blue xylene cyanole	80% 0.5x

Table 3-9: Buffers for *in vitro* transcription experiments.

3.1.4 Nucleic acids

A) *Nucleotides*

For polymerase chain reaction (PCR) deoxynucleotides were purchased from New England Biolabs (dNTPmix, 10mM each). Nucleotides for *in vitro* transcription were bought from GE Healthcare in separate vials (rNTP set, 100mM each). Radiolabeled [α–^{32}P]-CTP was purchased from Hartmann Analytic GmbH at a concentration of 10µCi/µl and a specific activity of 400 Ci/mmol.

B) *Oligonucleotides*

Oligonucleotides were purchased from Eurofins MWG Operon. For cloning purposes, standard purification was chosen, modified oligos were ordered HPLC purified.

#	name	seqence	gene/ locus	function
-	T7 terminator	TATGCTAGTTATTGCTCAG		sequencing
-	M13 rev	AACAGCTATGACCATG		sequencing
723	M13	GTCAGACTGTGTCAACGGT GTAGAT		sequencing
2038	Bla_rev	AGCAAAAACAGGAAGGCAA A		sequencing
2479	rDNA4 Th fo	CTTGTCTCAAAGATTAAGCC ATGC	rDNA	qPCR
2480	rDNA4 Th re	ACCACAGTTATACCATGTAG TAAAGGAACT	rDNA	qPCR
2551	5' for A135 seq	TGT TGG TGG TAA TGA AAC AA	A135	sequencing A135 with #2552
2552	3' rev A135 seq	GTT TTA AAA CCT AAG AGT CA	A135	sequencing A135 with #2551
2553	5' for B150 seq	TAT CGC GAA ATT AAA TCA TA	B150	Sequencing B150 with #2554
2554	3' rev B150 seq	TTC GTT TTA AAA CCT AAG AG	B150	sequencing B150 with #2553
2555	5' for C128 seq	ATG GGC TAT AGT GGT TGG TG	C128	sequencing C128 with #2556
2556	3' rev C128 seq	TCG TTT TAA AAC CTA AGA GT	C128	sequencing C128 with #2555
2557	B150 H7 PA for II	CAT TAC ACC ACG TTT ATA TAC CGA TCG TTC GAG AGA TTT T	B150	tagging of B150 with 7x His and ProtA
2558	C128 H7 PA for II	CAT AGC CCC AAG ATT AAG ATT GGA AGA TAT CTT CCA GCA G	C128	tagging of C128 with 7x His and ProtA
2559	Reb1 inv up	TTA AGA ATT CTA TGA TTT TTT ACC CGG CAT GTA TTG TAT ATA TCT ATT A	rDNA	Reb1 binding site inverted for annealing with #2560

2560	Reb1 inv down	TAA TAG ATA TAT ACA ATA CAT GCC GGG TAA AAA ATC ATA GAA TTC	rDNA	Reb1 binding site inverted for annealing with #2559
2561	TFG1 fwd	GAT GGT ACC AAA AAT TGT GTC GAA AGG TTG GCA ATG ACC ACA TGG AAT TAA AGA AAG AGC GTA CGC TGC AGG TCG AC	TFG1	TFG1 tagging ProtA
2562	TFG1 rev	GAC CTC GAG AAA GAA CGA AAA CTA AAT AAC CTA TTA AGT ACA TAA CAT TAT AAA CTA ACA TCG ATG AAT TCG AGC TCG	TFG1	TFG1 tagging Prot A
2563	5' for mut HpaI	TAT CTA TTA TAA TAT ACG ATG AGG ATG ATA GTG TGT AAG AGT TAA CCA TTT ACT AAT GTA TGT AAG	rDNA	primer to introduce a mutation in the Reb1 binding site
2564	3' rev AvaI Ydr	CGT TCG CTC GAG ATT GAT TTG TTC CAA CAA TG	Ydr026c	primer for amplification of Ydr026c introducing a AvaI site
2592	3'_rev_SacI_FOB1	CTAGTGAGCTCTTACAATTC CATTGATGTGC	FOB1	amplification of FOB1 and introduction of BamHI/SacI sites for insertion into pFL Flag TEV
2593	3'_rev_SacI_HMO1	CTAGTGAGCTCTCAAATAGA AGAGTTGGATT	HMO1	amplification of HMO1 and introduction of BamHI/SacI sites for insertion into pFL Flag TEV
2594	3'_rev_SacI_mTTF1	TAGTGAGCTCTCACTGCACA TCAGAGGCGC	TTF1	amplification of TTF1 and introduction of BamHI/SacI sites for insertion into pFL Flag TEV
2595	3'_rev_SacI_PAF1	TAGTGAGCTCCTATTCTTCTT GTAAAGTTT	PAF1	amplification of PAF1 and introduction of BamHI/SacI sites for insertion into pFL Flag TEV
2596	3'_rev_SacI_REB1	TAGTGAGCTCTTAATTTTCT GTTTTCATTG	REB1	amplification of REB1 and introduction of BamHI/SacI sites for insertion into pFL Flag TEV
2597	3'_rev_SacI_Y	TAGTGAGCTCTTAATTGATT	YDR026c	amplification of YDR026c and

	DR026c	TGTTCCAACA		introduction of BamHI/SacI sites for insertion into pFL Flag TEV
2598	5'_for_BamHI_FOB1	CTAAGGATCCATGACGAAACCGCGTTACAA	FOB1	amplification of FOB1 and introduction of BamHI/SacI sites for insertion into pFL Flag TEV
2599	5'_for_BamHI_HMO1	CTAAGGATCCATGACTACAGATCCTTCTGT	HMO1	amplification of HMO1 and introduction of BamHI/SacI sites for insertion into pFL Flag TEV
2600	5'_for_BamHI_mTTF1	CTAAGGATCCATGAAAGGGGGCACAAGCAA	TTF1	amplification of TTF1 and introduction of BamHI/SacI sites for insertion into pFL Flag TEV
2601	5'_for_BamHI_PAF1	CTAAGGATCCATGTCCAAAAAACAGGAATA	PAF1	amplification of PAF1 and introduction of BamHI/SacI sites for insertion into pFL Flag TEV
2602	5'_for_BamHI_REB1	CTAAGGATCCATGCCTTCAGGTCATAACGA	REB1	amplification of REB1 and introduction of BamHI/SacI sites for insertion into pFL Flag TEV
2603	5'_for_BamHI_YDR026c	CTAAGGATCCATGGACAGCGTGTCAAACCT	YDR026c	amplification of YDR026c and introduction of BamHI/SacI sites for insertion into pFL Flag TEV
2604	5'_for_YDR_new	TGTCTGCGTCAAGAAGAAAGA	YDR026c	amplification of YDR026c and introduction of BamHI/SacI sites for insertion into pFL Flag TEV (newly designed primers)
2605	3'_rev_YDR_new	TGTTTGGGAAAGTAACCCTTC	YDR026c	amplification of YDR026c and introduction of BamHI/SacI sites for insertion into pFL Flag TEV (new designed primers)
2606	5'_for_cDNA	CATTCCCTACAATTCTACTT		generation of cDNA from the tail g- 5xTTF1 transcript
2607	3'_rev_cDNA	CTGGCACGACAGGTTTCCCG		generation of cDNA from the tail g- 5xTTF1 transcript
2608	5'_for_EMSA	ATCACCTTACCCTATACTTACTCGC		generation of EMSA templates possible on all pUC19 tail g- vectors

2609	3'_rev_EMSA	CTGGCACGACAGGTTTCCC		generation of EMSA templates possible on all pUC19 tail g-vectors
2610	LexA shift up	AACGAATTCCATGGTGCTGTATATAAAACCAGTGGTTATATGTACAGTAG		small fragment for EMSA with one LexA binding site for annealing
2611	LexA shift down	CTACTGTACATATAACCACTGGTTTTATATACAGCACCATGGAATTCGTT		small fragment for EMSA with one LexA binding site for annealing
2612	top Ala tRNA	ATGAATTCGGGCACATGGCGCAGTTGGTAGCGCGCTTCCCTTGCAAGGAAGAGGTCATCGGTTCGATTCCGGTTGCGTCCAAAGCTTATAT	tRNA Ala	annealing oligo for insertion of the alanine tRNA via EcoRI /HindIII into pUC19 tail g-constructs
2613	down Ala tRNA	ATATAAGCTTTGGACGCAACCGGAATCGAACCGATGACCTCTTCCTTGCAAGGGAAGCGCGCTACCAACTGCGCCATGTGCCCGAATTCAT	tRNA Ala	annealing oligo for insertion of the alanine tRNA via EcoRI /HindIII into pUC19 tail g-constructs
2614	5'_for_BamHI_LacI	ACTGGATCCGTGAAACCAGTAACGTTATAC	LACI	amplification of LACI from pGEX 4T1 and insertion of BamHI site
2615	3'_rev_NotI_LacI	GATAAGCGGCCGCGTTTTTCTTTTCACCAGTGA	LACI	amplification of LACI from pGEX 4T1 and insertion of NotI site TRUNCATED!
2616	3'_rev_LacI_2	TAATGCGGCCGCTCACTGCCCGCTTTCCAGT	LACI	amplification of LACI from pGEX 4T1 and insertion of NotI site FULL Length
2617	T7 Promoter	TAATACGACTCACTATAGGG		sequencing
2618	SP6 Promoter	CTATTTAGGTGACACTATAG		sequencing
2619	top 2xLacR	CTTGTGGATCCTTAAGTGTGGAATTGTGAGCGGATAACAATTTCACAAATTGTGAGCGGATAACAATTCTTAACTGCAGTTCAG	LacO	top strand annealing oligo for insertion of 2 LacI binding sites via BamHI/PstI in pUC19 tail g-Enh
2620	bottom 2xLacR	CTGAACTGCAGTTAAGAATT	LacO	bottom strand annealing oligo

		GTTATCCGCTCACAATTTGT GAAATTGTTATCCGCTCACA ATTCCACACTTAAGGATCCA CAAG		for insertion of 2 LacI binding sites via BamHI/PstI in pUC19 tail g- Enh
2621	top 1xLacR	CTTGTGGATCCTGTGGAATT GTGAGCGGATAACAATTTCA CACTGCAGTTCAG	LacO	top strand annealing oligo for insertion of 1 LacI binding site via BamHI/PstI in pUC19 tail g- Enh
2622	bottom 1x LacR	CTGAACTGCAGTGTGAAATT GTTATCCGCTCACAATTCCA CAGGATCCACAAG	LacO	bottom strand annealing oligo for insertion of 1 LacI binding site via BamHI/PstI in pUC19 tail g- Enh
2623	top LacO	GTCCTGAATTCGGCGGCTCG TATGTTGTGTGGAATTGTGA GCGGATAACAATTTCACACA GGAAACAGCCAAGCTTGGC GA	LacO	top strand annealing oligo for insertion of the Lac Operator via EcoRI/ HindIII into pUC19 tail g- 3xLexA
2624	bottom LacO	TCGCCAAGCTTGGCTGTTTC CTGTGTGAAATTGTTATCCG CTCACAATTCCACACAACAT ACGAGCCGCCGAATTCAGG AC	LacO	bottom strand annealing oligo for insertion of the Lac Operator via EcoRI/ HindIII into pUC19 tail g- 3xLexA
2625	1xLacI E/H up	GATGAATTCTGTGGAATTGT GAGCGGATAACAATTTCACA AAGCTTGATG	LacO	top strand annealing oligo for creation of pUC19 tail g- 1xLacI ; insertion via EcoRI/ Hind III
2626	1x LacI E/H down	CATCAAGCTTTGTGAAATTG TTATCCGCTCACAATTCCAC AGAATTCATC	LAcO	bottom strand annealing oligo for creation of pUC19 tail g- 1xLacI ; insertion via EcoRI/ Hind III
3050	5’ for TER SacI	GAGGGAGCTCTCTCTATAAA TTTTATTTGT	rDNA	amplification of Pol I terminator introducing SacI site
3051	3’ rev TER BamHI	GATGGATCCACTATAGGAA ATGAGCTTTTC	rDNA	amplification of Pol I terminator introducing BamHI site
3052	5’ for Rnt TER SacI	GAGGGAGCTCGCCTTTGTT GTCTGATTTGT	rDNA	amplification of Pol I terminator plus Rnt1 site introducing SacI site

3053	5’ for SOE SacI rDNA	AAGGATTGACAGATTGAGA GTTCTTTCTTG	rDNA	SOE primer eliminating the SacI site in the yeast rDNA with #3056
3054	3’ rev SOE SacI rDNA	CCCACAAAATCAAGAAAGA ACTCTCAATCT	rDNA	SOE primer eliminating the SacI site in the yeast rDNA with #3055
3055	5’ for SacI rDNA	TTCGAGCTCGAGTAGGCTTG TCGTTCGTT	rDNA	outer primer for rDNA SOE PCR introducing a SacI site with #3054
3056	3’ rev BamHI rDNA	TCTGGATCCCACCATATCTT CATAACCTG	rDNA	outer primer for rDNA SOE PCR introducing a BamHI site with #3053
3057	3' EMSA rev Cy5	CTGGCACGACAGGTTTCCC		universal reverse primer for amplification of all IVT constructs together with 5' EMSA for labeled with Cy5
3094	3' rev XhoI REB1	GCACTCGAGTTAATTTTCTG TTTTCATTG	REB1	introduction of Xho1 site 3' of REB1 ORF
3095	pGEX 3'	CCGGGAGCTGCATGTGTCA GAGG		sequencing
3096	3' rev NotI YDR026c	ATATGCGGCCGCTTAATTGA TTTGTTCCAACA	YDR026c	introduction of Not1 site 3' of YDR026c ORF
3097	3' rev NotI HMO1	ATATGCGGCCGCTCAAATAG AAGAGTTGGATT	HMO1	introduction of Not1 site 3' of HMO1 ORF
3098	3' rev NotI REB1	ATATGCGGCCGCTTAATTTT CTGTTTTCATTG	REB1	introduction of Not1 site 3' of REB1 ORF
3099	3' rev NotI PAF1	ATATGCGGCCGCCTATTCTT CTTGTAAAGTTT	PAF1	introduction of Not1 site 3' of PAF1 ORF
3100	3' rev NotI FOB1	ATATGCGGCCGCTTACAATT CCATTGATGTGC	FOB1	introduction of Not1 site 3' of FOB1 ORF
3101	3' rev NotI mTTF1	ATATGCGGCCGCTCACTGCA CATCAGAGGCGC	TTF1	introduction of Not1 site 3' of TTF1 ORF
3102	pGEX 5'	GGGCTGGCAAGCCACGTTT GGTG		sequencing
3103	5' for bluescr	CGCCTCCATCCAGTCTATTA		amplification of 758bp from bluescript for elongation of IVT templates
3104	3' rev bluescr	GCACTTTTCGGGGAAATGT		amplification of 758bp from

		G		bluescript for elongation of IVT templates
3105	3' rev blue seq	CAATGATGAGCACTTTTAAA		sequencing
3106	shift fragment 5' TER	ATAAATTTTATTTGTCTTAAGAATTCTATGATCCGGGTAAAAACATGTATTGTATATATC	rDNA	for EMSA / NanoTemper, together with shift fragment 3' TER
3107	shift fragment TTFI	CCATTTTTTCCCCCCCAACTTCGGAGGTCGACCAGTACTCCGGGCGACACTTTGT	rDNA	EMSA and Nanotemper studies, anneal with reverse complement
3108	shift fragment TTFI rc	ACAAAGTGTCGCCCGGAGTACTGGTCGACCTCCGAAGTTGGGGGGGAAAAAATGG	rDNA	EMSA and Nanotemper studies, anneal with reverse complement, 5' Cy5
3109	shift fragment TER	ATAAATTTTATTTGTCTTAAGAATTCTATGATCCGGGTAAAAACATGTATTGTATATATC	rDNA	EMSA and Nanotemper studies, anneal with reverse complement
3110	shift fragment TER rc	GATATATACAATACATGTTTTTACCCGGATCATAGAATTCTTAAGACAAATAAAATTTAT	rDNA	EMSA and Nanotemper studies, anneal with reverse complement, 5' Cy5
3111	shift fragment w/o BS	CCAATTCAACACAAGGGTGAAAAGAGTTTGGAAACGAATTAGCTTGGCGTAATCA		EMSA and Nanotemper studies, anneal with reverse complement
3112	shift fragment w/o BS rc	TGATTACGCCAAGCTAATTCGTTTCCAAACTCTTTTCACCCTTGTGTTGAATTGG		EMSA and Nanotemper studies, anneal with reverse complement, 5' Cy3
3113	shift fragment ENH	AAAAGAGTTTGGAAACGAATTCTATGATCCGGGTAAAAACATGTATTGTATATATC	rDNA	EMSA and Nanotemper studies, anneal with reverse complement
3114	shift fragment ENH rc	GATATATACAATACATGTTTTTACCCGGATCATAGAATTCGTTTCCAAACTCTTTT	rDNA	EMSA and Nanotemper studies, anneal with reverse complement, 5' Cy5
3115	LexA shift fragment	AACGAATTCCATGGTGCTGTATATAAAACCAGTGGTTATATGTACAGTAG		EMSA and Nanotemper studies, anneal with reverse complement
3116	LexA shift fragment rc	CTACTGTACATATAACCACTGGTTTTATATACAGCACCAT		EMSA and Nanotemper studies, anneal with reverse complement,

		GGAATTCGTT		5' Cy5
3117	5' for g-less	ATACCAAACCAATTCAACACAAGGG		sequencing
3118	tail complement FAM	UGCAUUUCACCUUACCCUAUACUUACUCG		5' FAM labeled RNA for hybridisation to a tailed template according to P.Cramer as a primer RNA
3119	TspRI linker up	GACCGGCACTGGGTTTACGC		introducing a TspRI site via blunt end cloning, 5' phosphorylated with #3120
3120	TspRI linker down	GCGTAAACCCAGTGCCGGTC		introducing a TspRI site via blunt end cloning, 5' phosphorylated, rc with #3119
3121	NDS59	ACTTACAGCCATCGAGAGGGACACGGCGAAAAGCCAACCCAAGCGACACCGGCACTGGG		non template strand for Studitsky IVT templates, 5' biotinylated
3122	TDS50	GGTGTCGCTTGGGTTGGCTTTTCGGGCTGTCCCTCTCGATGGCTGTAAGT		template strand for Studitsky IVT templates
3123	RNA9	AUCGAGAGGG		primer RNA for Studitsky IVT templates
3476	TER 3'	GATATATACAATACATGTTTTTACCCGGATCATAGAATTCTTAAGACAAATAAAATTTAT	rDNA	for EMSA / NanoTemper, together with TER 5' shift fragment
3477	ENH 3'	GATATATACAATACATGTTTTTACCCGGATCATAGAATTCGTTTCCAAACTCTTTT	rDNA	for EMSA / NanoTemper, together with ENH 5' shift fragment
3478	RFB3 up Cy5	CATGCAAGCTTAAGAGAAGGGCTTTCACAAAGGGATCCGAGTCGG	rDNA	for EMSA/ NanoTemper, RFB3 site, for annealing
3479	RFB3 up	CATGCAAGCTTAAGAGAAGGGCTTTCACAAAGGGATCCGAGTCGG	rDNA	for EMSA/ NanoTemper, RFB3 site, for annealing
3480	RFB3 down	CCGACTCGGATCCCTTTGTG	rDNA	for EMSA/ NanoTemper, RFB3

		AAAGCCCTTCTCTTAAGCTTGCATG		site, for annealing
3481	RFB1 up Cy5	CATGCAAGCTTATGAGTGCTTGTATAAGTTTGGATCCGAGTCGG	rDNA	for EMSA/ NanoTemper, RFB1 site, for annealing
3482	RFB1 up	CATGCAAGCTTATGAGTGCTTGTATAAGTTTGGATCCGAGTCGG	rDNA	for EMSA/ NanoTemper, RFB1 site, for annealing with #3483
3483	RFB1 down	CCGACTCGGATCCAAACTTATACAAGCACTCATAAGCTTGCATG	rDNA	for EMSA/ NanoTemper, RFB1site, for annealing with #3482
3484	5' forRFB compl Cy5	CGTTGCAAAGATGGGTTGAAAGAGAAGGGC	rDNA	primer for amplification of the RFB, 5’ Cy5 labeled
3485	5' for RFB compl	CGTTGCAAAGATGGGTTGAAAGAGAAGGGC	rDNA	primer for amplification of the RFB
3486	5' for TER SacI Cy5	GAGGGAGCTCTCTCTATAAATTTTATTTGT	rDNA	primer for amplification of the rDNA terminator, 5’ Cy5 labeled
3792	5‘ for AflII Rebinv	ATTTGTCTTAAGAATTCTATGAATTTTTACCCGGCATGTATTGTATATATCTATTATAATATAC	rDNA	PCR primer for introduction of an inverted Reb1 BS in pUC19 tail g-TER elong with 2105
3793	5‘ for AflII noReb	ATTTGTCTTAAGAATTCTATGATCATGTATTGTATATATCTATTAT	rDNA	PCR primer for deletionof the Reb1 BS in pUC19 tail g- TER elong with 2105
3794	5‘ for AflII LexA	ATTTGTCTTAAGCATGGTGCTGTATATAAA		PCR primer for exchange of the Reb1 BS in pUC19tailg- TER elong with a LexA BS together with #3795
3795	3‘ rev BamHI LexA new	GATCGGATCCAACGTACTACTGTACATATAACCACTG		PCR primer for exchange of the Reb1 BS in pUC19tailg- TER elong with a LexA BS together with #3794
3796	5‘ for pUC19 compl	TGAGGATGATAGTGTGTAAGAGTGTACC		PCR primer for amplification of pUC19 tail g- TER elong and introduction of a PsiI site in the

				Abf1 binding site via introduction of a point mutation with #3797
3797	3‘ rev pUC19 compl	TCGTATATTATAATAGATATATACAATACATGTTTTTAC		PCR primer for amplification of pUC19 tail g- TER elong and introduction of a PsiI site in the Abf1 binding site via introduction of a point mutation with #3796
3798	5‘ for elong EcoRI	GATCGGAATTCCTTGTCTCAAAGATTAAGCCATG		PCR primer for amplification of the PCR product obtained with #2479 and #2480 with introduction of a KpnI and EcoRI site for cloning into pUC19 tail g-601 together with # 3799
3799	3‘ rev elong KpnI	GATCTGGTACCCCACAGTTATACCATGTAGTAAAGGAAC		PCR primer for amplification of the PCR product obtained with #2479 and #2480 with introduction of a KpnI and EcoRI site for cloning into pUC19 tail g-601 together with # 3798
3800	3‘ rev EMSA biotin	CTGGCACGACAGGTTTCCC		PCR primer for amplification with #2608 biotinylated
3801	3‘ rev M13 FAM	AACAGCTATGACCATG		PCR primer M13 rev FAM label

Table 3-10: Oligonucleotides.

C) *Plasmids*

#	name	description	cloning	function	origin
1	pBluescript KS(+/-)	T3 und T7 Promoter M13-20, T7, und SK Primer		cloning	Stratagene
44	pYM 9	module for TEV-ProA-7His-tag kanMX6		yeast tagging	(Knop et al. 1999)
45	pYM 10	module for TEV-ProA-		yeast	(Knop et

		7His-tag HISMX6		tagging	al. 1999)
190	pNOY373	rDNA mit Promoter, Start bei -206 mit XhoI-NotI flanked enhancer			(Wai et al. 2000)
375	pT11	Constuct for propagation approach in delta rdn yeast strains. L/RS/rDNA/lexA/RS/L/R (RS: recombination side, lexA: lexA binding side)			Griesenbeck, Joachim
1245	pRS316 SIRT G-less	SIRT fragment and G-less cassette	unknown, beware of sequence mistakes!!!!	in vitro transcription template	Philipp Merkl/ Max Felle/ Axel Berger
1247	pUC19 PIP G- 601	contains Pol I promoter dependent 601 template for in vitro transcription	EcoRI/EcoRV digested amplicon from pRS316 SIRT G-less with 2107/2108 into KasI, blunted/EcoRI digested pUC19 601	in vitro transcription template	Philipp Merkl
1248	pUC19 PIP G- 3xLexA	contains Pol I promoter dependent 3xLexA template for in vitro transcription	EcoRI/HindIII digested amplicon from pT11 with 2109/2110 into same digested pUC19 PIP G-601	in vitro transcription template	Philipp Merkl
1249	pUC19 PIP G- 5xTTF1	contains Pol I promoter dependent 5xTTF1 template for in vitro transcription	EcoRI/HindIII digested amplicon from pMrEnIL9T5 with 2111/2112 into same digested pUC19 PIP G-601	in vitro transcription template	Philipp Merkl
1250	pUC19 PIP G- 5xTTF1 inv	contains Pol I promoter dependent 5xTTF1 inv template	EcoRI/HindIII digested amplicon from pMrEnIL9T5 with 2113/2114 into same	in vitro transcription	Philipp Merkl

		for in vitro transcription	digested pUC19 PIP G-601	template	
1251	pUC19 PIP G- Enh	contains Pol I promoter dependent Enh template for in vitro transcription	EcoRI/BamHI digested amplicon from pRS316 SIRT G-less with 2105/2106 into same digested pUC19 PIP G-601	in vitro transcription template	Philipp Merkl
1252	pUC19 PIP G- 12x601	contains Pol I promoter dependent 12x601 template for in vitro transcription	EcoRI/HindIII digested fragment from pUC18 12x601 into same digested pUC19 PIP G-601	in vitro transcription template	Philipp Merkl
1253	pUC19 tail G- 601	contains tailed template 601 for in vitro transcription	KasI/EcoRI digested amplicon from pRS316 SIRT G-less with 2115/2107 into same digested pUC19 601	in vitro transcription template	Philipp Merkl
1254	pUC19 tail G- 3xLexA	contains tailed template 3xLexA for in vitro transcription	EcoRI/HindIII digested amplicon from pT11 with 2109/2110 into same digested pUC19 tail G-601	in vitro transcription template	Philipp Merkl
1255	pUC19 tail G- 5xTTF1	contains tailed template 5xTTF1 for in vitro transcription	EcoRI/HindIII digested amplicon from pMrEnIL9T5 with 2111/2112 into same digested pUC19 tail G-601	in vitro transcription template	Philipp Merkl
1256	pUC19 tail G- 5xTTF1 inv	contains tailed template 5xTTF1 inv for in vitro transcription	EcoRI/HindIII digested amplicon from pMrEnIL9T5 with 2113/2114 into same digested pUC19 tail G-601	in vitro transcription template	Philipp Merkl
1257	pUC19 tail G- Enh	contains tailed template Enh for in vitro transcription	EcoRI/BamHI digested amplicon from pRS316 SIRT G-less with 2105/2106 into same digested pUC19 tail G-601	in vitro transcription template	Philipp Merkl
1258	pUC19 tail G- 12x601	contains tailed template 12x601 for in vitro transcription	EcoRI/HindIII digested fragment from pUC18 12x601 into same digested pUC19 PIP G-601	in vitro transcription template	Philipp Merkl
1275	pET21a	vector for expression	AvaI/BamHI insertion of REB1	Expressio	Philipp

	REB1	of Reb1p with a C terminal His tag	ORF amplified from genomic yeast DNA	n of Reb1p with a C terminal His tag	Merkl
1561	pUC19 tail g- 1xLacR	contains tailed template with 1 Lac repressor binding site for in vitro transcription	EcoRI/ HindIII fragment of annealed oligos 2625/2626 into EcoRI/ HindIII cut pUC19 tail g- 3xLexA	in vitro transcription	Philipp Merkl
1562	pUC19 PIP g- 1xLacR	contains Pol I promoter template with 1 Lac repressor binding site for in vitro transcription	EcoRI/ HindIII fragment of annealed oligos 2625/2626 into EcoRI/ HindIII cut pUC19 PIP g- 3xLexA	in vitro transcription	Philipp Merkl
1563	pUC19 tail g- 2xLacR	contains tailed template with 2 Lac repressor binding sites for in vitro transcription	EcoRI/ BamHI fragment of annealed 2xLacR up and down oligos (Alarich) into EcoRI/ BamHI cut pUC19 tail g- Enh	in vitro transcription	Philipp Merkl
1564	pUC19 PIP g- 2xLacR	contains Pol I promoter template with 2 Lac repressor binding sites for in vitro transcription	EcoRI/ BamHI fragment of annealed 2xLacR up and down oligos (Alarich) into EcoRI/ BamHI cut pUC19 PIP g- Enh	in vitro transcription	Philipp Merkl
1565	pFL FLAG TEV REB1	Acceptor vector for Multibac system with REB1 ORF	ORF from yeast genomic DNA with primers 2596/2602, restricted with BamHI/ SacI into BamHI/SacI cut pFL FLAG TEV	SF21 expression	Philipp Merkl
1566	pFL FLAG TEV PAF1	Acceptor vector for Multibac system with PAF1 ORF	ORF from yeast genomic DNA with primers 2595/2601, restricted with BamHI/ SacI into BamHI/SacI cut pFL FLAG TEV	SF21 expression	Philipp Merkl

1567	pFL FLAG TEV HMO1	Acceptor vector for Multibac system with HMO1 ORF	ORF from yeast genomic DNA with primers 2593/2599, restricted with BamHI/ SacI into BamHI/SacI cut pFL FLAG TEV	SF21 expression	Philipp Merkl
1568	pFL FLAG TEV FOB1	Acceptor vector for Multibac system with FOB1 ORF	ORF from yeast genomic DNA with primers 2592/2598, restricted with BamHI/ SacI into BamHI/SacI cut pFL FLAG TEV	SF21 expression	Philipp Merkl
1569	pFL FLAG TEV YDR026c	Acceptor vector for Multibac system with YDR026c ORF	ORF from yeast genomic DNA with primers 2604/2605, restricted with BamHI/ SacI into BamHI/SacI cut pFL FLAG TEV	SF21 expression	Philipp Merkl
1570	pFL FLAG TEV mTTF1	Acceptor vector for Multibac system with mTTF1 ORF	ORF from yeast genomic DNA with primers 2594/2600, restricted with BamHI/ SacI into BamHI/SacI cut pFL FLAG TEV	SF21 expression	Philipp Merkl
1571	pUC19 tail g- Enh 2xLacR	contains tailed template with 2 Lac repressor binding sites after the rDNA Enhancer for in vitro transcription	BamHI/ PstI fragment of annealed oligos 2619/2620 into BamHI / PstI cut pUC19 tail g- Enh	in vitro transcription	Philipp Merkl
1572	pUC19 tail g- LacO	contains tailed template with the Lac Operator for in vitro transcription	EcoRI/ HindIII fragment of annealed oligos 2623/2624 into EcoRI/ Hind III cut pUC19 tail g- 3x LexA	in vitro transcription	Philipp Merkl
1573	pUC19 tail g-	contains tailed template without any binding sites for in vitro transcription	EcoRI /Hind III cut pUC19 tail g- 3xLexA blunted and re-ligated	in vitro transcription	Philipp Merkl
1574	pUC19 tail	contains tailed	EcoRI/ HindIII fragment of	in vitro	Philipp

	g- tRNA Ala	template with the yeast alanine tRNA for in vitro transcription	annealed oligos 2612/2613 into EcoRI/ Hind III cut pUC19 tail g- 3x LexA	transcription	Merkl
1575	pGST 4T1 LACI	expression of LacI as an N terminal GST fusion	ORF from pGST 4T1 with primers 2614/2616 restricted with BamHI /NotI into BamHI/ NotI cut pGST 4T1	E. coli expression	Philipp Merkl
1576	pGST LEXA	expression of LexA as an N terminal GST fusion		E. coli expression	Griesenbeck, Joachim
1959	pUC19 PIP g- w/o BS	contains Pol I promoter template with no protein binding site for in vitro transcription	cut #1248 with EcoRI/HindIII, blunt, re-ligate	in vitro txn	Philipp Merkl
1960	pUC19 tail g- TER	contains tailed template with rDNA terminator including T1 T-rich element for in vitro transcription	SacI/BamHI cut terminator region amplified with primers #3050/3051 was cloned into SacI/BamHI cut vector #1253	in vitro txn	Philipp Merkl
1961	pUC19 PIP g- TER	contains Pol I promoter template with rDNA terminator including T1 T-rich element for in vitro transcription	SacI/BamHI cut terminator region amplified with primers #3050/3051 was cloned into SacI/BamHI cut vector #1247	in vitro txn	Philipp Merkl
1962	pUC19 tail g- Rnt TER	contains tailed template with rDNA terminator including T1 T-rich element and Rnt1 cleavage site for in vitro transcription	SacI/BamHI cut terminator region amplified with primers #3052/3051 was cloned into SacI/BamHI cut vector #1253	in vitro txn	Philipp Merkl
1963	pUC19 PIP g- Rnt TER	contains Pol I promoter template with rDNA terminator	SacI/BamHI cut terminator region amplified with primers #3052/3051 was cloned into	in vitro txn	Philipp Merkl

		including T1 T-rich element and Rnt1 cleavage site for in vitro transcription	SacI/BamHI cut vector #1247		
1964	pUC19 tail g- rDNA BamHI SacI frag	contains tailed template with the BamHI SacI fragment of the rDNA, for further cloning	SacI/BamHI rDNA fragment from pNOY373 was inserted into SacI/BamHI cut vector #1253	in vitro txn	Philipp Merkl
1965	pUC19 PIP g- rDNA BamHI SacI frag	contains Pol I promoter template with the BamHI SacI fragment of the rDNA, for further cloning	SacI/BamHI rDNA fragment from pNOY373 was inserted into SacI/BamHI cut vector #1247	in vitro txn	Philipp Merkl
1966	pUC19 tail g- rDNA	contains tailed template with complete rDNA for in vitro transcription	pUC19 tail g- rDNA BamHI/SacI frag was cut with SacI, blunted and the blunted PCR amplicon from pNOY373 with primers #3055/3056 was inserted	in vitro txn	Philipp Merkl
1967	pUC19 PIP g- rDNA	contains Pol I promoter template with complete rDNA for in vitro transcription	pUC19 PIP g- rDNA BamHI/SacI frag was cut with SacI, blunted and the blunted PCR amplicon from pNOY373 with primers #3055/3056 was inserted	in vitro txn	Philipp Merkl
1968	pUC19 tail g- TspRI TER	contains 3' part of a Studitsky in vitro txn template with the rDNA terminator including the T1 T-rich element	blunt end ligation of a linker created via annealing of two oligos containing a TspRI restriction site into SacI cut pUC19 tail g- TER	in vitro txn	Philipp Merkl
1969	pUC19 tail g- TspRI 5xTTF1	contains 3' part of a Studitsky in vitro txn template with 5 TTF1	blunt end ligation of a linker created via annealing of two oligos containing a TspRI	in vitro txn	Philipp Merkl

		binding sites	restriction site into EcoRI cut #1255		
1970	pUC19 tail g- TspRI w/o BS	contains 3' part of a Studitsky in vitro txn template without binding sites	blunt end ligation of a linker created via annealing of two oligos containing a TspRI restriction site into EcoRV cut #1573	in vitro txn	Philipp Merkl
1971	pUC19 PIP g- TspRI 601	contains 3' part of a Studitsky in vitro txn template with one 601 sequence	blunt end ligation of a linker created via annealing of two oligos containing a TspRI restriction site into EcoRI cut #1247	in vitro txn	Philipp Merkl
1972	pUC19 tail g- TspRI 3xLexA	contains 3' part of a Studitsky in vitro txn template with 3 LexA binding sites	blunt end ligation of a linker created via annealing of two oligos containing a TspRI restriction site into EcoRI cut #1254	in vitro txn	Philipp Merkl
1973	pGEX 4T1 PAF1	Expression of Paf1 as a GST fusion protein	ORF from yeast genomic DNA amplified with primers introducing a 5' BamHI and 3' NotI site into BamHI NotI cut pGEX 4T1	protein expressio n	Philipp Merkl
1974	pGEX 4T1 HMO1	Expression of Hmo1 as a GST fusion protein	ORF from yeast genomic DNA amplified with primers introducing a 5' BamHI and 3' NotI site into BamHI NotI cut pGEX 4T1	protein expressio n	Philipp Merkl
1975	pGEX 4T1 FOB1	Expression of Fob1 as a GST fusion protein	ORF from yeast genomic DNA amplified with primers introducing a 5' BamHI and 3' NotI site into BamHI NotI cut pGEX 4T1	protein expressio n	Philipp Merkl
1976	pGEX 4T1 Ydr026c	Expression of Ydr026c as a GST fusion protein	ORF from yeast genomic DNA amplified with primers introducing a 5' BamHI and 3'	protein expressio n	Philipp Merkl

			NotI site into BamHI NotI cut pGEX 4T1		
2144	pUC 19 tail g- ENH elongated	a sequence 5' of the ENH was inserted to give a longer transcription product /better detection	amplicon of primers #2479 and #2480 from pT11 phosphorylated and cloned into EcoRI cut #1257	in vitro txn	Philipp Merkl
2145	pUC 19 tail g- TER elongated	a sequence 5' of the ENH was inserted to give a longer transcription product /better detection	amplicon of primers #2479 and #2480 from pT11 phosphorylated and cloned into SacI cut #1960	in vitro txn	Philipp Merkl
2146	pUC 19 tail g- Rnt TER elongated	a sequence 5' of the ENH was inserted to give a longer transcription product /better detection	amplicon of primers #2479 and #2480 from pT11 phosphorylated and cloned into SacI cut #1962	in vitro txn	Philipp Merkl
2147	pUC 19 PIP g- ENH elongated	a sequence 5' of the ENH was inserted to give a longer transcription product /better detection	amplicon of primers #2479 and #2480 from pT11 phosphorylated and cloned into EcoRI cut #1251	in vitro txn	Philipp Merkl
2148	pUC 19 PIP g- TER elongated	a sequence 5' of the ENH was inserted to give a longer transcription product /better detection	amplicon of primers #2479 and #2480 from pT11 phosphorylated and cloned into SacI cut #1961	in vitro txn	Philipp Merkl
2149	pUC 19 PIP g- Rnt TER elongated	a sequence 5' of the ENH was inserted to give a longer transcription product /better detection	amplicon of primers #2479 and #2480 from pT11 phosphorylated and cloned into SacI cut #1963	in vitro txn	Philipp Merkl
2150	pET21a Ydr026c	C terminal His tagging of Ydr026c	BamHI / AvaI fragment of amplicon of primers #2604 and #3096 from a PCR product	expressio n	Philipp Merkl

			with primers 2604# and #2605 from yeast genomic DNA (NOY505) cloned into pET21a		
2244	pUC19 tail G- 3xLexA elong	contains tailed template 3xLexA for in vitro transcription, insertion of 124bp 5‘ of the first LexA BS	amplicon from pT11 with #2479 and #2480 in EcoRI cut and blunted #1254	in vitro transcription template	Philipp Merkl
2245	pUC 19 tail g- TER Reb1 inv elongated	contains tailed template with rDNA terminator including T1 T-rich element for in vitro transcription, Reb1 BS is inverted	AflII/BamHI digested amplicon of primers #3792 and #2105 in likewise digested #2145	in vitro txn	Philipp Merkl
2246	pUC 19 tail g- TER noReb1 BS elongated	contains tailed template with rDNA terminator including T1 T-rich element for in vitro transcription, Reb1 BS is deleted	AflII/BamHI digested amplicon of primers #3793 and #2105 in likewise digested #2145	in vitro txn	Philipp Merkl
2247	pUC 19 tail g- TER PsiI elongated	contains tailed template with rDNA terminator including T1 T-rich element for in vitro transcription, introduction of a PsiI site in the Abf1 BS via a point mutation	amplicon of primers #3796 and #3797 was re-ligated, template #2145	in vitro txn	Philipp Merkl
2248	pUC 19 tail g- ENH PsiI elongated	contains tailed template with rDNA terminator including T1 T-rich element for in vitro transcription, introduction of a PsiI site in the Abf1 BS via	amplicon of primers #3796 and #3797 was re-ligated, template #2144	in vitro txn	Philipp Merkl

		a point mutation			
2249	pUC19 tail g- 601 elong	contains tailed template 601 for in vitro transcription, insertion of 124bp 5‘ of the 601 sequence	EcoRI and KpnI digested PCR product obtained with primers #3798 and #3799 (template pT11) was ligated into vector #1253 cut with EcoRI and KpnI	in vitro transcription template	Philipp Merkl

Table 3-11: Plasmids.

D) *DNA and RNA size markers*

1kb ladder: NEB

fragment size [bp]: 10002, 8001, 6001, 5001, 4001, 3001, 2000, 1500, 1000, 517, 500

100bp ladder: NEB

fragment size [bp]: 1517, 1200, 1000, 900, 800, 700, 600, 517, 500, 400, 300, 200, 100

GeneRuler™ 1kb Plus DNA ladder: Fermentas

fragment size [bp]: 75, 200, 300, 400, 500, 700, 1000, 1500, 2000, 3000, 4000, 5000, 7000, 10000, 20000

Century™ Plus RNA marker templates: Ambion

Transcribed *in vitro* with T7 RNA polymerase (3.2.11 E), transcript sizes [nt]: 100, 200, 300, 400, 500, 750, 1000

All marker solutions were prepared according to the standard operating protocols of the manufacturers.

3.1.5 Enzymes and polypeptides

All enzymes were used with the provided buffers.

enzyme	supplier
Calf Intestinal Phosphatase	New England Biolabs
GoTaq DNA Polymerase	Promega
Herculase II Fusion DNA Polymerase	Stratagene
iProof High-Fidelity DNA Polymerase	Bio Rad
M-MLV Reverse Transcriptase	Invitrogen
Proteinase K	Sigma Aldrich
Restriction endonucleases	New England Biolabs
RNase A	Invitrogen
RNase H	Roche
T4 DNA Ligase	New England Biolabs
T4 DNA Polymerase	New England Biolabs
T4 Polynucleotide Kinase	New England Biolabs
T7 RNA Polymerase	New England Biolabs
Tobacco Etch Virus Protease (TEV)	in-lab-prepared
Trypsin Sequencing Grade	Roche
PreScission Protease	GE Healthcare
Thrombin	Sigma Aldrich
RNasin® Plus RNase inhibitor	Promega
Proteinase K (from Tritiarchium album)	Sigma

Table 3-12: Enzymes and polypeptides.

3.1.6 Antibodies

#	antibody	species	dilution	origin
10	anti A49	rabbit	1:50000	
12	anti A43	rabbit	1:10000	
13	anti A135	rabbit	1:30000	(Buhler et al. 1980)
32	anti A190	rabbit	1:5000	
33	anti Reb1	rabbit	1:5000	
50	anti Pol III	rabbit	1:5000	
59/1	anti TFG1	rabbit	1:5000	Stefan Bjorklund

59/2	anti TFG3	rabbit	1:5000	Stefan Bjorklund
75	anti HA (3F10)	rat	1:5000	Roche
77	anti Pol II complete (8WG16)	mouse	1:2000	HISS
78	anti Rabbit IgG (H+L) [peroxidase conjugated]	goat	1:5000	Dianova
79	anti mouse IgG (H+L) [peroxidase conjugated]	goat	1:5000	Dianova
81	anti rat IgG (H+L) [peroxidase conjugate]	goat	1:5000	Dianova
83	anti FLAG M2	mouse	1:5000	Sigma Aldrich
98	anti GST	rabbit	1:5000	Santa Cruz
102	anti CBP	goat	1:5000	
104	anti goat IgG (H+L) [peroxidase conjugated]	donkey	1:5000	Dianova
105	anti Protein A (PAP)	goat	1:5000	Sigma Aldrich
110	anti A12.2	rabbit	1:5000	Christophe Carles

Table 3-13: Antibodies.

3.1.7 Organisms

A) *Escherichia coli strains*

strain	genotype
Escherichia coli (E. coli) XL1 blue	*endA1 gyrA96(nal^R) thi-1 recA1 relA1 lac glnV44* F'*[::Tn10 proAB$^+$ lacI^q Δ(lacZ)M15] hsdR17(r_K^- m_K^+)*
E. coli BL21 (DE3)	F$^-$ *ompT gal dcm lon hsdS$_B$(r_B^- m_B^-) λ(DE3 [lacI lacUV5-T7 gene 1 ind1 sam7 nin5])*
E. coli K12 TB1	F$^-$ *ara Δ(lac-proAB) [Φ80dlac Δ(lacZ)M15] rpsL*(Str^R) *thi hsdR*
E.coli DH10Bac eYFP	pMON7124 (*bom+, tra-, mob-*), bMON14272 – *eYFP*, F– *mcrA (mrr-hsdRMS-mcrBC) 80lacZΔ M15 lacX74 recA1 endA1 araD139 (ara, leu)7697 galU galK – rpsL nupG*

E. coli DH5α	F– Φ80*lac*ZΔM15 Δ(*lac*ZYA-*arg*F) U169 *rec*A1 *end*A1 *hsd*R17 (rK–, mK+) *pho*A *sup*E44 λ– *thi*-1 *gyr*A96 *rel*A1

Table 3-14: *E. coli* strains.

B) *Saccharomyces cerevisiae strains*

#	name	genotype	origin
-	NOY222 RPA135-ProtA A190 SallA	MATα trp1-1 his4-401 leu2-3,112 ura3-52 can r rpa190::URA3 RPA135-ProtA::kanMX6 pRS314 rpa190 SallA	Jorge Perez-Fernandez
-	NOY222 RPA135-ProtA A190 SallD	MATα trp1-1 his4-401 leu2-3,112 ura3-52 can r rpa190::URA3 RPA135-ProtA::kanMX6 pRS314 rpa190 SallD	Jorge Perez-Fernandez
-	NOY222 RPA135-ProtA A190 S936A	MATα trp1-1 his4-401 leu2-3,112 ura3-52 can r rpa190::URA3 RPA135-ProtA::kanMX6 pRS314 rpa190 S936A	Jorge Perez-Fernandez
-	NOY222 RPA135-ProtA A190 S936D	MATα trp1-1 his4-401 leu2-3,112 ura3-52 can r rpa190::URA3 RPA135-ProtA::kanMX6 pRS314 rpa190 S936D	Jorge Perez-Fernandez
-	NOY222 RPA135-ProtA A190 S941A	MATα trp1-1 his4-401 leu2-3,112 ura3-52 can r rpa190::URA3 RPA135-ProtA::kanMX6 pRS314 rpa190 S941A	Jorge Perez-Fernandez
-	NOY222 RPA135-ProtA A190 S941D	MATα trp1-1 his4-401 leu2-3,112 ura3-52 can r rpa190::URA3 RPA135-ProtA::kanMX6 pRS314 rpa190 S941D	Jorge Perez-Fernandez
206	BY4741	MATa, his3-1 leu2-0 met15-0 ura3-0	Euroscarf (Brachmann et al. 1998)
207	BY4742	MATα, his3-1 leu2-0 met15-0 ura3-0	Euroscarf (Brachmann et al. 1998)
531	NOY222 RPA135-ProtA	MATα trp1-1 his4-401 leu2-3,112 ura3-52 can r rpa190::URA3 RPA135-ProtA::kanMX6	Jochen Gerber
601	Y06861 (BY4741 ΔA12)	MATa, his3-1 leu2-0 met15-0 ura3-0	Alarich Reiter

		YJR063w::kanMX4	
779	NOY222 A190 S685A	MATα trp1-1 his4-401 leu2-3,112 ura3-52 can r rpa190::URA3 pRS314-rpa190-p5	Jochen Gerber
780	NOY222 A190 S685D	MATα trp1-1 his4-401 leu2-3,112 ura3-52 can r rpa190::URA3 pRS314-rpa190-p6	Jochen Gerber
2018	NOY505 Fob1-TAP (ySH38)	MATa ade2-1 ura3-1 trp1-1 leu2-3,112 his3-11 can1-100 Fob1-TAP-kanMX6 PHO5 RDN	Stephan Hamperl
2423	BY4741 A135-TEV-ProtA	MATa, his3-1 leu2-0 met15-0 ura3-0 rpa135::RPA135-TEV-ProtA-kanMX6	Jochen Gerber
2424	BY4741 Rpb2-TEV-ProtA	MATa, his3-1 leu2-0 met15-0 ura3-0 rpb2::RPB2-TEV-ProtA-kanMX6	Jochen Gerber
2425	BY4741 C128-TEV-ProtA	MATa, his3-1 leu2-0 met15-0 ura3-0 c128::C128-TEV-ProtA-kanMX6	Jochen Gerber
2559	BY4741 Spt16-TAP	MATa leu2-0 met15-0 ura3-0 YGL207w-TAP HIS3MX6	Open Biosystems
2560	BY4741 pob3-TAP	MATa leu2-0 met15-0 ura3-0 YML069w-TAP HIS3MX6	Open Biosystems
2670	yJPF162-1a	MATα, his3-1 leu2-0 lys2 ura3-0 RPA135-TEV-ProtA::kanMX6 HIS3MX::GAL::HA-RPA49	Jorge Pérez-Fernández
2994	DSY5 Int3	MATα leu2 trp1 ura3-52 his3::PGAL1-GAL4 pep4 prb1-1122 YGR186W (leu2) YGR005C-TAP (trp1) YPL129W (ura3)	(Chen et al. 2010)
3051	BY4741 A135 His_7 ProtA His_7	MATa, his3-1 leu2-0 met15-0 ura3-0 rpa135::RPA135-His_7-ProtA-His_7 (his3)	this study
3052	BY4741 Rpb2 His_7 ProtA His_7	MATa, his3-1 leu2-0 met15-0 ura3-0 rpb2::RPB2-His_7-ProtA-His_7 (his3)	this study
3053	BY4741 C128 His_7 ProtA His_7	MATa, his3-1 leu2-0 met15-0 ura3-0 c128::C128-His_7-ProtA-His_7 (his3)	this study

Table 3-15: Yeast strains.

C) *SF21 insect cells*

The SF21 cell line is developed from primary explants of pupal tissue from the insect Spodoptera frugiperda (Vaughn et al., 1977). Cells were purchased from Invitrogen™.

3.1.8 Baculoviruses

#	expressed protein	MultiBac parent vector	origin
46	FLAG-TEV-Reb1	pFL-FLAG-TEV	this study
47	FLAG-TEV-Paf1	pFL-FLAG-TEV	this study
48	FLAG-TEV-Hmo1	pFL-FLAG-TEV	this study
49	FLAG-TEV-Fob1	pFL-FLAG-TEV	this study
50	FLAG-TEV-Ydr026c	pFL-FLAG-TEV	this study
51	FLAG-TEV-mTTF-I	pFL-FLAG-TEV	this study

Table 3-16: Baculoviruses.

3.1.9 Kits

name	manufacturer
peqGOLD Plasmid Miniprep kit	Peqlab
peqGOLD Gel Extraction kit	Peqlab
peqGOLD MicroSpin CyclePure kit	Peqlab
QIAprep Spin Miniprep kit	QIAGEN
QIAquick gel extraction kit	QIAGEN
QIAquick PCR purification kit	QIAGEN
QIAEX II Gel Extraction kit	QIAGEN
PureLink® HiPure Plasmid Filter Maxiprep Kit	Invitrogen™
PureLink® HiPure Plasmid Filter Midiprep Kit	Invitrogen™
iTRAQ™ labeling kit	Life Technologies™

Table 3-17: Kits.

3.1.10 Equipment

name	manufacturer
4800 Proteomics analyzer MALDI TOF/TOF	Applied Biosystems
-80°C Fridge Ultra Low	Sanyo
Avanti J-26 XP centrifuge	Beckman Coulter
AxioCam MR CCD camera	Carl Zeiss
Axiovert 200M microscope	Carl Zeiss
BAS cassette 2040	Fuji
BAS III imaging plate	Fuji
Bc-Mag Separator-24	Bioclone Inc.
Bc-Mag Separator-50	Bioclone Inc.
Biofuge Fresco refrigerated tabletop centrifuge	Heraeus
Biofuge Pico tabletop centrifuge	Heraeus
C412 centrifuge	Jouan
C422 r centrifuge	Jouan
Centrifuge 1-14	Sigma
Centrifuge 5-14	Sigma
Centrikon T-324 centrifuge	Kontron Instruments
Contamat FHT 111M	Thermo Scientific
ECPS 3000/150 Power supply	Pharmacia Biotech
Electrophoresis system model 45-2010-i	Peqlab
Eraser	Raytest
FlexCycler Thermocycler Twinblock 48x48	Analytic Jena
Fluorescent Image Analyzer FLA 3000	Fuji
Gel max UV transilluminator	Intas
Hemocytometer Neubauer II	Neubauer
HB-1000 Hybridization Oven	UVP
IKA-Vibrax VXR	IKA
Incubators	Memmert
Insect cell incubator	Binder
IX 50 microscope	Olympus
LAS 3000 chemiluminescence imager	Fuji

Microcentrifuge 5415 r	Eppendorf
Microcentrifuge MC6	Sarstedt
MicroPulser electroporation apparatus	Bio-Rad
Microwave	Privileg
NanoDrop ND-1000 spectrophotometer	Peqlab
PerfectBlot Hybridisation Oven	Peqlab
PIPETMAN® Classic P2, P10, P200, P1000	Gilson Inc.
Power Pac 3000 Power supplies	Bio-Rad
ProBot MALDI Target Spotter	Dionex / Thermo Scientific
Pumpdrive 5001	Heidolph
PURELAB Ultra	ELGA
QIAcube	QIAGEN
Shake incubators Multitron/Minitron	Infors
SMART system	Pharmacia Biotech
Sonifier 250	Branson
Speed Vac Concentrator	Savan
Sterile bench LaminAir HLB2472GS	Heraeus
Sub-Cell GT Agarose Gel Electrophoresis System	Bio-Rad
Superose 12 PC 3.2/30	GE Healthcare
Thermomixer® Dry block heating shaker	Eppendorf
Trans Blot SD semi-dry transfer cell	Bio-Rad
Ultimate 3000 nanoHPLC	Dionex
Unimax 2010 shaker	Heidolph
UV/Vis Spectrophotometer Ultraspec 3100pro	Amersham Biosciences
Vacufuge Plus Concentrator	Eppendorf
Vortex-Genie 2	Scientific Industries

Table 3-18: Equipment.

3.1.11 Consumables

name	supplier
Anti-FLAG M2 Affinity Resin	Sigma Aldrich

BcMag™ Epoxy-Activated Magnetic Beads	Bioclone Inc.
Bis-Tris Novex® NuPAGE® 4-12% gel	Invitrogen
Blotting Papers MN 827 B	
BM Chemiluminescence Blotting Substrate (POD)	Roche
Calmodulin Affinity Resin	Stratagene
Century™ RNA Plus marker templates	Ambion®
Color Plus Prestained Protein Marker Broad Range (7-175kDa)	New England Biolabs
Filter paper 3MM	Whatman
FLAG peptide	Sigma Aldrich
FuGene HD Transfection reagent	Promega
Gene Pulser cuvettes	Bio Rad
Glass beads (ø 0.75-1mm)	Roth
glycogen solution (5mg/ml)	Ambion®
Immobilon-P transfer membrane	Millipore
Multiwell plates (6 wells, 24 wells)	Sarstedt
Ni-NTA superflow Affinity Resin	QIAGEN
NuPAGE® MES buffer	Invitrogen
NuPAGE® MOPS buffer	Invitrogen
Protein Assay Dye Reagent Concentrate	Bio Rad
Rabbit IgG	Sigma Aldrich
SimplyBlue™ SafeStain	Invitrogen
SYBR Safe DNA Gel stain	Invitrogen

Table 3-19: Consumables.

3.1.12 Software

name	manufacturer
4000 Series Explorer	Applied Biosystems
Acrobat 7.0 Professional	Adobe Systems
Axio Vision Rel. 4.7	Carl Zeiss
Data Explorer v. 4.5C	Applied Biosystems

GPS Explorer v. 3.5	Applied Biosystems
Illustrator CS3	Adobe Systems
Image Reader FLA3000 v. 1.8	Fuji
Image Reader LAS3000 v2.2	Fuji
Mascot	Matrix Science
Microsoft Office 2007	Microsoft
MultiGauge v. 3.0	Fuji
ND1000 v. 3.5.2	Peqlab
Photoshop Elements 6.0	Adobe Systems
Sigma Plot	Systat
Vector NTI Advance™ 11	Invitrogen™

Table 3-20: Software.

3.2 Methods

3.2.1 Enzymatic DNA manipulation

A) Polymerase chain reaction (PCR)

A standard PCR reaction had a volume of 20-50µl. It contained the DNA to be amplified (1-10ng), 250µM desoxynucleotides, 20pmol of each the forward and the reverse primer, the buffer supplied with the polymerase in a final 1x concentration and the appropriate polymerase. If applicable, a mastermix was prepared from the components. PCR reactions were carried out in 0.2ml thin-wall PCR tubes. For cloning purposes, the Herculase system (Stratagene) was used, for colony PCR the GoTaq system (Promega) was applied. Herculase polymerase has proof-reading activity, Taq polymerase has not. PCR was performed in a semi-hotstart manner to reduce primer-polymerase interactions, mispriming due to secondary structure formation and formation of primer dimers. Thus, the tubes were placed in the PCR machine when the block had reached 95°C or 98°C and initial denaturation of the DNA was carried out for 3min. DNA amplification was done for 35 cycles. A standard PCR cycle starts with an initial denaturation step (95°C for 20s), followed by annealing of the primers to their complementary DNA sequence (5°C below the calculated primer T_M for 30s) and

the amplification step (72°C, 30s per kb for Herculase, 1min per kb for Taq polymerase). For primers with non-complementary 5' overhangs >10nt, the first three cycles were performed at an annealing temperature of the complementary part of the primer. A final elongation step (72°C for 3min) is added after 35 cycles. Upon completion of the PCR, the samples were slowly cooled down and stored at 4°C.

B) Sequence specific restriction digest

Restriction endonucleases hydrolyze DNA phosphodiester bonds at specific recognition sites. All restriction digests were performed in 20µl-100µl reactions at the temperatures and buffer conditions advised by NEB. The used restriction enzyme volume correlated with the amount of DNA but never exceeded 10% of the reaction volume due to glycerol in the enzyme storage buffer.

C) Introduction of single strand breaks

In the context of *in vitro* transcription with tailed templates (3.2.12), the introduction of single strand breaks in DNA is needed. For this purpose, the enzyme Nb.BsmI (NEB) was used. It has the same recognition sequence as BsmI (5'-NG'CATTC-3') but hydrolyzes only the DNA strand with the given sequence. The cutting site is indicated with an apostrophe. The reaction contains the template, NEB buffer 3 and the enzyme and is carried out at 65°C for 1.5h. Afterwards, Nb.BsmI is heat-inactivated at 80°C for 20min.

D) *Blunting of single strand DNA overhangs*

T4 DNA polymerase (NEB) was used to fill in 5' overhangs and to digest 3' overhangs after restriction digest. Thus, both DNA strands within a duplex have the same length afterwards (blunt ends). The reaction contains 100µM dNTPs, 1U T4 DNA polymerase per µg DNA and the template. It is directly carried out in the restriction digest buffer. Incubation conditions are 15min sharp at 12°C. Afterwards, the reaction is stopped by DNA purification with the PCR cleanup kit (3.1.9).

E) *Dephosphorylation at the 5' end*

After restriction digest, a terminal orthophosphate group remains at the 5' end of each DNA strand. To prevent re-ligation of matching ends of a DNA vector, treatment with calf intestinal phosphatase (CIP, NEB) is necessary. This is done by incubation of the restriction digest with 1µl of the enzyme at 37°C.

F) DNA Ligation

DNA fragments with matching or blunt ends can be ligated with T4 DNA ligase (NEB). A standard reaction was 10µl and contained 100ng of plasmid DNA and a 3- to 5-molar excess of insert DNA. It was carried out in the supplemented buffer containing ATP with 0.5µl DNA ligase. Reaction time varied from 1h at room temperature to overnight incubation at 16 °C. 1-2 µl were used for transformation of *E. coli.*

G) DNA sequencing

For DNA sequencing, samples were sent to GENEART (Life Technologies). The obtained sequences were compared to annotated database sequences with vector NTI (Invitrogen).

3.2.2 DNA purification and analysis

A) Plasmid DNA purification

Plasmid DNA was isolated from *E. coli* XL1 Blue overnight cultures with kits. The amount of purified plasmid DNA corresponds with culture size. "Minipreps" (2-5ml culture volume, yield of approximately 20µg of DNA) were done with a Peqlab "peqGold plasmid miniprep" kit), "Maxipreps" (150ml culture, 200µg of DNA) were prepared with an Invitrogen "PureLink® HiPure Plasmid Maxiprep" kit. In general, the manufacturer's protocol was always followed. In a first step, the pelleted cells are lysed in a buffer containing NaOH, SDS and RNase A. After 5min incubation at RT,

the mixture is neutralized with potassium acetate (KOAc), which results in precipitation of the proteins and the genomic DNA. The precipitate is removed from the solution by centrifugation. The plasmid DNA-containing supernatant is transferred onto an anion-exchange column (Maxiprep) or a silica-based column (Miniprep), to which the DNA binds at low salt conditions. Residual RNAs and proteins are washed away. Plasmid DNA is eluted under high salt conditions. Excess salt is removed by isopropanol or ethanol precipitation and the precipitated DNA dissolved in water, EB or TE buffer. Plasmid DNA is stored at -20°C.

B) Purification of genomic DNA from yeast

Cells from an overnight culture (100ml YPD, OD_{600} 0.6), were harvested by centrifugation (45ml, 4000rpm, 15min, 4°C). The cells were resuspended in 2.5ml buffer AE (3.1.3) and split into 5 samples. To each sample, 50µl 10% SDS and 500µl Phenol equilibrated in AE were added, the solution vortexed and incubated at 65°C for 7min in a thermoblock. The suspension was chilled on ice for 2min and centrifuged for 2min at 16000g and 4°C in a tabletop centrifuge. The RNA in the supernatant was sequentially extracted with 500µl Phenol/AE and 500µl chloroform and then subjected to EtOH precipitation. After each step, the solution was centrifuged for 2min at 16000g and 4°C. After precipitation, the pellet was dissolved in RNase free water and the RNA concentration was determined (3.2.2 G).

C) PCR purification

PCR products and DNA from restriction digests were purified with the “QIAquick PCR purification” kit (Qiagen) or the “peqGOLD cycle pure” kit (Peqlab). The manual of the manufacturer was always followed. The DNA above a certain exclusion size is bound to a silica-based column and proteins, salts, nucleotides and primers are washed away. The exclusion limit depends on the manufacturer and the reaction conditions. DNA is eluted in water or EB buffer.

D) DNA extraction from agarose gels

Purification of one DNA fragment from a mixture of different DNA species was done via agarose gel electrophoresis. The "QIAquick gel extraction" kit (Qiagen) was used and the manufacturer's protocol was followed. First, the band of interest is excised from the gel and weighed in a reaction tube. The gel slice is dissolved in the appropriate volume of a buffer containing chaotropic salts at 50°C. Afterwards, the DNA is bound to a silica-based column and residual agarose and salts are washed away. The DNA is eluted in water or EB buffer.

E) Precipitation of DNA and RNA

Nucleic acids are precipitated by ethanol or isopropanol in presence of monovalent cations. This method is applied to concentrate or desalt DNA solutions. 10% of the sample volume from a 3M sodium acetate (NaOAc) solution are added to the tube followed by 2.5 sample volumes of ethanol (EtOH) or 1 volume of isopropanol. Precipitation time was 1h at -20°C. The DNA is pelleted by spinning in a tabletop microcentrifuge at 16000g for 20min at 4°C. Residual salts are washed away with 70% ethanol and the centrifugation step is carried out again. The pellet is air-dried and dissolved in water or EB.

F) Agarose gel electrophoresis

Agarose gel electrophoresis was used to separate DNA fragments of different lengths. Agarose forms a three-dimensional matrix with defined spacing, in which separation in an electric field depends on size and charge. DNA is negatively charged with the charge correlating with its size. Thus, separation during electrophoresis depends on molecule size. By default, 0.8% (m/v), 1% and 1.5% agarose gels containing 1xTBE and Sybr® Safe (Invitrogen) were used. The running buffer was 1xTBE and gels were run at 2-7 V/cm. After electrophoresis, the DNA was visualized on an UV imaging system (Intas). To determine the size of the DNA fragments, 1µg of the DNA standards "1kb ladder" or "100bp ladder", (NEB) were loaded.

G) UV spectrometric DNA concentration analysis

DNA concentrations were determined with a Nano Drop device (Peqlab). After equilibration with the respective buffer, 1.7µl of the sample were applied. The DNA concentration is measured at 260nm wavelength. Contamination with proteins was simultaneously detected at 280nm. Pure DNA has an OD_{260}/OD_{280} ratio of 1.8 -2.0. The DNA concentration is calculated according to the following formula:

$$c\left[\frac{\mu g}{ml}\right] = 50\frac{\mu g}{ml} \times volume^{-1} \times OD_{260}$$

3.2.3 Techniques with *Escherichia coli*

A) Preparation of electrocompetent E. coli

For preparation of electrocompetent *E. coli* XL1 Blue, an overnight culture in SOB medium (3.1.2) was diluted 1:1000 in pre-warmed (37°C) SOB. This culture was then grown with vigorous shaking to an OD_{600} of 0.4 to 0.6 for 3h. Afterwards, the culture was chilled on ice for 15min and centrifuged at 1000g for 10min at 4°C. The pellet was washed with 400ml of sterile ice-cold water. Centrifugation and resuspension (200ml) were repeated. After a next centrifugation step, the washed cells were resuspended in 10ml sterile 10% (v/v) glycerol and pelleted at 5000g for 10min at 4°C. Finally, the cells were resuspended in 1.5ml of the 10% glycerol solution, 50-100µl aliquots were prepared and stored at -80°C.

B) Preparation of chemical competent E. coli

200 ml SOB medium were inoculated from a stationary *E. coli* culture to an OD_{600} of 0.2 and grown at 37°C to an OD_{600} of 0.5. Cells were harvested by centrifugation (50ml, 4500 rpm, 10 min, 4°C), resuspended in 15 ml cold Tfb-I buffer (3.1.3), incubated on ice for 20 min and spun down again. The

pellets were dissolved and combined in a total volume of 4 ml cold Tfb-II buffer (3.1.3) and incubated on ice for 20 min. Chemical competent *E. coli* were stored in 100µl aliquots at -80°C

C) Liquid culture of E. coli

Liquid cultures of *E. coli* were started in three different ways. Either, a single colony was picked from a freshly streaked selective plate or a glycerol culture was used or a fresh overnight culture was taken. Inoculation was done using a sterile loop or pipette tip. If necessary, antibiotics were added to the medium. Culture sizes ranged from 2ml for Minipreps to 2l for recombinant protein expression.

D) Transformation of electrocompetent E. coli

The required competent cell aliquots were thawed on ice. Upon liquefaction, about 1ng of plasmid DNA or 1-2µl of a ligation reaction were added to the cells and mixed carefully. As a control, one aliquot of competent cells was used without adding DNA. The solution was transferred into a pre-cooled electroporation cuvette with a 2mm gap. Electroporation was performed in a micropulser (BioRad) at setting EC2 (1.8kV output, 9V/cm, 8ms duration). Immediately afterwards, 1ml of prewarmed (37°C) LB medium was added, the cell suspension transferred to a microreaction tube followed by an incubation step at 37°C for 30min. 100µl of this suspension were directly plated on LB_x, the rest was spun down at 5000g for 1min in a microcentrifuge and all but 100µl of the supernatant were removed and the pellet resuspended. The resulting suspension was then also plated on LB_x and the plates were incubated at 37°C over night.

E) Transformation of chemical competent E. coli

The required competent cell aliquots were thawed on ice. Upon liquefaction, about 10ng of plasmid DNA or 1-2µl of a ligation reaction were added to the cells and mixed carefully. As a control, one aliquot of competent cells was used without adding DNA. The solution was incubated on ice for 5min, subjected to a heat shock (42°C, 40s) and incubated on ice for another 3min. Immediately afterwards, 1ml of prewarmed (37°C) LB medium was added, the cell suspension transferred to a microreaction tube followed by an incubation step at 37°C for 30min. 100µl of this suspension were

directly plated on LB_x, the rest was spun down at 5000g for 1min in a microcentrifuge and all but 100µl of the supernatant were removed and the pellet resuspended. The resulting suspension was then also plated on LB_x and the plates were incubated at 37°C over night.

3.2.4 Techniques with *Saccharomyces cerevisiae*

A) Preparation of competent yeast cells

Treatment of yeast cells with monovalent cations (e.g. Li^+, Cs^+, K^+) induces competence for the uptake of linear and circular DNA molecules. Competent yeast cells were prepared from 50ml of an exponentially growing liquid culture. The cells were pelleted (500g, 5min, RT) and first washed with 25ml sterile H_2O, followed by a washing step with 5ml SORB (3.1.3). After a next centrifugation step, the cells were resuspended in 500µl LitSORB (3.1.3), transferred to a reaction tube and spun down again. 360µl SORB and 40µl of boiled (95°C, 5min) salmon sperm DNA were added to the pellet and the suspension carefully mixed. Competent yeast cells were stored at -80°C in 50µl aliquots.

B) *Transformation of S. cerevisiae*

The required competent cell aliquots were thawed on ice. Upon liquefaction, 2-8µg (corresponding to less than 10µl) of DNA were added and the cells were mixed carefully. As a control, one aliquot of competent cells was used without adding DNA. In the next step, 6 volumes of LitPEG (3.1.3) were added and the suspension thoroughly mixed, followed by 30min incubation at RT. Sterile dimethylsulfoxide (DMSO) was added to an extent of 1/9 of the total sample volume and the mixture was heat-shocked at 42°C for 15min. Afterwards, the cells were spun down (2000g, RT, 2min), the supernatant discarded and the pellet resuspended in rich medium. The cells were then transferred into a culturing tube and regenerated at 30°C for 3h. Then, the cells were centrifuged and 90% of the supernatant was discarded. The cells were resuspended in the remaining liquid, plated on selective media and the plates were incubated at 30°C.

C) *Liquid culture of S. cerevisiae*

Liquid cultures of *S. cerevisiae* were started in three different ways. Either, a single colony was picked from a freshly streaked selective plate or a glycerol culture was used or a fresh overnight culture was taken. Inoculation was done using a sterile loop or pipette tip. If necessary, antibiotics were added to the respective medium. Culture sizes ranged from 2ml for preparation of genomic DNA to 2l for affinity purification of proteins.

D) *Permanent glycerol culture of S. cerevisiae*

For glycerol cultures, 2ml of a culture which had just reached stationary phase were mixed with 1ml of sterile 50% glycerol. The suspension was divided in two aliquots, frozen on dry ice and stored at -80°C.

E) *Spot test analysis of yeast strains*

Overnight cultures of the yeast strains to be tested were diluted to OD_{600} = 0.1 with sterile H_2O. 7-10 µl of this cell suspension and of serial 1:10, 1:100, and 1:1000 dilutions with sterile H_2O were spotted on the appropriate test plates. Phenotypes were monitored after incubation for 2-4 days at 24°C, 30°C, and 37°C, respectively.

F) Generation of yeast strains with affinity tagged proteins

In this work, yeast strains with the tandem affinity purification (TAP) tag were created. The TAP tag is a succession of protein A (Prot A), a tobacco etch virus (TEV) cleavage site and the calmodulin binding protein (CBP). In the fusion protein, CBP is connected to the C-terminus of the protein of interest. In general, these strategies have been outlined in (Knop et al. 1999; Puig et al. 2001). Briefly, tagging cassettes were generated by PCR and transformed into yeast cells. Stable integration into the genome is achieved by homologous recombination. Positive clones are selected via resistance to

antibiotics or auxotrophy markers integrated in the tagging cassettes. The used oligonucleotides and plasmids are listed in **Table 3-10Fehler! Verweisquelle konnte nicht gefunden werden.** and **Table 3-11**, resulting yeast strains are given in **Table 3-15**

3.2.5 Heterologous protein expression in SF21 insect cells using recombinant baculoviruses

A) *Overview*

Expression of recombinant proteins with the baculovirus-mediated SF21 insect cell system was performed according to (Berger et al. 2004; Fitzgerald et al. 2006). Expression of eukaryotic proteins in *E. coli* can lead to non-functionality due to the lack of posttranslational modifications or problems with solubility. Independent purification of affinity tagged proteins directly from their host cells bears the risk of cross-contamination with other factors of interest and yields less material than recombinant techniques. These issues are even more significant, if protein complexes are to be analyzed. The baculovirus-mediated recombinant expression system combines the advantages of recombinant techniques with correct (or similar) posttranslational modifications and solubility. In this work, the system was used to express single proteins from *S. cerevisiae*.

B) *Cultivation of SF21 cells*

Techniques directly involving SF21 cells were executed in a sterile bench in a separate tissue culture room SF21 insect cells were cultivated in SFII 900 SFM medium (Life Technologies) at 27°C on a platform shaker at 100rpm (Heidolph Unimax 2010). Culture density and purity were monitored daily under a microscope with a hemocytometer (Neubauer II). Cells were kept in logarithmic growth by adjusting the density to $0.5x10^6$ cells/ml every day. If cell viability dropped below approximately 95% or the culture had reached passage number 30, the cells were trashed. Erlenmeyer flasks for cell culture were cleaned with 1% acetic acid and water and adherent cells removed mechanically. Afterwards, the flasks were twice autoclaved.

C) *Long term storage of SF21 cells*

Long-term storage cultures were prepared at a low passage number (< 10). A total of $60x10^6$ cells were harvested per aliquot (500g, 10min, RT), resuspended in 1ml medium supplemented with 30°C fetal calf serum (FCS) and 10% sterile DMSO. This suspension was frozen in -20°C cold isopropanol and stored at -80°C. A maintenance culture was started by permanent addition of just thawed cells of one cryo-culture to 60ml medium supplemented with 10% FCS. This culture was grown for 48h before the first determination of the cell density.

D) *Cloning, generation and isolation of bacmids*

Yeast genes of interest were inserted into the multiple cloning site 2 of the acceptor vector pFL-FLAG-TEV (#1212) by standard cloning techniques. Thus, the gene will be expressed in SF21 cells under control of the strong viral polyhedrin promoter as an N-terminal FLAG tag fusion protein.

The resulting plasmid was then integrated *in vivo* into a modified viral genome (bacmid) via Tn7 transposition sites present in the pFL vector. For this, the respective plasmid was transformed into the *E. coli* strain DH10MultiBac-eYFP, which carries the bacmid and a helper plasmid pMON7124 encoding the DNA recombinase Tn7 transposase (see Bac-to-Bac® Baculovirus Expression System manual; Invitrogen). Transformation was in general carried out as described in 3.2.3 E, but cells were allowed to regenerate overnight. Transformed DH10MultiBac-eYFP cells were subjected to blue/white colony screening and thus plated on LB supplemented with ampicillin (100µg/ml), gentamycin (10µg/ml), tetracycline (10µg/ml), IPTG (0.5mM) and X-GAL (5-bromo-4-chloro-3-indolyl-β-D-galactopyranoside, 50mg/ml) and incubated overnight at 37°C. Three positive (white) colonies and one negative (blue) colony were streaked out again on the respective plates to confirm integration of the plasmid in the bacmid.

For isolation of recombinant bacmid from *E. coli* DH10MultiBac-eYFP cells, 3ml of an overnight culture of a positive clone in $LB_{Amp\ Tetra\ Genta}$ were spun down (5min, 4000rpm, RT) and cells were resuspended in 0.3ml solution I (**Table 3-2**). Cells were lysed by addition of 0.3ml solution II (**Table 3-2**) and incubated for 5min at RT. Proteins were precipitated by addition of 0.3ml 3M KOAc pH 5.5, the solution incubated on ice for 10min and centrifuged for 10min at 16000g and RT in a tabletop centrifuge. The bacmid DNA in the supernatant was precipitated with isopropanol as described (3.2.2 E) and the air-dried pellet resuspended in 50µl sterile H_2O.

E) *Transfection of SF21 cells*

Transfection of SF21 cells was done in 6-well plates. For each transfection, $1x10^6$ cells were seeded in two wells each. As mock and medium control, one additional well with cells and one well with medium only was prepared. The plate was incubated for 15min at RT to let the cells adhere to the bottom, the supernatant was removed and 3ml fresh medium were added. To 20µl bacmid solution (50-100ng DNA), 300µl medium and 10µl transcfection reagent (FuGene, Promega) were added in a microreaction tube. The solution was carefully mixed and incubated for 30min at RT. Of this mixture, 160µl were added to each well. Mock controls did not contain bacmid DNA. Cells were incubated at 27°C and transcfection success monitored by fluorescence microscopy. Usually, after 48h - 60h, the virus-containing supernatant (V_0) was harvested and stored at 4°C.

F) *Amplification of recombinant baculoviruses*

Recombinant baculoviruses were amplified by infecting 50ml SF21 cultures (passage 5-15, $0.5x10^6$ cells/ml) with 50µl V_0 followed by incubation at 27°C under shaking. Cell density was monitored daily at the same time and cells were diluted to $0.5x10^6$ cells/ml. Infection success was also monitored daily under a fluorescence microscope. Growth arrest was defined as the inability to reach a density of $1x10^6$ cells/ml in 24h and occurred usually 72h post infection. Then, the culture was incubated for another 24h and cells were harvested at 130g for 15min at RT. The supernatant (V_1) contains the amplified virus and is stored at 4°C. The cells were used for protein expression and purification tests.

G) *Large scale expression of recombinant proteins in SF21 cells*

For large scale infections, cells from passages between 5 and 10 were used. A large scale culture usually was 200ml in a 1l Erlenmeyer flask with a cell density of $1x10^6$ cells/ml. Infection was performed with 5ml V_1 and cultures were incubated at 27°C for 48h. The infection was monitored under a fluorescence microscope. Cells were harvested in $50x10^6$ cells aliquots (130g, 15min, RT), frozen in liquid nitrogen and stored at -20°C.

3.2.6 Protein biochemical methods

A) *Denaturing protein extraction from yeast cells*

Denaturing protein extraction was performed as a first step in the verification of protein tags in before manipulated yeast cells. 1ml of an overnight culture was harvested in a microcentrifuge (5min, 5000rpm, RT). Cells were resuspended in 1ml ice-cold water and 150µl of pre-treatment solution (1.85M NaOH, 1M β-mercaptoethanol) were added. The solution was incubated on ice for 15min. Proteins were precipitated by adding 150µl 55% trichloroacetic acid (TCA) and incubating on ice for 10min. The precipitate was spun down at 13000rpm for 10min at 4°C in a table-top centrifuge. The pellet was resuspended in 5µl HU buffer and the solution neutralized with NH_4OH gas, if the buffer turns yellow. A neutral pH is indicated by a blue buffer colour. Denaturation was performed at 65°C for 10min and approximately half of the sample was analyzed in Western blot.

B) *Methanol/chloroform precipitation*

For mass-spectrometric analyses, proteins were precipitated with methanol and chloroform according to (Wessel & Flügge 1984). The sample was first adjusted to 150µl with H_2O. Afterwards, 4 volumes (600µl) methanol (MeOH), one volume (150µl) of chloroform and three volumes (450µl) of H_2O were added. After every step, the sample was thoroughly mixed. Phase separation was achieved by centrifugation in a table-top centrifuge for 5min at RT and 13000rpm. The upper phase is discarded without distortion of the protein containing interphase. Another 3 volumes (450µl) MeOH were added, the solution was vortexed and spun down again (13000rpm, 5min, RT). The supernatant was removed and the pellet was air-dried at RT.

C) TCA precipitation

Proteins can be precipitated with TCA to reduce sample volumes. 0.2 sample volumes of 100% TCA were added and the reaction tube was kept on ice for 30min. Afterwards, the precipitate was pelleted at 13000rpm for 30min at 4°C in a table-top centrifuge. The supernatant was discarded and

the pellet dissolved in an appropriate volume of SDS sample buffer. If the colour of the buffer was yellow, the solution was neutralized with NH_4OH gas until it turned blue. The proteins were denatured at 95°C for 5min and then subjected to SDS-PAGE.

D) Ammonium sulfate precipitation

Ammonium sulfate precipitation is a classical approach for fractionation of cell extracts and is thus used in early stages of protein purification (Sambrook et al. 1989). With increasing concentration of $(NH_4)_2SO_4$, the ionic strength of the solution rises. This first leads to enhanced protein solubility (salting in). After reaching a solubility optimum, proteins start to precipitate (salting out). Thus, fractionation is based on differences in solubility at certain $(NH_4)_2SO_4$ concentrations with the protein of interest being precipitated. In this work, it was included in the purification of Reb1. To one sample volume, 3 volumes of a 4°C cold, saturated $(NH_4)_2SO_4$ solution were added slowly (75% fractionation). The saturated solution was prepared by dissolving more than 70.6g $(NH_4)_2SO_4$ per 100ml water at RT. The solution was constantly stirred and upon use allowed to form a precipitate. The clear supernatant is the saturated solution. The cell extract supplemented with $(NH_4)_2SO_4$ was kept on ice for 30min and the precipitate harvested at 16000g and 4°C for 1h. The pellet containing the protein of interest is then further processed.

E) Protein concentration measurement

Protein concentrations were measured in two different ways. First, the Bio-Rad protein assay was employed, which is based on the Bradford assay (Bradford 1976) to measure total protein concentration of a fraction. Briefly, 1µl of the fraction of interest was mixed with 800µl H_2O and 200µl of the protein assay stock solution. The mixture was incubated for 5min at RT and the optical density (OD) monitored with a UV/vis spectrophotometer at 595nm. The approximate protein concentration in mg/ml can be calculated by multiplying the absorbance with factor 23 resulting from a calibration curve with BSA. In cases, where protein preparations were not completely pure, the concentration of the protein of interest had to be further calculated. After Coomassie staining of the SDS gel, a profile analysis was performed with the respective gel lane (function “profile” in Multi Gauge). Background and peaks were assigned automatically and the percentage of the peak of

interest calculated based on the peak areas. Finally, the concentration obtained by Bradford measurement was corrected by this percentage.

Second, protein concentrations were determined with BSA calibration curves on SDS gels. Defined amounts of BSA ranging from 100 to 1000ng were loaded on a SDS gel together with a defined volume of the protein fraction of interest. After Coomassie staining, protein bands were quantified with the function "quant" in the program Multi Gauge (Fuji) and a calibration curve was calculated to evaluate the unknown concentration.

If protein concentrations had to be calculated for EMSAs (3.2.6 K) or *in vitro* transcription (3.2.12), both methods were applied and the average of both obtained concentrations was determined.

F) SDS-polyacrylamide gel electrophoresis (PAGE)

Proteins are separated according to their molecular weight by vertical discontinuous gel electrophoresis (Laemmli 1970). In this work, 10% polyacrylamide separating gels and 4% stacking gels were used:

substance	separating gel	stacking gel
30% AA/ 0.8% bisAA solution	4.16ml	0.65ml
Lower Tris buffer	2.5ml	-
Upper Tris buffer	-	1.25ml
10% APS	40µl	30µl
TEMED	10µl	6µl
water	4.16ml	3.1ml

Table 3-21: SDS polyacrylamide gel recipe.

Electrophoresis was performed at constant voltage (120-180V) in SDS-PAGE running buffer until the bromophenol blue band reached the end of the gel. To estimate the molecular weight of the proteins, 8µl of a pre-stained marker solution (NEB) were applied on the gel.

For mass spectrometry, precast 4%-12% gradient Bis-Tris Novex® NuPAGE® gels (Life Technologies) were used. The running buffer was either NuPAGE® MES ((2-N-morpholino)ethanesulfonic acid) or MOPS (3-N-morpholino)propanesulfonic acid), complemented with the NuPAGE® antioxidant reagent. Electrophoresis was carried out according to the manufacturer's protocol (200V constant, 35 [MES] or 50min [MOPS] running time).

G) Coomassie staining

After SDS-PAGE, proteins were visualized with Coomassie or silver staining. For standard analytical purposes, the gel was stained for 30min in the Coomassie staining solution (**Table 3-3Table 3-8**) containing the Coomassie brilliant blue R250 dye. Destaining was done in the appropriate solution (**Table 3-3**) until the gel background was clear (Meyer & Lamberts 1965).

For mass spectrometry or more sensitive analyses, the visualization was done with the SimplyBlue SafeStain® (Life Technologies). This staining solution is based on colloidal Coomassie brilliant blue G250 (Diezel et al. 1972). Briefly, the gel was washed 3 times with ultrapure water to remove SDS and salts. Staining was done for 1h at RT. The gel was destained in ultrapure water until the background was clear.

H) Silver staining

Gels containing low amounts of protein were stained with the more sensitive silver staining method based on studies by (Switzer et al. 1979). The detection limit is between 1 and 10ng protein per band. First, the gel was incubated with the fixation solution for >1h and then washed in 50% EtOH for 20min. Next, the gel was washed with pretreatment solution for 1min followed by three rinsing steps with ultrapure water for 20s each. The gel was then soaked with staining solution for 20min and again rinsed with water twice. Finally, the protein bands were made visible by applying the developing solution. The staining process was ended upon treatment with 1% acetic acid (HOAc). The composition of the solutions is listed in (**Table 3-3**)

I) Western blotting and protein detection with immuno-chemiluminescence

Transfer of proteins from an SDS gel to a membrane was first described by (Renart et al. 1979; Towbin et al. 1979). After electrophoresis, the proteins are associated with SDS and thus negatively charged. Therefore, they can be transferred to a PVDF (polyvinylidene fluoride) membrane in an electric field. Three layers of whatman paper were soaked in blotting buffer, and put on the anode of the blotting apparatus avoiding air bubbles. The membrane (Immobilon PSQ 0.2µm, Millipore) was

activated in MeOH and then washed in blotting buffer. Next, the SDS gel was transferred onto the membrane and both put on top of the whatman papers. Finally, the gel was covered with three layers of wet whatman paper. Remaining air bubbles were carefully removed and blotting was performed at constant 24V for 75min. Afterwards, the stack was disassembled and the lanes were marked on the membrane with a pen.

The transfer success was verified by putting the membrane in Ponceau S staining solution (**Table 3-2**) for 2min. The diazo dye Ponceau S reversibly binds the amino groups of the proteins. Thus, after detection, it can be washed away with water.

For protein detection via immune-chemiluminescence, the membrane was first put in a 5% milk powder solution in PBST for 1h under shaking to saturate the unspecific protein binding capacity of the membrane. Then, the membrane was wrapped and put into a 50ml falcon tube containing the primary antibody in its appropriate dilution in 1ml PBST with 1% milk powder. The tube was attached to a rotating wheel and incubated for 45min at RT. Next, the membrane was washed three times with PBST for 5min. Again, the membrane was wrapped and put into a 50ml tube containing the secondary antibody in its appropriate dilution in 1ml PBST with 1% milk powder and rotated for 30min at RT. This was followed by three washing steps in 5ml PBST for 5min each. The secondary antibodies are coupled to horseradish peroxidase (HRP) which catalyses the oxidation of diacylhydrazides via an activated intermediate that decays to the ground state by emission of light in the visible range. The blots were developed with the chemiluminescence substrate and a starter (BM chemiluminescence blotting susbtrate (POD), Roche), transferred to a translucent plastic bag and the positions of the prestained marker protein bands were indicated with a fluorescent pen. The readout was done with a LAS 3000 fluorescence reader (Fuji) with the setting “increment”.

J) *Protein gel filtration chromatography*

Gel filtration of recombinant proteins was performed to determine oligomerization state and homogeneity. They were analyzed on the Smart system (Pharmacia Biotech) with a Superose 6 PC 3.2/30 gel filtration column (GE Healtcare) equilibrated with the respective protein storage buffer. Buffers for gel filtration did not contain detergents present in the storage buffers. Samples were loaded with a Hamilton syringe on a 50µl loop. Separation was performed according to the program ROSUP61 at 4°C and a flow rate of20µl/min. Thirty 50µl fractions were collected starting with the void volume for subsequent SDS PAGE analysis. For molecular weight and thus oligomerization estimations, calibration curves were calculated based on retention times of a set of standard

proteins (thyreoglobulin, bovine serum albumin (BSA), immune globulin G, catalase, glutathione-S-transferase, ferredoxin and cytochrome c).

K) Electrophoretic mobility shift assay

Electrophoretic mobility shift assays were used to analyze the DNA binding ability of recombinant protein factors and to determine optimal binding conditions, respectively. Proteins of interest were purified (3.2.9) and their concentration calculated (3.2.6 E). DNA templates were obtained via annealing of oligonucleotides (**Table 3-10**) for templates up to 50bp or PCR, with one of the oligonucleotides/primers carrying a 5' Cy5 fluorescent label. PCR products were purified and concentrated via EtOH precipitation. The final DNA concentration in the assay was 10nM. Template, buffer and protein(s) of interest were mixed in a reaction tube in a total volume of 10µl and incubated for 15min at RT. Binding conditions (buffer, template concentration, ionic strength) were chosen identically to *in vitro* transcription. After incubation, 2µl of 6x EMSA loading buffer (**Table 3-2**) were added and the mixture was separated on a native 6% polyacrylamide 0.4x TBE gel. Gels were pre-run in 0.4xTBE for 1h and electrophoresis was performed at 100V constant with a Novex® XCell™ sure lock Mini cell gel apparatus (Invitrogen). Gels were analyzed with a FLA3000 imaging device (Fuji).

Native 6% PA 0.4x TBE gel	**1x**	**6x**
Rotiphorese Gel 30 AA/Bis-AA solution 37.5:1 (Roth)	2ml	10ml
5x TBE	0.8ml	4ml
water	7.2ml	36ml
10% APS	80µl	400µl
TEMED	8µl	12µl
total	10ml	50ml

Table 3-22: Native polyacrylamide gel recipe.

L) Cleavage of GST fusion proteins

GST fusion proteins expressed from pGEX6-P1 contain a cleavage site recognized by PreScission protease (GE Healthcare) and fusion proteins expressed from pGEX4-T1 contain a cleavage site for

thrombin, respectively. The cleavage sites are located between the N-terminus of the protein of interest and the GST tag. Cleavage with PreScission protease was performed according to the manufacturer's protocol with 1U/100µg fusion protein at 4°C over night. Thrombin was used according to the manufacturer's protocol at 1U/100µg fusion protein at 12°C over night. Cleavage success was monitored via SDS PAGE.

M) Formation of the Pol II-TFIIF complex

The Pol II-TFIIF complex was reconstituted from one-step purified yeast Pol II (KCl conditions, strain #2424, see 3.2.10 A) and TFIIF purified with 500mM KCl from strain #2994 (3.2.10 C). 20µl of Pol II and TFIIF were mixed, adjusted to a volume of 200µl with buffer C1 (**Table 3-4**) and incubated on ice for 15min (input). The mixture was added to 50µl of Calmodulin resin (Stratagene) equilibrated in C1 and incubated rotating for 2h at 4°C. The FT was collected and the beads washed twice with 1ml C2. The beads were resuspended in 40µl C2. 10µl of input and flowthrough, 20µl of the washing steps and 20µl of beads were boiled in SDS sample buffer and analyzed via SDS PAGE.

3.2.7 Mass spectrometry

A) *Identification of proteins with MALDI TOF/TOF*

Protein bands of interest were cut out of Coomassie stained gels and processed as in principle described in (Shevchenko et al. 1996; Shevchenko et al. 2006). Briefly, the bands were cut into small pieces and washed first with 600µl 50mM NH_4HCO_3 for 30min at RT in a thermomixer. The supernatant was discarded and the gel pieces incubated again under the same conditions with 60µl of 50mM NH_4HCO_3 supplemented with 25% (v/v) acetonitrile (AcN) and a final washing step was performed with 600µl of 50mM NH_4HCO_3 + 50% (v/v) AcN. The supernatant was discarded and the gel pieces lyophilized for 1h. The dried gel pieces were re-hydrated in an equal volume (approx. 10µl) of a 10mM NH_4HCO_3 solution containing sequencing grade trypsin (Roche) to a final concentration of 0.1µg/µl (approx. 1µg trypsin per sample). Re-hydration was done for 45min at 37°C followed by addition of another volume of the trypsin containing solution. The tryptic digest was carried out over

night at 37°C and the supernatant transferred to a new reaction tube. The tryptic peptides were eluted by diffusion in a series of washing steps with twice 15µl of 100mM NH_4HCO_3 and 15µl of 100mM NH_4HCO_3 + 35% (v/v) AcN. Incubation time was 1h for each step at 37°C under shaking. The supernatants were all pooled and then lyophilized. Afterwards, 25µl 1% (v/v) acetic acid (HOAc) were added to remove carbonates followed by another lyophilization step. The peptides were solubilized in 5µl freshly prepared matrix solution (2 mg/ml α-cyano-4-hydroxycinnamic acid (CHCA), 50% (v/v) acetonitrile, 0.1% (v/v) TFA) and spotted on a cleaned MALDI plate manually.

Peptide mass fingerprints (PMF) and MS/MS analyses were performed on a 4800 Proteomics Analyzer MALDI-TOF/TOF mass spectrometer (ABI) operated in positive ion reflector mode and evaluated by searching the NCBInr protein sequence database with Mascot implemented in GPS Explorer v.3.5 (ABI).

B) *Semi-quantitative comparative iTRAQ LC MALDI TOF/TOF analysis*

Isobaric tags for relative and absolute quantification (iTRAQ™ (Ross et al. 2004)) were used for comparative analysis of the protein content of RNA polymerase and transcription factor preparations from yeast. As a maximum, comparisons of four different preparations were performed with usually 10-20µl of the elution fraction per sample (see 3.2.9). Labeling was done with the iTRAQ™ labeling kit (Life Technologies).

To reduce the unspecific protein content, His_6-tagged tobacco etch virus protease (TEV) was depleted from the samples. 40µl Ni-nitrilotriacetic acid (NTA) agarose slurry (QIAGEN) per sample were washed with 400µl and then equilibrated on a rotating wheel for 1h at 4°C with 500µl of the respective elution buffer (3.1.3). The protein fraction volume was adjusted to 150µl with elution buffer and the solution applied to the column. TEV binding was done at 4°C on a rotating wheel for 30min. The flowthrough was collected and methanol/chloroform precipitated (3.2.6 B).

The precipitate was solubilized in in 20µl iRTAQ™ dissolution buffer and reduced with 2µl iTRAQ™ reducing agent (5mM Tris-(2-carboxyethyl)phosphine). Incubation time was 1h at 60°C in a thermomixer. Cystein sulfhydryl groups were modified with 1µl iTRAQ™ cystein blocking reagent (10mM methyl-methanethiosulfonate (MMTS)) at room temperature for 10min. 25µg sequencing grade trypsin (Roche) were resuspended in 25µl water and 6µl of this suspension were added to each sample. The tryptic digest was carried out over night at 37°C.

The tryptic peptides were labeled with different combinations of iTRAQ™ reagents according to the manufacturer's protocol. Briefly, one unique labeling reagent was assigned to one protein preparation of interest, re-dissolved in 70µl 70% (v/v) EtOH and incubated with the tryptic peptide solution for ≥ 1.5h. Afterwards, up to four differently labeled samples were unified and lyophilized.

The lyophilized sample was dissolved in 30µl 0.1% (v/v) trifluoroacetic acid (TFA) and spun down at 13000rpm for 10min in a tabletop centrifuge. The supernatant was loaded on a nano-flow HPLC system (Dionex) harbouring a C18-Pep-Mep column (LC-Packings). The peptides were separated by a gradient of 5% to 95% of buffer B (80% acetonitrile/0.05% TFA) and fractions were mixed with 5 volumes of CHCA (alpha-cyano-4-hydroxy cinnamic acid; Sigma) matrix (2mg/ml in 70% acetonitrile/0.1%TFA) and spotted on-line via the Probot system (Dionex) on a MALDI plate.

MS/MS analyses were performed on an Applied Biosystems 4800 Proteomics Analyzer. MALDI-TOF/TOF mass spectrometer operated in positive ion reflector mode and evaluated by searching the NCBInr protein sequence database with the Mascot search engine (Matrix Science) implemented in the GPS Explorer software (Applied Biosystems). Laser intensity was adjusted due to laser condition and sample concentration. The ten most intense peptide peaks per spot detected in the MS mode were further fragmented yielding the respective MS/MS spectra.

Only proteins identified by peptides with a Confidence Interval > 95% were included in the analysis. The peak area for iTRAQ™ reporter ions were interpreted and corrected by the GPS-Explorer software (Applied Biosystems) and Excel (Microsoft). An average iTRAQ ratio of all peptides of a given protein was calculated and outliers were deleted by manual evaluation.

3.2.8 *In vitro* chromatin assembly

In vitro assembly of chromatin via salt gradient dialysis is a well established technique in the field (Kleiman & Huang 1972; Woodcock 1977; Wilhelm et al. 1978; Gadski & Chae 1976). Purified core histones H2A, H2B, H3 and H4 from chicken erythrocytes (as first described by (NEELIN & BUTLER 1959)) were a kind gift from the Längst lab. Chromatin was reconstituted on templates for *in vitro* transcription containing one or multiple 601 nucleosome positioning sequences (**Table 3-11**) (Lowary & Widom 1998). This results in defined positions of the nucleosomes and thus homogeneity of the chromatin templates.

For *in vitro* transcription, only fully assembled template DNA was used. To determine optimal assembly conditions, histones were titrated to the DNA:

ratio histones : DNA	**0.4 : 1**	**0.6 : 1**	**0.8 : 1**	**1 : 1**
high salt buffer	44µl	42.75µl	41.5µl	40.25µl
BSA (10mg/ml)	1µl			
DNA template (2µg/µl)	2.5µl			
chicken histones (0.8mg/ml)	2.5µl	3.75µl	5µl	6.25µl
total volume	50µl			

Table 3-23: Assembly titration series scheme.

Dialysis chambers were prepared from siliconized microreaction tubes (Eppendorf) by clipping off the conical part and perforation of the cap with a red-hot metal rod (ø 0.5cm). The dialysis membrane (molecular weight cutoff 6.8kDa) was pre-wet in high salt buffer (**Table 3-8**) and fixed between tube and cap. The dialysis chambers were put in a floater in a bucket containing 300ml high salt buffer, air bubbles were removed and the mixture of histones and DNA was applied to the chambers. Dialysis from 2M NaCl to 0.23M NaCl was performed over night at RT with constant stirring and at a low salt buffer flow rate of 200ml/h (3l total). Upon completion, the assembly solution was transferred to a siliconized tube, its volume was measured and chromatin was stored at 4°C. To determine the assembly success, 5µl of the reaction were supplemented with 1µl loading buffer (**Table 3-8**) and analyzed on a 6% polyacrylamide, 0.4xTBE gel as described (3.2.6 K). Gels were stained in 0.4xTBE containing ethidium bromide for 15min, washed in 0.4xTBE for 15min and read out on a FLA3000 imager (Fuji).

3.2.9 Recombinant protein affinity purification

A) Purification via the FLAG tag [Nsi1, Fob1, Paf1]

Nsi1, Fob1 and Paf1 were expressed as N-terminal FLAG tag fusion proteins in SF21 insect cells (3.2.5). A recognition site for TEV protease is located between the FLAG tag and the protein of

interest. 50x10^6 infected SF21 cells were resuspended in 40ml TAP 300 (**Table 3-5**) and a crude cell extract was prepared by sonication for 5min with a pattern of 30s pulse and 30s pause using the macrotip (output 5, Branson sonifier). Cell debris were removed by centrifugation (4000g, 15min, 4°C) and the supernatant added to 50µl (100µl slurry) anti-FLAG M2 beads (Sigma Aldrich) equilibrated three times with 5ml TAP300. The suspension was incubated on a rotating wheel at 4°C for 2h. After centrifugation (130g, 5min, 4°C) the supernatant was removed and the beads washed three times with 10ml TAP 100 (w/o PIs) each. For elution, the beads were resuspended in 100µl TAP 100 (w/o PIs), transferred to a microreaction tube and incubated with 8µl of in-lab-prepared TEV protease for 2h at 16°C in a thermomix. The suspension was centrifuged at 16000g for 5min at 4°C and the supernatant loaded on a MobiCol column (MoBiTec). For removal of remaining beads, the column was spun again (16000g, 5min, 4°C). Each sample taken during the purification process was analyzed via SDS PAGE to monitor the purification success and the protein concentration in the elution fraction was determined.

B) Purification via the hexahistidine (His_6) tag [Reb1, Hmo1, A49/A34.5 dimer]

Reb1, Hmo1 and the RNA polymerase I (Pol I) subunits A49 and A34.5 were expressed in *E. coli* BL21 (DE3). Reb1 and Hmo1 were cloned into the expression vector pET21a and thus expressed as fusion proteins with a C-terminal His_6 tag. The vector expressing A49-His_6 and A34.5 subunits (pET28b) was a generous gift from the Cramer lab and cloning was described in (Geiger et al. 2010). All purification steps were carried out on ice in a 4°C room. In first place, an overnight culture (20ml LB supplemented with the respective antibiotic) was inoculated from a single colony picked from a freshly streaked selective plate. The culture was grown at 37°C over night. On the next day, the main culture (800ml LB with the respective antibiotic) was inoculated to an OD_{600} of 0.1 and grown at 37°C until an OD_{600} of 0.6 to 0.8 was reached. Then, protein expression was induced by adding isopropyl-β-thiogalactopyranoside (IPTG) to a final concentration of 1mM. After 3h at 37°C, the cells were harvested at 4000g for 20min at 4°C. From here, different strategies were followed.

i. Reb1 and Hmo1

The Reb1and Hmo1 purification strategy was adapted from (Morrow et al. 1990; Morrow et al. 1993). The amount of cells representing 250ml of the main culture was directly used for purification.

First, cells were resuspended in 20ml resuspension buffer 1 (**Table 3-6**) and lysed via sonication for a total of 5min with a pattern of 30s pulse and 30s pause using the macrotip (output 5, Branson sonifier). The cell debris were removed via centrifugation (16000g, 30min, 4°C) and the soluble fraction subjected to 75% ammonium sulfate precipitation (3.2.6 D). The precipitate was solubilized in resuspension buffer 2 and loaded on a Ni-NTA agarose column with a bed volume of 0.5ml (1ml slurry) equilibrated with resuspension buffer 2. The column was drained by gravity flow and washed in two steps with each 30ml washing buffer 1 and 2. Reb1-His_6 and Hmo1-His_6 were eluted in 5 steps with 0.5ml elution buffer each. Each sample taken during the purification process was analyzed via SDS PAGE to monitor the purification success and the protein concentration in each elution fraction was determined.

ii. A49/A34.5 dimer

The harvested cells were washed in buffer A (**Table 3-7**), divided into aliquots reflecting 200ml of the main culture and spun down again. The cells were frozen in liquid nitrogen and stored at -80°C.

A standard purification was from one cell aliquot and the purification strategy was adapted from (Geiger et al. 2010). Cells were resuspended in 40ml buffer B (**Table 3-7**). A crude cell extract was prepared by sonication for a total of 5min with a pattern of 30s pulse and 30s pause using the macrotip (output 5, Branson sonifier). The cell debris were pelleted at 16000g and 4°C for 40min. The supernatant was loaded on a Ni-NTA agarose column with a bed volume of 0.6ml (1.2ml slurry) equilibrated with buffer B. The column was drained by gravity flow and washed first with 25ml buffer C and subsequently with 15ml buffer D (**Table 3-7**). The A49-His_6/34.5 dimer was eluted from the column in four steps with 0.6ml buffer E (**Table 3-7**) each. Each sample taken during the purification process was analyzed via SDS PAGE to monitor the purification success and the protein concentration in each elution fraction was determined.

C) Purification via the glutathione-S-transferase (GST) tag [LexA, LacI]

LexA and LacI were expressed in *E. coli* BL21 (DE3). LexA was cloned into pGEX6-P1 and LacI was cloned into pGEX4-T1 thus resulting in expression of N-terminal GST fusion proteins. All purification steps were carried out on ice in a 4°C room. In first place, an overnight culture (20ml LB supplemented with the respective antibiotic) was inoculated from a single colony picked from a

freshly streaked selective plate. The culture was grown at 37°C over night. On the next day, the main culture (500ml LB with the respective antibiotic) was inoculated to an OD_{600} of 0.1 and grown at 37°C until an OD_{600} of 0.6 to 0.8 was reached. Then, protein expression was induced by adding isopropyl-β-thiogalactopyranoside (IPTG) to a final concentration of 1mM. After 3h at 37°C, the cells were harvested at 4000g for 20min at 4°C, washed with phosphate buffered saline (PBS) and pelleted again. Cell pellets were frozen in liquid nitrogen and stored at -80°C.

Upon purification, the cells were resuspended in 25ml PBS supplemented with 3mM β-mercaptoethanol and PIs. A crude cell extract was prepared by sonication (Branson Sonifier) for a total of 5min with a pattern of 30s pulse and 30s pause using the macrotip. The cell debris were pelleted at 9000g and 4°C for 20min. The supernatant was loaded on a glutathione agarose column with a bed volume of 1ml (2ml slurry) which was equilibrated with 20ml PBS + 3mM β-mercaptoethanol before. Binding of GST-LexA/GST LacI was done for 30min on a rotating wheel.

The column was drained by gravity flow and washed three times with 10ml PBS + 3mM β-mercaptoethanol. GST fusion proteins were eluted in six steps with 1.5ml PBS + 10mM glutathione (reduced) each. Each sample taken during the purification process was analyzed via SDS PAGE to monitor the purification success and the protein concentration in each elution fraction was determined. If applicable, the GST tag was cleaved off with thrombin (GST-LacI) or PreScission protease (GST-LexA) (**Table 3-12**).

3.2.10 Purification of yeast RNA polymerases and transcription factors

A) Wild-type RNA polymerases

Wild-type RNA polymerases I, II and III (Pol I, II and III) were purified from yeast strains # 2423 (Pol I), # 2424 (Pol II) and # 2425 Pol III (**Table 3-15**) via the protein A affinity tag. In each strain, the second largest subunit of one polymerase is expressed as a C-terminal fusion protein with protein A tag. Between the subunit's C-terminus and the protein A part, a recognition site for TEV protease is located. A 20ml YPD culture was grown to stationary phase at 30°C. From this culture, 2l of YPD were inoculated to an OD_{600} such that it would result in an OD_{600} of 1.5 after overnight cultivation at 30°C. At OD_{600} 1.5, the cells were harvested (4000g, 6min, RT) and washed in ice cold water. Cells were

split in aliquots representing 400ml culture volume and again spun down (4000g, 6min, 4°C). Cell aliquots were frozen in liquid nitrogen and stored at -20°C.

Polymerase purification was performed with 1-4 cell aliquots under two different conditions in a 4°C room. The buffers used during lysis and washing either contained 200mM KOAc or 200mM KCl (**Table 3-4**), elution was always done in KOAc conditions (P2 KOAc). Cells were thawed, washed in 5ml P1 + protease inhibitors (PIs) and spun down again (4000g, 6min, 4°C). The pellet was weighed and resuspended in 1.5ml of the respective P1 + PIs per gram. 0.7ml of this solution were added to 2ml reaction tubes containing 1.4g glass beads (diameter 0.75-1mm, Roth). Cells were lysed on an IKA Vibrax VXR basic shaker with 2200 rpm at 4°C for 15 min, followed by 5 min on ice. This procedure was repeated four times. The cell extract was cleared from glass beads by perforation of the cup at bottom and cap and a centrifugation step (150g, 1min, 4°C). Cell debris were removed by centrifugation at 16000g and 4°C for 30min. The protein content of the supernatant and thus lysis success were determined with the Bradford assay. The lysate was supplemented with NP40 to a concentration of 0.5% and PIs were added. Equal protein amounts (usually 1ml cell extract, 30-40mg) were incubated with 200 µl of IgG (rabbit serum, I5006-100MG, Sigma) coupled magnetic beads slurry (1 mm BcMag, FC-102, Bioclone) for 1h on a rotating wheel. The slurry had previously been equilibrated three times with 500µl of the respective P2. The beads were washed three times with 700µl of the respective P2 +PIs and then washed three times with 700µl P2 (KOAc). For elution, the beads were resuspended in 25µl P2 (KOAc) supplemented with 3µl of in-lab-prepared TEV protease. Cleavage was performed for 2h at 16°C in a thermomix at 1000rpm. The supernatant was collected, the beads were washed with 25µl P2 (KOAc) and both fractions combined. This elution fraction containing either Pol I, II or III was split in 10µl aliquots, frozen in liquid nitrogen and stored at -80°C. Each sample taken during the purification process was analyzed via SDS PAGE to monitor the purification success and the protein concentration in the elution fraction was determined.

B) Mutants of RNA polymerase I

Mutants of Pol I were purified in the same way than wild-type polymerases with the exception of Pol I ΔA49. It was purified from yeast strain #2670 , a BY4742 derivative with a chromosomal knockout of A49, rescued by A49 being expressed from a plasmid under the control of the GAL promoter. To ensure optimal growth, a 20ml YPG culture was inoculated to an OD_{600} of 0.1 and grown overnight at 30°C. Depletion of A49 was carried out for ~ 48h in two steps. First, 50ml YPD were inoculated to an OD_{600} of 0.05 and grown for 24h at 30°C. The main culture (2l YPD) was then started at an OD_{600} of

0.005 and grown at 30°C under shaking to an OD_{600} of 1.5 (≥ 24h). From here, the described protocol was followed (3.2.10 A). Absence of subunit A49 was controlled with Western analysis and iTRAQ LC MALDI-MS/MS and the growth phenotype was monitored.

C) Transcription factor IIF (TFIIF)

TFIIF was purified from yeast strain #2994 (DSY5 Int3), a kind gift from the Cramer lab. Cloning and yeast genetic manipulation are explained in (Chen et al. 2010). In this strain, the TFIIF subunits Tfg1, 2 and 3 are expressed under the ADH promoter, with Tfg2 being expressed as a fusion protein with a C-terminal tandem affinity purification (TAP) tag. A 20ml YPD culture was grown to stationary phase at 30°C. From this culture, 2l of YPD were inoculated to an OD_{600} such that it would result in an OD_{600} of 1.5 after overnight cultivation at 30°C. At OD_{600} 1.5, the cells were harvested (4000g, 6min, RT) and washed in ice cold water. Cells were split in aliquots representing 800ml culture volume and again spun down (4000g, 6min, 4°C). Cell aliquots were frozen in liquid nitrogen and stored at -20°C.

TFIIF was purified in general like wild-type RNA polymerases as described (3.2.10 A). Diverging from this protocol, TFIIF purifications were performed in three different salt conditions (200mM, 300mM or 500mM KCl). TFIIF was eluted in P2 (KOAc).

3.2.11 Cloning strategy for the *in vitro* transcription template library

The constructed library was developed using the set of template-containing plasmids created in (Merkl 2009) and was further extended in the same systematical approach.

A first subset of templates contains cis-elements of the 35S rDNA terminator (**Fig. 4-1**). It is based on vectors #1960 (pUC19 tail G- TER), #1961 (pUC19 PIP G- TER), #1251 (pUC19 PIP G-ENH) and #1257 (pUC19 tail G- ENH). Here, "TER" refers to the terminator region spanning trom the T-rich 1 element to the 3' end of the RFB, whereas "ENH" templates lack the first T-rich site (4.1.2). Reeder and co-workers showed that Reb1 is involved in the termination of Pol I transcription *in vitro* and *in vivo* (Morrow et al. 1993; Reeder et al. 1999) and stated, that a fraction of Pol I is terminated at T1. In our *in vitro* transcription system this results in short RNAs (<100nt) whose detection is at the technical limit of the gel system. Therefore, 125bp of the 18S rDNA amplified with primers #2479 and #2480

were inserted into EcoRI cut and blunted vectors #1251 and #1257 and SacI cut and blunted vectors #1961 and #1960. This resulted in plasmids #2148 (pUC19 PIP G- TER elong), #2145 (pUC19 tail G- TER elong), #2147 (pUC19 PIP G- ENH elong) and #2144 (pUC19 tail G- ENH elong) carrying additional 125bp upstream of the rDNA terminator cis-elements. To include the possibility of studies involving Rnt1, template vectors were constructed containing a larger version of TER starting at -20bp with respect to the end of the 25S rDNA hence including the Rnt1 cleavage site (#1963 [pUC19 PIP G- Rnt TER] and #1962 [pUC19 tail G- Rnt1 TER]). Elongated template vectors were obtained as described before (#2149 [pUC19 PIP G- Rnt1 TER elong] and #2146 [pUC19 tail G- Rnt1 TER elong]). To study the cis-element dependency of elongation roadblocks or termination events, templates were constructed lacking or carrying an inverted version of the Reb1 BS (#2246 [pUC19 tail G- TER noReb elong] and #2245[pUC19 tail G- TER Reb1inv elong]). Deletion (inversion) of the Reb1 BS was achieved by insertion of the AflII/ BamHI digested PCR amplicons obtained with primers #3793 (#3792) and #2105 on plasmid #1960 into equally cut vector #2145, respectively. This also involved the creation of a blunt-end PsiI cutting site in the Abf1 binding site by introduction of a point mutation. Thus, from these vectors templates with or without the RFB can be prepared. The PsiI site was also introduced in plasmid #2247 (pUC19 tail G- TER elong PsiI) by amplification and re-ligation of the complete plasmid #2145 with primers #3796 and #3797.

A series of templates for *in vitro* transcription containing one or multiple 601 nucleosome positioning sequences (Lowary & Widom 1998) was created (**Fig. 4-2**). The subset is comprised of the vectors #1247 (pUC19 PIP G- 601), #1253 (pUC19 tail G- 601), #1252 (pUC19 PIP G- 12x601), #1258 (pUC19 tail G- 12x601) and #2249 (pUC19 tail G- 601 elong). The first four constructs are described in detail in (Merkl 2009). #2249 was created by insertion of an EcoRI/KpnI digested amplicon with primers #3798 and #3799 (18S rDNA, 125bp) into the equally cut vector #1253. The insertion was made upstream of the 601 sequence, to increase length and thus detectability of prematurely terminated/abortive transcripts.

Vectors #1573 (pUC19 tail G- w/o BS) and #1959 (pUC19 PIP G- w/o BS) were constructed by re-ligation of the EcoRI/HindIII fragment of vectors #1254 and #1248, respectively. The resulting templates do not contain binding sites for one of the investigated DNA-binding proteins (**Fig. 4-1**).

Templates with a cluster of three LexA binding sites were described in (Merkl 2009). An elongated version of the tailed template vector was created by insertion of 125bp upstream of the LexA binding sites as described before, resulting in vector #2244 (pUC19 tail G- 3xLexA elong). In (Merkl 2009) template vectors with a part of the mouse rDNA terminator region containing 5 binding sites for the termination factor TTF-I were created (#1249, #1250, #1255 and #1256). Digestion of plasmid #1255 with EcoRV/DraI, EcoRV/SapI and EcoRV/SalI followed by agarose gel purification resulted in

derivative templates containing two, one or a half binding site, respectively. Based on studies by Tschochner and co-workers (Tschochne & Milkereit 1997), template vectors were designed containing one (#1561 [pUC19 tail G- 1xLacR] and #1562 [pUC19 PIP G- 1xLacR]) or two (#1563 [pUC19 tail G- 2xLacR] and 1564 [pUC19 PIP G- 2xLacR]) binding sites for the Lac repressor LacI or the complete Lac operator DNA sequence (#1572 [pUC19 tail G- LacO]). Hence, the annealed oligos #2619/#2620, #2621/#2622 or #2623/#2624 were cloned into the EcoRI/BamHI digested vectors #1247 or #1253, respectively. Furthermore, a hybrid template with the ENH region followed by two LacI binding sites was created (#1571 [pUC19 tail G- ENH 2xLacR]). Plasmid #1574 (pUC19 tail G-tRNA Ala) contains the yeast alanyl tRNA gene to provide a template which is transcribed by Pol III *in vivo*.

Vectors containing a complete yeast rDNA repeat or a BamHI/SacI fragment thereof were constructed. Plasmids #1965 (pUC19 PIP rDNA BamHI/SacI) and #1964 (pUC19 tail G- rDNA BamHI/SacI) were constructed by insertion of the SacI/BamHI rDNA fragment from vector #190 into the equally digested vectors #1247 and #1253, respectively. The missing part of the 18S rDNA gene was introduced via ligation of the SacI digested amplicon obtained by PCR with primers #3055 and 18S_end_rev on vector #190 with the equally digested plasmids #1965 and 1964, respectively. This resulted in plasmids #1967 (pUC19 PIP G- rDNA) and #1966 (pUC19 tail G- rDNA).

To adapt the *in vitro* transcription system to the assay established by the Kashlev group (Komissarova et al. 2003; Kireeva et al. 2000), a recognition site for TspRI was introduced upstream of the third template module (4.1.1) in plasmids #1247, #1255, #1960, #1573 and #1254. The annealed oligos #3119 and #3120 were introduced at the respective 5' restriction site of the third module via blunt-end ligation which resulted in plasmids #1968, #1969, #1970, #1971 and #1972.

3.2.12 *In vitro* transcription

In general, the protocol for *in vitro* transcription is based on the method published by Tschochner and co-workers (Tschochner 1996). The assay was further developed, partially newly established (Merkl 2009) and used in this work. As in most *in vitro* transcription systems, the underlying principle is homogeneous incorporation (body labeling) of radioactively labeled nucleotides. In this case, [α-^{32}P]-CTP was used. All ingredients were purchased RNAse free or checked for RNase contamination by incubation with genomic RNA from *S. cerevisiae*. The RNA was then separated on a

polyacrylamide gel and visualized under UV light. RNase free water was obtained from the standard water purification apparatus.

A) Template preparation

The system is suitable for transcription from promoter containing templates (Tschochner 1996) as well as for tailed templates (Keener et al. 1998). Template plasmid libraries were generated as described in (Merkl 2009) and an overview of available constructs is given in (**Table 3-11**). Plasmids containing *in vitro* transcription templates with the Pol I promoter were linearized with PvuII (1.5h, 37°C). The restriction enzyme was then heat inactivated at 80°C for 20min, the DNA was EtOH precipitated (3.2.2 E) and redissolved in RNase free water.

Tailed templates were first cut out of the respective vector with EcoRV and PvuII or EcoRV and PsiI (1.5h, 37°C), followed by incubation for 20min at 65°C to inactivate EcoRV. The DNA was EtOH precipitated, washed with 70% EtOH (3.2.2 E) and resuspended in RNase free water. Next, the DNA was treated with the sequence specific nicking endonuclease Nb.BsmI (NEB) at 65°C for 1.5h to introduce a single strand break in the coding strand. PvuII and Nb.BsmI were heat inactivated by incubation at 80°C for 20min. After 10min, a competitor oligo (#2207) with the same sequence as the 24nt tail overhang was added in excess to anneal with the 5' single strand DNA released upon the nicking reaction. The DNA was subjected to EtOH precipitation, resuspended in RNase free water and its concentration determined.
Transcription on a tailed template starts right at the point, where the DNA becomes double stranded again. Pol I promoter template transcription starts in the core element (CE I), 8 bp from its 3’ end.

B) Reaction setup and RNA extraction

Buffers and solutions are summarized in (**Table 3-9**). A standard basic reaction contained:

substance	***final concentration/quantity***
template DNA	~200fmol (30-100ng)
[α-^{32}P]-CTP (400Ci/mmol, 10µCi/µl, Hartmann Analytic)	1.25µM (1µl)
cold CTP (100µM)	24µM (4,8µl)
mix of cold ATP, UTP and GTP (10mM each)	0.5mM each (1µl)

2.5M KOAc	50mM/150mM (0,4µl/1.2µl)
10x new transcription buffer (NTB)	1x (2µl)
RNasin	10-20U (0.5µl)
RNA polymerase (3.2.10)	1µl
RNase free H_2O	to 20µl

Table 3-24: Standard basic *in vitro* transcription reaction.

All substances were thawed and kept on ice until the start of the reaction and filter tips were always used. If multiple reactions were carried out, a mastermix was prepared from the constituents except recombinant proteins, chromatin and RNA polymerases. If applicable, protein factors binding to cis elements on the transcription template were added and the reaction was mixed and incubated for 15min at RT. The reaction was always started by addition of the polymerase, immediately mixed thoroughly and incubated for 30min at 30°C. Incubation was done in a hybridization oven, to overcome condensation of water on the microreaction tube lid and thus altering salt concentrations.

Transcription was stopped by addition of 200µl Proteinase K mix and subsequent incubation at 37°C for 15min. Afterwards, 22µl of 3M NaOAc, 2µl glycogen solution (5mg/ml, Ambion) and 750µl EtOH were added and the RNA precipitated at -20°C over night. The precipitate was spun down by centrifugation at 16000g for 20min at 4°C, the supernatant was discarded and the pellet was washed with 50µl 70% EtOH. After a second centrifugation step at 16000g for 20min at 4°C, the pellet was dried at 90°C for 15s. For gel electrophoresis, the sample was redissolved in 9µl of loading buffer. RNA secondary structures were denatured by heating the solution to 70°C for 10min followed by immediate incubation on ice.

Transcription with T7 RNA polymerase (NEB) was conducted as described in the manufacturer's protocol, incubation time was 1h at 37°C and the RNA workup was done as described before.

C) Denaturing gel electrophoresis and transcript visualization

The transcripts were separated via denaturing PAGE. Electrophoresis was carried out on a vertical, 0.4mm thick polyacrylamide gel of approximately 25x10cm. The glass plates, spacers and the comb were treated with 0.1% SDS to remove RNases, washed with RNase free water and 70% ethanol. One plate was silanized with the GelSave solution (Applichem) and the gel was cast. The usual concentration of acrylamide was 5% with 0.3% bisacrylamide. The buffer was 0.5x TBE and the denaturing agent urea at a concentration of 7M. The recipe is given here:

Ingredient	*10% gel*	*5% gel*
30% AA /0.8% BisAA stock solution (Roth)	6.6ml	3.3ml
5xTBE	2ml	2ml
H_2O	4.7ml	8ml
urea	6.4g	6.4g
TEMED	20µl	20µl
20% APS	100µl	100µl

Table 3-25: Denaturing polyacrylamide gels for RNA electrophoresis.

After polymerization, the gel was kept for no longer than one day at 4°C and then used. The gel was inserted into the apparatus, the tanks were filled with 0.5xTBE buffer and the comb was removed. Not polymerized acrylamide in the pockets and air bubbles were removed by flushing with a syringe. To avoid inhomogeneous running behavior of the gel due to temperature gradients, a pre-electrophoresis was done at constant 25W and a limit of 1150V for 1h. Afterwards, the pockets were flushed again, to remove urea, diffusing from the gel. Electrophoresis was carried out at constant 25W with a limit of 1150V for approximately 30min. The gel was transferred to whatman filter paper and dried at 80°C for 45min.

The radioactive transcripts were visualized by exposure to a previously erased imaging plate (Fuji) and the read-out was done on a FLA 3000 phosphoimager (Fuji).

D) Transcript quantification

In vitro transcription images were quantified with Multi Gauge (Fuji). Compared to the template of interest, equal molar amounts of a reference template (tail g- w/o BS) were co-transcribed in every reaction. Thus every lane of the resulting gel showed a signal obtained from this transcript which served as an internal control. All lanes were quantified with the function “profile” and the background was subtracted automatically as a polygonal line. Peaks were assigned by the software according to the default settings and the assignment was manually reviewed. Signal intensities were calculated as $\frac{total\ pixels - background}{peak\ area}$ and normalized to the signal intensity of the reference transcript.

For absolute determination of transcript mass, a dilution series of a solution with known concentration of [α-^{32}P]-CTP was created. Equal volumes of the diluted solutions were spotted in duplicate on whatman paper and exposed together with the gel of interest. After visualization, the spots were quantified with the function "quant" in Multi Gauge and a calibration curve generated. The signal intensities of the bands of interest were also determined with "quant" and absolute transcript mass was calculated by correlation with the calibration curve.

E) Preparation of an *in vitro* transcribed RNA marker

To determine the length of *in vitro* transcribed RNAs, a radioactively labeled RNA marker was included in every gel run. RNA marker templates were purchased (Century™ Plus RNA marker, Ambion) and transcribed with T7 RNA polymerase according to the manufacturer's protocol. Briefly, 0.5µg of the template mix were incubated with 3µl of [α-^{32}P]-CTP (400Ci/mmol, 10µCi/µl), 0.5mM of each NTP, 0.5µl RNasin and 50U of T7 RNA polymerase in T7 RNA polymerase buffer. The reaction volume was 20µl and incubation was done at 37°C for 1h. The RNA workup was performed as described (3.2.11 B). Transcription of the marker templates results in a mixture of RNAs with lengths of 100, 200, 300, 400, 500, 750 and 1000nt.

CHAPTER IV – RESULTS

4.1 Creation of a template library for *in vitro* transcription

4.1.1 Outline

Development of a template library was the first step in establishment of a solid *in vitro* transcription system. To address the questions outlined in 2.5, the respective templates had to contain i) yeast Pol I terminator cis elements, ii) recognition sites for the DNA binding factors which were analyzed regarding their ability to serve as elongation obstacles or iii) positioning sequences for nucleosomes. The constructed library is based on the set of template-containing plasmids created in (Merkl 2009) and was further developed in the same systematical approach.

Each template consists of three main DNA modules. The first module carries elements for transcription initiation. This is either the RNA polymerase I (Pol I) promoter (PIP) from *Saccharomyces cerevisiae* (*S. cerevisiae*, yeast) (Kempers-Veenstra et al. 1985) or a single stranded 3' extension (tail) to the template strand (Dedrick & Chamberlin 1985). PIP templates can be transcribed by the PA600 extract (Tschochner 1996) or a mixture of core factor (CF) and the Pol I-Rrn3 complex (unpublished data), thus allowing promoter-specific initiation in analogy to the *in vivo* situation. Initiation on tailed templates does not depend on additional factors, which allows comparative investigation of elongation and termination of various RNA polymerases. The second module serves to stall elongating RNA polymerases. This is achieved by a G-less cassette of 22nt length, which contains no cytosine in the template strand. Thus, if GTP is missing in the reaction, the polymerase will stop when encountering three cytosine residues. Transcription can be resumed upon addition of GTP. The third DNA module is variable and contains different cis-elements. These elements allow comparison of DNA binding factor-dependent elongation and termination of RNA polymerases in absence or

presence of the respective factor. A schematic overview of the templates is given in **Fig. 4-1** and **Fig. 4-2** and all parent vectors are listed in **Table 3-11**. Cloning strategies are explained in (3.2.11). Several templates exist in short and long versions ("elong"). If not indicated otherwise, the elongated versions were used in the assays.

4.1.2 Template cis-element combinations

A) Templates containing elements of the yeast rDNA terminator

A subset of templates contains different cis-elements of the yeast rDNA terminator and combinations thereof. The respective tailed templates are listed in **Fig. 4-1**. In this context, "TER" refers to a sequence in the rDNA terminator region between +70 and +414bp downstream of the end of the 25S rRNA gene, covering the first T-rich stretch (T-rich 1), the Reb1 binding site (Reb1 BS), an Abf1 binding site, the second T-rich stretch (T-rich 2) and the replication fork barrier (RFB, 2.3.3 A). In contrast, the "Reb1 BS RFB" template contains a truncated version of the TER DNA sequence starting at +96bp and thus missing T-rich 1. To include the possibility of studies involving Rnt1, template vectors were constructed containing a larger version of TER, starting at -20bp with respect to the end of the 25S rDNA, hence including the Rnt1 cleavage site. To study the cis-element dependency of elongation roadblocks or termination events, templates were constructed lacking or carrying an inverted version of the Reb1 BS or missing the RFB (**Fig. 4-1**).

B) Templates containing the 601 nucleosome positioning sequence

RNA polymerases encounter nucleosomes during transcription *in vivo*. To investigate how different RNA polymerases deal with an elongation obstacle like the nucleosome, templates for *in vitro* transcription containing one (1x 601) or multiple (12x 601) 601 nucleosome positioning sequences (Lowary & Widom 1998) were created (**Fig. 4-2**).

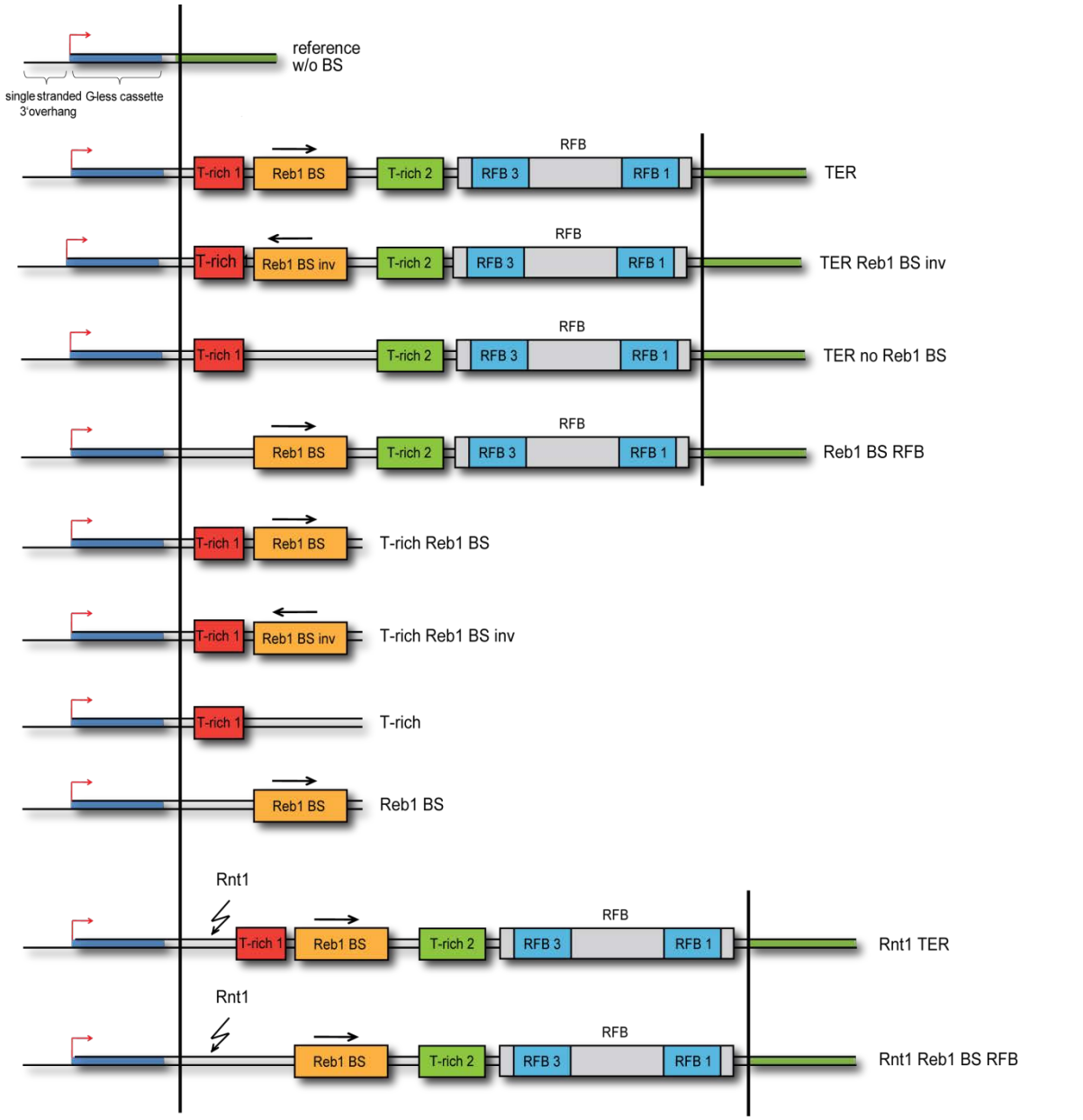

Fig. 4-1: Schematic representation of tailed templates containing different cis elements of the yeast rDNA terminator region. The initiation sequence and the G-less cassette are indicated. The red arrow marks the transcription start site. Selected cis elements of the rDNA terminator are represented by colored boxes. Exact positions of the respective elements in the rDNA are given in the text. Arrows indicate whether the cis element was inserted in the same orientation compared to an enlongating RNA polymerase *in vivo* or inverted. The Rnt1 cleavage site is visualized by a flash.

C) Internal reference template

The Internal reference template (reference w/o BS) does not contain binding sites for one of the investigated DNA-binding proteins (**Fig. 4-1**). Furthermore, it was demonstrated, that the factors of interest do not interact specifically with the template DNA nor interfere in *in vitro* transcription

(4.5.2, 4.3.1, 4.3.2, 4.3.3, 4.3.4). Thus, transcript signal intensities from these templates were used as a *bona fide* internal control for normalization during quantification and the templates were included in every *in vitro* transcription reaction.

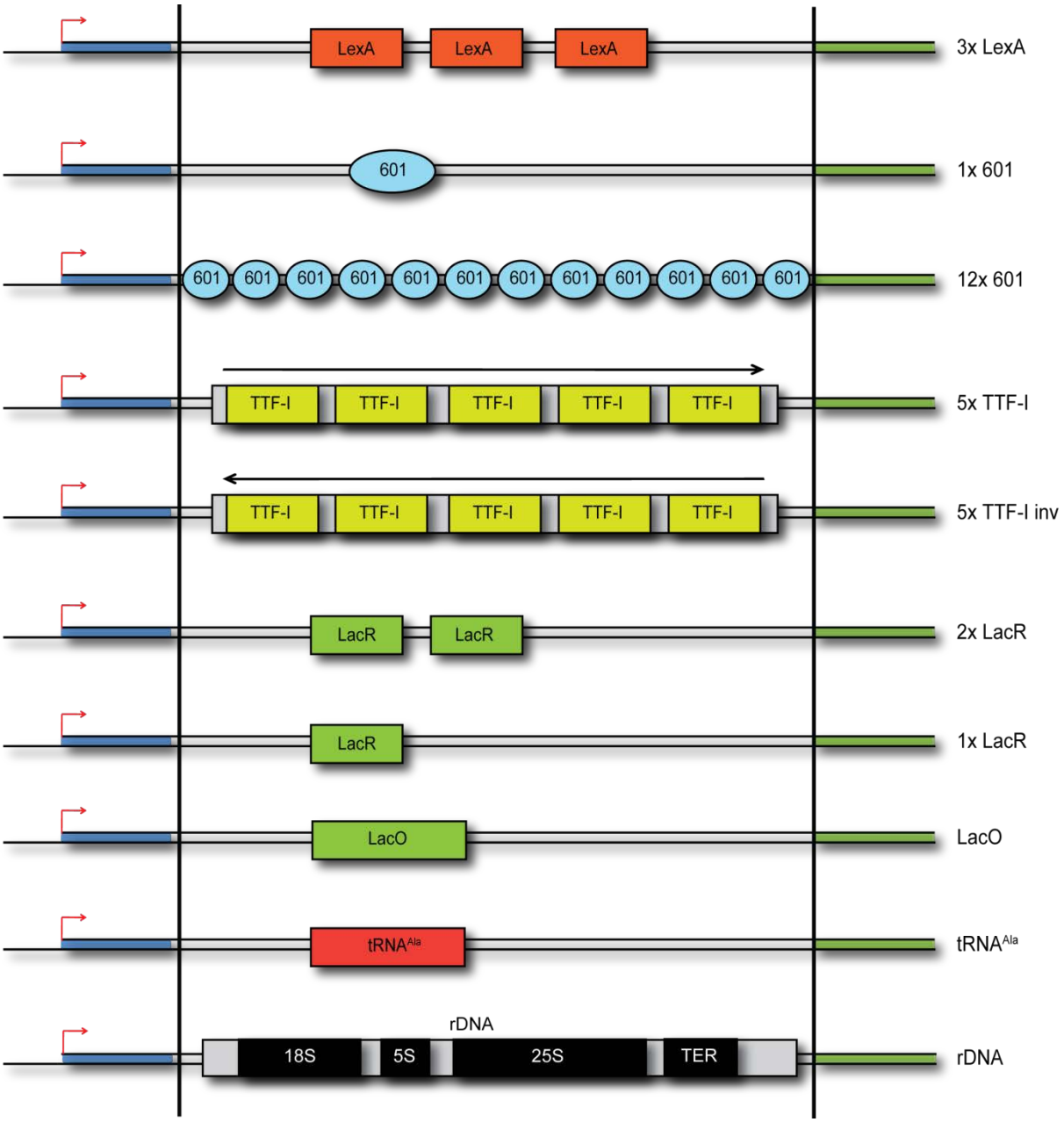

Fig. 4-2: Selected tailed templates containing different cis elements. The red arrow marks the transcription start site. Cis elements are represented by colored boxes and ellipses. Identity of the respective elements in the rDNA is discussed in the text. Arrows indicate, whether the cis element is in the same orientation compared to an enlongating RNA polymerase *in vivo* or inverted.

D) Templates with binding sites for non-yeast proteins

Templates with binding sites for non-yeast proteins were constructed to elucidate RNA polymerase diversity at transcriptional roadblocks (**Fig. 4-2**). In (Merkl 2009), templates containing a cluster of three LexA binding sites (3x LexA) or a part of the mouse rDNA terminator region harboring 5 binding sites for the termination factor TTF-I (5x TTF-I) were described. Based on observations that termination by TTF-I is dependent on the orientation of its binding sites (Jansa et al. 2001; Grummt, Rosenbauer, et al. 1986; Schnapp et al. 1996), a template with the inverted mouse rDNA terminator sequence was constructed (**Fig. 4-2**). According to studies by Tschochner and co-workers (Tschochne & Milkereit 1997), template vectors were designed containing one (1xLacR) or two (2xLacR) binding sites for the Lac repressor LacI or the complete Lac operator DNA sequence (LacO) (**Fig. 4-2**).

E) Other templates

Template "$tRNA^{Ala}$" contains the yeast alanyl tRNA gene to provide a template which is transcribed by Pol III *in vivo* (**Fig. 4-2**). Vectors containing a complete yeast rDNA repeat (rDNA) or a BamHI/SacI fragment thereof (rDNA BamHI/SacI) were constructed, to compare transcription of the naked 35S rDNA with *ex vivo* purified 35S rDNA (Hamperl 2012) *in vitro* (**Fig. 4-2**).

4.2 Purification and characterization of RNA Pol I, II and III from *S. cerevisiae*

4.2.1 Outline

Objectives of this study included the comparison of Pol I, II and III in their capability to deal with elongation obstacles and the comparison of wild-type Pol I with Pol I mutants in transcription termination. To assay different RNA polymerases in comparable conditions, it was necessary to purify

Pol I, II and III equally. In this regard, a standardized purification protocol was established combined with thorough characterization of the protein content of the polymerase fraction.

4.2.2 Wild-type and mutant RNA polymerases can be purified in one step

Yeast RNA polymerases were purified in one step as described in (3.2.10). Cells were harvested in logarithmic phase to ensure maximum polymerase activity and expression levels. The purification strategy is based on immunoprecipitation of a C-terminal Protein A (Prot A) tag on one of the second largest subunits A135, Rpb2 or C128 with IgG-coupled magnetic beads. This purification method was chosen because recently Oeffinger and co-workers demonstrated that IgG-coupled magnetic beads reduce background contaminants and improve the yield in affinity purification of yeast RNP complexes (Oeffinger et al. 2007). In general, a slightly modified protocol of Oeffinger was followed using IgG-coupled magnetic beads. Upon elution, the ProtA tag was cleaved off with TEV protease to rule out diminished activity due to steric hindrance (**Fig. 4-3 A**).

First purifications were carried out with buffers containing 200mM KOAc (**Table 3-4**) which yielded elution fractions (E), in which the respective RNA polymerase was sufficiently enriched and pure for *in vitro* transcription. On Coomassie-stained SDS gels, the two largest subunits A190/A135, Rpb1/Rpb2 or C160/C128 could be detected in the lane containing the eluate (10µl, 10%) together with TEV protease (**Fig. 4-3 A**). Presence or absence and identity of the ProtA tag and single subunits were confirmed by Western analysis. Mono Q anion exchange chromatography (Jochen Gerber) (**Fig. 4-3 B)**, LC-MALDI MS/MS analysis (**Fig. 4-4)** and silver staining (data not shown) revealed the presence of the remaining subunits. Polymerase activity was finally demonstrated by *in vitro* transcription.

To this end, wild-type Pol I, II, III and several Pol I mutants were purified. The Pol I mutant library includes Pol I deletion mutants lacking either subunit A12.2 or the A49/34.5 dimer. Deletion of A49 or A49/A34.5 results in reduced Pol I activity and thus a reduced growth phenoptype (Huet et al. 1975; Liljelund et al. 1992). The dimer is believed to be a built-in elongation factor with similar function like TFIIF in Pol II (Kuhn et al. 2007). Thus, Pol I Δ A49 is an interesting candidate for *in vitro* elongation/termination analysis. Subunit A12.2 is required for cleavage of the nascent RNA (Kuhn et al. 2007) like its homolog C11 in Pol III (Chédin et al. 1998) and was identified as a Pol I termination factor (Prescott et al. 2004). Furthermore, deletion of A12.2 is synthetically lethal, if serine residue 685 in subunit A190 is mutated to aspartate (Gerber et al. 2008, **Fig. 4-3 D**). Therefore, Pol I Δ A12.2,

Pol I A190 S685A and Pol I S685D were candidates to be included in the subsequent analyses. Furthermore, a series of Pol I phosphomutants was purified based on results of a mutagenesis screen of the A190 serine residues (J. Pérez-Fernández, unpublished data) and the work described in (Gerber et al. 2008). Hence, one or all serine residues which were identified as phosphosites in the largest subunit A190 were exchanged to alanine or aspartate which includes mutations A190 SallA, A190 SallD, A190 S936A, A190 S936D, A190 S941A and A190 S941D.

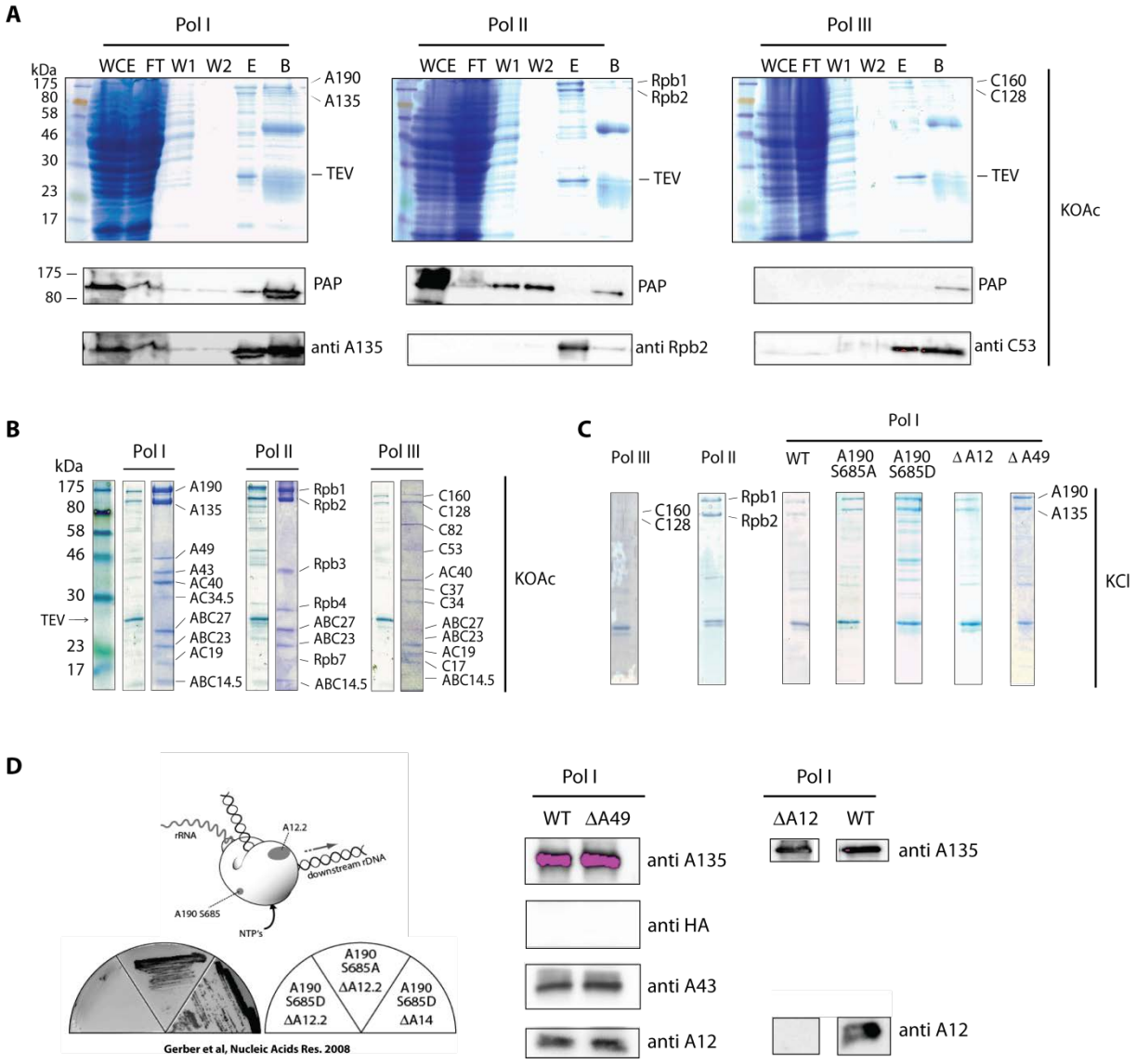

Fig. 4-3: Yeast RNA polymerases can be purified in one step. (A) Coomassie stained 10% SDS gels of wild-type Pol I, II and III purifications in KOAc conditions. Fractions from left to right: whole cell extract (WCE, 0.6%), flowthrough of the IP (FT, 0.6%), washing steps (W1, 0.7%; W2, 0.7%) elution fraction (E, 10%) and beads after elution (B, 50%). The two largest subunits of Pol I, II or III and TEV protease are indicated. Western blots representing the same fractions as above were developed with antibodies directed against Protein A (PAP) or the specific polymerase subunits A135, Rpb2 and C53. **(B)** One-step purified polymerases (KOAc conditions) and the polymerase peak fractions after MonoQ ion exchange chromatography were separated on a 10% SDS gel. **(C)** Coomassie stained 10% SDS gels of one-step purified RNA polymerases and Pol I mutants (KCl conditions, 10% of IP). **(D)** Western blots of Pol I, II and III purifications (KCl conditions)

were developed with antibodies against specific subunits A135, Rpb2 and C53. Fraction abbreviations and loading are explained in (A). Western blots developed with the anti C53 antibody exhibit signals around 50kDa due to cross-reactivity with the IgG heavy chain. **(E)** Cartoon from (Gerber et al. 2008) visualizing the synthetic lethality of mutation A190 S685D in combination with deletion of subunit A12.2. Western blots of Pol I ΔA12 and Pol I ΔA49 in comparison with the wild-type were done after separation on a 10% SDS gel. Blots were developed with antibodies recognizing subunits A135, A43, A12.2 and the 3xHA tag.

The absence of subunit A12.2 from the respective Pol I mutant purification was confirmed by Western blotting and development with an antibody recognizing A12.2 (**Fig. 4-3 E**). Pol I ΔA49 was purified from BY4742 ΔA49 pGAL A49-3xHA in which the chromosomal copy of the A49 gene is knocked out and A49 is expressed from a plasmid under the control of the GAL promoter. Hence, the purification was carried out after A49 had been depleted for 48h after shifting to glucose. Since loss of A49 is believed to destabilize the polymerase, the presence of subunits A135, A43 and A12.2 was verified by Western blot. In the respective strain, A49 was 3xHA tagged. The tag could not be detected in Western analysis of a Pol I ΔA49 preparation thus pointing towards homogeneity of Pol I ΔA49 (**Fig. 4-3 E**). Note that the absence of subunit A34.5 was not formally proven in this study but other studies demonstated that A49 and A34.5 form a distinct subcomplex which is associated with the Pol I core (Geiger et al. 2010). In a Pol I ΔA34.5 also A49 was missing (Gadal et al. 1997) and a Pol I ΔA49 was lacking subunit A34.5 (Beckouet et al. 2008). Therefore it can be hypothesized that our Pol I ΔA49 also lacks subunit A34.5.

4.2.3 Purified RNA polymerases are not cross-contaminated

To show that the purified polymerase fractions were not cross-contaminated with transcription factors and other RNA polymerases, Western analyses and mass spectrometric analyses with the isobaric tags for relative and absolute quantification (iTRAQ) were carried out (3.2.7)(Ross et al. 2004). Polymerase samples were first depleted of the His-tagged TEV protease by incubation with Ni-NTA agarose to avoid overloading of HPLC and mass spectrometer and thus diminished detection sensitivity. After digestion with trypsin, the resulting peptides were separately labeled with two, three or four different isotopic iTRAQ reagents depending on the number of fractions to be compared. Chemically, a covalent bond is formed between the peptide reactive group of the iTRAQ reagent and the peptide N-terminal α-amino groups as well as ε-amino groups of lysines. The differentially labeled fractions were combined and the peptides separated by reversed-phase high performance liquid chromatography (HPLC) followed by MALDI MS/MS analysis (3.2.7). A database

search based on the fragmentation data identified the peptides and so the respective proteins. Fragmentation of the isobaric tag creates unique reporter ions in the low m/z region of the respective MS/MS spectra. Reporter ion signal intensities allow calculation of the relative abundance of a peptide (single iTRAQ ratio) and thus of the protein of interest (average iTRAQ ratio).

Comparative analysis of Pol I, Pol II and Pol III purifications revealed, that specific polymerase subunits were enriched in the respective purification up to factor 100 with regard to the other purified polymerase fractions (**Fig. 4-4**). Subunits common to all three polymerases could be detected at roughly equal levels. If Pol I and Pol III were compared, the two common subunits AC40 and AC19 were present at similar levels. Note that common subunits sometimes do not result in an expected iTRAQ ratio of 1 as the protein concentration slightly varies between purifications of Pol I, II or III. The obtained results allow to state that purified RNA polymerases are not significantly cross-contaminated.

However, iTRAQ analysis showed, that the Pol II purification (KOAc conditions) contained subunits Tfg1, Tfg2 and Taf14 of transcription factor IIF (TFIIF) as well as transcription factors Spt5 and Spt6 (data not shown). Hence, a more stringent purification procedure had to be established to rule out that effects seen in an *in vitro* transcription assay are due to the co-purified factors. Polymerase purification was then switched to new buffers containing 200mM KCl instead of KOAc (**Table 3-4**). Albeit the second washing step and elution were still done in KOAc buffer conditions to ensure comparability of the differently purified polymerases in the transcription assay. In general, yield, enrichment and purity of the polymerase fractions were comparable to the previous conditions (**Fig. 4-3 C**). With antibodies recognizing subunits A135, Rpb2 or C53, specific signals were only obtained in Western analysis of the respective polymerase preparation (**Fig. 4-3 D**) indicating absence of polymerase cross-contamination. Subsequent MALDI analysis demonstrated that if the purification was done with 200mM KCl, TFIIF Spt4 and 5 could not be detected in the Pol II fraction (**Fig. 4-4**).

In all purifications, a similar content of ribosomal proteins (data not shown) and housekeeping proteins could be detected via mass spectrometry. Proteins belonging to these groups mostly had an average iTRAQ ratio of close to 1 and were often identified with only one peptide. Therefore, their abundance was generally low and comparable in the analyzed purifications.

In summary, the established protocol for RNA polymerase purification is complying with the three prerequisites for *in vitro* transcription formulated above. If not stated otherwise, all *in vitro* transcription experiments were executed with KCl-purified polymerases.

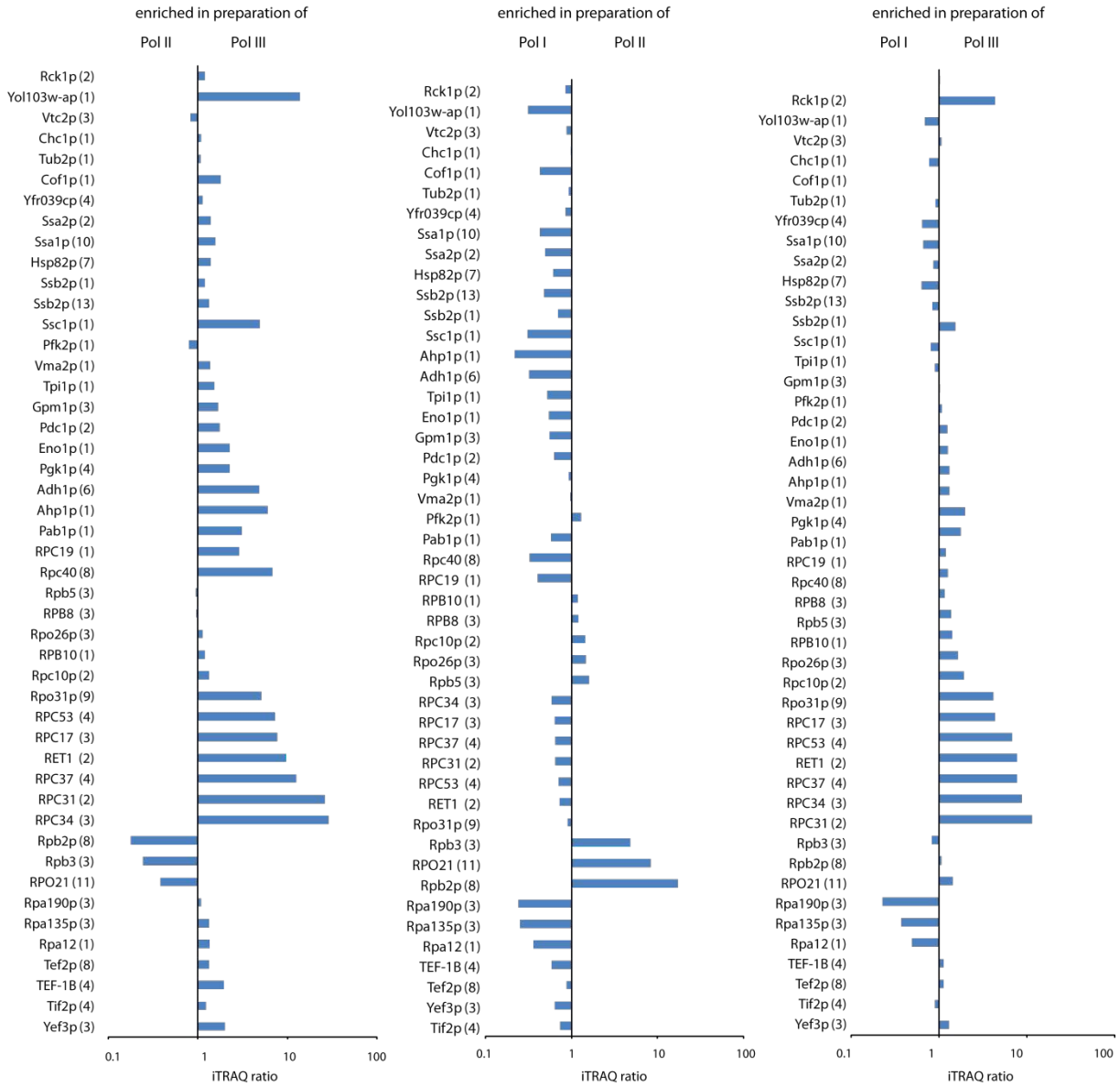

Fig. 4-4: Comparative iTRAQ analysis of RNA polymerase preparations purified with KCl demonstrates selective enrichment. Pol I, II and III preparations were subjected to comparative iTRAQ analysis versus each other. Average iTRAQ ratios of identified proteins were plotted against a list enumerating all identified proteins. The number of allocated peptides per protein is given in brackets. Robosomal proteins were excluded from the diagrams. Note the log 10 scale of the x-axis.

4.3 Purification and characterization of trans-acting protein factors

4.3.1 Reb1-His_6

A) Reb1-His_6 can be purified in high yield and purity in a two-step procedure

The yeast rDNA repeat contains two binding sites for Reb1, one of them in close proximity to the Pol I promoter region and a second one in the 5' part of the enhancer/terminator region (Morrow et al. 1989; Chasman et al. 1990). Additionally, binding sites for Reb1 occur frequently in promoter regions of Pol II genes (Liaw & Brandl 1994). Reb1 was described by the Reeder group as a potent Pol I termination factor *in vitro* and *in vivo* (Reeder et al. 1999; Morrow et al. 1993; Lang & Reeder 1995). However, recent data indicate that efficient transcription termination requires further factors (Reiter et al. 2012). For comparison, Reb1 has to be included in any analysis of Pol I transcription termination.

A first purification protocol for recombinant Reb1 from *E. coli* was established by Morrow and co-workers (Morrow et al. 1990; Morrow et al. 1993) and further developed in (Merkl 2009, **Fig. 4- A**). Nonetheless, baculovirus-mediated expression in SF21 insect cells would have been advantageous. In general, this expression system leads to better solubility of the proteins and post-translational modifications of this cell line are similar to the ones observed in yeast. However, the attempts to express Reb1 in SF21 cells failed (data not shown). Therefore, the original protocol was refined to yield highly purified Reb1-His_6 in large quantities (3.2.9). Purification was done as described by Morrow and co-workers and the results are shown in (**Fig. 4-5**). The apparent molecular weight of Reb1-His_6 was calculated from a calibration curve resulting in 103kDa with an error of 1%, which is above the theoretical value (92.7kDa) (**Fig. 4-5 C**). Quantification of the Reb1-His_6 protein concentration (3.2.6 E) resulted in 1.27mg/ml (13.7µM) for fraction E2 and 0.81mg/ml (8.7µM) for E3, respectively.

However, the elution fraction lanes contained further Coomassie stained bands. Western analysis with the INDIA His probe indicated that some of the additional bands could be N-terminal truncations of Reb1-His_6. Nonetheless, a visible background of contaminating proteins presumably from *E. coli* remained. To assess, if those proteins influence further downstream applications like *in*

vitro transcription, an equal mock purification was carried out from an *E. coli* culture transformed with the empty vector. Notably, the band pattern observed in SDS PAGE analysis of the mock elution fractions, showed similarity to the background in Reb1-His_6 elution fractions.

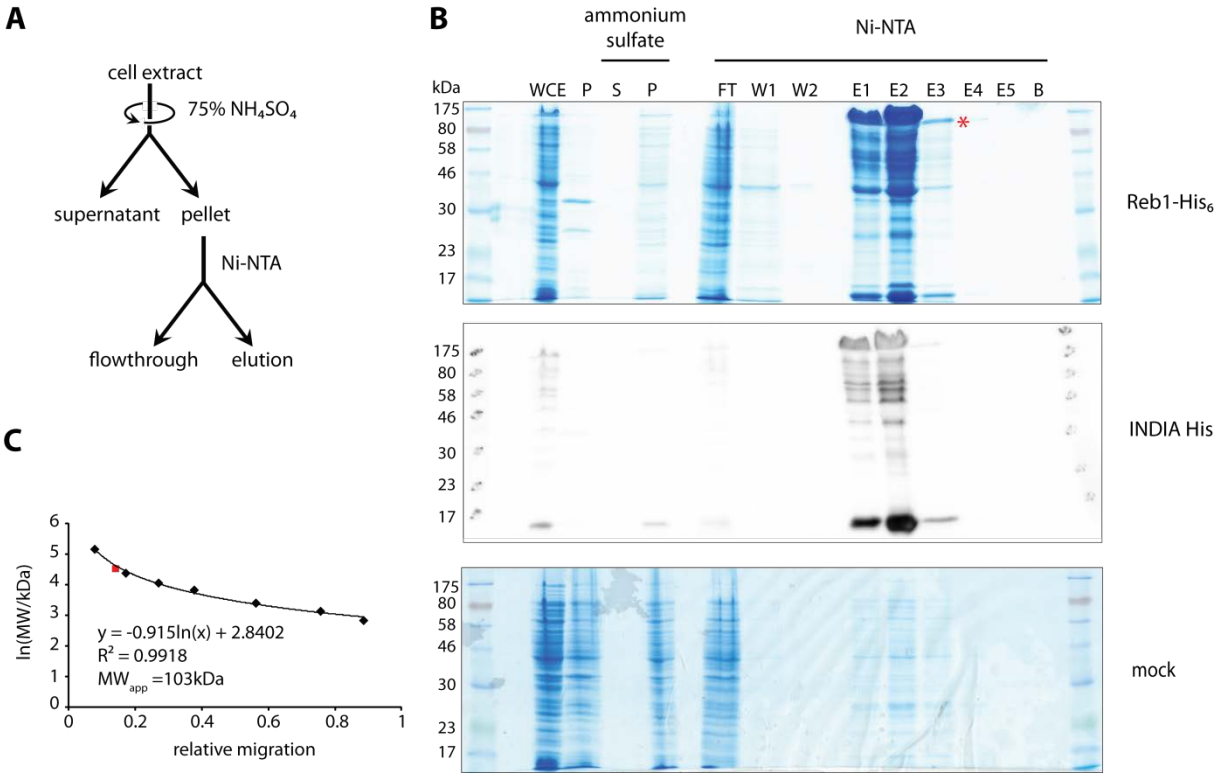

Fig. 4-5: Reb1-His_6 is purified in a two-step procedure. (A) The cleared cell extract was fractionated by addition of ammonium sulfate to 75%. The precipitate was redissolved and subjected to Ni-NTA affinity chromatography. **(B)** Fractions collected during the Reb1 purification were separated on a 10% SDS gel. From left to right: whole cell extract (WCE, 0.1%), insoluble fraction (P, 0.1%), supernatant of the ammonium sulfate precipitation (S, 0.027%), pellet of the ammonium sulfate precipitation (P, 0.2%), flowthrough of the Ni-NTA column (FT, 0.2%), washing steps (W1 & W2, 0.07%), elution frations (E1-E5, 4%), beads after elution (B, 50%). The band representing Reb1-His_6 is marked with a red asterisk (*). For Western analysis, identical amounts were analyzed. The blot was developed with a probe detecting the His_6 epitope. Fractions collected during a respective mock purification from *E. coli* were separated on a 10% SDS gel and visualized with Coomassie blue. **(C)** A calibration curve for the determination of the apparent MW of Reb1-His_6 was calculated from the migration distances of the marker proteins in the topmost gel of (B). The curve was approximated with a logarithmic function and the apparent MW calculated. The red dot indicates the ln of the MW of Reb1-His_6.

B) In gel filtration chromatography, Reb1-His_6 behaves like a pentamer

Gel filtration of Reb1-His_6 was performed to assess the question of sample homogeneity. 50µl of elution fraction E2 (**Fig. 4-5**) were separated on a Superose6 column as described (3.2.6 J) with Reb1 elution buffer as the eluent. The collected fractions were subjected to SDS PAGE and the proteins

were detected with Coomassie staining (**Fig. 4-6**). The chromatogram showed a minor peak at the beginning, representing the void volume (fractions 3-4) and two major peaks (fractions 13-15 [P1] and 22-25[P2]). Between the two major peaks, absorption did not reach background levels nor form a single peak either (fractions 17-21 [P3]). Correlation with the SDS gel revealed that P3 contained contaminating proteins of different sizes and P2 mainly consisted of the major low molecular weight contaminant (< 17kDa). In contrast, most of the full length Reb1-His_6 was detected in P1. This indicated that fraction E2 and thus presumably the other elution fractions contained an almost homogeneous population of Reb1-His_6. To address the question of the multimerization state, a calibration curve was calculated from elution volumes of marker proteins with known molecular weights. Taken the apparent molecular weight of 103 kDa as a basis, Reb1-His_6 seems to form a pentamer (510kDa). However, further studies on the multimerization of the trans-acting factors were not within the scope of this work.

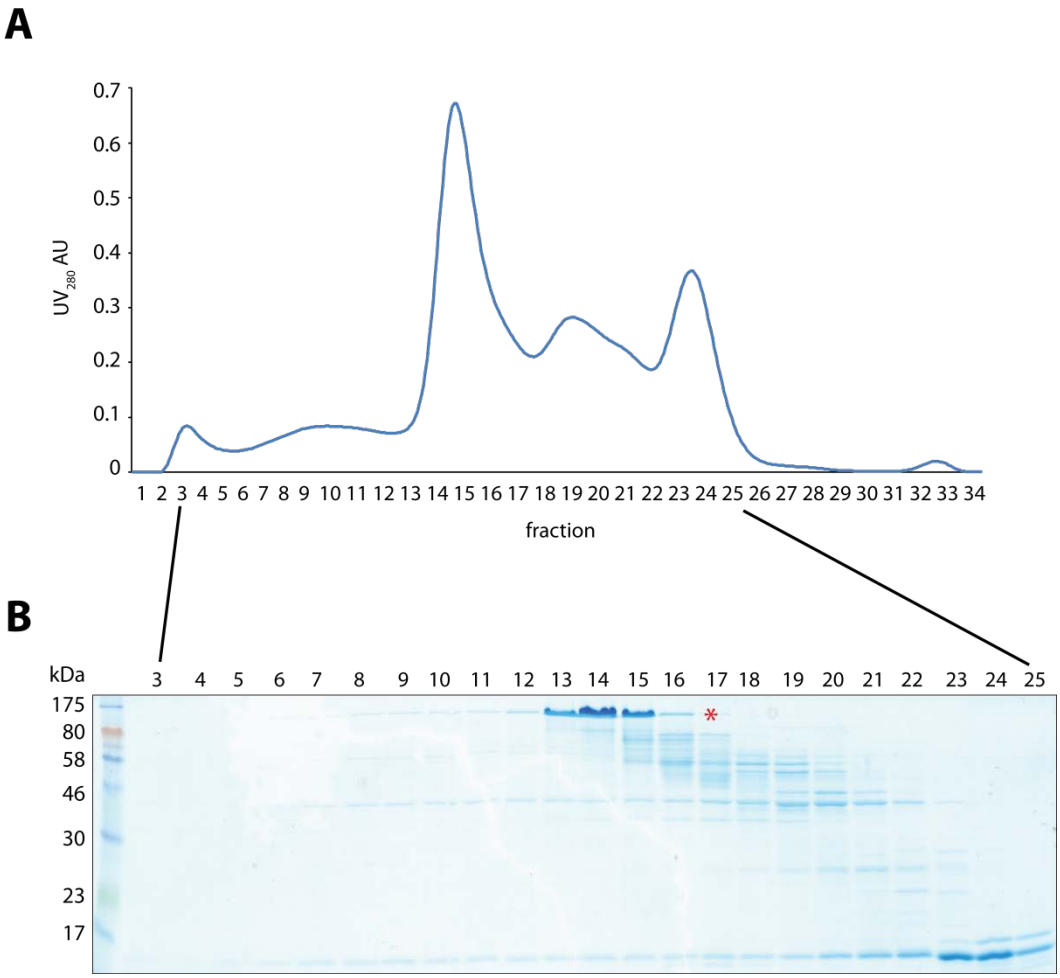

Fig. 4-6: Gel filtration analysis reveals a homogeneous population of Reb1-His_6. (A) Gel filtration was performed with 50µl of fraction E2 (**Fig. 4-5**) on a Superose6 column with a SMART system. UV_{280} absorption was detected and arbitrary units were plotted against the fraction number. **(B)** 4% of fractions 3 to 25 collected during the run were analyzed on a 10% SDS gel. The band respresentng Reb1-His_6 is marked with a red asterisk (*).

C) Reb1-His$_6$ specifically recognizes its binding site in the rDNA terminator

Reb1-His$_6$ was further characterized by testing its ability to bind its designated recognition site in the rDNA terminator and the specificity thereof. Additionally, it was crucial to determine an optimal Reb1-His$_6$ concentration where the binding site was fully occupied. In (Wang & Warner 1998), Reb1 binding to three recognition sites named A, B and C 5' upstream of its own gene was analyzed. K_D values of 25nM (A), 70nM (C) and 250-700nM were estimated from gel shift experiments. Thus, electrophoretic mobility shift assays (EMSA) were conducted as described (3.2.6 K). EMSA templates, specific and unspecific competitors were designed mimicking the *in vitro* transcription situation as closely as possible. Furthermore, buffer, ionic strength and template concentration were chosen equally to *in vitro* transcription conditions. This allowed drawing direct conclusions of binding site occupancy in a respectively performed transcription assay.

Experiments were conducted with three different specific DNA targets. The first target (T-rich Reb1 BS) was created by annealing oligos #3109 and #3110 resulting in a 60bp DNA fragment with a Cy5 label. It contained the sequence reaching from +75bp to +135bp downstream of the end of the 25S rDNA gene including T1 and the Reb1 binding site. The second target (Reb1 BS) contained the sequence between +95bp and +135bp including the Reb1 BS and a random 5' part. It was obtained by annealing oligos #3113 and #3114 resulting in a 56bp Cy5-labeled DNA fragment. The third target (TER) was created via PCR using primers #3051 and #3486 producing a 344bp Cy5 labeled amplicon representing the complete terminator region including the RFB (+70bp to +414bp). Equal constructs were created with unlabeled oligos (#3476, #3477 and #3050) to test the specificity of the DNA binding activity. For unspecific competition experiments, a Cy3-labeled 55bp DNA was chosen, which is a part of the third module of the reference *in vitro* transcription template (4.1.2 C). Therefore, oligos #3111 and #3112 (55nt) were annealed.

In titration assays with a constant DNA concentration of 10nM and the Reb1-His$_6$ concentration ranging from 17.5nM to 1.4µM, DNA binding activity could be verified on all three templates (**Fig. 4-7 A, B, E**). Gel electrophoresis revealed a band resembling shifted DNA which appeared first at roughly 50nM Reb-His$_6$ and increased in intensity when Reb1-His$_6$ was added up to 175nM. Above this concentration, slower migrating bands could be detected probably due to an emerging superstructure. At the highest concentration of Reb1-His$_6$, the DNA did not enter the gel, pointing to the formation of random protein-DNA aggregates. The binding behavior did not significantly depend on the template used, leading to the conclusion that the only cis-element within the rDNA terminator

influencing Reb1 binding was its designated binding site. Specific and unspecific competition assays were performed at fixed Reb1-His_6 concentrations of 175nM (Reb1 BS) or 350nM (T-rich Reb1-BS) and 10nM template DNA (**Fig. 4-7 C, D**). Specific and unspecific competitor DNA were titrated in stepwise from 10nM to 0.5µM. The specific competitor induced a significant decrease in signal intensity of the shifted DNA band starting at low concentrations. Contrary, the signal intensity decreased very slightly even at high concentrations of the unspecific competitor.

In summary, Reb1-His_6 binds specifically to the binding site in the rDNA terminator. The binding is not influenced by other cis elements present in a DNA stretch ranging from position +70bp to +414bp from the end of the 25S rDNA gene. In *in vitro* transcription, Reb1 is used at 700nM final concentration if not otherwise stated, which marks full occupancy of the template DNA (**Fig. 4-7 E**).

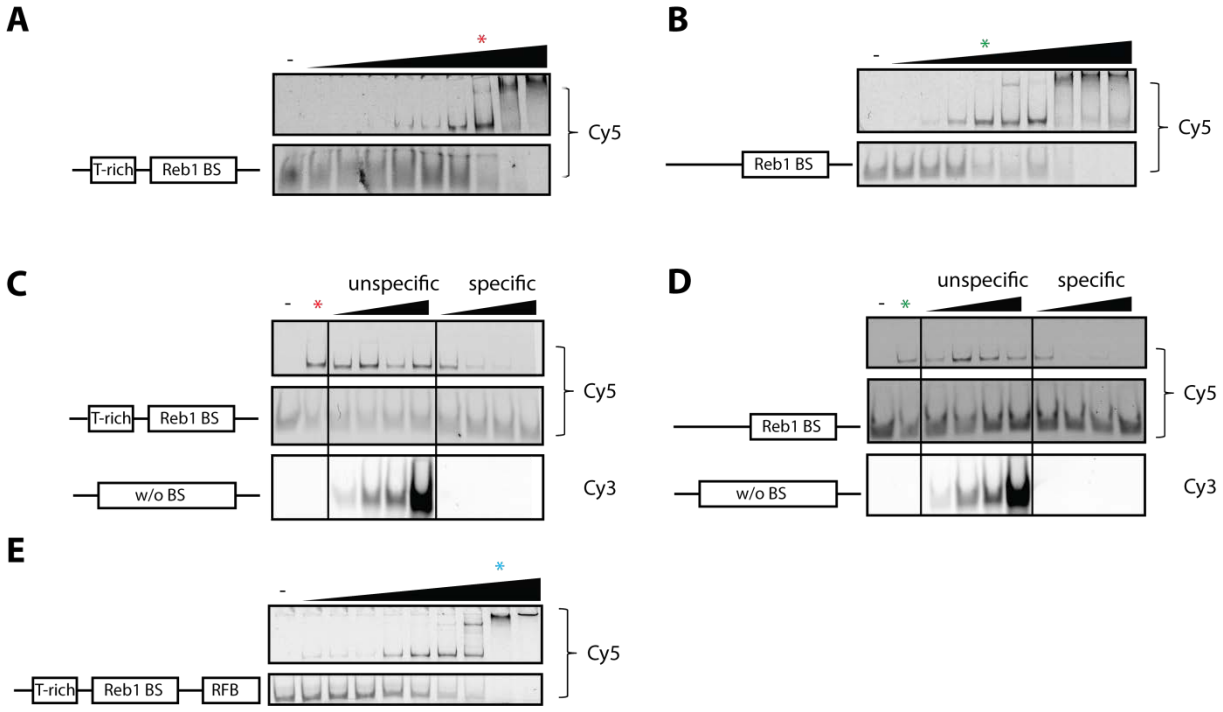

Fig. 4-7: EMSAs demonstrate specific binding of Reb1-His_6 to the yeast rDNA terminator Reb1 binding site. Reb1 was titrated on Cy5-labeled templates containing the T-rich element and the Reb1 BS **(A)** or only the Reb1 BS **(B)** or the complete rDNA terminator region **(E)**. From left to right: No protein control, titration of Reb1 in steps (17.5nM, 26.25nM, 35nM, 61,25nM, 87.5nM, 175nM, 350nM, 700nM, 1.4µM). Template DNA concentration was 10nM. **(C)** and **(D)**: Specificity of Reb1 binding was challenged in competition assays with templates containing the T-rich element and the Reb1 BS or only the Reb1 BS. From left to right: No protein control, positive control (marked with red or green asterisk), titration series of the unspecific competitor in 4 steps 10nM, 50nM, 100nM, 500nM, titration series of the unspecific competitor in 4 steps 10nM, 50nM, 100nM, 500nM. The blue asterisk (E) marks full occupancy of the template and thus the condition used in *in vitro* transcription. Samples were allowed to equilibrate for 15min at RT and then separated on a 6% native PA gel. DNA bands were visualized in a FLA3000 fluorescence reader. Titration of the unspecific competitor was monitored via Cy3 fluorescence.

4.3.2 Nsi1 / Ydr026c

A) Establishment of a strategy to purify Nsi1 from SF21 insect cells

Nsi1 or Ydr026c was just recently described as a *bona fide* termination factor for Pol I *in vivo* in yeast (Reiter et al. 2012). Moreover, Ha and colleagues suggested that Nsi1 plays a role in silencing of rDNA repeats (Ha et al. 2012, p.1). Thus, Nsi1 is an obvious candidate for thorough analysis in an *in vitro* transcription system for elongation/termination. In a newly developed strategy, recombinant Nsi1 was expressed in SF21 insect cells using the MultiBac system (3.2.5) as an N-terminal FLAG tag fusion protein (**Fig. 4-8 A**). FLAG-Nsi1 was purified via immunoprecipitation (IP) with an anti-FLAG M2 agarose matrix as described (3.2.9 A). For elution, two different methods were tested: Addition of the FLAG peptide or cleavage with TEV protease via a recognition site between the tag and Nsi1. Elution efficiency turned out to be comparable however, TEV cleavage results in an untagged version of Nsi1 which is preferable. Hence, all further purifications were carried out with TEV protease. The purification success was monitored by SDS PAGE and Western analysis.

SDS PAGE and Coomassie staining revealed that the elution fraction (E) contained only the two characteristic bands for TEV protease as well as an additional band with the expected size of Nsi1 (66.5kDa) (**Fig. 4-8 B**). No antibody is available for Nsi1. Nonetheless, Western analysis of the whole cell extract (WCE) and the elution (E) fractions with an antibody detecting Reb1 resulted in a signal at the position where Nsi1 is expected (apparent MW 62.4kDa)) (**Fig. 4-8 C**). Since Nsi1 was purified recombinantly from insect cells and the molecular weight of yeast Reb1 is 92kDa, presence of a 66.5kDa truncated version of Reb1 was very unlikely. Albeit it is speculative, the structural similarity of Reb1 and Nsi1 may explain a cross-reactivity of the polyclonal antibody. The purifications yielded highly purified Nsi1 in low amounts. Different purifications were very comparable with Nsi1 concentrations (3.2.6 E) ranging from 1.4µM to 1.7µM.

Strategies to express Nsi1 in larger quantities in *E. coli* with a C-terminal His_6 tag and an N-terminal GST tag were successful on the purification level, however failed as no road-blocking activity could be detected in *in vitro* transcription (data not shown). Purification of Nsi1 from yeast with a C-terminal TAP tag according to the polymerase purification protocol was unsuccessful (data not shown).

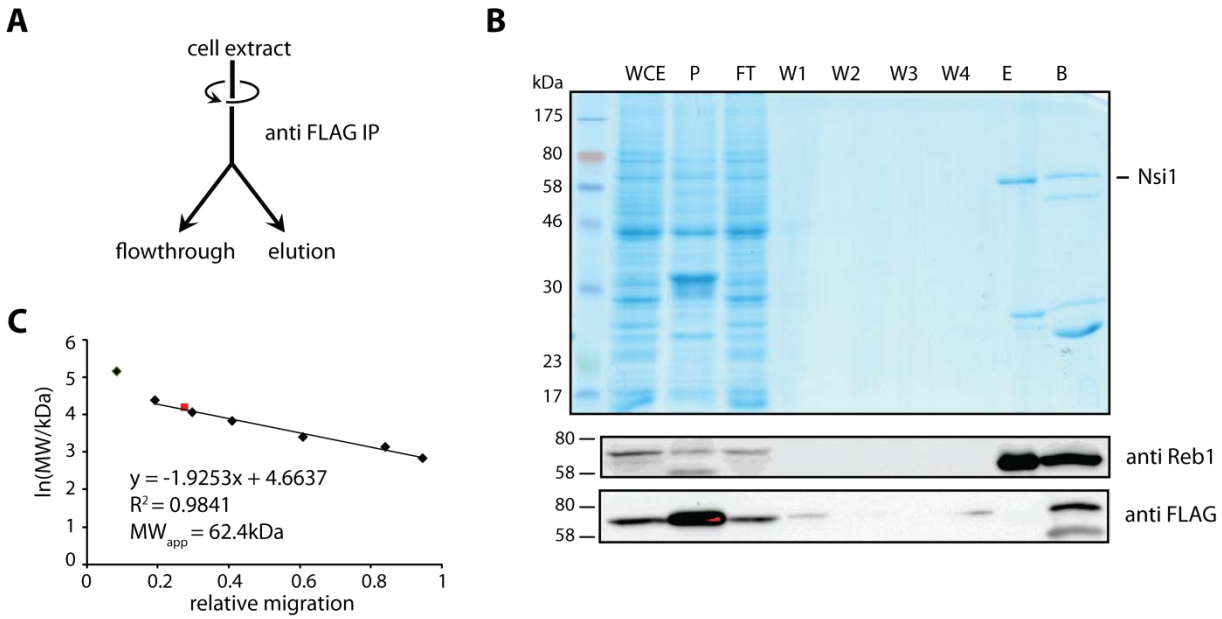

Fig. 4-8: Nsi1 is purified in one step from SF21 insect cells. (A) The clear cell extract from 50x10^6 cells was subjected to anti FLAG immune precipitation. Nsi1 was eluted with the FLAG peptide or via TEV cleavage of the FLAG tag. **(B)** Fractions collected during the purification of Nsi1 (TEV cleavage) were separated on a 10% SDS gel and visualized by Coomassie staining. From left to right: whole cell extract (WCE, 0.04%), pellet (P, 0.04%), flowthrough of the IP (FT, 0.04%), washing steps (W1 – W4, 0.2%), elution fraction (E, 5%), beads after elution (50%). For Western analysis, identical amounts were separated on a 10% SDS gel. The blot was developed with antibodies directed against Reb1 and the FLAG epitope. **(C)** A calibration curve for the determination of the apparent MW of Nsi1 was calculated from the migration distances of the marker proteins in the Coomassie gel. The curve was approximated with a linear function and the apparent MW calculated. The red dot indicates the ln of the MW of Nsi1.

B) Nsi1 exhibits DNA binding activity in gel shift experiments

A binding motif for Nsi1 which is nearly identical with the recognition site of Reb1 was identified in a mass spectrometry based yeast proteome screen (Fleischer et al. 2006). Therefore, templates T-rich Reb1 BS and TER (4.3.1 C) were used to characterize the DNA binding ability of Nsi1. EMSAs were conducted as described in (3.2.6 K) and designed to mimic the *in vitro* transcription situation as closely as possible (4.3.1 C). The main focus laid on determination of template occupancy by Nsi1. Thus, experiments were carried out with the template DNA concentration held constant at 10nM and Nsi1 being titrated from 3.2nM to 320nM. In contrast to EMSAs with Reb1 and Fob1, only a faintly stained blurred band representing the shifted DNA could be detected (**Fig. 4-9**). Additionally, upon higher concentrations of Nsi1, signals were observed in the gel pockets pointing to random aggregate formation. This suggests that either EMSA conditions were not optimal to detect this interaction, Nsi1 concentration was to low or Nsi1 binding is mediated by other factors. However, the amount of

free DNA clearly decreased upon increased levels of Nsi1. The binding pattern slightly changed, if the TER template was used. Here, the free DNA signal vanished when 320nM Nsi1 were used. In summary, it was shown that Nsi1 exhibits DNA binding activity. Specificity thereof could not be addressed, due to the low signal intensity of the shifted DNA. Therefore, the question of functionality had to be addressed in *in vitro* transcription assays (**Fig. 4-24**) in which unless otherwise stated the standard Nsi1 concentration was 88nM.

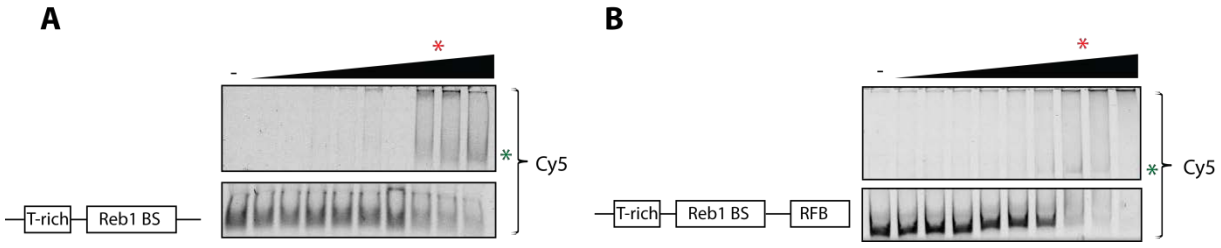

Fig. 4-9: Nsi1 binds to templates containing cis elements of the yeast rDNA terminator. Nsi1 was titrated on Cy5-labeled templates containing the T-rich element and the Reb1 BS **(A)** or the complete rDNA terminator region **(B)**. From left to right: No protein control, titration of Nsi1 in steps (3.2nM, 4.8nM, 6.4nM, 11.3nM, 16.1nM, 40.3nM, 80.5nM, 161nM, 320nM). Template DNA concentration was 10nM. Samples were allowed to equilibrate for 15min at RT and then separated on a 6% native PA gel. DNA bands were visualized in a FLA3000 fluorescence reader. The red asterisk marks the Nsi1 concnetration which was used in *in vitro* transcription, the green asterisk marks the blurred band representing shifted DNA.

4.3.3 Fob1

A) Establishment of a strategy to purify Fob1 from SF21 insect cells

Fob1 was described as a factor involved in blocking of the DNA replication fork from entering the 35S rDNA, and was linked to homologous recombination events of the yeast rDNA (Kobayashi & Horiuchi 1996). Additionally, Fob1 was implicated to function in Pol I transcription termination (El Hage et al. 2008). A known target to which Fob1 binds *in vivo* is the replication fork barrier (RFB) in which three sites (RFB 1-3) were identified as being responsible for the blocking activity (Ward et al. 2000; Kobayashi 2003). One aim of this study was to elucidate the influence of Fob1 on Pol I transcription termination and its general road-blocking ability for RNA polymerases.

Fob1 was expressed as an N-terminal FLAG fusion protein in SF21 cells as described in (3.2.5). Like Nsi1 (4.3.2), Fob1 was purified via IP with anti-FLAG M2 beads (3.2.9 A). Elution was either performed by addition of the FLAG peptide or cleavage with TEV protease. Both methods yielded

Fob1 in comparable amounts and purity. TEV-eluted Fob1 was used in all further described experiments if not stated otherwise. The purification was monitored via SDS-PAGE and Western blotting. On a Coomassie stained SDS gel including all fractions collected during the purification, the lane containing a sample of the elution fraction (E) showed three distinct bands (**Fig. 4-10 B**). Around 25kDa, two bands probably representing TEV protease were visible while the third band was in the range of the theoretical molecular weight of Fob1 (65.3kDa). Other contaminants could not be detected on Coomassie level. No antibody was available recognizing Fob1. Therefore, a purification where elution was done with the FLAG peptide was used for Western analysis. FLAG-Fob1 was detected with antibody #83 directed against the FLAG epitope. The fusion protein was detected in every fraction of the purification including the eluate. Note that the Western blot showed two signals in the lane of the eluate fraction, which could be due to a C-terminal proteolytic fragment of Fob1. This second band was also visible in other Coomassie gels of Fob1 purifications. An apparent MW of 64.2kDa was calculated.

In summary, a strategy for purification of recombinant Fob1 from SF21 cells was developed, yielding highly pure protein. In repetitive purifications, Fob1 concentrations ranged from 6.5µM to 8.5µM. Attempts to purify Fob1 from *E. coli* as a GST fusion protein or from yeast with a C-terminal TAP tag, failed (data not shown).

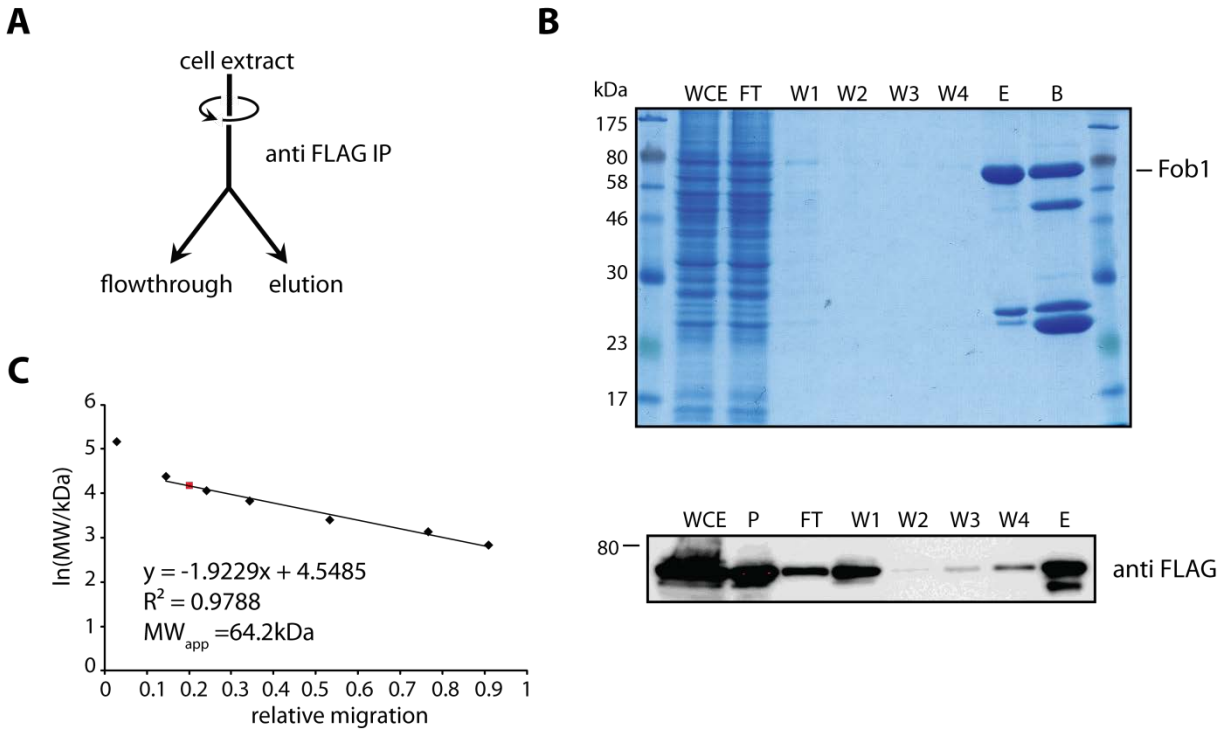

Fig. 4-10: Fob1 is purified in one step from SF21 insect cells. (A) The clear cell extract from 50x10^6 cells was subjected to anti FLAG immune precipitation. Fob1 was eluted with the FLAG peptide or via TEV cleavage of the FLAG tag. **(B)** Fractions collected during the purification of Nsi1 (TEV cleavage) were separated on a 10% SDS gel and visualized by Coomassie staining. From left to right: whole cell extract (WCE, 0.04%), pellet (P, 0.04%), flowthrough of the IP (FT, 0.04%), washing

steps (W1 – W4, 0.2%), elution fraction (E, 5%), beads after elution (50%). For Western analysis, identical amounts were separated on a 10% SDS gel. The blot was developed with an antibody directed against the FLAG epitope. **(C)** A calibration curve for the determination of the apparent MW of Fob1 was calculated from the migration distances of the marker proteins in the Coomassie gel. The curve was approximated with a linear function and the apparent MW calculated. The red dot indicates the ln of the MW of Nsi1.

B) Gel filtration suggests multimerization of Fob1

Gel filtration of Fob1 was performed as described (3.2.6 J) to shed light on sample homogeneity. 50µl of purified Fob1 eluted with the FLAG peptide were separated on a Superose6 column with TAP100 buffer (**Table 3-5**) as the eluent. Fractions were collected and analyzed via SDS-PAGE and Coomassie staining. The chromatogram showed three distinct peaks, of which the first (fractions 2-4) represented the void volume (**Fig. 4-11**).

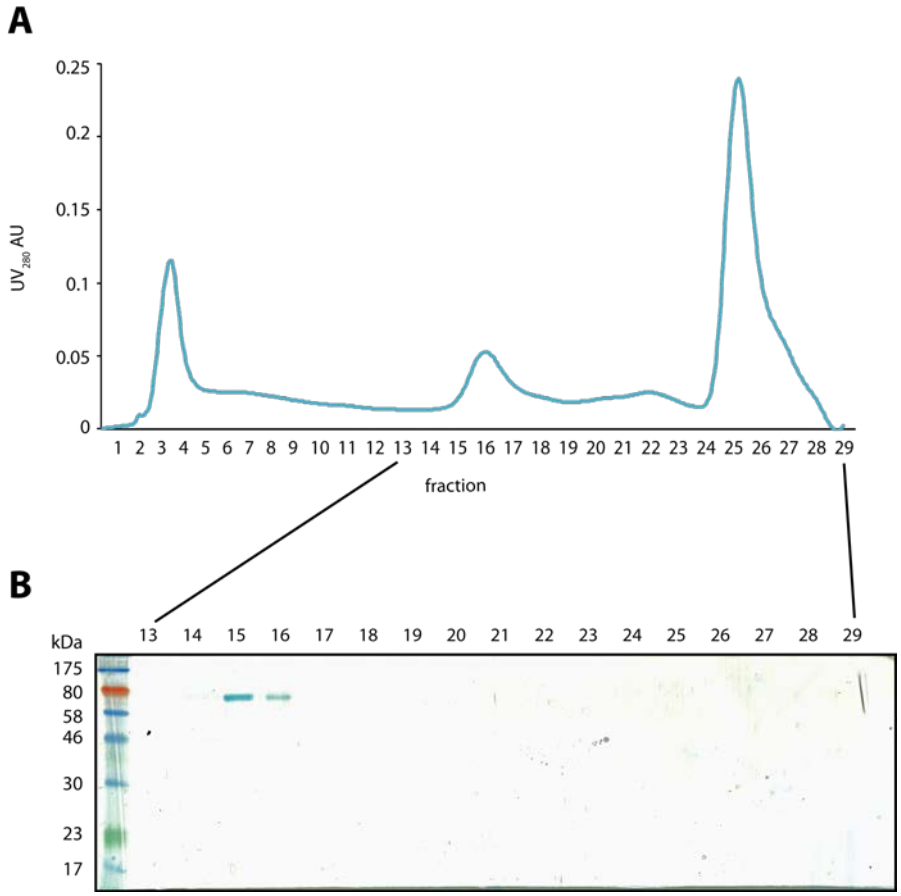

Fig. 4-11: Gel filtration analysis of Fob1. (A) Gel filtration was performed with 50µl of fraction E (**Fig. 4-10**) on a Superose6 column with a SMART system. UV_{280} absorption was detected and arbitrary units were plotted against the fraction number. **(B)** 4% of fractions 13 to 29 collected during the run were analyzed on a 10% SDS gel.

Peak two reached from fraction 15-17 and the third and largest peak was detected around fractions 25-27. Fractions up to 7 could not be analyzed due to malfunction of the sample collector. SDS gel analysis of fractions 13-30 demonstrated that peak two consisted of Fob1, whereas peak three most certainly contained the FLAG octapeptide, which could not be resolved in a standard gel system.

This indicated that the population of Fob1 obtained by the described purification method was almost homogeneous, albeit not excluding the possibility that the first peak could be due to Fob1 aggregates. The question of possible Fob1 multimerization was addressed by calculation of a calibration curve made up of elution volumes of proteins with known molecular weights. Fob1 eluted at an apparent molecular weight of 252kDa, which is roughly 4 times the apparent molecular weight of 64.2kDa indicating a tetrameric state.

C) Fob1 specifically binds its RFB recognition sites in EMSA experiments

Kobayashi demonstrated that RFB 1 and 3 are specifically bound by GST-Fob1 (Kobayashi 2003) whereas RFB 2 exhibits no or very low Fob1 binding activity. Based on this study, EMSAs were conducted as outlined in (3.2.6 K). To draw conclusions about template occupancy in *in vitro* transcription assays, gel shift conditions were chosen respectively (4.3.1 C). To verify the results of Kobayashi and to elucidate the influence of further rDNA terminator cis elements, a series of Cy5-labeled templates was created. Template RFB 1 (44bp) contained the equally named sequence identified by Kobayashi (+363bp - +383bp from the end of the 25S gene) flanked by random DNA. It was obtained by annealing of oligos #3482 and #3483. Annealing of oligos #3478 and #3480 resulted in template RFB 3 (45bp), which consisted of the RFB 3 region (+265bp – +286bp) flanked by random sequences. In his work of 2003, Kobayashi claimed that the RFB is wrapped around Fob1, implying concurrent binding to both RFB 1 and 3. Therefore, a template with both binding sites was created via PCR with oligos #3051 and #3484 (RFB 1 -3, 160bp) spanning from position +244bp to +404bp. For specific competition assays, an equal set of unlabeled templates was manufactured with oligos #3497 [RFB 3], #3482[RFB1] and 3485[RFB 1-3]). The unspecific competitor was identical to the one used before (4.3.1 C).

In a first approach, Fob1 was titrated from 16nM to 1.2µM on all templates at constant 10nM template concentration (**Fig. 4-12 A, B**). With templates RFB 1 and 3, a band representing shifted DNA was visible upon addition of the lowest amount of Fob1. This band increased in intensity whereas the signal of the free DNA vanished. The highest concentrations of Fob1 led to supershifting likely due to random Fob1 binding activity. However, EMSAs with RFB 1 and RFB 3 showed subtle differences (**Fig.**

4-12 E). With RFB 3, the free DNA signal was not detectable when Fob1 was present at 160nM, whereas with RFB 1 this point was reached between 55nM and 80nM Fob1. Taken into account that Fob1 came from the same purification and the templates were annealed from oligos side by side, uncertainties regarding protein or DNA concentration could be ruled out. Hence, the result suggested, that Fob1 has a bigger affinity for RFB 1 than for RFB 3. This is in agreement with the Kobayashi data from 2003 although it was not commented in the manuscript.

When both RFB 1 and RFB 3 were present in the template, shifted DNA first formed a double band which could represent two states of single occupancy of either the RFB 1 or RFB 3 site (**Fig. 4-12 E**). Upon higher Fob1 concentrations a second, slower migrating sharp band appeared, correlating with vanishing of the free DNA (5nM-80nM). This species might occur when the template was bound by two Fob1 proteins. Further increase in Fob1 probably resulted in formation of random aggregates which could not enter the gel. Interestingly, full occupancy of the RFB 1-3 template was reached at a similar Fob1 concentration than observed with the RFB 1 template, implicating that binding of the RFB1 site is the decisive event. Finally, gel shifts were conducted with the TER template (4.3.1 C), giving similar results as observed with the RFB 1-3 template (**Fig. 4-12 G**).

For specific and unspecific competition studies on RFB 1 and 3 templates, DNA concentration was fixed at 10nM and Fob1 concentration was held constant at 55nM (RFB 1) and 160nM (RFB 3) representing the states of complete shifting. Specific and unspecific competitor DNA was added in four steps between 10nM and 0.5µM. Unspecific competition with both RFB 1 and 3 lead to a minor decrease in the shifted DNA signal (**Fig. 4-12 C, D**). Upon addition of a specific competitor, signal intensity of the shifted DNA decreased substantially. Notably, RFB 1 and RFB 3 show different behavior in this regard as well. Whereas with RFB 1 free DNA signals could only be detected if high amounts of competitor DNA were present, free RFB 3 template was visible at low amounts thereof already. Competition assays performed with the RFB 1-3 template were done at 10nM template and 80nM Fob1 concentrations (**Fig. 4-12 F**). Unspecific competitor was added like before and exerted little effect on the shifted DNA signal. Specific competition was done in two steps with 10nM and 50nM resulting in significant decrease of the shifted band signal.

In summary, data from (Kobayashi 2003) could be verified. Fob1 specifically bound DNA fragments containing the RFB 1 or RFB 3 site. Further EMSAs revealed that other cis elements present in the rDNA terminator did not influence Fob1 binding. Interestingly, binding to the RFB 1 site seemed to occur with a lower affinity than binding to RFB 3.

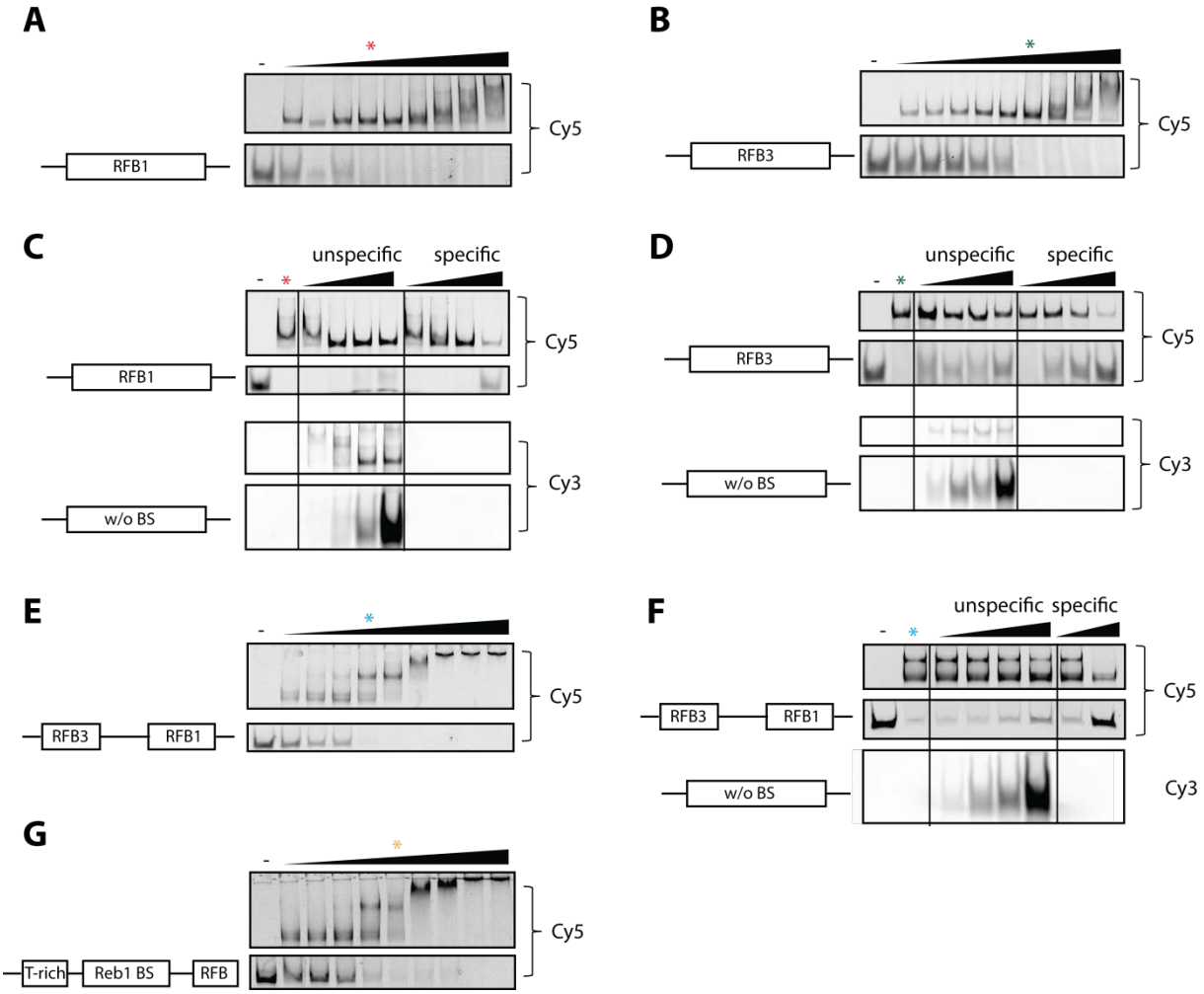

Fig. 4-12: EMSAs demonstrate specific binding of Fob1 to the replication fork barrier. Fob1 was titrated on Cy5-labeled templates containing the RFB1 **(A)**, RFB3 **(B)**, the complete RFB **(E)** or the complete rDNA terminator region **(G)**. From left to right: No protein control, titration of Fob1 in steps (16nM, 24nM, 32nM, 56nM, 80nM, 158nM, 317nM, 635nM, 1.2µM). Template DNA concentration was 10nM. The red (RFB1), green (RFB3) and cyan (RFB1&3) asterisks represent the Fob1 concentrations used in later competition experiments. **(C)**, **(D)** and **(F)**: Specificity of Fob1 binding was challenged in competition assays with templates containing RFB1, RFB3 or the complete RFB. From left to right: No protein control, positive control (marked with red, green or cyan asterisk), titration series of the unspecific competitor in 4 steps (10nM, 50nM, 100nM, 500nM), titration series of the unspecific competitor in 4 steps (10nM, 50nM, 100nM, 500nM). Titration of the unspecific competitor was monitored via Cy3 fluorescence. In (F), the specific competitor was titrated in two steps at concentrations of 10nM and 50nM. The orange asterisk in (G) marks the Fob1 concentration used in transcription experiments. Samples were allowed to equilibrate for 15min at RT and then separated on a 6% native PA gel. DNA bands were visualized in a FLA3000 fluorescence reader.

4.3.4 LexA

A) LexA is purified from *E. coli* as a GST fusion protein

LexA is a well studied strong DNA binding protein in bacteria. Together with RecA, it is one of the major effectors within the SOS system thus being involved in maintenance of genome stability and DNA damage repair (Butala et al. 2009). LexA consists of an N-terminal domain responsible for its DNA binding activity and a C-terminal domain involved in LexA dimerization. Specific DNA binding activity occurs in the context of recognition sites called SOS boxes (CTGTN$_8$ACAG) in dimeric state. As a strong DNA binding protein in a bacterial system, LexA was used as an external reference to elucidate differences in road blocking of eukaryotic polymerases.

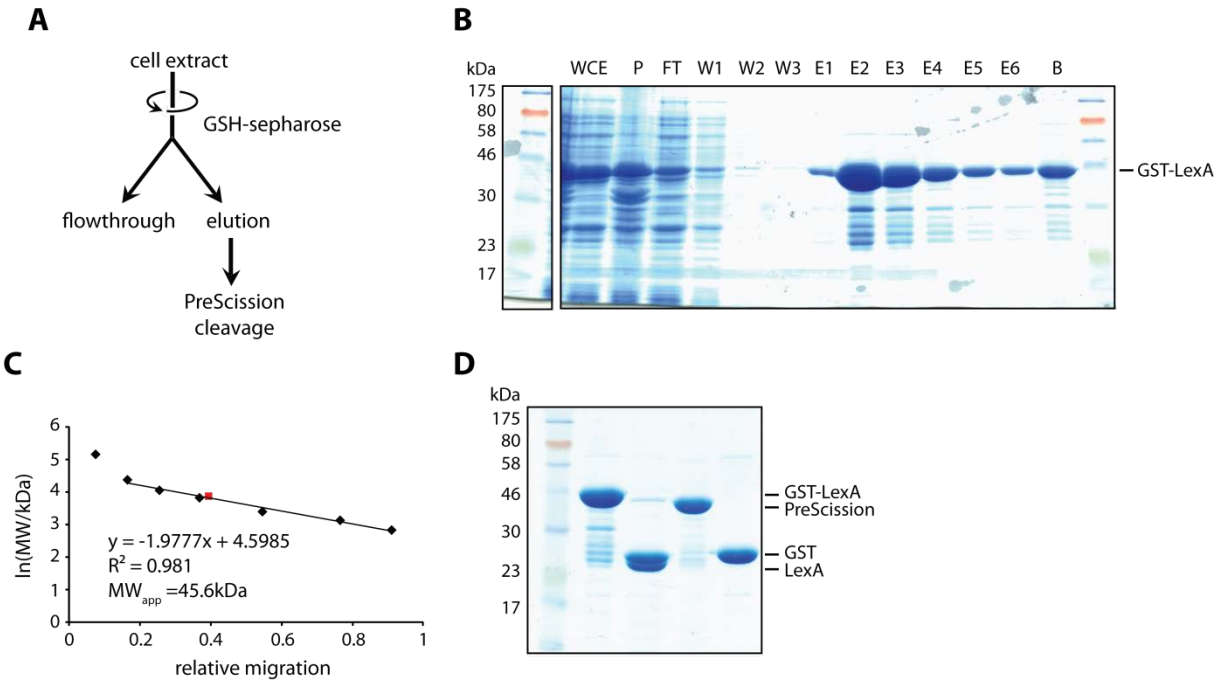

Fig. 4-13: GST-LexA is purified from *E. coli* in two steps. (A) The clear cell extract was subjected to GSH-sepharose affinity chromatography. GST-LexA was eluted by addition of GSH. PreScission protease cleaves the fusion protein to yield GST and LexA (3.2.6 L). **(B)** Coomassie stained SDS gel of all fractions collected during the purification. From left to right: cell extract (WCE, 0.04%), insoluble fraction (P, 0.04%), flowthrough of the GSH sepharose column (FT, 0.04%), washing steps (W1-3, 0.1%), elution steps (E1-6, 0.67%), beads after elution (B, 0.5%). The band representing GST-LexA is indicated. **(C)** A calibration curve for the determination of the apparent MW of GST-LexA was calculated from the migration distances of the marker proteins in the Coomassie gel (B). The curve was approximated with a linear function and the apparent MW calculated. The red dot indicates the ln of the MW of Nsi1. **(D)** The GST and LexA mixture was separated on a 10% SDS gel. From left to right: GST-LexA before cleavage, GST and LexA after cleavage, PreScission protease control, GST control.

LexA was purified as from *E. coli* as described (3.2.9 C) according to a protocol developed by Joachim Griesenbeck (**Fig. 4-13 A**). Expression was done from pGEX-6P-1 resulting in an N-terminal GST fusion protein. After cell lysis and centrifugation, the whole cell extract (WCE) was subjected to affinity purification via glutathione (GSH) agarose. Following binding (FT) and washing (W1-W3), GST-LexA was eluted in 6 steps (E1 - E6) with a buffer containing 10mM GSH. Fractions of every purification step were collected and analyzed via SDS PAGE and Coomassie staining (**Fig. 4-13 B**). All elution fraction lanes contained a strong signal in the range of 46kDa, which presumably represented GST-LexA (48.4kDa). Calculation of its apparent molecular weight with a calibration curve resulted in 45.6kDa with an error of 2% (**Fig. 4-13 C**). However, in elution fractions 2, 3 and 4, additional bands with lower molecular weights were detected. Mass spectrometry (3.2.7 A) after gel filtration revealed that these bands represent fragments of the fusion protein (see also 4.3.4 B).

B) LexA behaves like a monomer in gel filtration

The question of homogeneity of the GST-LexA preparation was addressed in gel filtration experiments (3.2.6 J). 50µl of fraction E2 were separated on a Superose 6 column with PBS as the eluent (**Fig. 4-14 A**). The chromatogram consisted of a broad peak spanning from fractions 10 to 23 with two summits. SDS gel analysis of the collected fractions followed by Coomassie staining demonstrated that this peak consisted of GST-LexA. This random distribution suggests that purified GST LexA represents a mixture of different multimerization states, presumably due to the dimerization capacity of both LexA and GST. Notably, several bands at lower molecular weights were detected in every fraction containing GST-LexA, in a similar pattern as observed before (4.3.4 A). To clarify, whether these were proteolytic fragments of GST-LexA, selected bands were excised and subjected to mass spectrometry as described (3.2.7 A). The result proved the hypothesis, as only peptides of GST or LexA were found with a significant score. However, the question remained, why proteins of different molecular weights co-eluted in one peak. Possible explanations included complex formation of full-length GST-LexA with its fragments or instability of the fusion protein during the experimental procedure.

For further characterization, the fusion protein was cleaved (3.2.6 L) with PreScission protease at a recognition site between GST tag and LexA. Separation on a SDS gel demonstrated the successful cleavage of GST-LexA (**Fig. 4-13 D**). Two bands in the range of the molecular weights of LexA (22.4kDa) and GST (26kDa) appeared upon protease treatment. With a MW close to 46kDa, PreScission

protease was detected, whereas GST-LexA was absent. Most interestingly, no LexA and GST fragments were visible after digestion of the fusion protein.

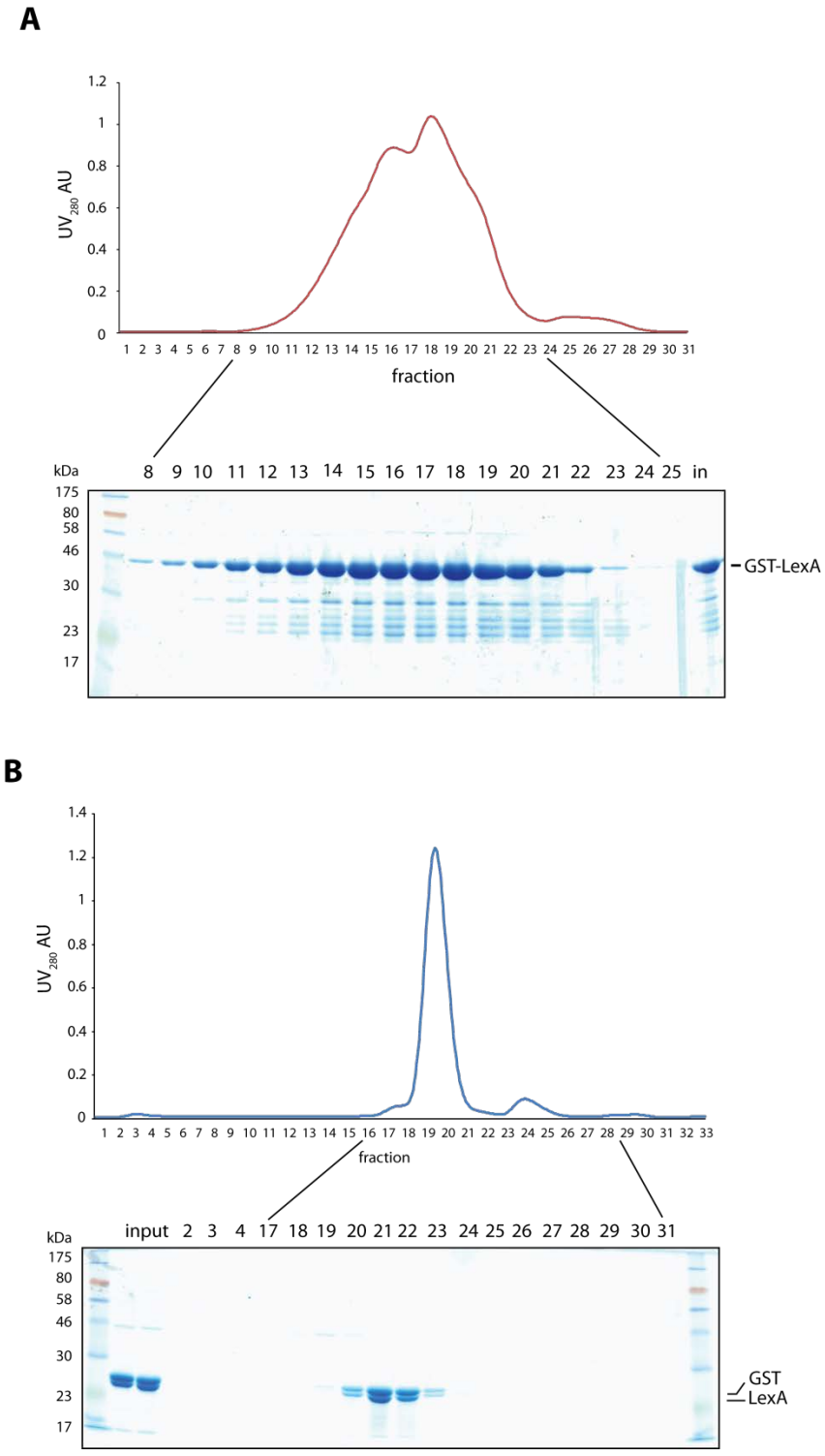

Fig. 4-14: Gel filtration analysis reveals a fairly homogeneous population of LexA. (A) Gel filtration was performed with 50µl of GST LexA (fraction E2, **Fig. 4-13**) on a Superose6 column with a SMART system. UV_{280} absorption was detected and arbitrary units were plotted against the fraction number. 4% of fractions 8 to 25 collected during the run were analyzed on a 10% SDS gel. **(B)** Gel filtration of LexA and GST was performed with 50µl of the cleaved fusion protein on a Superose6 column with a SMART system. UV_{280} absorption was detected and arbitrary units were plotted against the fraction number.

4% of fractions 8 to 4 and 17 to 31 collected during the run were analyzed on a 10% SDS gel. “in” represents the gel filtration input.

The mixture of LexA and GST was again characterized by separation on a Superose 6 column followed by SDS PAGE analysis of the collected fractions (**Fig. 4-14 B**). The chromatogram contained one major (fractions 20-22) and one minor (fractions 25-27) peak. With Coomassie staining, it was demonstrated that the major peak contained LexA and GST which were not resolved, while no signals were obtained for the minor peak. An apparent molecular weight of 24kDa was calculated via a calibration curve leading to the assumption that LexA and GST were in monomeric state. The GST and LexA mixture was referred to as LexA only in further studies.

C) LexA binds to SOS box-containing templates *in vitro*

EMSA experiments with GST-LexA were successful in conditions different from *in vitro* transcription (data not shown & bachelor thesis Sonja Blumenstock) making the results not conclusive for downstream applications. However, GST-LexA and LexA were also successfully used in EMSAs conducted in the conditions mentioned before (4.3.1 C). Two DNA targets with either one (1x LexA BS) or three (3x LexA BS) LexA binding sites (SOS boxes) were designed: Template 1x LexA BS was obtained by annealing of oligos #3115 and #3116 resulting in a Cy5-labeled 50bp DNA. For template 3x LexA BS, a PCR was done with primers #3801 and #3117 on vector #1254 yielding a FAM-labeled 265bp DNA representing nearly the complete transcription template which was used later on. In titration experiments with 1x LexA BS, template concentration was held constant at 10nM and GST-LexA or LexA concentrations were ranging from 165nM to 8,26µM or 112nM to 5.63µM, respectively. Both titrations with GST-LexA and LexA did not lead to full template occupancy (**Fig. 4-15 A, B**). However, upon rising protein concentrations, two (LexA) or three (GST-LexA) bands with lower electrophoretic mobility became visible. These shifted DNA species could represent templates bound to one, two or three proteins, given the facts that LexA binds SOS boxes as a dimer and GST is also able to dimerize (Liew et al. 2008). In an equally performed shift assay with the 3x LexA BS template, results differed substantially. In a low LexA concentration range from 220nM to 450nM, a pattern of three distinct bands was observed besides the free DNA, presumably representing templates occupied by one, two or three LexA proteins or LexA dimers (**Fig. 4-15 C**). Upon rising LexA concentrations, the triple-occupied template became the predominant species (1.1µM – 1.7µM). The highest LexA concentrations resulted in fuzzy bands suggesting random aggregate formation.

In summary, GST-LexA could be purified in vast amounts and high purity. GST LexA showed a random distribution in gel filtration probably due to multimerization domains in both LexA and GST. The fusion protein was successfully cleaved with PreScission protease to yield an equimolar mix of LexA and GST. Gel filtration of this mixture suggested that LexA and GST were eluting as monomers. A LexA concentration of 56.3µM was calculated (3.2.6 E). In gel shift experiments, DNA-binding activity of both GST-LexA and LexA to SOS boxes was confirmed as expected from literature. Specificity of LexA binding was already addressed in other studies (Butala et al. 2007; A. P. P. Zhang et al. 2010).

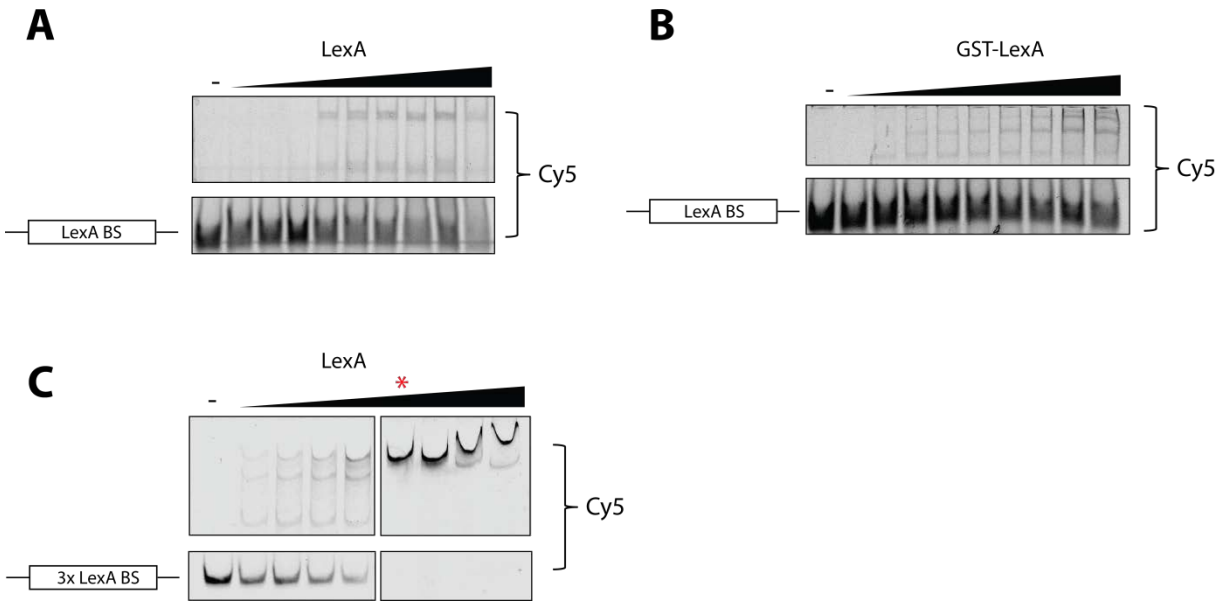

Fig. 4-15: LexA binds to templates containing SOS boxes. LexA or GST-LexA were titrated on Cy5-labeled templates containing one **(A), (B)** or three **(C)** SOS boxes. From left to right: No protein control, titration of GST-LexA (165nM, 248nM, 330nM, 413nM, 660nM, 826nM, 1.6µM, 4.1µM, 8.26µM) or LexA (112nM, 168nM, 225nM, 281nM, 450nM, 562nM, 1.1µM, 2.8µM, 5.63µM) in steps. Template DNA concentration was 10nM. Samples were allowed to equilibrate for 15min at RT and then separated on a 6% native PA gel. DNA bands were visualized in a FLA3000 fluorescence reader. The red asterisk marks the LexA concnetration which was used in *in vitro* transcription.

4.3.5 LacI

A) LacI is purified from *E. coli* as a GST fusion protein

The Lac repressor protein (LacI) is a key regulator of gene expression in bacteria which was first described by (JACOB & MONOD 1961) in context of the lac operon. Its *in vivo* target are three binding

sites in the lac operator region. LacI binds DNA as a tetramer, recognizing a GAATTGTGAGCGCTCACAATT consensus sequence or slight variations thereof. LacI exhibited road-blocking activity for elongating yeast RNA Pol I in *vitro* (Tschochne & Milkereit 1997), thus making it an interesting reference in this study.

LacI was purified as descried (3.2.9 C) from *E. coli* as an N-terminal GST fusion protein. The same strategy was followed as was used for GST-LexA (4.3.4), except that expression was from pGEX-4T-1 (**Fig. 4-16 A**). Thus, GST-LacI contained a recognition site for thrombin between LacI and GST. SDS gel analysis of the collected fractions showed that a large percentage of GST-LacI was unsoluble (P) (**Fig. 4-16 B**). Elution fractions 1 to 6 were mainly composed of a protein in the range of 58kDa, which matched with the theoretical MW of GST-LacI (64kDa). MW calculation via a calibration curve resulted in 57.1kDa with an error of 2% (**Fig. 4-16 C**). Only minor amounts of contaminants were detected in either of the elution fractions. GST-LacI was cleaved with thrombin as described (3.2.6 L) resulting in an equimolar mix of GST and LacI (**Fig. 4-16 D**).

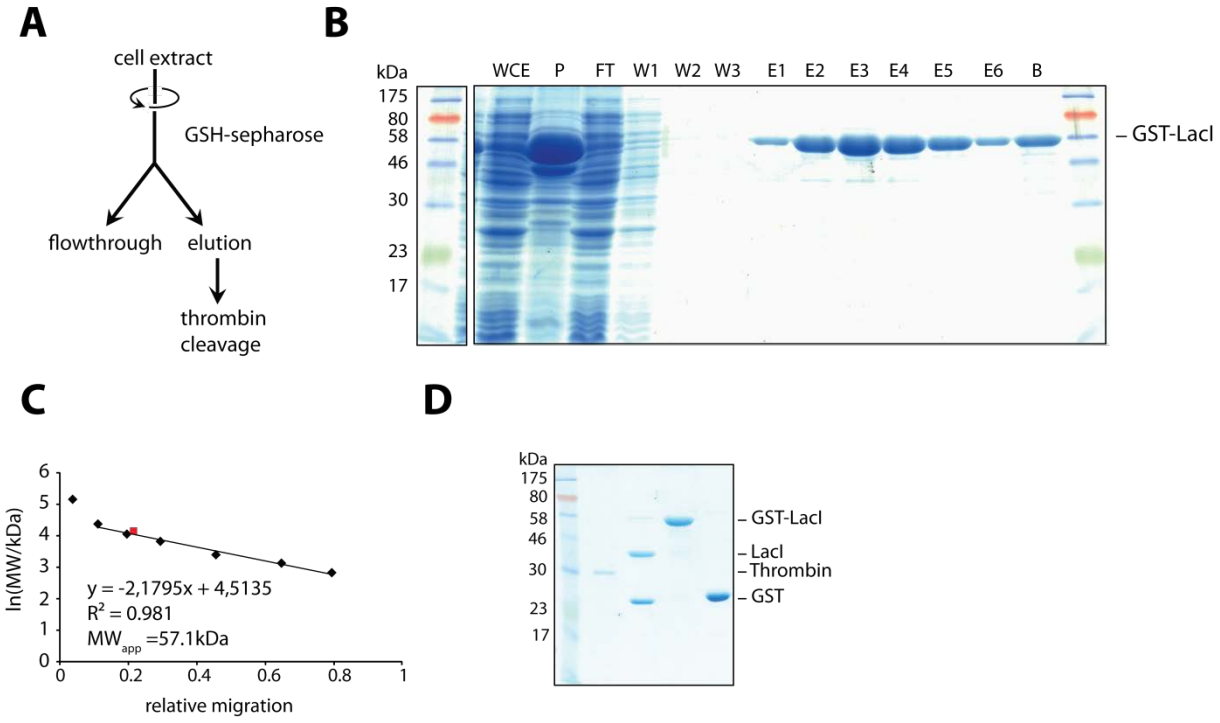

Fig. 4-16: LacI is purified from *E. coli* in two steps. (A) The clear cell extract was subjected to GSH-sepharose affinity chromatography. GST-LacI was eluted by addition of GSH. Thrombin cleaves the fusion protein to yield GST and LacI (3.2.6 L). **(B)** Coomassie stained SDS gel of all fractions collected during the purification. From left to right: cell extract (WCE, 0.04%), insoluble fraction (P, 0.04%), flowthrough of the GSH sepharose column (FT, 0.04%), washing steps (W1-3, 0.1%), elution steps (E1-6, 0.67%), beads after elution (B, 0.5%). The band representing GST-LacI is indicated. **(C)** A calibration curve for the determination of the apparent MW of GST-LacI was calculated from the migration distances of the marker proteins in the Coomassie gel (B). The curve was approximated with a linear function and the apparent MW calculated. The red dot indicates the ln of the ln of the MW of Nsi1. **(D)** The GST and LacI mixture was separated on a 10% SDS gel. From left to right: Thrombin, GST and LacI after cleavage, uncleaved GST-LacI, GST control.

B) Gel filtration suggests a multimeric state of GST-LacI

A Superose 6 column was used to assess the homogeneity and multimerization of the GST-LacI preparation.

A

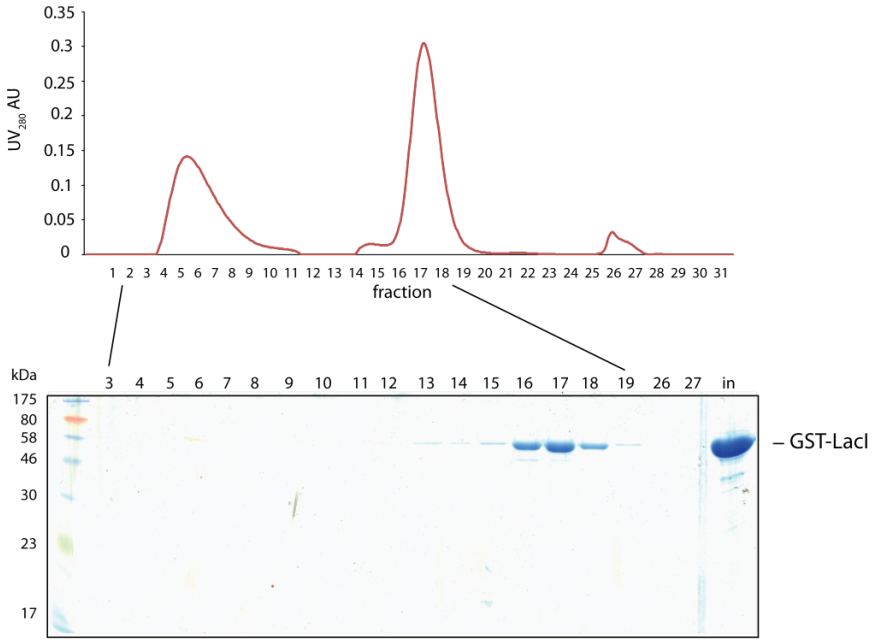

B

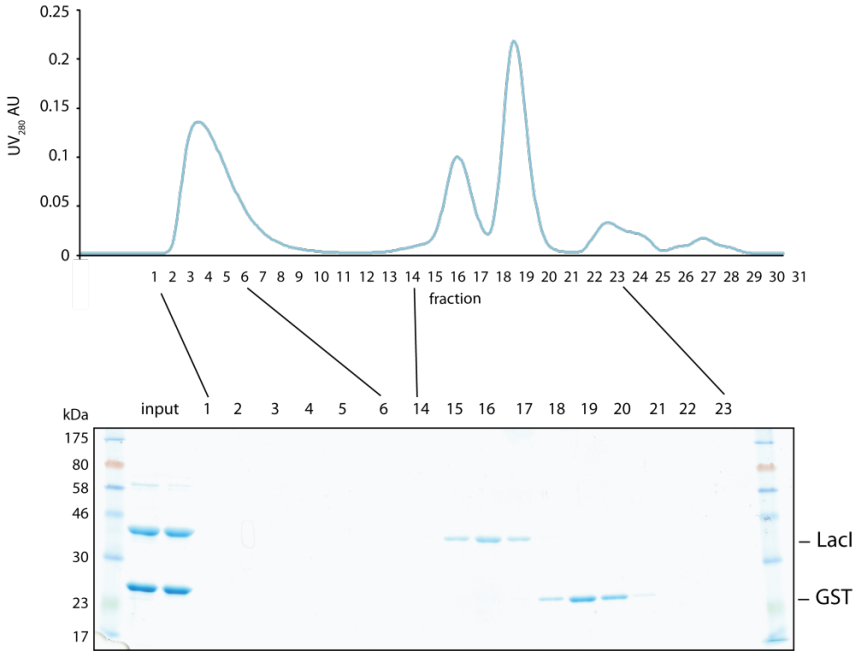

Fig. 4-17: Gel filtration analysis reveals an almost homogeneous population of LacI. (A) Gel filtration was performed with 50µl of GST LacI (fraction E2, **Fig. 4-16**) on a Superose6 column with a SMART system. UV_{280} absorption was detected and arbitrary units were plotted against the fraction number. 4% of fractions 3 to 19 and 26 to 27 collected during the run were analyzed on a 10% SDS gel. **(B)** Gel filtration of LacI and GST was performed with 50µl of the cleaved fusion protein on a Superose6 column with a SMART system. UV_{280} absorption was detected and arbitrary units were plotted against the fraction number. 4% of fractions 1 to 6 and 14 to 23 collected during the run were analyzed on a 10% SDS gel. "in" represents the gel filtration input.

In the chromatogram two peaks were visible including fractions 4 to 7 and 16 to 18. While for the first peak no signals were obtained after Coomassie staining, the second peak was comprised of GST-LacI (**Fig. 4-17 A**). Calculation of the apparent MW of GST-LacI with a calibration curve resulted in 163kDa, suggesting a dimeric or trimeric state. However, purified GST-LacI was a fairly homogeneous fraction eluting in one peak. After cleavage, three peaks were visible in the gel filtration chromatogram (**Fig. 4-17 B**). On a SDS gel, no signal was obtained for the first peak representing the void volume, whereas the second and third peak consisted of LacI and GST, respectively. Compared to a calibration curve of standard proteins, LacI eluted at 152kDa, suggesting a tetrameric state (monomer MW 38kDa) in good agreement with the literature (Pace et al. 1990).

4.3.6 TFIIF

TFIIF stimulates Pol II elongation rates and decreases elongation pausing (Flores et al. 1989; Price et al. 1989; Bengal et al. 1991; Izban & Luse 1992; Tan et al. 1994). It was extensively studied and further described as an initiation factor, albeit this role is being challenged (Luse 2012). Yeast TFIIF is comprised of three subunits Tfg1 (82.2kDa), Tfg2 (46.6kDa) and Tfg3 (Taf14, 27.4kDa). It was shown, that Tfg1 and Tfg2 are partially structurally related to the Pol I subunits A49 and A34.5 (Kuhn et al. 2007; Geiger et al. 2010). The A49/A34.5 dimer is being discussed as a built-in elongation factor for Pol I (Kuhn et al. 2007). Thus, we wanted to compare TFIIF and the A49/A34.5 dimer regarding their functions in transcription elongation.

A) TFIIF is purified from yeast via immunoprecipitation

TFIIF was purified as described (3.2.10 C) from yeast strain #2994 via IP with IgG coupled magnetic beads (**Fig. 4-18 B**). All three TFIIF subunits were expressed under the control of the ADH promoter,

with a C-terminal TAP tag on the second largest subunit Tfg2 (Chen et al. 2010). First purifications were carried out with buffers containing 200mM KCl (**Table 3-4**) yielding a complex mixture of proteins after elution via TEV cleavage (E). Analysis of the elution fraction via SDS PAGE showed four predominant bands, of which three were in the MW range of the TFIIF subunits (**Fig. 4-18 A**). The identity of the three TFIIF subunits was proven in mass spectrometry and Western analysis with antibodies detecting Tfg1, Tfg3 and CBP. Furthermore, two bands representing Rpb1 and Rpb2 (*) were detected with Coomassie staining and identified by Western blot and mass spectrometry, leading to the assumption that Pol II was co-purified with TFIIF in these conditions. In *in vitro* transcription experiments, the TFIIF preparation exhibited polymerase activity, thus proving the hypothesis (**Fig. 4-18 D**). Interestingly, TFIIF did not co-purify with Pol II in similar conditions (200mM KCl), if Rpb2-ProtA was the bait (4.2.3). Mass spectrometry did not return a significant result for the co-purifying protein with a MW between Tfg1 and Tfg2-CBP (*).

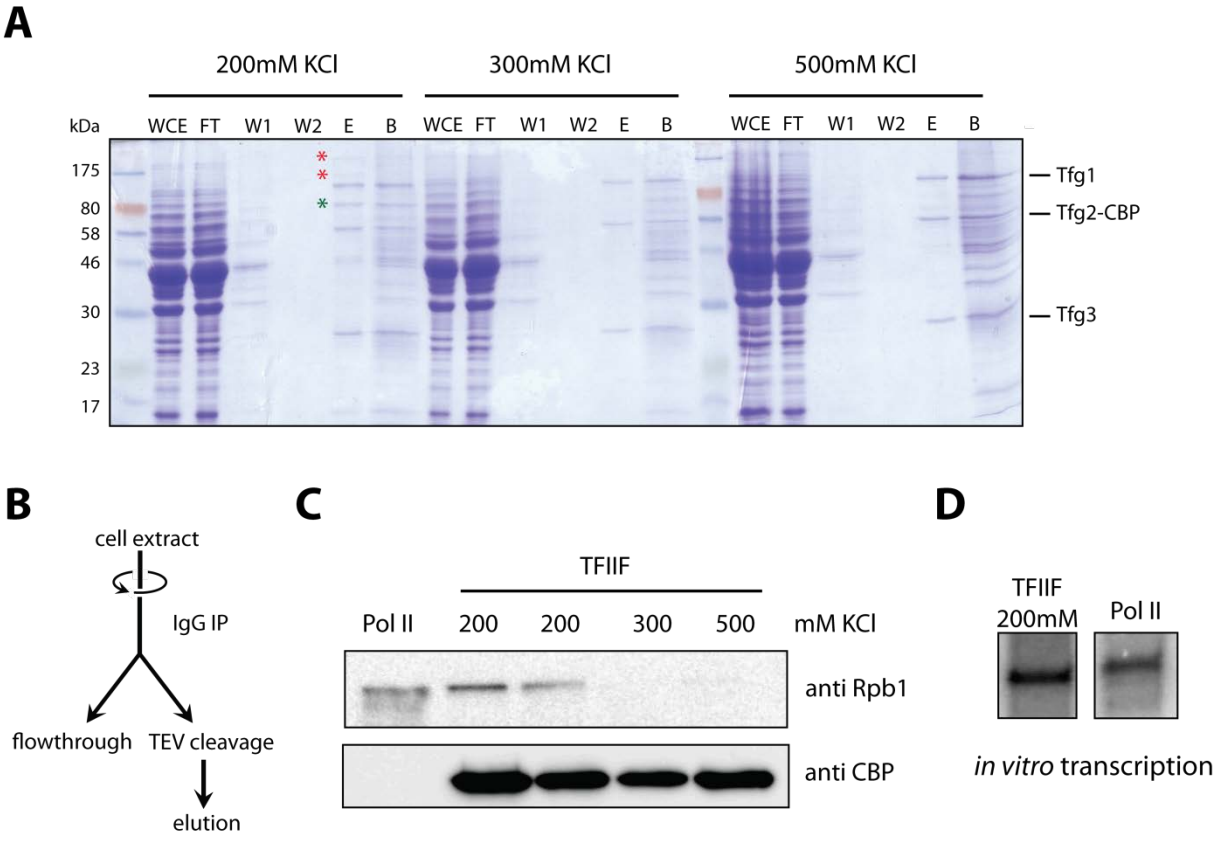

Fig. 4-18: TFIIF is purified from yeast in one step. (A) Fractions collected during purification of TFIIF in three different salt concentrations were separated on a 10% SDS gel and visualized by Coomassie staining. From left to right: cell extract (WCE, 0.6%), flowthrough of the IP (FT, 0.6%), washing steps (W1, 2, 0.7%), elution fraction (E, 10%), beads after elution (B, 50%). Bands representing TFIIF subunits are indicated. Two red asterisks mark Rpb1 and Rpb2. The green asterisk indicates an unknown major contaminant. **(B)** The cleared cell extract is subjected to immune precipitation with IgG coupled magnetic beads with Tfg2-TAP as the bait. TFIIF is eluted by addition of TEV protease and cleavage of the TAP tag. **(C)** Western analysis was done with identical amounts of the elution fractions from the different TFIIF purifications and a Pol II preparation. The blot was developed with two antibodies against Rpb1 and CBP. **(D)** Comparative *in vitro* transcription was

conducted with TFIIF prepared with 200mM KCl and Pol II using the tailed reference template (**Fig. 4-1**). 1µl of Pol II or TFIIF were used in a 20µl standard reaction and exposure was 1h. Transcriptional activity of a TFIIF (500) preparation is shown in **Fig. 4-37**.

B) Pol II is co-purified with TFIIF depending on ionic strength of the buffers

Aim of this part of the study was to purify only TFIIF. Therefore, purifications were carried out in buffers with different ionic strength, ranging from 200mM KCl to 500mM KCl (**Table 3-4**). Side-by-side analysis of the respective elution fractions revealed significant differences (**Fig. 4-18 A, C**). With Coomassie staining, Rpb1 and Rpb2 could not be detected in 300mM and 500mM KCl conditions, the background decreased in general and the significant band with a MW between Tfg1 and Tfg2-CBP vanished. In Western analysis, roughly equal amounts of Tfg2-CBP were observed in all TFIIF purifications, while Rpb1 was detected at 200mM, faintly at 300mM but not at 500mM KCl. Therefore, TFIIF purified with 500mM KCl was used in all further studies, unless indicated otherwise.

C) Interactions between Pol II and TFIIF *in vitro*

Next, the question was addressed, whether a TFIIF-Pol II complex could be reconstituted from TFIIF purified with 500mM KCl and purified Pol II (4.2). After the purification, Tfg2 was still fused to the CBP part of the TAP tag, making an affinity capture via Calmodulin beads possible. The complex formation was conducted as described (3.2.6 M). TFIIF and Pol II concentrations were calculated (3.2.6 E) and mixes with equal amounts or excess TFIIF were prepared. Respective amounts of either purified Pol II or TFIIF which were treated equally served as controls. After incubation with the affinity matrix, unbound proteins were separated (FT) and 2 washing steps (W1, W2) were performed with a buffer containing 100mM KCl. The beads were boiled in SDS sample buffer to determine associated proteins. The collected fractions were separated by SDS PAGE followed by silver staining or Western blot in parallel (**Fig. 4-19**). TFIIF alone was present in input and beads fractions, thus confirming the expected result. In the polymerase control, Pol II was mainly detected in the input (IN) and FT. However minor amounts were associated with the beads, thus determining the Pol II background. In both Pol II/TFIIF mixtures, the beads fraction contained Pol II and TFIIF with Pol II signal intensity being elevated in comparison with the Pol II background. With rising amounts of TFIIF, more Pol II was recruited, as visible in silver staining and Western blot. However, Pol II was never completely bound to the beads.

In summary, TFIIF could be purified from yeast in a strategy adapted from (Chen et al. 2010). Depending on the ionic strength of the buffers, Pol II co-purified with TFIIF. Our results indicate interactions of Pol II with TFIIF *in vitro*. TFIIF concentration (500mM KCl) was calculated as 2.5µM.

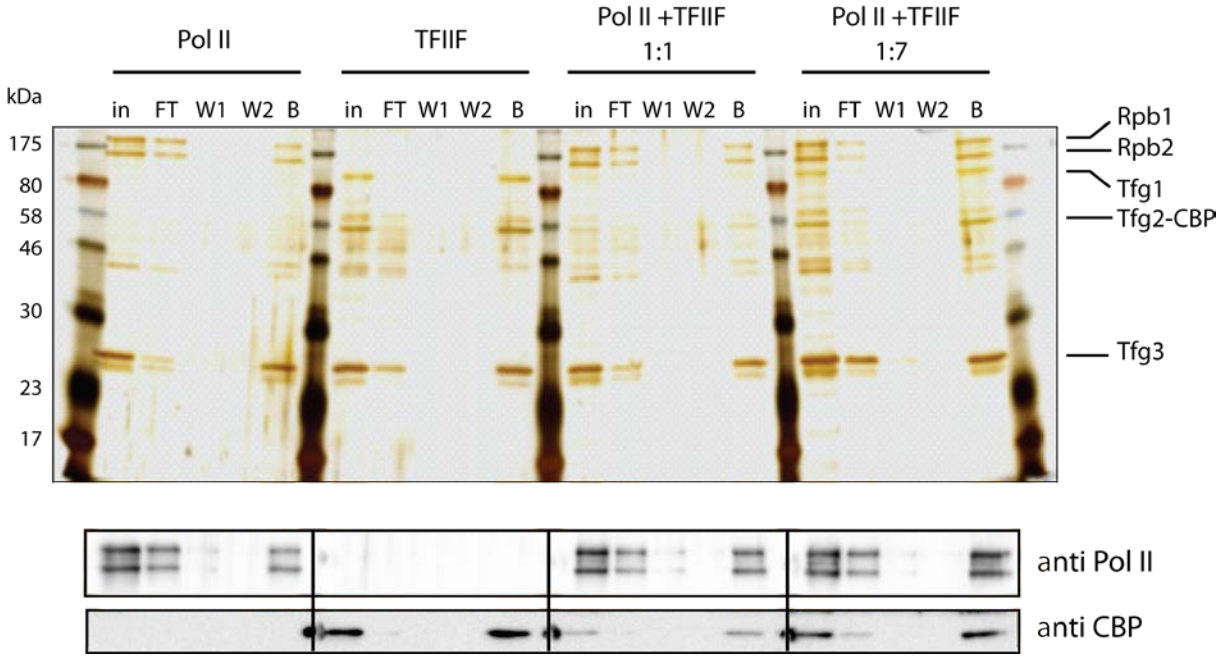

Fig. 4-19: *In vitro* interaction between Pol II and TFIIF. Pol II and TFIIF were incubated on ice for 15min in a buffer containing 50mM NaCl. The sample was incubated with Calmodulin beads for 2h at 4°C. The flowthrough was collected and the affinity resin washed twice with a buffer containing 100mM NaCl. Fractions were analyzed on a 10% SDS gel and the proteins visualized with silver staining. From left to right: Pol II control, TFIIF control, Pol II + TFIIF , Pol II + excess TFIIF; input (in, 6.7%), flowthrough of the Calmodulin column (FT, 7.7%), washing steps (W1, 2, 2%), beads after washing (B, 25%). The TFIIF amount in 1:1 was the same than in the TFIIF control, in 1:7 7x the TFIIF amount was used. Western blots were performed respectively and developed with antibodies against complete Pol II and CBP.

4.3.7 A49/A34.5

A) The A49/A34.5 dimer is purified from *E. coli* via a His_6 tag

The recombinant A49/A34.5 dimer was purified as described (3.2.9 B ii) according to a protocol adapted from (Geiger et al. 2010). Both Pol I subunits were expressed from pET28b resulting in a C-terminal A49-His_6 fusion protein. After cell lysis, the whole cell extract was subjected to Ni-NTA affinity chromatography (**Fig. 4-20 A**). A49-His_6 and A34.5 were eluted from the beads in four steps with 200mM imidazole. Fractions of every purification step were collected, separated by SDS PAGE

and analyzed either by Coomassie staining or Western blotting. The elution fractions (E1-4) showed a slightly changing band pattern with less different proteins in later fractions (**Fig. 4-20 B**). However, three main protein bands were observed, of which two were in the range of the theoretical size of A49-His_6 and A34.5. Western analysis with antibody #10 confirmed the identity of subunit A49. The three bands of interest were excised and subjected to mass spectrometry (3.2.7 A), resulting again in identification of A49 and A34.5. No significant result was obtained for the third band in a yeast database search, which suggests that it was an *E. coli* protein. Protein concentration measurement (3.2.6 E) of the A49/A34.5 dimer in fraction E4, which was used in further experiments, resulted in 3.0µM.

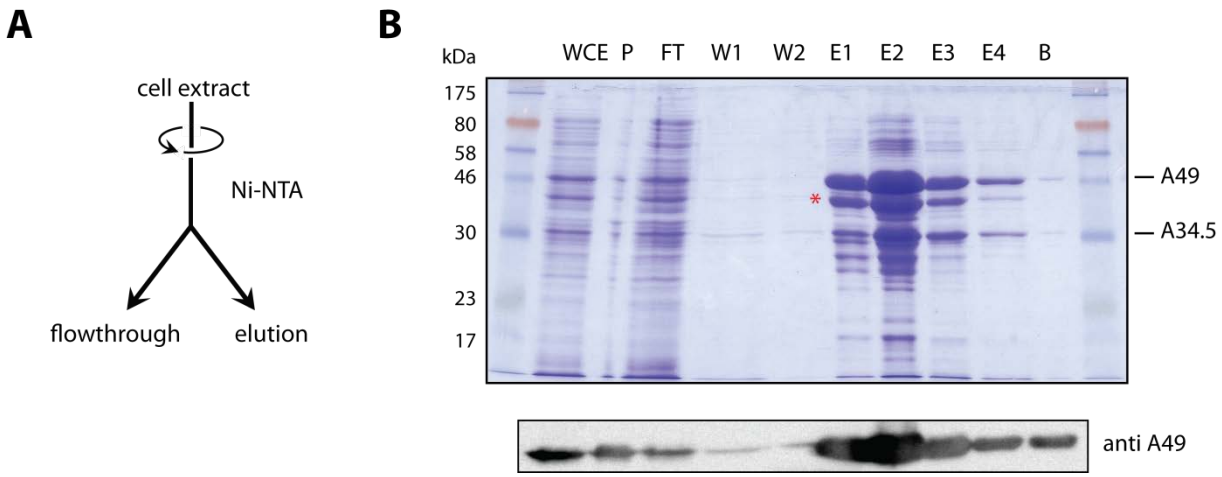

Fig. 4-20: The A49/A34.5 dimer is purified from *E. coli* in one step. (A) The cleared cell extract is incubated with Ni-NTA affinity resin and A49/A34.5 is eluted stepwise with a buffer containing imidazole. **(B)** Fractions collected during the purification were analyzed on a 10% SDS gel. From left to right: Cell extract (WCE, 0.05%), insoluble fraction (P, 0.05%), flowthrough of the nickel column (FT, 0.05%), washing steps (W1, 2, 0.08%), elution fractions (E1-4, 1.6%), beads after elution (B, 2%). The positions of A49 and A34.5 are indicated. The red asterisk points out a major unidentified contaminant. Western analysis was done respectively with an antibody detecting subunit A49.

4.4 Determination of *in vitro* transcription system parameters

4.4.1 Optimal Pol I, II and III activity depends on ionic strength

To compare Pol I, II and III in *in vitro* transcription, it was crucial to determine activity optima of the respective polymerases. Since the NTB buffer (**Table 3-9**) contained only standard components and

nearly no salt, optimal conditions thereof had to be determined. Hence, to standard *in vitro* transcription reactions conducted with Pol I, II and III, KOAc was titrated from 50mM to 400mM. The template of choice was the reference template (**Fig. 4-1**). The three polymerases showed distinctly different behavior. While Pol II activity was highest without additional KOAc ,Pol I reached the activity optimum at 100mM (**Fig. 4-21**). At higher salt concentrations, both polymerase activities declined. Contrary, Pol III activity increased with rising KOAc concentrations. Same results were observed with polymerases purified under KOAc conditions (data not shown). Thus, in the beginning, transcription experiments were conducted in two salt conditions (50mM and 150mM KOAc) ensuring that robust signals were obtained with all polymerases. Furthermore, misguided interpretations of salt-dependent effects upon addition of protein factors in transcription experiments could be excluded. However, later experiments showed that the results obtained in both KOAc conditions were comparable. Thus, *in vitro* transcription experiments were carried out at 50mM KOAc, if not otherwise stated.

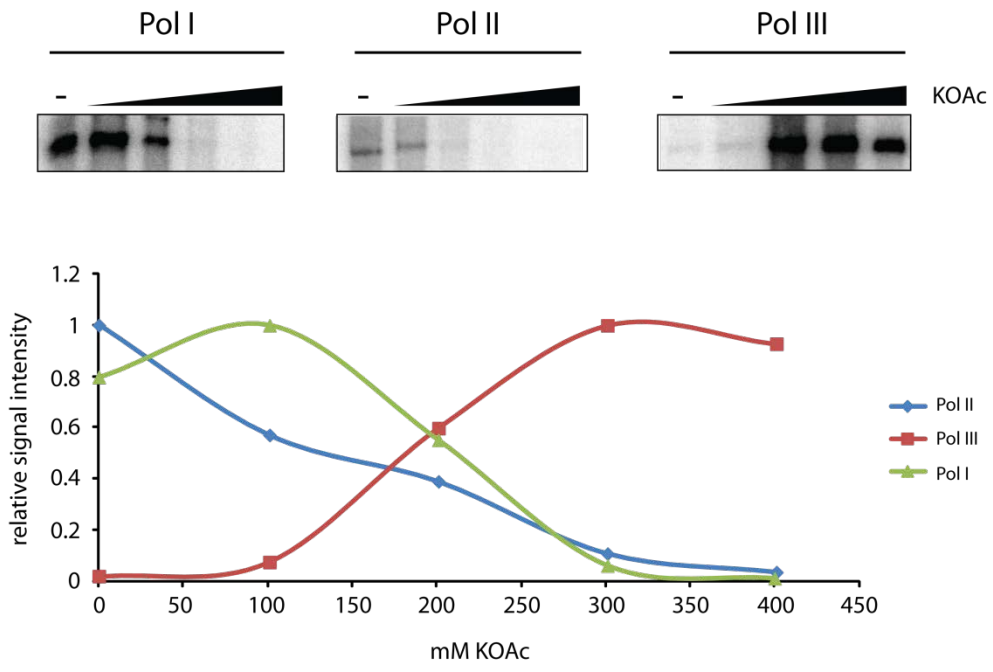

Fig. 4-21: RNA polymerase I, II and III have different activity optima with regard to ionic strength. Transcription reactions were performed as described with 10nM of the reference template and 1µl of each polymerase preparation. Isolated RNAs were separated on a 5% denaturing PA gel. Exposition time of the dried gel was 1h. The signal intensities of the tail full length transcripts were calculated and plotted against the KOAc concentration. The maximum signal intensity in every graph was set to 1.

4.4.2 Tailed template usage in *in vitro* transcription is 10%

The molar ratio of generated transcript to template is defined as the template usage. It is an important characteristic of an *in vitro* transcription system and was hence calculated for the tailed template assay. The used template was a derivative of tail G- Reb1 BS RFB (**Fig. 4-1**) with a length of 667bp (412kDa) of which 100ng (242fmol) were included in the reaction. Via a calibration curve, the molar amount of the generated transcript can be correlated to the signal intensity of the respective band visualized by autoradiography. To establish a calibration curve, a titration series of the α-^{32}P-CTP solution was spotted on whatman filter paper and exposed side-by-side with the transcription gel (**Fig. 4-22 A**).

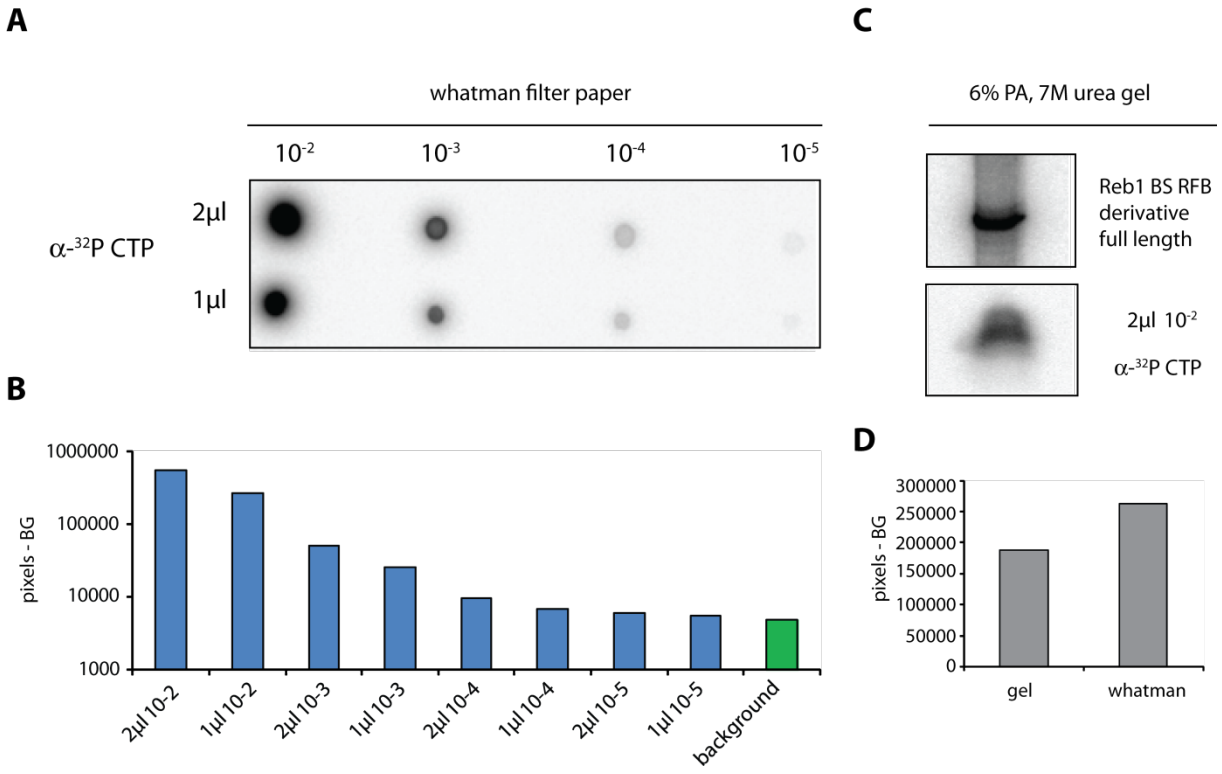

Fig. 4-22: Tailed template usage in *in vitro* transcription is 10%. (A) The α-^{32}P-CTP stock solution was spotted on whatman filter paper in serial dilutions and exposed together with the transcription gel. **(B)** Signal intensities of those spots were quantified and plotted against the dilution. **(C)** Transcription was performed as described with 10nM of the reference template and 1µl Pol I. The isolated RNA was separated on a 5% denaturing PA gel. 2µl of the 10^{-2} dilution of the α-^{32}P-CTP stock solution were applied on the gel shortly before the end of the run. Exposition time of the dried gel was 1h. **(D)** For determination of a quenching effect of the polyacrylamide gel, the signals obtained with 2µl of the 10^{-2} dilution of the α-^{32}P-CTP stock solution in (A) and (C) were compared.

The signal intensities of the spots were measured and plotted against the molar amount of radioactively labeled nucleotides taking into account the specific activity and the labeling efficiency of the nucleotide stock solution as well as the radioactive decay (**Fig. 4-22 B**). Next, the average number of incorporated α-^{32}P-CTP per transcript was calculated by multiplication of the number of cytosine residues in the transcript with the fraction of radioactive CTP in the transcription reaction. Taken together, this allowed determination the molar amount of transcript. To estimate signal quenching due to the polyacrylamide urea gel, 1µl of the 10^{-2} dilution of the α-^{32}P-CTP solution was applied on the gel shortly before the end of the run (**Fig. 4-22 C**). The signal intensities on the gel and on the filter paper were compared resulting in a quenching effect of roughly 30% (**Fig. 4-22 D**). Taken this into account, the molar amount of the generated RNA was 24fmol, leading to a template usage of 10%. In comparison with other *in vitro* transcription systems, this is a rather high value (personal communication, Herbert Tschochner, Philipp Milkereit).

4.4.3 Tailed templates are transcribed only once

Studies conducted by (Kadesch & Chamberlin 1982) indicated, that during *in vitro* transcription with tailed templates the two DNA strands are displaced and RNA-DNA hybrids are formed subsequently. In turn, this means that every template can be only transcribed once under the assumption that single stranded DNA cannot serve as a template. To challenge this hypothesis, the tailed template Reb1BS RFB was transcribed in different conditions in the presence of heparin. Heparin is a sulfated and thus negatively charged glucosaminoglycan with protein-binding features related to that of DNA. Heparin tightly binds to RNA polymerases forming a stable complex which is not initiation-competent in promoter dependent and independent transcription assays. If heparin was titrated to a standard *in vitro* transcription reaction conducted with T7 RNA polymerase, the signal intensity of the full length transcript decreased with rising concentration (**Fig. 4-23**) due to declining amount of polymerase. To mimic single round transcription, the polymerase was stalled at the G-less cassette, heparin was added and transcription resumed by addition of GTP. In this condition, roughly identical signal intensities were observed compared to the control without heparin, leading to the conclusion that tailed templates are transcribed only once (**Fig. 4-23**). This experiment was performed only with T7 RNA polymerase. However, strand displacement during transcription most probably is a template-inherent feature which suggests single round transcription also for transcription with Pol I, II and III.

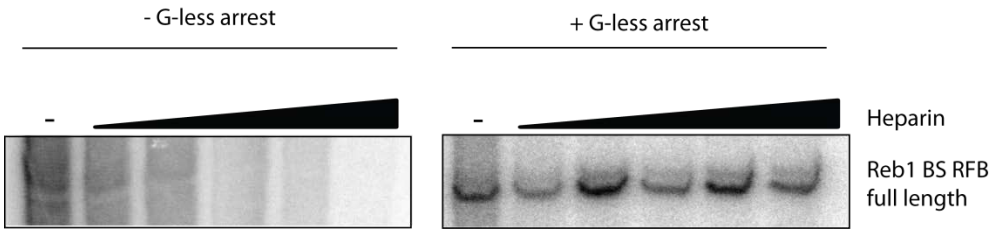

Fig. 4-23: Tailed templates are transcribed only once. Transcription reactions were performed as described with 10nM of the Reb1 BS RFB template and T7 RNA polymerase. Heparin was titrated to the samples before transcription was started (-G-less arrest) or during G-less arrest (+G-less arrest). After arrest, transcription was resumed by addition of GTP. Heparin concentrations ranged from 5ng/µl to 50ng/µl. Isolated RNAs were separated on a 5% denaturing PA gel. Exposition time of the dried gel was 1h. The signal intensities of the tail full length transcripts were calculated and

4.5 *In vitro* transcription with complexed templates reveals road-blocking ability of protein factors

This study addressed the question, whether the purified proteins possessed the ability to function as elongation road blocks or transcription termination factors. Thus, the respective templates complexed with Nsi1, Reb1, Fob1, LexA or TTF-I were transcribed *in vitro*, with the main focus on the yeast proteins. Since TTF-I, Nsi1 and Reb1 were identified as Pol I termination factors (Reiter et al. 2012; Lang & Reeder 1995; Evers et al. 1995), they will be referred to as such in the following chapters besides the terms elongation barriers/obstacles.

4.5.1 Reb1, Nsi1 and Fob1 impose barriers in *in vitro* transcription

In a first step, Reb1, Nsi1 or Fob1 were titrated to transcription reactions with Pol I and the tailed template TER (**Fig. 4-1**). Template concentration was 10nM and protein concentrations ranged from 13.8nM to 1380nM (Fob1), 8.7 to 870nM (Reb1) and 8nM to 320nM (Nsi1) corresponding to the respective EMSA conditions (**Fig. 4-12**, **Fig. 4-7**, **Fig. 4-9**). The samples were allowed to equilibrate at RT for 15min before the reactions were started by addition of the polymerase. *In vitro* transcription reactions were carried out as described in (3.2.12). Besides the bands representing the run-off TER

and reference transcripts, one further band was each detected on the gel upon addition of Reb1 and Nsi1 in the range of 205nt (**Fig. 4-24**). Addition of Fob1 resulted in two different extra signals of roughly 395nt and 490nt. RNA length calculations were based on calibration curves generated with an *in vitro* transcribed RNA marker which was applied on every gel. Comparison of the transcript sizes with the position of the cis elements in the template DNA indicated that the RNA obtained with Reb1 and Nsi1 was ending at the T-rich 1 element (209nt-221nt) and the two bands gained with Fob1 were mapping to the RFB3 (394nt-415nt) and RFB1 (492nt-512nt) sites. RNA lengths and cis element positions are referenced to the tailed template transcription start site. Quantification of the percentage of the remaining full-length transcript upon addition of a protein factor was done as described (3.2.12 D). This evaluation method was in general preferred over calculation of the percentage of the abortive or terminated transcript as the full length RNA bands always show robust signal intensities. However, in case of the titration series the respective vice versa calculation was performed as well to assess plausibility of the results.

Upon titration of Reb1, the fraction of TER run-off transcript was gradually reduced to 40% compared to the negative control (**Fig. 4-24 B**). This result was expected and in good agreement with earlier observations made by Reeder and co-workers (Morrow et al. 1993). The fraction of full-length transcript was plotted against the Reb1 concentration resulting in a curve best approximated by a logarithmic fit, seemingly reaching a plateau. This suggested that full template occupancy as determined in EMSA analysis (700nM Reb1, **Fig. 4-7**) also reflected the maximum effect in *in vitro* transcription. Note, that the overall signal intensity decreased with rising amounts of Reb1 present in the reaction thus leading to the hypothesis that Reb1 negatively influences transcription at high concentrations. This effect was not observed, if a mock purification from *E.* coli (**Fig. 4-5**) was titrated to a transcription reaction instead of Reb1 (data not shown).

Similarly, rising concentrations of Nsi1 led to a reduction of the TER full length transcript to roughly 60% (**Fig. 4-24 A**). The curve obtained by plotting the proportion of TER run-off transcript versus the Nsi1 concentration reached a plateau at the higher Nsi1 concentrations. At full template occupancy identified in EMSA experiments (88nM Nsi1, **Fig. 4-9**), the maximum road-blocking effect was not yet reached. However, technical limits prohibited addition of larger Nsi1 volumes and attempts to obtain more concentrated Nsi1 failed.

Fob1 was a less potent elongation obstacle for Pol I than Reb1 and Nsi1. Even at high concentrations, 75% of the full length transcript were obtained than without Fob1 (**Fig. 4-24 C**). Thus, in the respective plot of full length transcript fraction against Fob1 concentration, saturation was reached at lower concentrations. With Fob1, full template occupancy (276nM Fob1, **Fig. 4-12**) correlated with the maximum road-blocking effect.

In summary, we could verify the pausing effect described for Reb1 qualitatively and quantitatively. Furthermore, we could show that Nsi1 and Fob1 are elongation obstacles for Pol I.

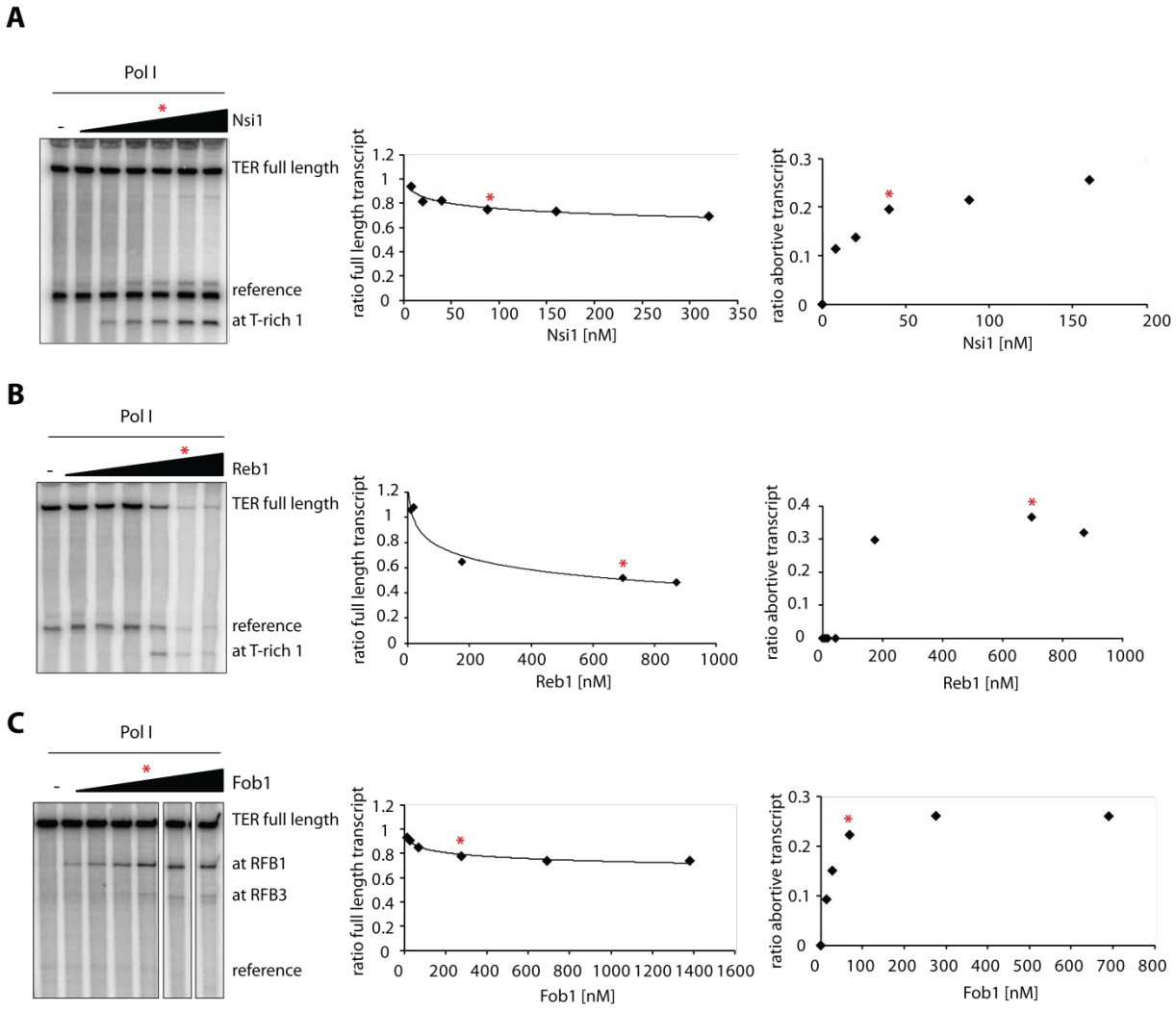

Fig. 4-24: Titration of Nsi1, Reb1 and Fob1 reveals road blocking ability in *in vitro* transcription reactions conducted with Pol I and the tailed template TER. (A) Transcription reactions were performed as described with 10nM of each template and 1µl Pol I preparation. Nsi1 was titrated from 8nM to 320nM. After addition of the respective factor, the sample was allowed to equilibrate for 15min at RT before the reaction was started. Isolated RNAs were separated on a 5% denaturing PA gel. Exposition time of the dried gel was 1h. Signals were normalized to the reference transcript and the ratio of the full length transcript signal intensities of the lane of interest versus the negative control was calculated. The proportion of the abortive transcript compared to the negative control was determined respectively. Red asterisks indicate the factor concentration at which full template occupancy was observed in EMSA experiments. **(B)** Reb1 was titrated from 8.7nM to 870nM. The experiment was carried out as described in (A). **(C)** Fob1 was titrated from 13.8nM to 1380nM. The experiment was carried out as described in (A)

4.5.2 Controls demonstrate that the observed effects can be traced back to the protein factors

In all *in vitro* studies, thorough controls are of great importance to draw solid conclusions. Therefore, multiple sets of experiments were conducted to exclude that observed effects were experimental artifacts.

As always two templates were present in the transcription reactions, it had to be clarified, whether the observed effects were due to the template of interest, or if the reference template was interfering. This was tested for Reb1, Nsi1, Fob1, LexA and TTF-I with KCl- and KOAc-purified RNA polymerases and the respective templates TER, 3xLexA or 5xTTF-I in transcription reactions containing additional 50mM or 150mM KOAc. **Fig. 4-25** exemplary shows the results for Nsi1, Reb1 and Fob1 with Pol I (KOAc-purified) in reactions containing 50mM KOAc. It could be demonstrated that the effects caused by Nsi1, Reb1 or Fob1 depended specifically on the presence of the TER template. Transcription of the reference template was not affected by the presence of either of the factors. Same results were obtained if Pol II or III were used, if the reactions contained 150mM KOAc or if the polymerases were KCl-purified (data not shown). All possible combinations thereof were tested. The results were also in coordinance with the results obtained by gel shift experiments with competitor DNA (**Fig. 4-12**, **Fig. 4-7**).

Furthermore, it had to be excluded that the protein elution buffers evoked significant effects. Thus, equal amounts of Reb1 elution buffer and TAP300 (with regard to the normally applied volumes of the elution fractions) were included in transcriptions. Reactions were conducted with Pol I, II and III (KOAc-purified) in presence of additional 50mM KOAc and compared to a negative control. Visual evaluation of the transcription gel lead to the conclusion, that neither buffer significantly influenced transcription by either polymerase (**Fig. 4-25**). For Pol I and II, transcript singal intensities seemed to decrease slightly upon addition of either buffer in accordance with general salt-dependency of the two polymerases (**Fig. 4-21**).

Concerning the possible dependency of the results on the amount of additional KOAc in the reaction, it could be shown that the quality of the statements did not change with minor effects on absolute numbers (data not shown).

Finally, the question was addressed, whether the polymerase purification protocol influenced the results. In **Fig. 4-31** and **Fig. 4-25**, results of identical transcription experiments are depicted conducted

with KCl- and KOAc-purified Pol I. In these experiments, the tailed template TER and reference were transcribed in presence of Fob1, Nsi1 or Reb1. Visual and mathematical comparison of the respective results showed that the observed effects did not depend on the polymerase purification method (calculations only shown for KCl polymerases).

In summary, it could be demonstrated that the results obtained in the in vitro transcription assay were robust and reproducible.

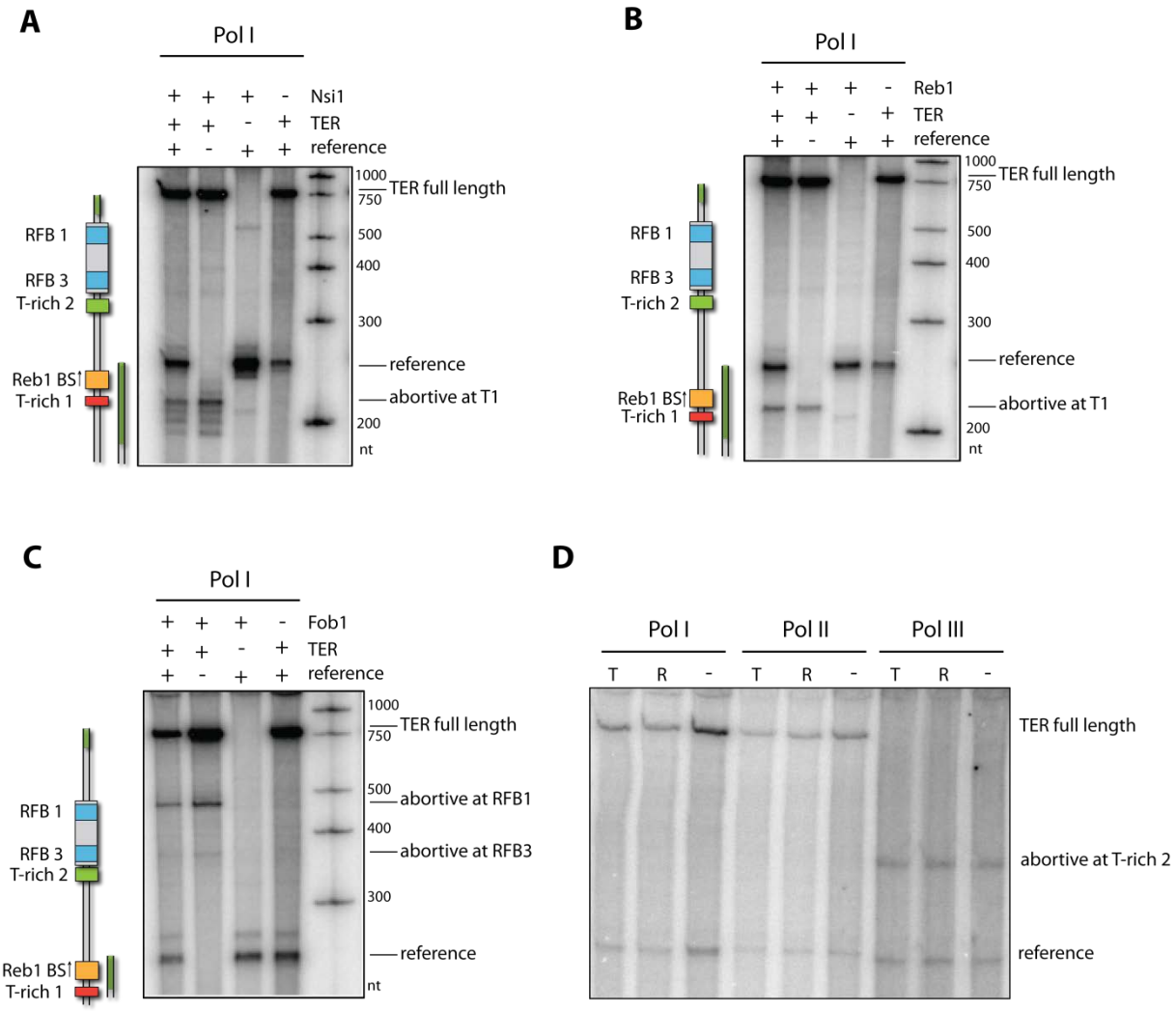

Fig. 4-25: Template, buffer, polymerase and RNA marker controls. (A) Transcription reactions were performed as described with 10nM of each tailed template and 1µl Pol I preparation (**KOAc conditions**). Either both or one of the templates TER or reference were present in the reactions. Nsi1 was used at 88nM concentration. After addition of Nsi1, the sample was allowed to equilibrate for 15min at RT before the reaction was started. Isolated RNAs were separated on a 5% denaturing PA gel. Exposition time of the dried gel was 1h. Cartoons of the templates indicate the identity and length of the RNAs. Transcript length calculations were based on calibration curves obtained from a set of RNA marker bands. Identical experiments were performed at 50mM KOAc and 150mM KOAc. The gel pictures represent the 50mMKOAc situation. **(B)** Description see (A), except not Nsi1 but Reb1 was used at 700nM concentration. **(C)** Description see (A), except not Nsi1 but Fob1 was used at 276nM concentration. **(D)** Experiments were done as described in (A) with tailed templates TER and

reference. Instead of protein factors, equal amounts of the respective elution buffers were included in the reaction, with T standing for TAP300 buffer, R standing for Reb1 elution buffer and – indicating the negative control.

4.6 Efficient Pol I termination is dependent on the presence and orientation of the cis-elements in the rDNA terminator *in vitro*

4.6.1 The T-rich 1 element is required for efficient termination by Nsi1

Previous results had demonstrated that Nsi1 was required for Pol I termination. Since the region spanning from the T-rich 1 element to the RFB contains several identified cis-elements, the question arose which of these elements actually influenced of Nsi1-dependent termination. Thus, a series of tailed templates was created containing various rDNA terminator cis-element combinations (**Fig. 4-1**, 4.1.2). Transcription reactions were carried out with 10nM of each template, 88nM Nsi1, 1µl Pol I preparation and additional 50mM KOAc. The transcripts were separated on a 5% denaturing PA gel and visualized by exposure to an imaging plate for 1h. Calculations demonstrated that the least amount of run-off transcript (40%) was generated if the entire terminator region was present in the template (**Fig. 4-26**). Inversion or deletion of the Reb1 binding site led to complete alleviation of the effect. When the T-rich 1 sequence was missing, the abortive transcript was still visible, albeit termination efficiency dropped by factor two (80%). Equal results were obtained with respective constructs lacking the RFB. However, comparison of transcription with template TER and the template containing only the T-rich 1 element and the Reb1 BS resulted in a small difference in full-length transcript formation of 10%.

In summary, presence and correct orientation of the Reb1 binding site is necessary for Nsi1 dependent termination of Pol I. The T-rich element is required for efficient termination. The RFB slightly stimulates the effect.

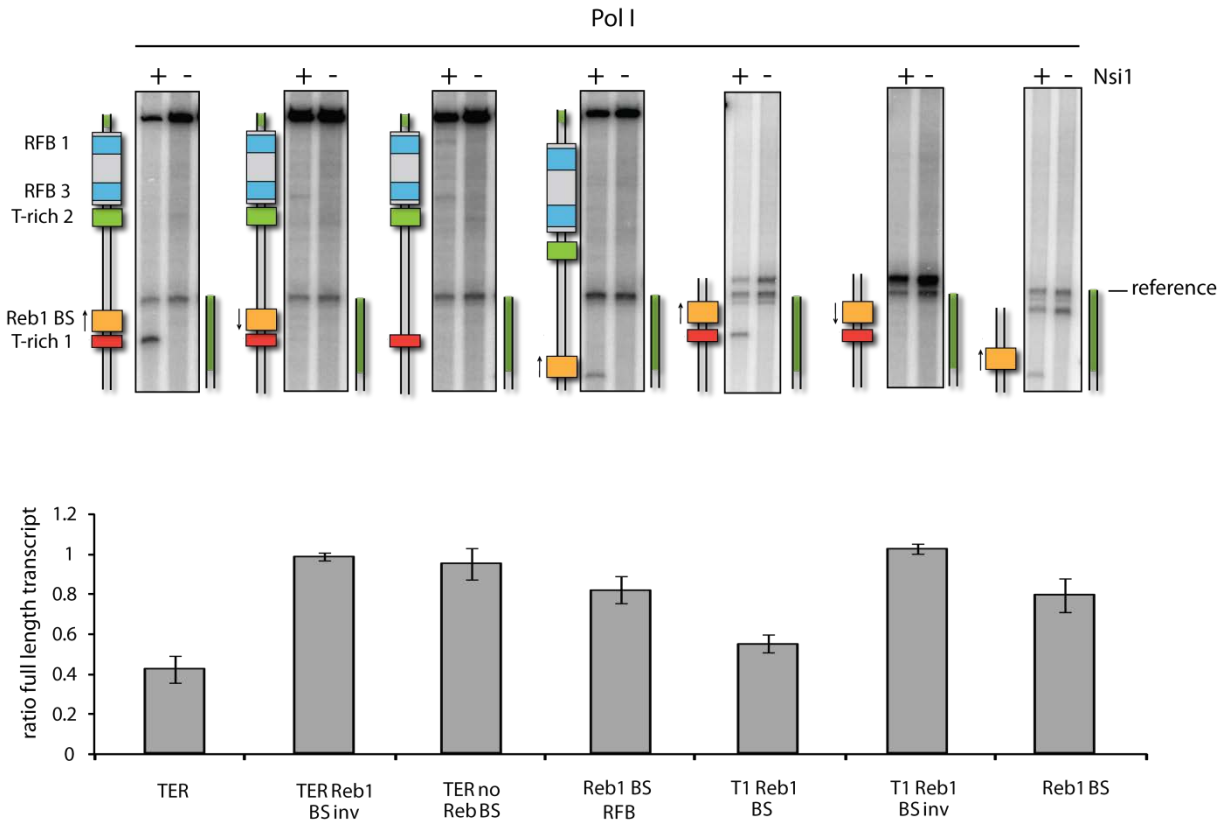

Fig. 4-26: Cis element analysis reveals that presence and orientation of the Reb1 BS are necessary for Nsi1-dependent Pol I termination and that the T-rich 1 element is required for efficient termination *in vitro*. Transcription reactions were performed in triplicate as described with 10nM of the respective tailed template and 1µl Pol I. Nsi1 was used at 88nM concentration. After addition of Nsi1, the sample was allowed to equilibrate for 15min at RT before the reaction was started. Isolated RNAs were separated on a 5% denaturing PA gel. Exposition time of the dried gel was 1h. Cartoons of the templates indicate the identity and length of the RNAs. Signals were normalized to the reference transcript and the ratios of the full length transcript signal intensities of the lanes of interest versus the negative control were calculated and plotted.

4.6.2 Reb1-dependent termination requires the T-rich 1 element and the Reb1 binding site

Reeder and co-workers observed that Reb1-dependent Pol I termination required the T-rich 1 element and the Reb1 BS *in vitro* (Lang et al. 1994). To compare the results obtained with Nsi1 with the published data, identical experiments as described in 4.6.1 were performed with Reb1 instead of Nsi1 to elucidate the cis-element dependency of Reb1-dependent Pol I termination *in vitro*. As usual, Reb1 concentration was set to 700nM. With templates missing the T-rich 1 element or the Reb1 BS, no termination was detected, which is in agreement with the literature. Most efficient termination

(40% full length transcript) was achieved if all cis elements were present in the template (**Fig. 4-27**). With templates TER and T-rich Reb1 BS, strong signals of abortive transcripts were observed. However, deletion of the RFB led to a minor decrease in termination efficiency (< 5%). Transcription of templates with an inverted Reb1 binding site resulted in a minor terminaton effect (70% full length transcript) compared to the respective templates with the correctly oriented binding site. Interestingly, the length of the abortive transcripts changed with the orientation of the Reb1 binding site. Upon correct orientation, transcripts were mapping to the T-rich 1 site as observed before. If the binding site was inverted, the (very faintly visible) abortive transcripts extended to the Reb1 binding site.

In summary the results demonstrated that the T-rich 1 element and the correctly oriented Reb1 BS were required for efficient Reb1-dependent Pol I termination. The percentage of terminated transcripts was reduced by roughly factor two if the Reb1 binding site was in inverted orientation.

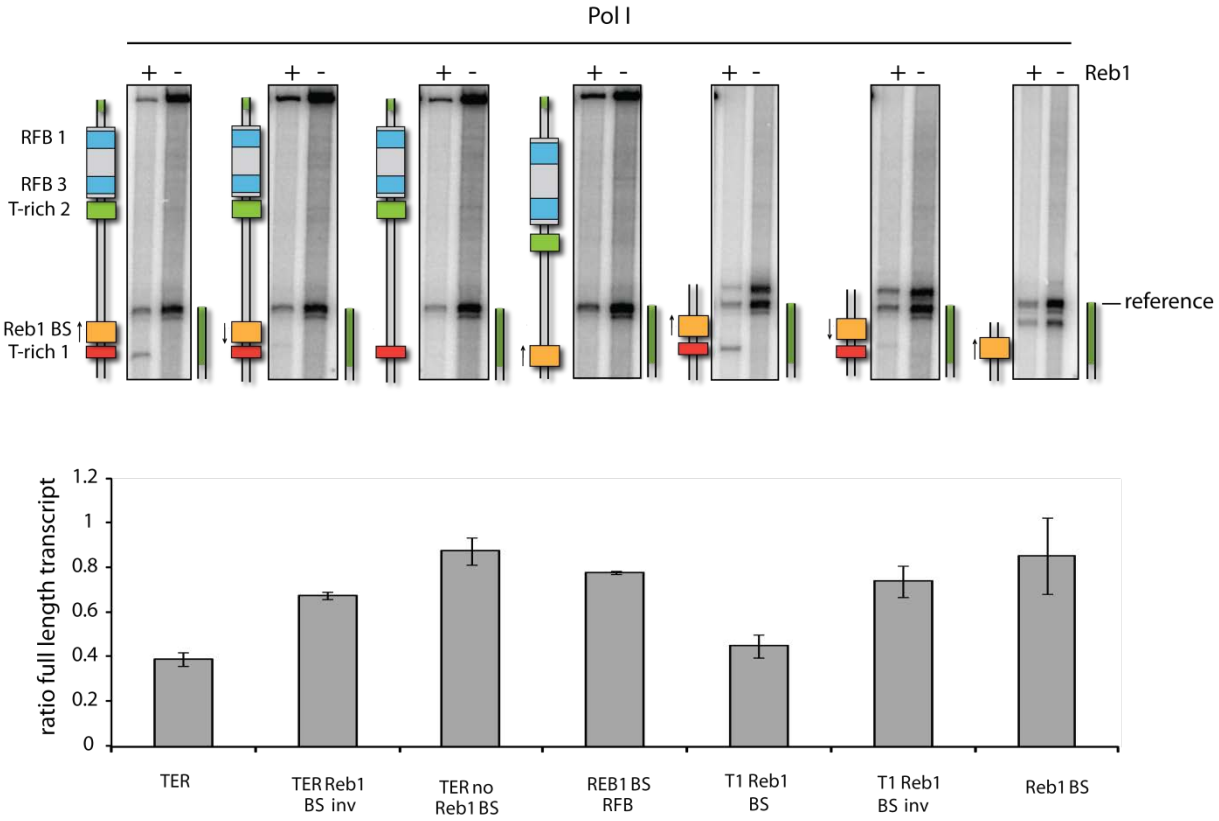

Fig. 4-27: Cis element analysis reveals that presence of the Reb1 BS and the T-rich 1 element are necessary for efficient Reb1-dependent Pol I termination *in vitro*. Description see Fig. 4-29, except that Reb1 was used at 700nM concentration instead of Nsi1.

4.7 Nsi1 and Fob1 exhibit cooperativity in Pol I transcription termination *in vitro*

Ha and co-workers suggested a cooperative effect between Nsi1 and Fob1 (Ha et al. 2012, p.1). Thus it was tried to determine, if Nsi1 and Fob1 acted cooperatively in Pol I termination *in vitro.* Transcription conditions were chosen such that the termination effect exerted by Nsi1 was minimally visible (20nM). Then Fob1 was titrated to the reactions in three steps (27.6nM, 276nM, 1380nM). Note that the amount of Fob1 representing full complexion of the template was 276nM. Samples only containing Fob1 or Nsi1 or no additional factors served as controls. Transcription reactions were assembled as usual and either Fob1 or Nsi1 or both were added. Equilibration time was 15min at RT. The autoradiography of the denaturing PA gel is depicted in **Fig. 4-28 A**. As expected, presence of Nsi1 resulted in a minimal fraction of terminated transcript (lane 2, green bar). Upon addition of rising amounts of Fob1 to samples containing Nsi1 (lanes 3, - 5, red bars) the signal intensity of the band representing the transcript terminated at the T-rich 1 site increased visibly. Furthermore, the two characteristic abortive transcripts at RFB1 and RFB3 appeared due to the presence of Fob1. However, the signal intensity of those bands seemed to be altered due to the presence of Nsi1. In a first step, the fractions of remaining full length transcript compared to the negative control (lane1) were calculated and plotted for every lane as usual, reflecting the made observations.

To address the question of cooperativity, diagrams with stacked columns were created from the dataset. First, the percentages of remaining run-off transcript obtained in the reactions with Fob1 and Nsi1 were plotted (red columns) like in the regular diagram. Then, the amount of transcripts terminated by Nsi1 was calculated as the difference between 100% and the amount of full-length transcript gained in the Nsi1 control (lane 2, green columns). The fraction of transcripts terminated by Fob1 was calculated alike (blue columns). The values obtained for Nsi1 and Fob1 were plotted on top of the red columns. If the effects exerted by Fob1 and Nsi1 were simply additive, this sum should be 100%. However, the values differed from 100% depending on the amount of Fob1 up to roughly 15%. This suggests a cooperative behaviour between Nsi1 and Fob1.

The result was challenged in an identical experiment conducted with the tailed template T-rich1 TER missing the RFB. The rationale was to further investigate whether simply the presence of Fob1 and thus probably a direct interaction between Nsi1 and Fob1 was imposing the cooperative effect or if the RFB DNA sequence was needed as well. The results are depicted in (**Fig. 4-28 B**). Contrary to the

previous experiment with the complete TER template, the signal intensity of the band representing the Nsi1-dependent terminated transcript did not increase visibly upon titration of Fob1. This impression was verified when the remaining amounts of the full-length transcripts were calculated. In the stacked column diagram, the fractions added up to 100% thus showing the additivity of the effects observed in this experiment. The results lead to the conclusion that the cooperative effect of Nsi1 and Fob1 in Pol I transcription termination depended on both presence of Fob1 and the RFB, which was also in good agreement with the cis-element analysis (**Fig. 4-26**).

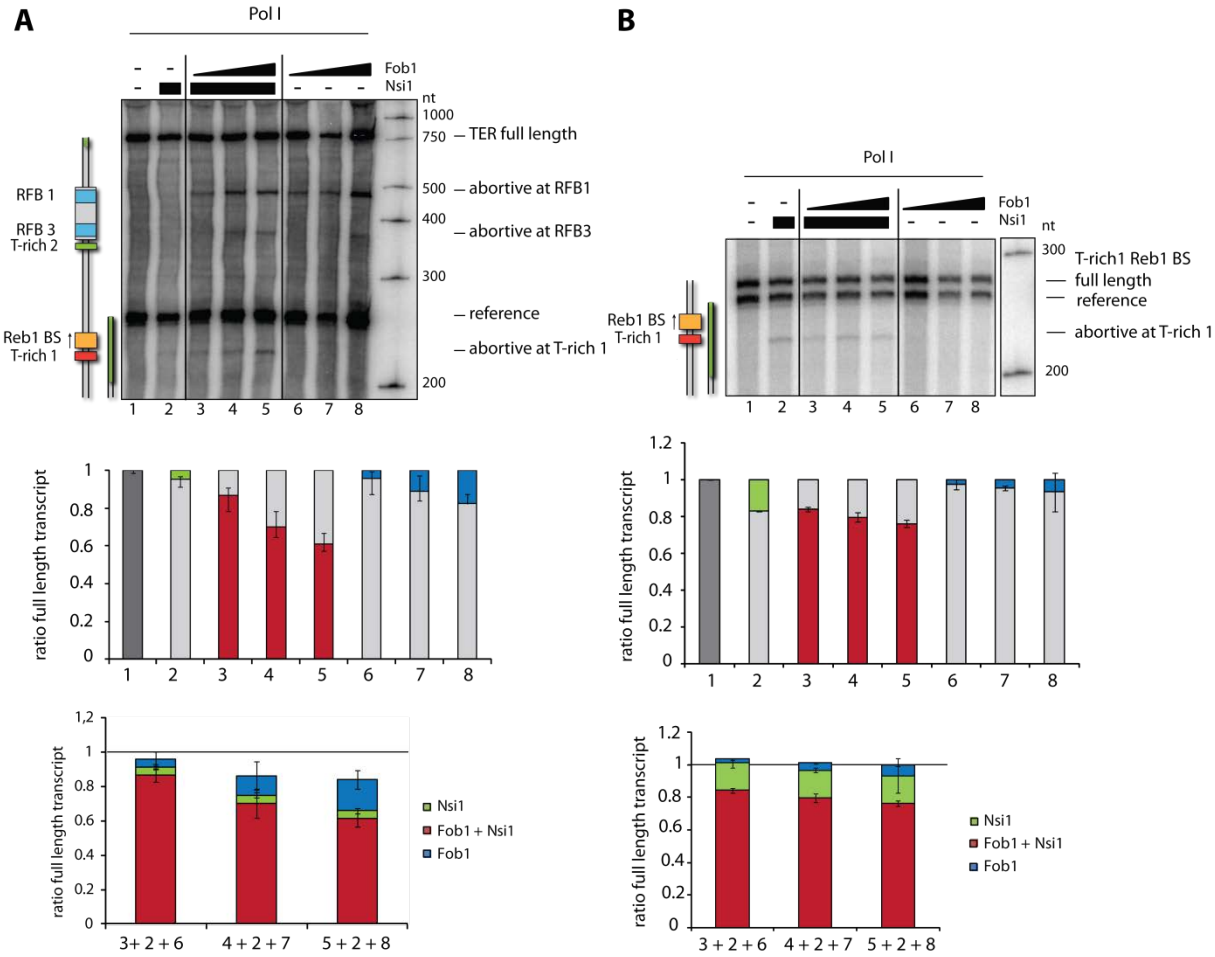

Fig. 4-28: Nsi1 and Fob1 exhibit cooperativity in Pol I transcription termination *in vitro.* (A) Transcription reactions were performed in duplicate as described with 10nM of the tailed template TER and 1µl Pol I. Nsi1 was used at 20nM concentration. Fob1 was titrated in three steps (27.6nM, 276nM, 1380nM) After addition of Nsi1 and/or Fob1, the sample was allowed to equilibrate for 15min at RT before the reaction was started. Isolated RNAs were separated on a 5% denaturing PA gel. Exposition time of the dried gel was 1h. A cartoon of the template indicates the identity and length of the RNAs. Signals were normalized to the reference transcript and the ratios of the full length transcript signal intensities of the lanes of interest versus the negative control were calculated and plotted. Grey bar: negative control; green bar: Nsi1 control, red bars: reactions with Nsi1 and Fob1; blue bars: Fob1 control titration. Red bars in the stacked diagram are identical to the red bars corresponding to lanes 3, 4 and 5. The percentages of terminated transcripts by Nsi1 (green bars) and Fob1 (blue bars) were calculated and plotted on top. **(B)** Explanation see (A) except that the tailed template T-rich 1 Reb1 BS was used instead of TER.

Obviously, the next question was whether Reb1 and Fob1 also exhibited a cooperative effect in Pol I transcription termination *in vitro*. An identical transcription experiment was carried out as described above with the template containing the complete rDNA terminator. Reb1 was used at 8.7nM, the least concentration at which a terminated transcript had been observed in titration experiments. The results can be seen in **Fig. 4-29**. In the Reb1 control lane (2), a very faint band corresponding to the abortive transcript at T-rich 1 was detected. Upon titration of Fob1 to samples containing Reb1, this signal did not visibly intensify (lanes 3-5). Comparison of the Fob1 control (lanes 6-8) with the lanes of interest (3-5) showed no difference in the intensity of the abortive transcript at RFB1.

First, the fractions of remaining full length transcript compared to the negative control (lane 1) were calculated and plotted for every lane as usual, confirming the observations. Then, diagrams with stacked columns were created from the dataset as outlined above. Contrary to the results obtained with Nsi1 on the same template, the signals added up to 100% thus indicating additivity of the effects.

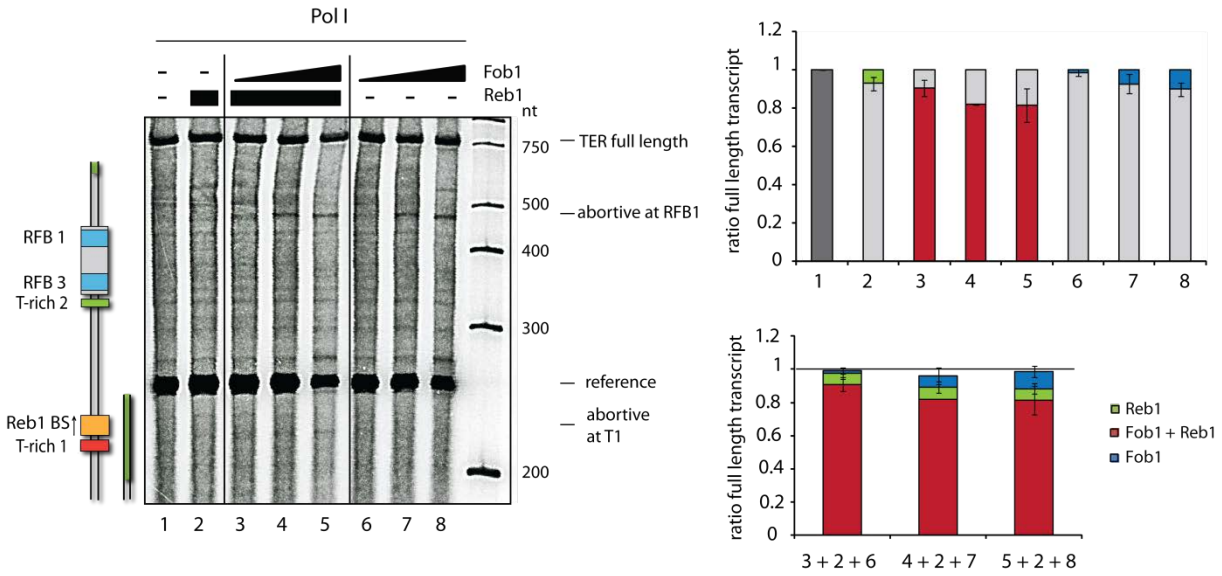

Fig. 4-29: Reb1 and Fob1 do not act cooperatively in Pol I transcription termination *in vitro*. (A) Description see Fig. 4-31 A. Instead of Nsi1, Reb1 was used at a concentration of 8.7nM. The contrast was adjusted compared to the original image.

4.8 Pol I mutants partly show altered behaviour in the termination assay compared to the wild-type

Since RNA Pol I subunits have been implicated to act in transcription termination, the question arose whether the termination effects observed with Nsi1, Reb1 and Fob1 *in vitro* could be traced back to a single subunit or a Pol I submodule. The analysis was based on previous reports indicating that subunit A12.2 was required for cleavage of the nascent RNA (Kuhn et al. 2007) and thus a key player in termination (Prescott et al. 2004). It was further demonstrated that deletion of A49 or the A49/A34.5 dimer resulted in reduced Pol I activity and hence in a growth phenotype (Huet et al. 1975; Liljelund et al. 1992). A more recent study structurally related TFIIF to the A49/A34.5 dimer (Kuhn et al. 2007) hence proposing a role as a built-in Pol I elongation factor. Therefore Pol I mutants lacking subunits A12.2 and A49 were purified (4.2.2) and employed in the analysis. Additionally it was reported that deletion of A12.2 was synthetically lethal (Gerber et al. 2008), if serine residue 685 in subunit A190 was mutated to aspartate (A190 S685D). Accordingly, the analyses were extended to Pol I A190 phosphomutants. Four mutants were selected in which either serine 685 or all serines which were identified as phosphosites were mutated to alanine or aspartate (A190 S685A, A190 S685D, A190 SallA, A190 SallD). Transcription experiments were carried out as usual with 10nM of the TER template complexed with either Nsi1 (88nM), Reb1 (700nM) or Fob1 (276nM) and 1µl of the respective polymerase fraction. The results are depicted in (**Fig. 4-30**).

When Pol I Δ A12 was transcribing the Nsi1-complexed template, an additional band was observed between the reference transcript and the transcript terminated at T-rich 1 compared to the wild-type situation (**Fig. 4-30 A**). According to a calibration curve derived from the RNA marker, it had a length of 232nt. Compared to the template, this size corresponds to the region just upstream of the Reb1 binding site. Furthermore, two transcript signals were obtained with Pol I Δ A12 mapping to the RFB1 and RFB 3 regions independently of the presence of an additional factor. The above observations were also made, if the Reb1-bound template was transcribed by Pol I Δ A12 (**Fig. 4-30 B**). One way of interpretation includes the hypothesis that the mutant is less termination-competent but eventually pauses upon reaching Nsi1. It can be speculated whether a distinct DNA structure is formed at the Reb1 binding site and the RFB which imposes an elongation obstacle for this Pol I mutant by itself. It might be envisioned that a special DNA structure could be a prerequisite for the cooperative effect on Pol I termination observed with Nsi1 and Fob1.

Compared to the wild-type, no differences could be detected, if the Nsi1-complexed template was transcribed with Pol I Δ A49 (**Fig. 4-30 A**). However, Reb1 or Fob1-dependent elongation blocking was roughly twice as efficient (**Fig. 4-30 B, C**). This observation would be generally in agreement with the role of A49/A34.5 as an elongation factor, albeit the question remains why results obtained with Nsi1 differed.

No major differences in termination efficiency were detected with Pol I A190 S685A and S685D in relation to the wild-type with Nsi1, Reb1 and Fob1 (**Fig. 4-30 A, B, C**). In contrast, for both the A190 SallA and SallD mutant the remaining proportion of run-off transcript was slightly elevated (70%-80% read-through) upon transcription of Reb1-, Nsi1- and Fob1-bound templates.

In summary, Pol I mutants partially show altered behaviour regarding transcription termination. However more thorough analyses of the observed effects and the respective polymerase mutants are necessary to draw mechanistic conclusions.

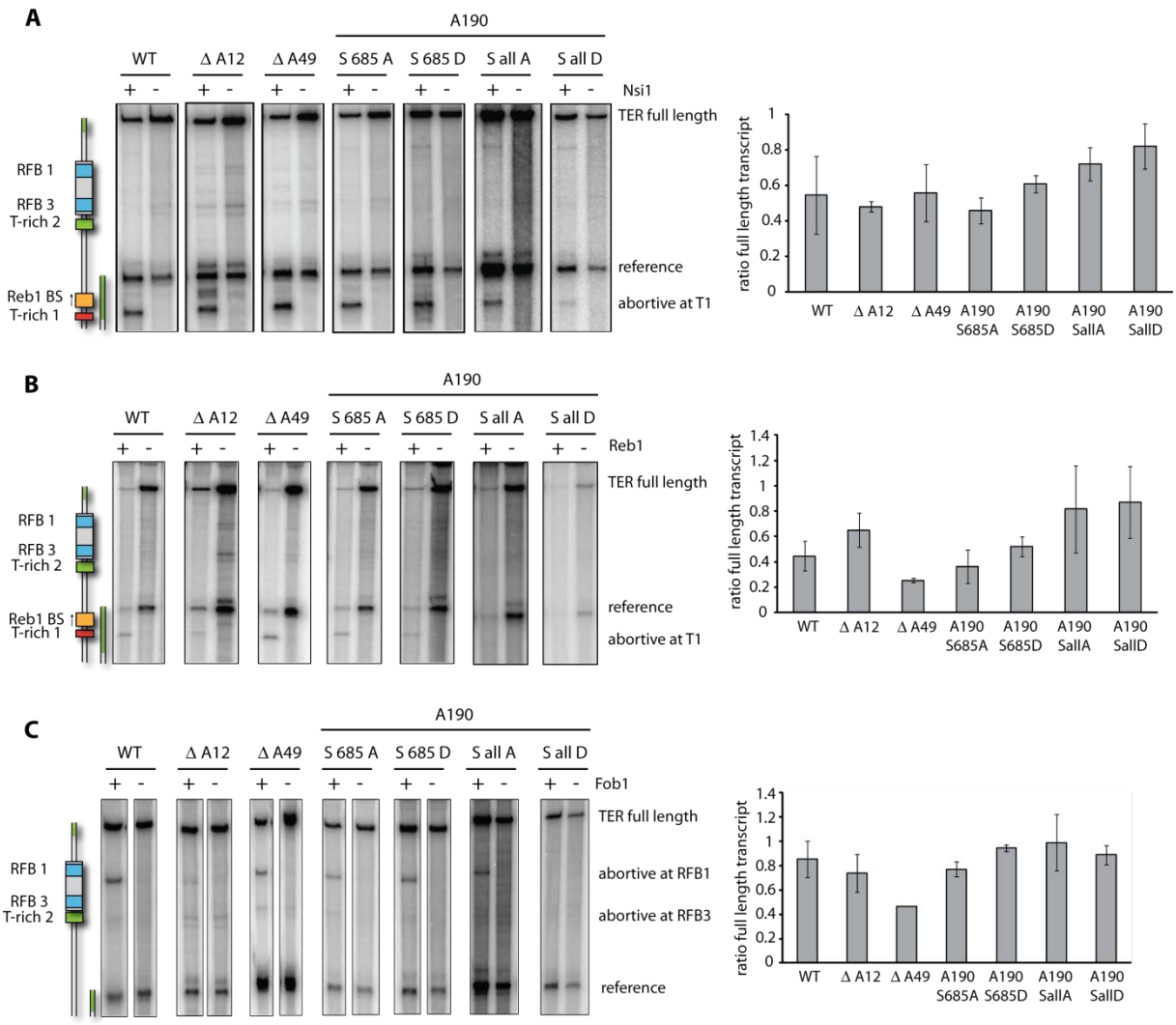

Fig. 4-30: Pol I mutants partially show altered transcription termination efficiency compared to the wild-type. (A) Transcription reactions were performed in triplicate as described with 10nM of the tailed template TER and 1µl of the

respective polymerase preparation. Nsi1 was used at 88nM concentration. After addition of Nsi1, the sample was allowed to equilibrate for 15min at RT before the reaction was started. Isolated RNAs were separated on a 5% denaturing PA gel. Exposition time of the dried gel was 1h. A cartoon of the template indicates the identity and length of the RNAs. Signals were normalized to the reference transcript and the ratios of the full length transcript signal intensities of the lanes of interest versus the negative control were calculated and plotted. **(B)** Description see (A) except that Reb1 was used at 700nM concentration instead of Nsi1. **(C)** Description see (A) except that Fob1 was used at 276nM concnentration instead of Nsi1.

4.9 Pol I, II and III deal differently with elongation obstacles *in vitro*

4.9.1 Only Pol I is significantly paused by Nsi1 and Reb1

A major goal of this study was to compare Pol I, II and III regarding their ability to handle elongation obstacles or in other words, if the purified trans-acting factors were elongation barriers for all of the polymerases or not. Therefore, comparative transcription assays with Pol I, II and III were performed in presence of Nsi1, Reb1 of Fob1. The sample containing the tailed template TER (**Fig. 4-1**) was incubated with 88nM Nsi1, 700nM Reb1 or 276nM for 15min at RT. Then transcription was started by addition of the polymerase and performed as described (3.2.12). The isolated RNA was separated on a 5% denaturing PA gel which was then exposed to an imaging plate for 1h. The experiments were done in triplicate and conducted in presence of 50mM KOAc or 150mM KOAc to exclude salt-dependency of observed effects. Size estimations of transcripts were based on calibration curves obtained with an RNA marker.

With Nsi1, abortive transcripts mapping to the T-rich 1 region were detected upon transcription with Pol I and in significantly lower intensity with Pol III but not with Pol II (**Fig. 4-31 A**). Note that with Pol III, the full length transcript cannot be formed due to the T-rich 2 element which serves as a Pol III terminator. Quantification (3.2.12 D) of the signals of the full length transcripts confirmed previous results showing that compared to the negative control, in presence of Nsi1 only 50%-60% of the full length transcript was obtained when transcription was done with Pol I. With Pol II or III still 80%-90% of the amount run-off transcript were detected. Albeit more full length transcript seemed to be produced in an environment with higher ionic strength, the general tendency was the same in both setups. It can be speculated, if higher KOAc concentration lowers the strength of the Nsi1-DNA interaction and thus favours run-off transcription.

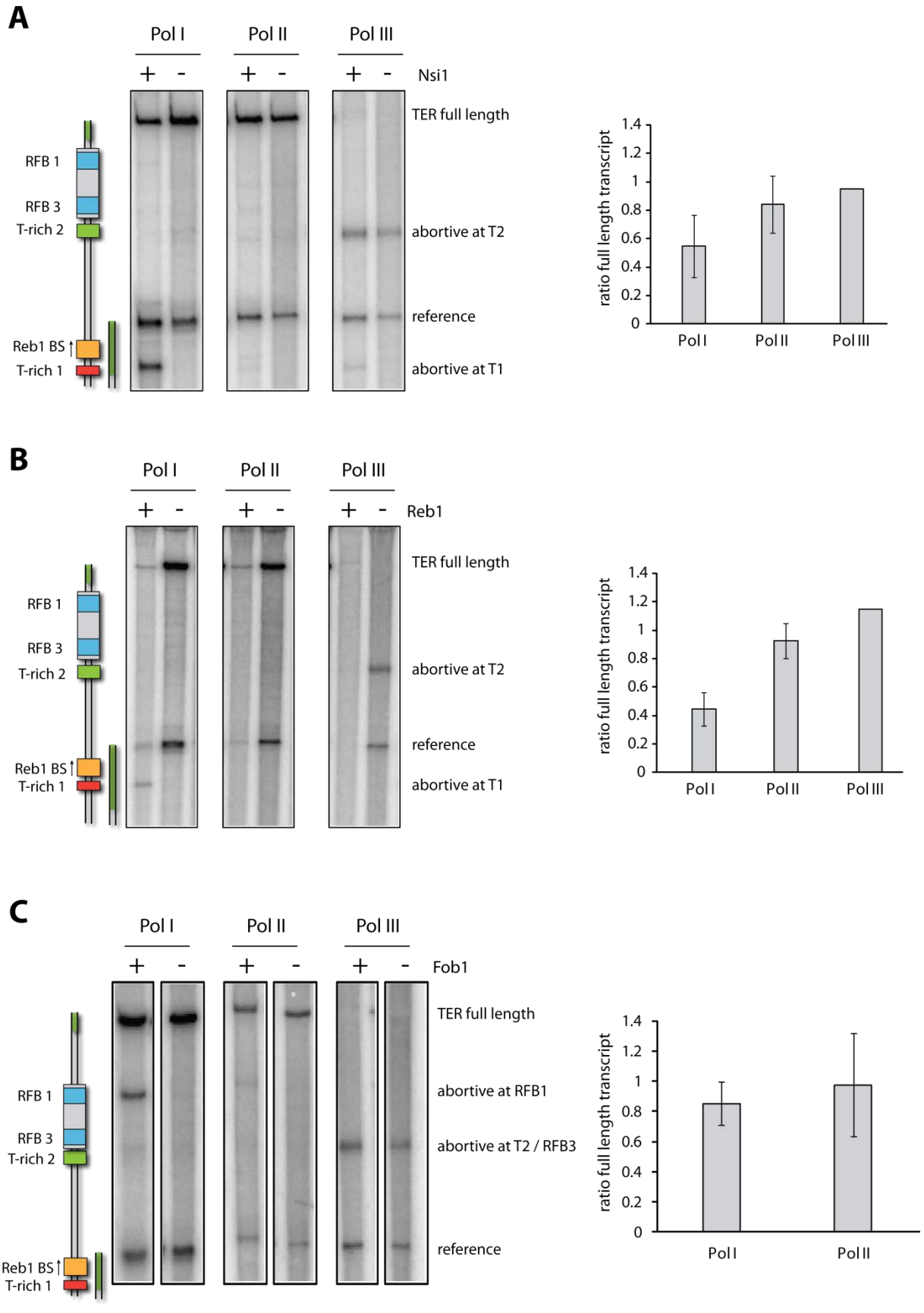

Fig. 4-31: Comparative transcription with Pol I, II and III using the tailed TER template complexed with Nsi1 or Reb1 reveals significant differences between the polymerases. (A) Transcription reactions were performed as described with

10nM tailed template TER and 1µl of the respective polymerase preparation. Nsi1 was used at 88nM concentration. After addition of Nsi1, the sample was allowed to equilibrate for 15min at RT before the reaction was started. Isolated RNAs were separated on a 5% denaturing PA gel. Exposition time of the dried gel was 1h. Cartoons of the templates indicate the identity and length of the RNAs. Signals were normalized to the reference transcript and the ratios of the full length transcript signal intensities of the lanes of interest versus the negative control were calculated and plotted. Identical experiments were performed at 50mM KOAc and 150mM KOAc The gel pictures and diagrams represent the 50mMKOAc situation. **(B)** Description see (A), except not Nsi1 but Reb1 was used at 700nM concentration. **(C)** Description see (A), except not Nsi1 but Fob1 was used at 276nM concentration

When Reb1 was included in the reactions, an abortive transcript mapping to the T-rich1 site was detected in Pol I transcription as previously shown (**Fig. 4-31 B**). This effect was not observed for Pol II or III. Quantification confirmed that upon addition of Reb1, only 30%-40% of full-length transcript were formed with Pol I. Contrary, the amount of RNA generated by Pol II or III was only minimally impaired. For Pol II, this was unexpected since it was proposed that Pol II transcription is terminated by Reb1 (Lang et al. 1998). The results did not qualitatively depend on the amount of salt in the reaction. Quantification for Pol III could not be performed due to insufficient signal intensity in the 50mM KOAc setup.

The effect of Fob1 could be investigated only for Pol I and Pol II as the RFB is located 3' downstream of the T-rich 2 element which terminates Pol III. Nonetheless a respective experiment with Pol III was carried out to determine if Fob1 interfered with Pol III transcription independently of its designated binding sites. However Fob1 did not impose an elongation obstacle for Pol III. Upon transcription of the Fob1-complexed TER template with Pol I, the two previously shown bands mapping to RFB1 and RFB3 could be observed (**Fig. 4-31 C**). As in earlier experiments, the signal correlated to RFB1 was stronger than the one at RFB3. Taken into consideration that in body labeling conditions, more α-^{32}P-CTP is incorporated in longer RNAs, still more transcripts seem to be aborted at RFB1. However, calculation of a remaining full-length transcript proportion of 80% revealed that Fob1 was only a minor roadblock for Pol I. Transcription with Pol II resulted in an additional, faintly visible transcript in the range of RFB1, though quantification yielded the same result as for Pol I.

In summary, it was shown that Nsi1, Reb1 and Fob1 specifically imposed elongation barriers of different strength for Pol I *in vitro*. Contrary, Pol II and Pol III transcription was not pronouncedly impaired by the presence of the mentioned factors in the way of the elongating polymerase. The effects were reproducible and only quantitatively dependent on the amount of KOAc present in the reaction.

4.9.2 LexA affects Pol II and III elongation but not Pol I

We further wanted to elucidate, whether the results how Pol I, II and III deal with proteins which bind to the 35S rDNA terminator during transcription was transferable to other elongation barriers. Therefore, it was an interesting option to extend this analysis to the strong DNA-binding bacterial protein LexA. Therefore, *in vitro* transcriptions were done with the tailed template containing three bacterial SOS boxes and therefore three binding sites for LexA (**Fig. 4-2**). The template (22nM) was fully complexed with LexA (1.6µM) as determined in gel shift analyses (**Fig. 4-15**). After addition of LexA, the sample was allowed to equilibrate at RT for 15min and then transcription was started by addition of the respective polymerase. Experiments were carried out in triplicate comparatively with Pol I, II and III as described. The isolated RNAs were separated on a 5% denaturing PA gel which was exposed to an imaging plate for 1h after drying. The amount of full length transcript was reduced visibly when Pol II was transcribing the complexed template and an additional smaller RNA was detected (**Fig. 4-32**). According to a calibration curve created with an RNA marker, the small fragment had a length of 188nt, which maps closely to the first SOS box (240nt-220nt) of the template.

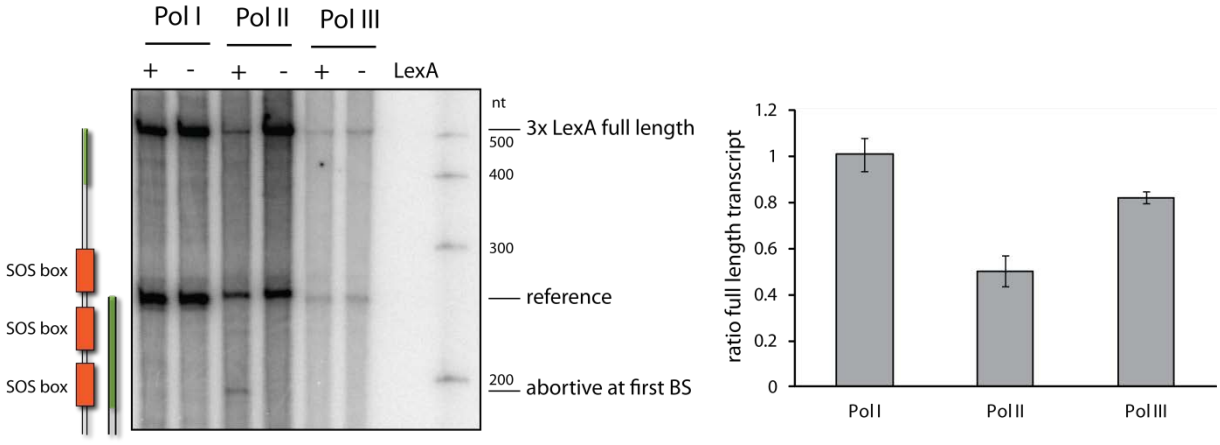

Fig. 4-32: LexA is an elongation obstacle for Pol II and III but not for Pol I. Transcription reactions were performed as described with 22nM tailed template 3x LexA and 1µl of the respective polymerase preparation. LexA was used at 1.7µM concentration. After addition of LexA, the sample was allowed to equilibrate for 15min at RT before the reaction was started. Isolated RNAs were separated on a 5% denaturing PA gel. Exposition time of the dried gel was 1h. Cartoons of the templates indicate the identity and length of the RNAs. Signals were normalized to the reference transcript and the ratios of the full length transcript signal intensities of the lanes of interest versus the negative control were calculated and plotted.

Calculation of the proportion of the remaining run-off transcript resulted in 50% for Pol II. Pol I was not affected and for Pol III a minor effect was observed, though no abortive transcript was visible. Unfortunately, the interesting comparison to T7 RNA polymerase could not be done as the

polymerase does not tolerate the ionic strength in the reaction and not all yeast polymerases work in the T7 polymerase buffer. As the tailed template assay does not answer the question of transcript release, no distinction can be made whether the observed effects are termination or polymerase pausing. Our results for Pol I are in good agreement with the literature, since recent *in vivo* experiments showed that LexA does not impose a transcriptional barrier for Pol I (Reiter et al. 2012).

4.9.3 TTF-I affects elongation of all three yeast RNA polymerases

We further characterized the three RNA polymerases by focusing on the question whether the well-studied Pol I termination factor TTF-I of higher eukaryotes would be an elongation obstacle and which polymerases would be affected. Respective transcription experiments used tailed templates incorporating a part of the mouse rDNA terminator which includes 5 TTF-I binding sites (5x TTF-I, **Fig. 4-2**). Additionally, a similar template with the inverted sequence was available (5x TTF-I inv) to investigate whether observed effects were direction-dependent. An N-terminal truncation variant of mouse TTF-I was used in the experiments (TTF-I ΔN348) which was a kind gift from Attila Nemeth (Németh et al. 2004, **Fig. 4-33 B**). Transcription experiments were only conducted with KOAc-purified polymerases with additional 150mM KOAc. Template concentration was 9.5nM and TTF-I ΔN348 was present at 7.6µM. After addition of TTF-I, the sample was equilibrated at RT for 15min and then transcription was started by addition of the respective polymerase. Experiments were carried out in duplicate comparatively with Pol I, II and III as described. The isolated RNAs were separated on a 5% denaturing PA gel which was exposed to an imaging plate for 1h after drying.

TTF-I imposed a major roadblock for all three polymerases (**Fig. 4-33 A**) albeit it cannot be discriminated between termination and pausing concerning Pol II and III. With Pol I, no full length transcript of the 5x TTF-I template was formed in presence of TTF-I, corresponding to 100% termination. Instead, two major bands mapping to the first and second TTF-I binding site were observed. Interestingly, if transcription was performed with a 5x TTF-I template containing the yeast rDNA promoter and an initiation-competent fraction containing Pol I (PA600, (Tschochne & Milkereit 1997)), all transcripts were terminated at the first binding site in presence of TTF-I (data not shown). Pol II was able to fully transcribe a fraction of the complexed template, but singals of transcripts in the range of the first three binding sites were detected. For Pol III it was impossible to transcribe the template completely due to a large T-rich region located shortly downstream of the second TTF-I binding site which acted as a terminator.

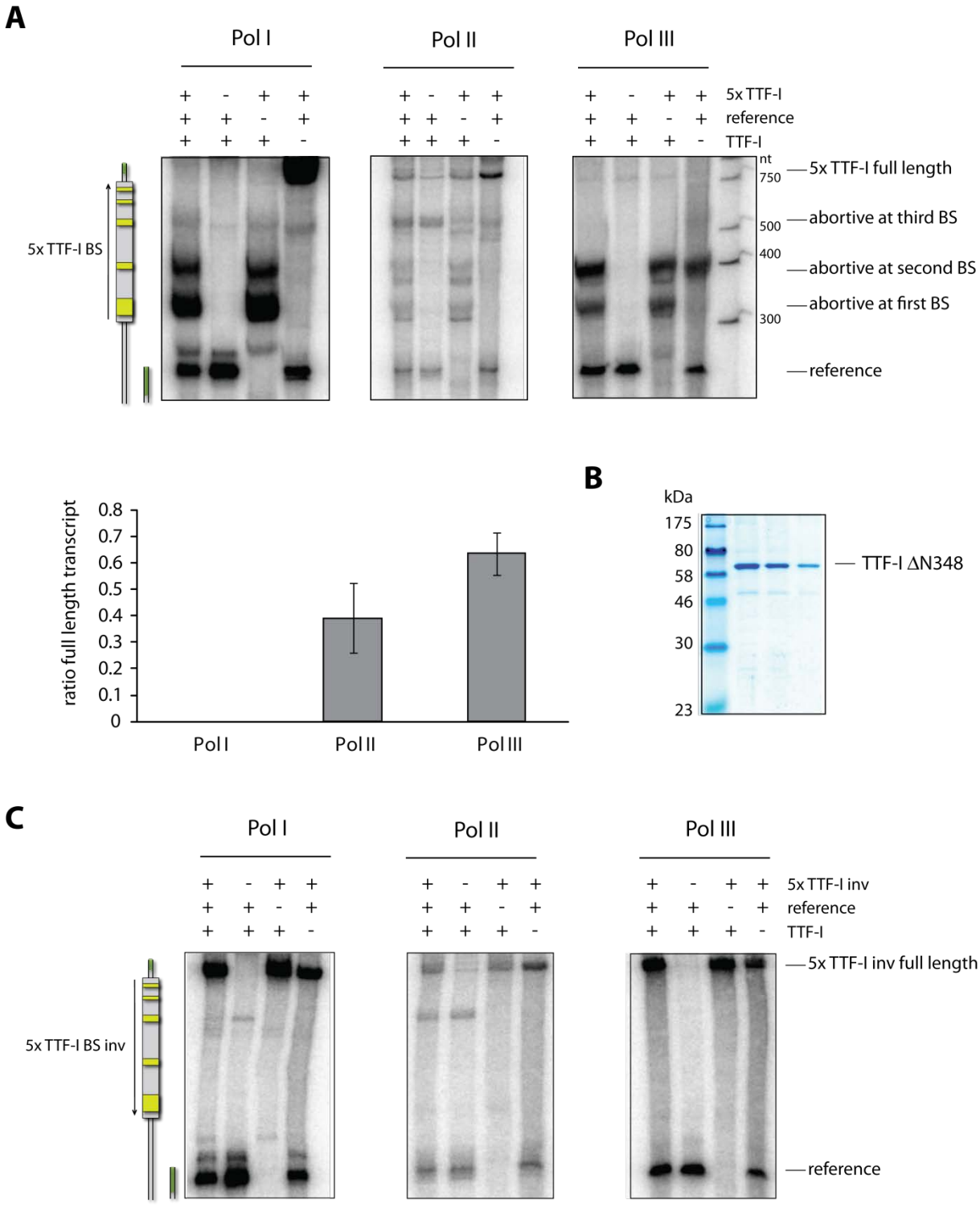

Fig. 4-33: TTF-I is a major roadblock for all three RNA polymerases. (A) Transcription reactions were performed as described with 9.5nM tailed template 5x TTF-I and 1µl of the respective polymerase preparation. TTF-I was used at 7.6µM concentration. After addition of TTF-I, the sample was allowed to equilibrate for 15min at RT before the reaction was started. Isolated RNAs were separated on a 5% denaturing PA gel. Exposition time of the dried gel was 1h. Cartoons of the templates indicate the identity and length of the RNAs. Signals were normalized to the reference transcript and the ratios of the full length transcript signal intensities of the lanes of interest versus the negative control were calculated and plotted. **(B)** TTF-I ΔN348 from Attila Nemeth was analysed on a 10% SDS gel. **(C)** Description see (A) except the template was 5x TTF-I inv.

However, a fraction of transcripts was elongated until the first binding site only. Size estimations were based on a calibration curve obtained with an RNA marker. Calculation of the proportion of the remaining run-off transcript resulted in 40% for Pol II and 60% for Pol III. Compared to all other investigated factors, only TTF-I represented an insuperable roadblock for one of the polymerases, in this case Pol I. Furthermore, in vitro transcription experiments with the tailed template 5x TTF-I inv demonstrated that the observed effects were dependent on the orientation of the binding sites with regard to the elongating polymerase (**Fig. 4-33 C**). The results for Pol I are in good agreement with published (Evers et al. 1995) and unpublished (Gernot Längst, personal communication) data.

4.10 Transcription of chromatin templates *in vitro*

In the cell, transcription occurs in the context of chromatin, a complex assembly of nucleic acids and proteins. The most abundant structural unit of chromatin is the nucleosome. As outlined in (2.4), studies on how Pol I, II and III deal with a nucleosomal template *in vitro* are hard to compare. Thus we wanted to study Pol I, II and III elongation on a nucleosomal template comparatively to learn more about the respective polymerase-inherent capability to overcome a nucleosomal barrier.

4.10.1 Establishment of nucleosomal templates

The reconstitution of the DNA-nucleosome complex in vitro is called chromatin assembly. Nucleosomes were assembled on tailed templates containing one or multiple 601 nucleosome positioning sequences (Lowary & Widom 1998) via salt dialysis *in vitro* (Kleiman & Huang 1972; Woodcock 1977; Wilhelm et al. 1978; Gadski & Chae 1976; Peterson 2008; Lee & Narlikar 2001). Due to the strong affinity of the 601 sequence to the histones, the nucleosome position is exactly determined. Hence this technique yields a homogeneous population of chromatin templates. As every template behaves differently in chromatin assembly, a titration series of assemblies with different histone:DNA ratios was conducted first. Samples contained 5µg of the tailed template with one 601 binding sequence, 10mg BSA and varying amounts of chicken histones in a total volume of 50µl high salt buffer. (**Table 3-8**). Purified chicken core histones H2A, H2B, H3 and H4 were a kind gift of the Längst lab (NEELIN & BUTLER 1959) (**Fig. 4-34**). The assembly was carried out as described

(3.2.8) and dialysis from 2M NaCl to 200mM was done over night at RT. Chromatin and free DNA were separated on a native 6% PA gel and the DNA was visualized with ethidium bromide (**Fig. 4-34**). Note that during tailed template preparation the vector backbone remained in the solution and thus two bands were visible in the negative control. The analysis revealed that upon rising histone concentrations first the 1x 601 template was occupied by a nucleosome followed by the vector backbone. This coincides with the strong affinity of the 601 sequence in comparison to random DNA. However once all 601 sites were occupied by nucleosomes, random nucleosome formation on the backbone started. Thus, the additional vector DNA served as a buffer against assembly of more than one nucleosome on the tailed template. For *in vitro* transcription, a mixture of assemblies with a ratio of 0.6:1 and 0.8:1 was used, which exhibited full template occupancy but not yet random assembly.

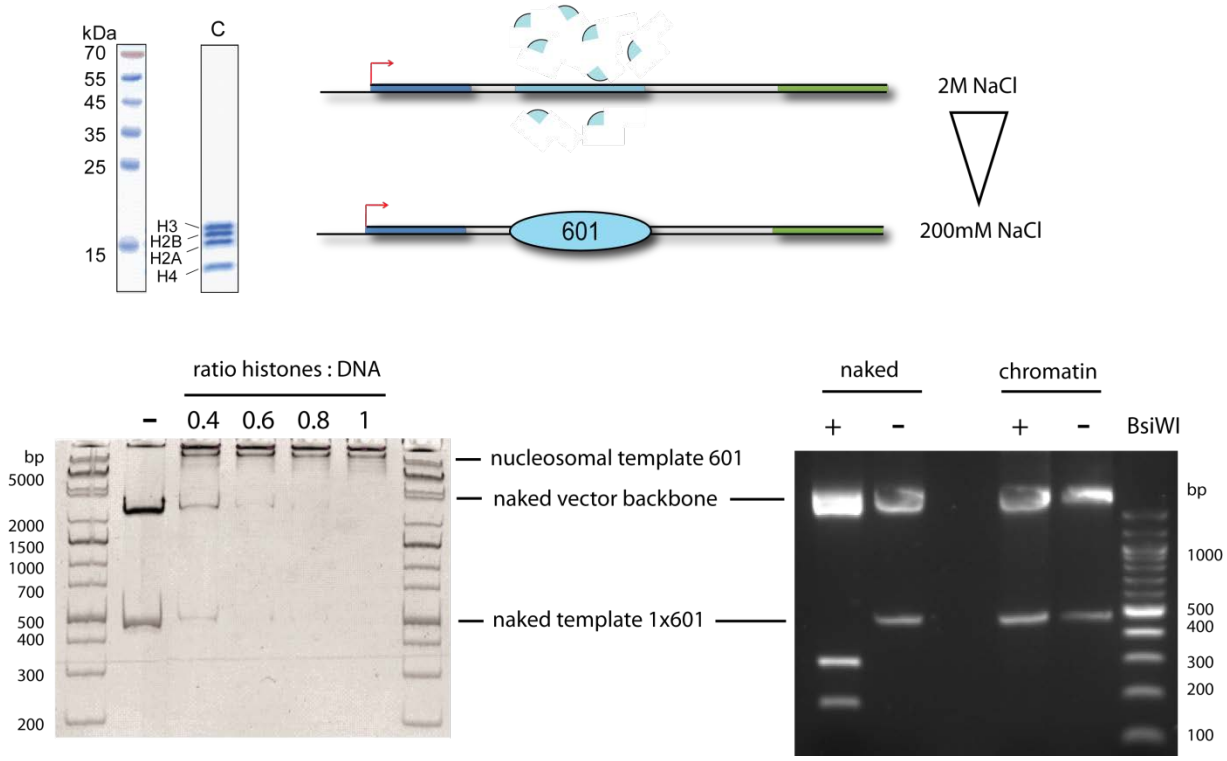

Fig. 4-34: Nucleosomes are assembled on templates containing 601 positioning sequences via salt dialysis. Chromatin was assembled via salt dialysis from 2M to 200mM over night. Assembly reactions contained 5µg 1x 601 tailed template DNA, 10mg BSA and varying amounts of histones in a total volume of 50µl. Purified histones from chicken erythrocytes were a kind gift of the Längst lab. 10% of the assembly reactions were separated on a native 6% PA gel and the DNA was visualized with ethidium bromide. Equal amounts of the mixture of 0.6:1 and 0.8:1 chromatin and naked template DNA were digested with BsiWI for 1h at 37°C. Samples were Proteinase K treated as described and EtOH precipitated. The pellet was redissolved and completely applied on a 1% agarose gel. DNA was visualized with SYBR Safe. Samples omitting BsiWI which were equally treated served as controls.

Due to the length of the standardly used elongated version of the 1x 601 template, formation of additional nucleosomes up- and downstream of the 601 sequence could not be excluded. A

downstream nucleosome would not compromise the later analyses as putative effects should be induced by the first nucleosome with known positioning. In contrast, a nucleosome positioned randomly upstream of the 601 sequence would make soild data analysis impossible. However, the short template version did not provide enough space to accommodate a second nucleosome upstream of the 601 sequence. Comparison of results obtained with the short (data not shown) and long (**Fig. 4-35**) version of the 1x 601 template (4.1.2) in identical in vitro transcription assays showed no significant differences in elongation behavior (4.10.2). This suggested that no additional nucleosome had been positioned upstream of the 601 sequence on the elongated template.

The amount of template which had actually been assembled was further determined by a restriction endonuclease protection assay. Therefore, equal amounts of naked DNA and chromatin were digested with BsiWI which has a recognition site in the 601 sequence close to the dyad axis of the nucleosome. Afterwards, the samples were Proteinase K digested and EtOH precipitated. As a control, naked DNA and chromatin samples were treated equally without adding the enzyme. The extracted DNA was then analyzed on a 1% agarose gel (**Fig. 4-34**). While the naked DNA had been digested upon addition of BsiWI, the chromatinized template DNA had been fully protected by the nucleosome. This result confirmed the previous assumption that the template DNA was fully assembled according to the sensitivity of the detection method.

4.10.2 *In vitro* interaction of Pol I, II and III with a nucleosomal transcription barrier

To determine how a single nucleosome would affect the elongation of Pol I, II and III, comparative *in vitro* transcription experiments were conducted as described (3.2.12). The reference template, 1x 601 naked DNA and chromatin were present at a final concentration of 17nM. Controls included reactions with only one of the three templates (reference, 1x 601 naked or chromatin) to trace effects back to one template. Reactions were started with 1µl of the respective polymerase preparation. Isolated RNAs were separated on a denaturing PA gel which was exposed for 1h or over night. The results are depicted in **Fig. 4-35**. Pol II did not manage to produce a detectable full-length transcript from the chromatin template as judged after 1h exposure. Upon over night exposure of the gel, an abortive transcript could be detected with a length of 218nt, which corresponds to the 5' end of the 601 sequence. A faint band between 400nt and 500nt (*) possibly could represent the full-length transcript, however the signal intensity was too low for quantification. Thus a nucleosome

imposed a very strong barrier for Pol II *in vitro*, which is in good agreement with the literature (see 2.4). In contrast, Pol I (60% readthrough) and Pol III (50%) elongation were only compromised.

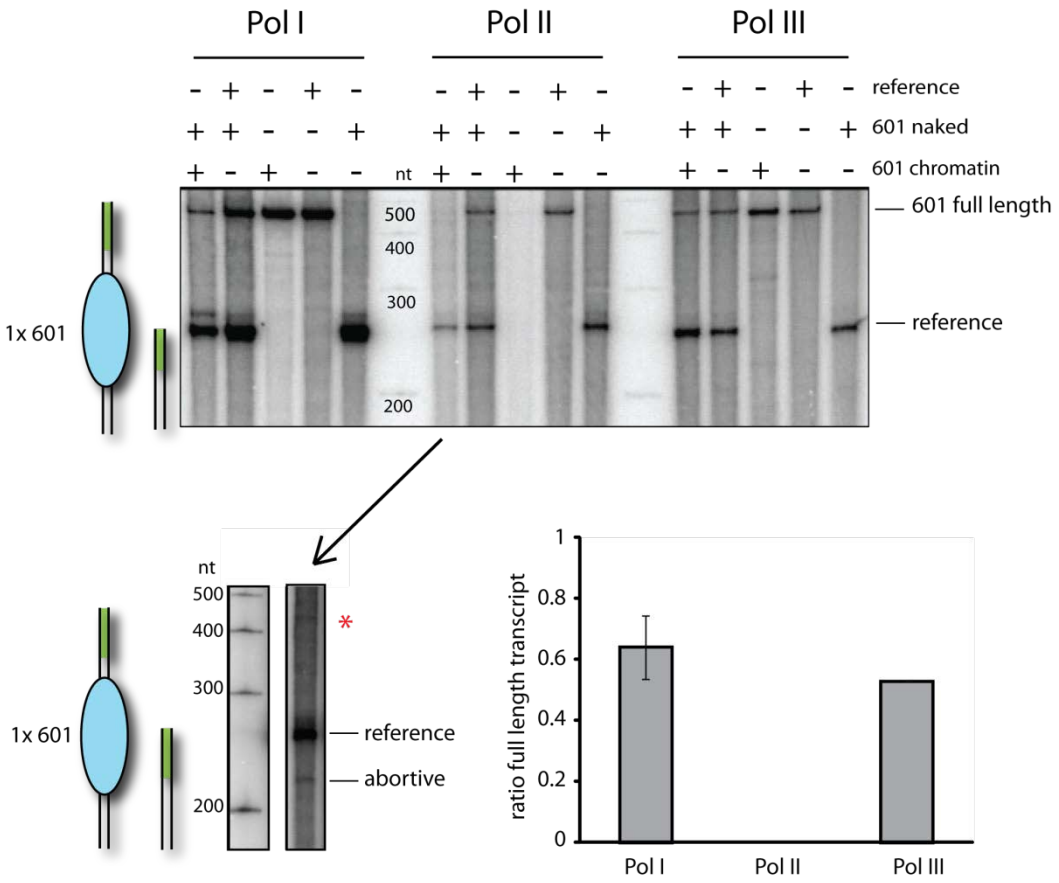

Fig. 4-35: A single nucleosome is a very strong barrier for Pol II and an elongation obstacle for Pol I and Pol III *in vitro*. Transcription reactions were performed in triplicate as described with 17nM of the tailed template 601 and the reference template. Reactions were started with 1µl of the respective polymerase preparation. Chromatinized 1x 601 template was used at 17nM. Isolated RNAs were separated on a 5% denaturing PA gel. Exposition time of the dried gel was 1h or over night to visualize the abortive transcript, respectively. A cartoon of the template indicates the identity and length of the RNAs. Signals were normalized to the reference transcript and the ratios of the full length transcript signal intensities of the lanes of interest versus the negative control were calculated and plotted. The red asterisk marks the possible run-off transcript produced by Pol II.

4.10.3 Subunit A49 significantly contributes to Pol I's ability to transcribe a nucleosomal template

Since Pol I was able to transcribe a nucleosomal template, the next question was whether this ability could be traced back to one or more subunits. Therefore, a subset of the already discussed Pol I mutants (4.2, 4.8) was tested in the *in vitro* transcription assay. Reactions were conducted as outlined above with 1µl of the respective polymerase preparation. Wild-type Pol I and the phosphomutant Pol I A190 S685A transcribed the chromatin template with 60% efficiency compared to naked DNA (**Fig. 4-36 A**). The fraction of full length transcript dropped to 45% when the chromatin template was transcribed by Pol I A190 S685D. However, the Pol I mutants lacking either subunits A12.2 or A49 generated only about 30% full length transcript in comparison to naked DNA. These results were in good accordance with the proposed role of subunit A49 as an elongation factor.

To formally demonstrate that the observed effect was due to the subunit A49, transcription experiments were conducted with equal amounts of wild-type Pol I, Pol I ΔA49 and different mixtures of Pol I ΔA49 and recombinant A49/A34.5 (4.3.7). All polymerases were preincubated on ice for 15min. Final concentration of the polymerases in the transcription reaction was roughly 7.5nM and A49 /A43.5 was titrated in four steps (7.5nM, 15nM, 75nM, 150nM final concentration). Interestingly, compared to the results above, the amount of full length transcript obtained with both wild-type Pol I and Pol I Δ A49 was lower than in previous experiments (45% and 10%) (**Fig. 4-36 A**). One possible explanation would be that the 15min incubation negatively influenced the integrity/activity/processivity of the polymerases. Nonetheless, upon titration of A49/A34.5 to Pol I Δ A49, wild-type read-through levels were reached. Note that in this experiment an abortive transcript was observed with Pol I ΔA49 which mapped to the 5' end of the 601 sequence. No polymerase activity was detected if transcription was carried out only in presence of recombinant A49/A34.5. Thus this suggests that subunit A49 plays a crucial role in transcription of nucleosomal templates by Pol I *in vitro*.

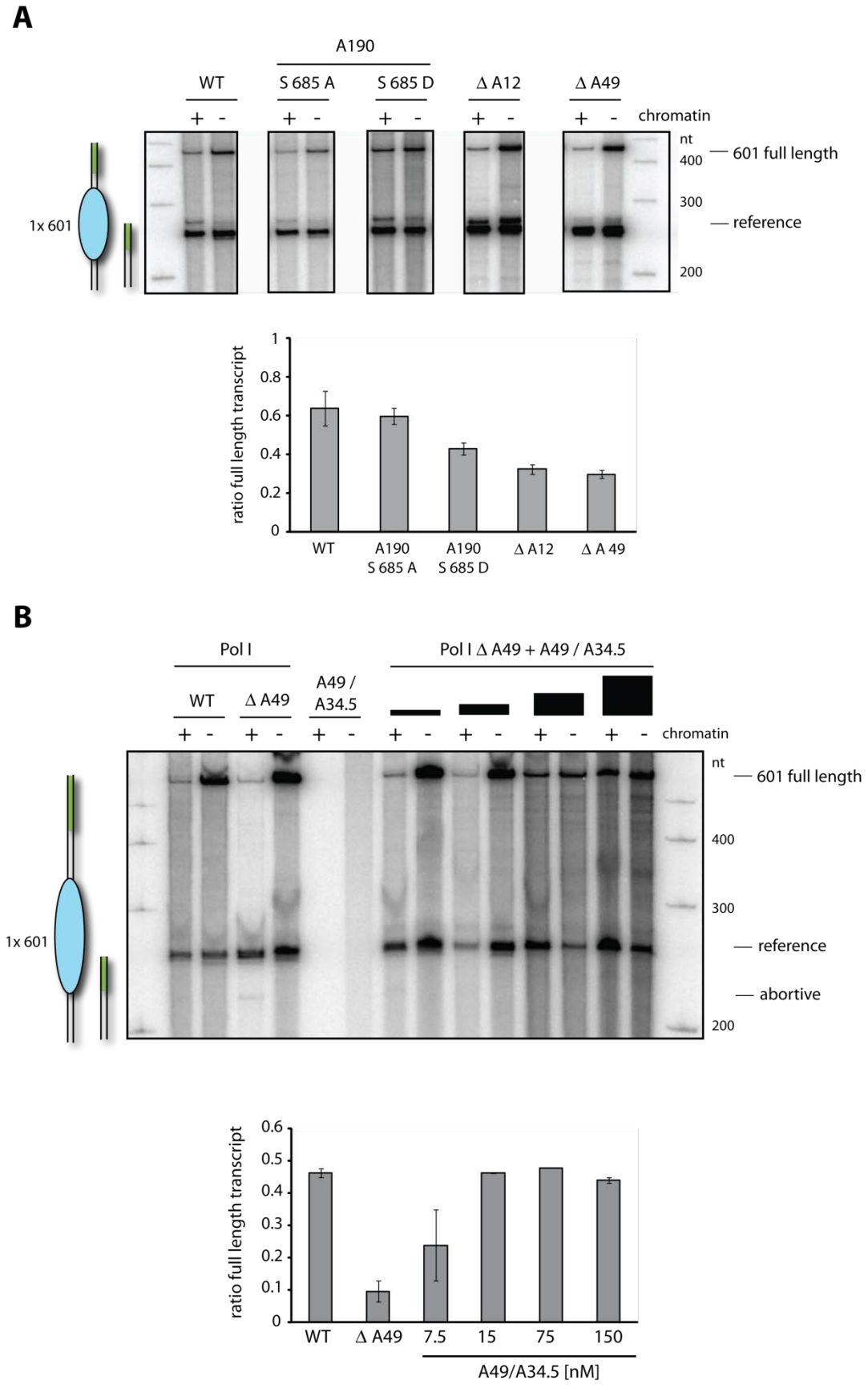

Fig. 4-36: Pol I subunits A49 and A12.2 significantly contribute to Pol I's ability to transcribe a nucleosomal template. (A) Transcription reactions were performed in triplicate as described with 17nM of the tailed template 601 and the reference template. Reactions were started with 1µl of the respective polymerase preparation. Chromatinized 1x 601 template was

used at 17nM. Isolated RNAs were separated on a 5% denaturing PA gel. Exposition time of the dried gel was 1h. A cartoon of the template indicates the identity and length of the RNAs. Signals were normalized to the reference transcript and the ratios of the full length transcript signal intensities of the lanes of interest versus the negative control were calculated and plotted. **(B)** Description of the transcription reactions an calculations see (A). Pol I Δ A49 (150nM) was incubated with recombinant A49/A34.5 (3µM) for 15min on ice. Final A49/34.5 concentrations in the transcription reactions were 7.5nM, 15nM, 75nM and 150nM with the final Pol I WT and Δ A49 concentration being 7.5nM.

4.10.4 TFIIF does not enable Pol II transcription through a nucleosome

After the confirmation that the A49/A34.5 dimer played a crucial role in transcription of chromatin templates by Pol I, it was logical to test its partial structural paralog TFIIF in this regard. Previously, Izban & Luse had reported that TFIIF exhibits no stimulatory effect on Pol II transcription of a nucleosomal template *in vitro* (Izban & Luse 1992). Transcription experiments were done as outlined for the titration of A49/A34.5 in (4.10.3). Reactions contained equal amounts of Pol II or mixtures of Pol II and purified TFIIF (500mM KCl condition, 4.3.6) respectively. As a negative control, transcription reactions were carried out with TFIIF alone. Pol II and the Pol II-TFIIF mixtures were incubated on ice for 15min prior to transcription to form the Pol II-TFIIF complex as shown in 4.3.6 C. The final Pol II concentration in the assay was 18nM and TFIIF was titrated in four steps (18nM, 25nM, 62.5nM, 125nM final concentration). All reactions were processed standardly and the extracted RNAs were separated on a 5% denaturing PA gel (**Fig. 4-37 A**). It was immediately obvious, that Pol II was not able to transcribe the chromatin template in the presence of TFIIF. Interestingly, the signal intensities of transcripts derived from naked DNA increased with rising amounts of TFIIF (**Fig. 4-37 A**). This is in accordance with published results indicating that TFIIF acts as a Pol II elongation factor on naked DNA by stimulation of the elongation rate and by decreasing elongation pausing (Flores et al. 1989; Price et al. 1989; Bengal et al. 1991; Izban & Luse 1992; Tan et al. 1994). Thus we propose that our TFIIF preparation is active.

It could not be excluded that only minor amounts of the Pol II-TFIIF complex were formed upon incubation. However in **Fig. 4-18** it was shown that Pol II was co-purified with TFIIF at 200mM KCl. Thus a fraction was available containing a certain amount of *ex vivo* purified Pol II-TFIIF complex. Albeit the percentage of Pol II-TFIIF complex in this preparation was unknown, it was demonstrated that the preparation exhibited polymerase activity (**Fig. 4-18**). Hence this fraction was used side-by-side with Pol II to transcribe the nucleosomal and naked template 1x 601 DNA (**Fig. 4-37 B**). Also in this experiment, no full length transcript originating from the chromatin template could be observed,

leading to the conclusion that Pol II-TFIIF was not able to transcribe a nucleosomal template, which confirmed previously published results (Izban & Luse 1992).

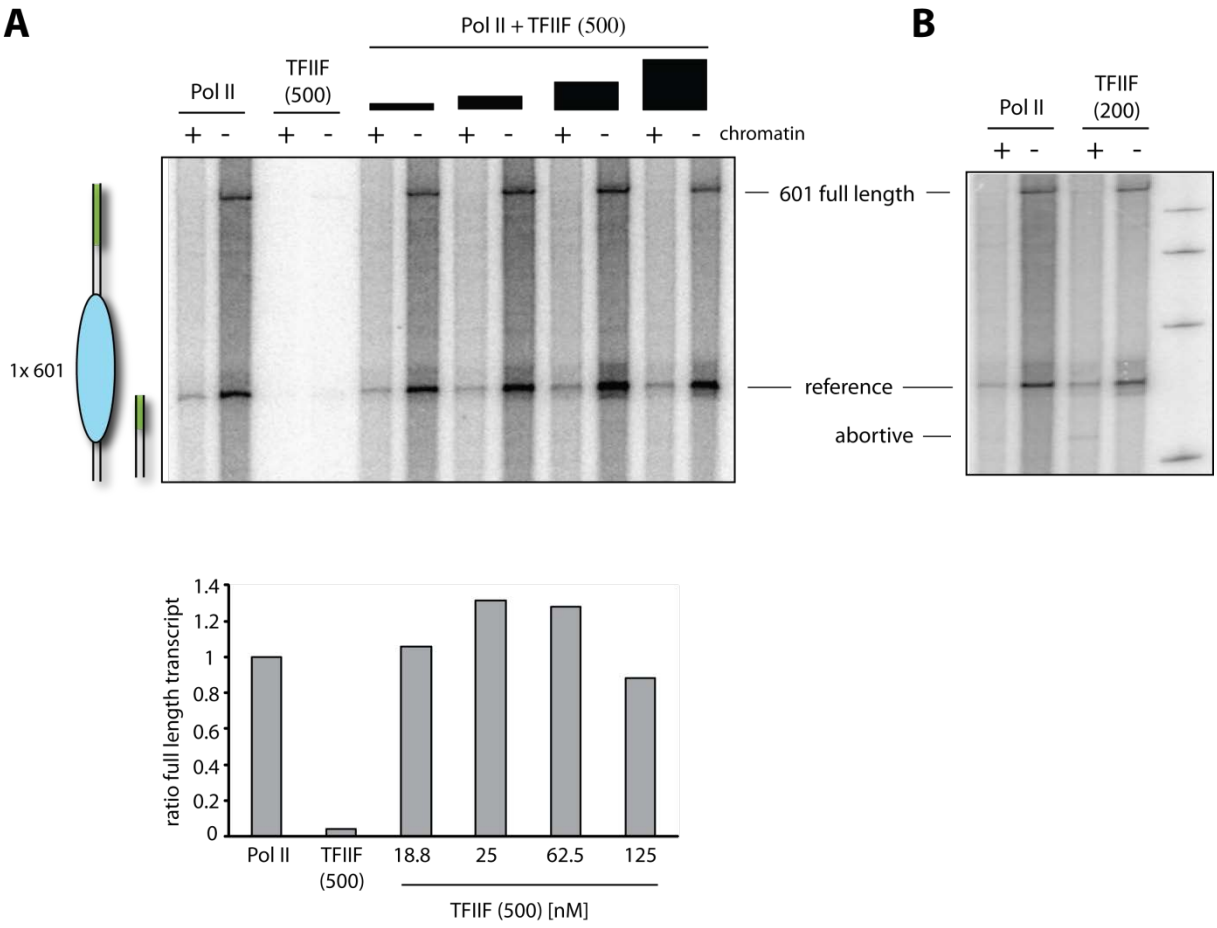

Fig. 4-37: TFIIF does not enable Pol II transcription through a nucleosome. (A) Transcription reactions were performed as described with 17nM of the tailed template 601 and the reference template. Reactions were started with 1µl of the respective polymerase preparation. Chromatinized 1x 601 template was used at 17nM. For the titration, Pol II was incubated with TFIIF purified at 500mM KCl for 15min on ice. Final TFIIF concentrations in the transcription were 18.8nM, 25nM, 62.5nM and 125nM. Isolated RNAs were separated on a 5% denaturing PA gel. Exposition time of the dried gel was 1h. A cartoon of the template indicates the identity and length of the RNAs. Signals were normalized to the reference transcript and the signal intensities of the 1x 601 full length transcripts in the lanes without chromatin were calculated and plotted.

CHAPTER V – DISCUSSION

5.1 Validation of the *in vitro* transcription system

Several factors were described to interact with the transcribing RNA Pol I at the terminator region. Two of these factors are Nsi1 and Fob1. We developed a novel approach to purify Nsi1 and Fob1 recombinantly from SF21 insect cells (3.2.9). The preparations were sufficiently pure to address their function in DNA binding and in *in vitro* transcription (4.3). The Fob1 fraction was purified close to homogeneity according to gel filtration. Interestingly, Fob1 eluted from the column as an apparent tetramer (4.3.3). Gel filtration analysis of Nsi1 was unsuccessful since it did not elute from the column. The trans-acting factors Reb1 and LexA were purified according to the published protocols or slight variations thereof (Morrow et al. 1990, Griesenbeck J.). LacI purification followed the protocol for LexA preparation (4.3.5). Gel filtration analysis revealed that the protein samples were purified close to homogeneity. Furthermore, multimerization of the factors was observed as they eluted from the column as an apparent pentamer (Reb1, 4.3.1), tetramer (LacI, 4.3.5) or monomer (LexA, 4.3.4). This is in good agreement with the literature for LexA and LacI (Bell & Lewis 2000; Butala et al. 2009). However, it is unknown, whether Reb1 forms multimers *in vivo* and if this has any implications in its designated function as a Pol I termination factor.

Specific binding of Reb1, Fob1 and LexA to their designated recognition sites according to the literature could be verified *in vitro* (Kobayashi 2003; Butala et al. 2009; Morrow et al. 1989). We could demonstrate that Nsi1 binds to the terminator-proximal Reb1 BS *in vitro* albeit optimal conditions could not be determined to this end (4.3.2). Note that association of Nsi1 with a template containing the complete terminator region seemed to have slightly altered binding behaviour compared to a template lacking the RFB.

Further, we report a one-step method for purification of all three yeast RNA polymerases based on immunoprecipiation. Judged based on the sensitivity of mass spectrometric analysis, polymerase fractions were not cross-contaminated with each other and devoid of transcription factors (4.2.2, 4.2.3).

In vitro transcription reactions were performed with tailed templates. This method was first described by the Chamberlin group (Dedrick & Chamberlin 1985; Kane & Chamberlin 1985; Kadesch & Chamberlin 1982). However our approach generates templates with an equal tail length of 20nt. In contrast, use of terminal nucleotide transferase as described before yields a mixture of different tail lengths and hence a set of templates with different initiation efficiencies. It was proposed that tailed templates can be only transcribed once. This is based on the observation that upon transcription of a tailed template an RNA-DNA hybrid is formed and the template strand gets displaced (Dedrick & Chamberlin 1985; Kane & Chamberlin 1985; Kadesch & Chamberlin 1982). Single stranded DNA was not reported as a template for RNA polymerases so far. It is obvious that tailed template transcription hence does not resemble the *in vivo* situation with a protruding transcription bubble. Thus the possibility exists that effects observed in such a system differ from the *in vivo* situation. In this regard, confirmation of the *in vitro* results in an *in vivo* approach is crucial. However, as will be explained below, our *in vitro* data match with our previously reported *in vivo* results (Reiter et al. 2012).

5.2 Nsi1 is a *bona fide* Pol I transcription termination factor

Currently, two models for yeast Pol I transcription termination are being discussed. A simple explanation for the Pol I termination mechanism was postulated by the Reeder group (“pause and release”). Extensive *in vitro* studies (Lang et al. 1994) support a hypothesis according to which Pol I is stalled by the presence of Reb1 at its cognate binding site. Termination subsequently occurs due to the presence of the T-rich 1 stretch upstream of the pausing site which promotes release of both transcript and Pol I by destabilization of the ternary elongation complex. However, Reb1 was not found to be associated with its binding site in the 35S terminator region *in vivo* above background levels (Kawauchi et al. 2008; Goetze et al. 2010; Reiter et al. 2012). Furthermore, depletion of Reb1 steady-state levels to roughly 25% did not result in significant termination defects (Kawauchi et al. 2008). In yeast strains deficient in the RNase III-like endonuclease Rnt1 which is necessary for 35S

rRNA 3' end formation, acculumation of Pol I transcripts extending to the T-rich 1 region and beyond was observed (Prescott et al. 2004; Reeder et al. 1999). The same was observed for cells expressing catalytically inactive mutants of the 5'->3' exonuclease Rat1 and the helicase Sen1 (Kawauchi et al. 2008). Furthermore, Pol I occupancy downstream of T1 increases in the before mentioned strains. Thus, a second model which shows similarity to the "torpedo" mechanism suggested for Pol II transcription termination was proposed by the Tollervey and Proudfoot groups based on transcription run-on (TRO) and ChIP analyses (Kawauchi et al. 2008; Braglia et al. 2011; El Hage et al. 2008). This model links transcription termination with 35S pre-rRNA processing. In a first step, Rnt1 cleaves the nascent 35S-pre-rRNA and hence provides an entry site for Rat1 which trails the elongating polymerase and degrades the transcript. In this model Reb1 also serves as a pausing element for Pol I allowing Rat1 to catch up with it. When Rat1 has reached Pol I, Sen1 unwinds the RNA-DNA hybrid and thus the ternary complex is destroyed.

In a publication by our group (Reiter et al. 2012), Nsi1, a Reb1 homologue, was introduced as a novel Pol I termination factor. *In vivo* association of Nsi1 with the terminator region was shown by ChIP (chromatin immunoprecipitation) and ChEC (chromatin endogeneous cleavage) analyses. Our data suggest that recombinant Nsi1 also binds to the Reb1 binding site of the Pol I terminator *in vitro*. This is in good agreement with the bioinformatical prediction of a consensus Nsi1 binding site (CCGGGTAA) which is identical to the 5' part of the Reb1 BS (Gordân et al. 2010). Although no binding constants were calculated, the *in vitro* binding affinity of Nsi1 seemed to be higher than that of Reb1. This is not explanatory for the observation that Nsi1 but not Reb1 is associated with the terminator-proximal Reb1 BS but matches with it (Reiter et al. 2012). Note that according to genome-wide analysis (Ghaemmaghami et al. 2003), Reb1 is believed to be present in roughly 7500 molecules per cell whereas Nsi1 is less abundant (~400 molecules). Additionally, it was shown that Reb1 but not Nsi1 is tightly associated with the promoter-proximal Reb1 binding site *in vivo* (Kawauchi et al. 2008; Goetze et al. 2010; Reiter et al. 2012). Analysis of mutant Reb1 binding sites with decreased (mut1) and increased (mut2) Reb1 binding affinities (Lang & Reeder 1993; Reeder et al. 1999) led to diminished or enhanced Pol I termination. If the terminator-proximal Reb1 BS was replaced my mut1 or mut2 in a yeast strain harbouring the rDNA terminator in the ITS1, Nsi1 binding was impaired (mut1) or enhanced (mut2) and the growth defect reduced (mut1) or enhanced (mut2) (Reiter et al. 2012). Thus the reason for recognition site selectivity of Reb1 and Nsi1 requires further investigation and may be mediated by other trans-acting factors like Fob1.

Additionally, we showed that Pol I elongation through an Nsi1-complexed template containing the complete terminator sequence was impaired *in vitro* (roughly 40% readthrough, 4.5.1). However, Reb1 imposed a stronger roadblock to Pol I (roughly 30% readthrough) which is matching with the

results from the Reeder group (Lang et al. 1994). Preliminary analyses of promoter-dependent Pol I transcription termination with recombinant CF, Rrn3 and yeast-purified Pol I confirm the results regarding Nsi1-mediated transcription termination obtained with tailed templates. Furthermore, not only pausing but also transcript release could be demonstrated upon transcription of immobilized Nsi1-bound templates (H. Tschochner, unpublished data).

Introduction of the terminator region in the ITS1 of the 35S rDNA leads to significant growth reduction of the respective yeast strain and this effect could be traced back to binding of Nsi1 (Reiter et al. 2012). However, the question remains, which terminator cis elements influence Nsi1-mediated termination. We could demonstrate that presence of the Reb1 BS alone was sufficient to induce Pol I pausing and/or release *in vitro* (4.6.1). Furthermore, the T-rich 1 element significantly enhanced this effect and presence of the RFB seemed to exhibit slightly stimulatory activity. In accordance, *in vivo*, integration of the terminator-proximal Reb1 BS into the ITS1 was sufficient to induce a growth defect, which was enhanced by the presence of the T-rich 1 element and the RFB (Merkl P. et al., manuscript in preparation, Pérez-Fernández, unpublished data). Additionally, the Nsi1-mediated polymerase pausing was dependent on the orientation of the Reb1 BS pointing towards a specific interaction between Nsi1 and the polymerase in contrast to simple elongation blocking. These observations are in good agreement with previous results demonstrating that Nsi1-mediated growth reduction in a yeast strain where the rDNA terminator was integrated in the ITS1 was dependent on the orientation of the Reb1 BS (Merkl P. et al., manuscript in preparation, Reiter et al. 2012).

In a study by Ha and coworkers (Ha et al. 2012), cooperativity between Fob1 and Nsi1 was suggested. This hypothesis is based on the finding that depletion of Fob1 seems to result in reduced Nsi1 recruitment to the Reb1 BS in the terminator region. Furthermore, interactions between Nsi1 and Fob1 were demonstrated based on yeast two-hybrid screens (Mohanty & Bastia 2004; Uetz et al. 2000). Our *in vitro* data further strengthen the view of cooperativity between Nsi1 and Fob1 since upon a constant level of Nsi1, titration of Fob1 increased Pol I termination at the T-rich 1 element (4.7). On the other hand, cooperativity between Reb1 and Fob1 could not be shown *in vitro*.

It was suggested that co-transcriptional 35S pre-rRNA processing is a prerequisite for correct termination *in vivo* (Kawauchi et al. 2008; Braglia et al. 2011; El Hage et al. 2008). In this regard, cleavage of the nascent RNA by Rnt1 would provide an entry site for Rat1. However, Reiter and co-workers showed that efficient termination *in vivo* also occurred in absence of the Rnt1 cleavage site (Reiter et al. 2012). It was further proposed that a failsafe termination mechanism exists in case of absence of Rnt1 or its cleavage site (Braglia et al. 2011). In this model, the T-rich stretch marks a second cleavage site for an unknown endonuclease which provides an alternative entry site for Rat1. This hypothesis is in contrast to earlier reports indicating that the T-rich region is necessary for RNA

release (Lang & Reeder 1995). This failsafe mechanism was postulated based on hybrid selection transcription run-on (hsTRO) analysis in WT and ΔRnt1 strains. hsTRO is a technique with which 3' end formation can be detected. However, proof of 3' end formation does not answer the question whether the 3' end results from a cleavage event or polymerization cessation and release. To confirm this hypothesis, detection of 5' end formation will be crucial. Furthermore, spatial requirements question the failsafe termination mechanism. The T-rich 1 stretch is located 16bp upstream of the Reb1 BS where Pol I is stalled due to binding of Reb1. Given the fact that Pol II is supposed to cover 25bp of DNA (Gnatt et al. 2001) it is hard to imagine how an endonuclease could get access to the T-rich stretch. In this regard, we were able to show that Pol I transcription is terminated *in vitro* in absence of both Rnt1 and the Rnt1 cleavage site only by Nsi1 or Reb1 binding to the template DNA. On the other hand, it can be imagined that RNA cleavage occurs not due to the presence of an unknown endonuclease, but is in intrinsic feature of Pol I. This explanation would facilitate termination in presence or absence of a T-rich stretch. In fact, it was reported previously, that subunit A12.2 is involved in transcription termination and RNA cleavage thus making it a possible candidate (Kuhn et al. 2007; Prescott et al. 2004). However, deletion of subunit A12.2 did not influence transcription termination at the T-rich 1 element (Braglia et al. 2011). According to our *in vitro* results, termination efficiencies of WT Pol I and Pol I ΔA12 are similar in the presence of Nsi1 (4.8). In respective experiments conducted with Reb1, Pol I ΔA12 exhibited a slightly reduced termination efficiency. Similarly, Nsi1-mediated Pol I termination was not influenced by the absence of subunit A49, whereas the Reb1-bound template imposed a stronger barrier for Pol I ΔA49 (4.8). Furthermore, the transcriptional roadblock induced by Fob1 was enhanced for Pol I ΔA49. In summary, these results argue for a putative interplay of subunits A12.2 and A49 with Reb1 and interaction of A49 with Fob1, although the physiological relevance and the implication for the termination mechanism remains to be clarified.

Concerning the Pol I A190 phosphomutants, no major changes in run-off transcript levels were observed with the S685A/D mutants compared to the WT when templates complexed with Reb1, Nsi1 or Fob1 were transcribed (4.8). Contrary, comparison of the SallA/D mutants with the WT revealed an elevated full-length transcript formation upon transcription of Nsi1 and Reb1 bound templates (4.8). Since both mutants with alanine or aspartate substitutions exhibit the same phenotype, we cannot draw meaningful conclusions from this set of experiments. However, phosphorylation of serine residues in A190 apart from S685 might affect transcription termination efficiency of Pol I.

Taken together, our in vitro data further strengthen the pause-and-release model originally proposed by the Reeder group. In accordance with our previous study (Reiter et al. 2012) we speculate that

Nsi1 fulfills the pausing and/or release function originally assigned to Reb1 *in vivo*. Our results are supported by *in vivo* studies conducted in our lab demonstrating that Pol I occupancy at the Reb1 BS and the RFB increase upon deletion of Nsi1 and are further elevated in a ∆nsi1 ∆fob1 strain (J. Pérez-Fernández, unpublished data). Nonetheless, a Reb1 function in Nsi1 recruitment, Nsi1 binding stabilization, or interaction with Pol I might be envisioned and will be the subject of further investigations. Concerning the torpedo termination model, it is possible that Rat1-mediated transcript degradation supports Pol I transcription termination. However, Nsi1 binding to the terminator-proximal Reb1 BS is sufficient to terminate at least a fraction of the transcribing Pol I *in vitro*. Nonetheless, our results do not exclude and comment on coupling of co-transcriptional 35S pre-rRNA processing to transcription termination. Furthermore, the physiological relevance of the apparent leakiness of Pol I transcription termination and hence the role of Nsi1 in rDNA integrity maintenance as suggested by Ha and coworkers (Ha et al. 2012) has to be investigated thoroughly.

Comparison of yeast Pol I termination to the RNA polymerase termination mechanisms proposed for T7 phage, bacteria and archaea reveals interesting similarities. According to our current knowledge, T7 and archaeal transcription are terminated by the presence of a T-rich stretch, albeit without any additional trans-acting factors (2.1.2, 2.1.3, 2.1.4). The described factor-independent termination mechanism in bacteria also requires a T-rich region. However, it is suggested that furthermore GC-rich inverted repeats which form an RNA hairpin structure contribute to bacterial RNAP termination. In this regard, bacterial and eukarotic Pol III seem to share related pathways according to most recent publications (Nielsen et al. 2013). For T7 RNAP, bacterial RNAP, yeast or mammalian Pol I, involvement of an RNA secondary structure in the termination process was not demonstrated so far. Note that the stem-loop structure in the pre-35S rRNA downstream of the 25S is an Rnt1 cleavage site and thus can not contribute to termination in the same allosteric mechanistic way as proposed for Pol III.

Concerning putative evolutionary relatedness, the second, Rho-dependent termination mechanism of bacterial RNAP (2.1.3) exhibits similarities to the torpedo termination model for eukaryotic Pol II (and Pol I). Whereas in Rho helicase and RNase activity are unified, eukaryotes apparently require two different factors (Rat1 and Sen1 in yeast). The concept of DNA binding factor-mediated polymerase stalling was solely introduced for eukaryotic RNA Pol I and may be implied in PAS-dependent Pol II termination (CPF, CF, 2.3.3). Clearly, Reb1 and/or Nsi1 function in polymerase pausing which is administrated by TTF-I in mammals. Release activity was shown to be executed by PTRF (Pol I and transcript release factor) in mouse *in vitro*, however its role and physiological relevance is questioned since PTRF null mice are viable. In yeast, transcript release was suggested to be mediated by the T-rich 1 element independently of Reb1 (Jeong et al. 1995; Lang & Reeder 1995)

(see also 5.3). Contrary, our most recent preliminary results indicate that Nsi1 alone is sufficient for transcript release *in vitro* (H. Tschochner, unpublished data).

Interestingly, *S. cerevisiae* differs from its close relative *S. pombe* regarding the molecular organization of Pol I termination and replication fork blocking. It was shown that the fission yeast Reb1 functions both as an rDNA termination factor and has replication fork barrier blocking ability (Zhao et al. 1997; Sánchez-Gorostiaga et al. 2004). This is similar to the role of TTF-I in higher eukaryotes which also exhibits termination and replication fork blocking activity (Gerber et al. 1997; López-Estraño et al. 1998), whereas *S. cerevisiae* in contrast seems to depend on the cooperation of at least two separate factors, Nsi1 and Fob1.

A recent report suggested that Nsi1 plays role in rDNA silencing and showed Nsi1 interactions with the RENT complex subunits Net1 and Sir2 (Ha et al. 2012). It remains to be clarified whether the function of Nsi1 in Pol I transcription termination and rDNA silencing are linked to each other and how this connection is reflected mechanistically. It can be speculated that the apparent leakiness of Pol I termination fulfills a physiological role regarding maintaining an open copy conformation or in rDNA integrity in general.

5.3 Comparative *in vitro* transcription reveals differences between Pol I, II and III

We demonstrated that the yeast RNA polymerases deal differently with elongation obstacles. All three physiological factors implicated in transcription termination Nsi1, Reb1 and Fob1 only influenced Pol I transcription significantly whereas Pol II and III elongation was minimally or not impaired (4.9.1). Interestingly, Reb1 exhibits a general negative effect on transcript signal intensities independent of the used polymerase. Since our transcription system is independent of initiation and reaction conditions are equal, the observed effects can be traced back to the polymerases. An easy explanation is provided by the hypothesis that Pol I has the lowest processivity and is hence easily stalled, whereas Pol II and III evict the factors from the DNA. However, if this assumption is true, Pol I should be most susceptible to all roadblocks. However, we showed that the strong DNA binding protein LexA was nearly no obstacle for Pol I but most significantly impaired Pol II traversal (4.9.2). Accordingly, incorporation of a cluster of three SOS boxes in the ITS1 of the 35S rDNA and concurrent

expression of LexA under the GAL promoter does not lead to a reduced growth phenotype although LexA is associated with its binding sites *in vivo* (Reiter et al. 2012). Thus, general differences in processivity can not explain our results.

Furthermore, the functional homolog to Reb1 and/or Nsi1 in mammals, TTF-I, provides a barrier for all three RNA polymerases albeit Pol I is again most severely affected (4.9.3). Selective blocking of yeast Pol I by yeast and mouse Pol I transcription termination factors might be explained due to evolutionary conservation in the actual termination mechanisms. Assuming that this hypothesis is true and given the fact that a torpedo termination mechanism for Pol I was not identified in mammals so far, this might be another hint supporting the pause-and-release termination model in yeast. Nonetheless, this is solely speculative since there are substantial differences in Pol I transcription termination between yeast and mammals as outlined in the introduction. Postulating full occupancy of the respective binding sites based on EMSA observations, the mammalian Pol I terminator seems to be more potent than its yeast counterpart however a direct comparison is not valid due to the different terminator architecture. It can be speculated whether the apparent leakiness of Pol I termination in yeast is an experimental artifact or whether it even fulfills a physiological role as outlined in 5.2.

Early studies by Reeder and co-workers suggested that LacI acts as an elongation obstacle for yeast RNA Pol I *in vitro* (Jeong et al. 1995). They further proposed that the blocking ability of LacI was independent of the surrounding DNA sequence and the orientation of the recognition site. However it was further reported that transcript release from LacI-stalled Pol I ternary complexes was enhanced by the presence of the T-rich 1 element but also worked without a specific surrounding DNA environment (Tschochne & Milkereit 1997). *In vivo* experiments to study the influence of LacI on Pol I elongation using a yeast strain with a LacI binding site in the rDNA ITS1 (Reiter A, 2012), as well as *in vitro* transcription analyses (data not shown), remained unconclusive.

The next obvious consideration is whether the difference in subunit composition evokes the diverse susceptibility to elongation obstacles. All three polymerases share a core comprised of 10 subunits of which 5 are identical in Pol I, II and III. Two further subunits, AC40 and AC19 are shared by Pol I and III. The two largest subunits which comprise the catalytically active center are homologous to each other, albeit are differing in molecular weight. Further, Pol I subunits A12.2, A43 and A14 have (partial) structural and functional homologs in Pol II and III (Vannini & Cramer 2012). To this end, all three polymerases are structurally related. However, only Pol I and III contain a specific subcomplex consisting of A49/A34.5 or C53/C37. Subunits Tfg1 and Tfg2 of the initiation and elongation factor TFIIF were identified as the respective homologs to the Pol I/III specific subcomplex (2.2.2). This would provide an explanation for the results obtained with LexA as an elongation obstacle. Addition

of TFIIF to reactions executed with Pol II and/or use of Pol I/III mutants lacking A49/A34.5 or C53/C37 should allow to clarify this hypothesis. Additionally, Pol III contains three subunits lacking in both Pol I and II (C82, C34, C31) of which C82 and C34 are related to TFIIE subunits. This could be part of an answer to the question why Pol III is nearly not affected by any of the trans-acting DNA binding factors during elongation.

In summary, we could show that under equal reaction conditions Pol I, II and III exhibit striking differences when encountering elongation barriers *in vitro*. Hypotheses to explain the observations with the different polymerase subunit composition remain speculative. Thorough polymerase mutant analysis and inclusion of the predicted structural and functional subunit homologs will be necessary to draw solid conclusions. However our results indicate fundamental inherent differences of Pol I, II and III in spite of their structural relatedness.

5.4 Pol I, II and III deal differently with a chromatin template

It is a long-standing question in the field how elongating RNA polymerases cope with a nucleosomal barrier. Many and mostly *in vitro* studies have been conducted as outlined in the introduction (2.4), however focusing usually on one RNA polymerase. With the established *in vitro* transcription system it was possible to compare the three yeast RNA polymerases side-by side regarding their ability to transcribe a nucleosomal template. To this end, mononucleosomal templates assembled via salt dialysis on the strong 601 positioning sequence (Lowary & Widom 1998) were incorporated in the analysis. We could demonstrate that Pol II is not able to overcome the nucleosomal barrier, whereas Pol I and III showed substantial levels of readthrough (4.10.2). Our observations regarding Pol II are in good agreement with the literature in which the nucleosome is described as a strong elongation barrier *in vitro* (Bondarenko et al. 2006; Hodges et al. 2009). Since the strength of the barrier depends on the magnitude of the actual histone-DNA interactions, it is coherent that we did not observe run-off transcripts with a template containing the very strong 601 sequence. Additionally, it was reported that Pol II is stalled after transcribing about 20-30nt of the nucleosome-covered DNA (Li et al. 2005). This is in good agreement with our observation of an abortive transcript mapping to the 5’ end of the 601 sequence.

Regarding Pol I, our data are partly challenging a recent publication by the Zomerdijk group focusing on chromatin transcription by human Pol I *in vitro* (Birch et al. 2009). In this paper, FACT is proposed as an elongation factor for Pol I which facilitates chromatin transcription. An equal role for FACT had been shown earlier for Pol II transcription elongation. Most strikingly, we observe a Pol I read-through efficiency of roughly 60% on a nucleosomal template. Contrary, Birch and co-workers report an efficiency of 10% with a Pol I fraction already containing the histone chaperone FACT. Based on the sensitivity of mass spectrometry, we can rule out cross-contamination of our Pol I preparation with the yeast FACT subunits Spt16 and Pob3. Additionally, transcription experiments were performed by Birch and co-workers with a polymerase fraction incubated with an antibody selectively recognizing one FACT subunit hence mimicking a "core" Pol I state. This resulted in a further reduction of full length transcript formation to roughly 2.5% which led to the conclusion that FACT is a Pol I elongation factor. Nonetheless, it cannot be ruled out that binding of the antibody to the proposed FACT-Pol I complex masks Pol I surfaces which are necessary for elongation and thus decreases elongation efficiency. We further conducted respective *in vitro* transcription experiments with Pol I on nucleosomal templates in presence of purified yeast FACT. To exclude the possibility that an affinity tag was compromising putative FACT activity, two different purifications with both possible baits Spt16-TAP and Pob3-TAP were used. However, no stimulation of Pol I readthrough levels could be demonstrated (data not shown). A previous report further suggested that FACT was not associated with *ex vivo* purified 35S rDNA chromatin (Hamperl 2012) based on mass spectrometric analysis. Additionally, FACT could not be detected co-precipitating with Pol I but with Pol II after formaldehyde crosslink (Hierlmeier et al. 2013).

Taken together, in our hands Pol I is able to cope with a nucleosomal template on its own *in vitro*. The discrepancy of our results with the literature obviously could be explained by different Pol I elongation mechanisms in human and yeast. Thus, a role of FACT in Pol I transcription through nucleosomal templates can not be excluded but requires more investigation.

We were further able to demonstrate that Pol I A190 S685D, Pol I ΔA12.2 and Pol I ΔA49 were impaired in transcription of the nucleosomal template (4.10.3). For Pol I ΔA49, the WT readthrough efficiency was restored upon pre-incubation with recombinant A49/A34.5. Therefore, we conclude that the A49/A34.5 dimer plays a crucial role in Pol I transcription elongation of nucleosomal templates. Our observations are in agreement with the literature which suggests that A12.2 and the A49/A34.5 dimer are necessary for proper Pol I elongation (Kuhn et al. 2007; Geiger et al. 2010). Although the synthetic lethality of Pol I ΔA12.2 with the S to D substitution of serine 685 in A190 was reported (Gerber et al. 2008), it remains unclear how both mutations affect elongation fidelity exactly.

TFIIF subunits Tfg1 and Tfg2 were identified as partial structural homologs to A49 and A34.5. Thus, we asked the question, whether TFIIF would help Pol II to overcome the nucleosomal barrier like it was shown for A49/A34.5 and Pol I. Concerning the question of TFIIF fidelity, we were able to demonstrate that presence of TFIIF enhanced run-off transcript levels of naked DNA by roughly 20%, therefore suggesting that our TFIIF preparation is active (4.10.4). Additionally, we have good evidence that incubation of Pol II with TFIIF leads to complex formation *in vitro*. In spite of this, we were not able to demonstrate stimulatory activity of TFIIF for Pol II traversal of a nucleosomal template. The same observation was made, if an *ex vivo* purified Pol II-TFIIF complex was used. In summary, this suggests that TFIIF by itself does not provide Pol II with the capability to overcome the nucleosomal barrier *in vitro,* which is accordance with previously published data (Izban & Luse 1992).

Regarding Pol III, our experiments indicate an intrinsic ability to overcome nucleosomal barriers *in vitro*. This observation is in accordance with the literature (Studitsky et al. 1997). Although, no chromatin remodeling activity or histone tail modification changing activities were needed for transcription through a single nucleosome as proposed for a nucleosomal array *in vitro* (Englander et al. 1993; Ura et al. 1997; Tse et al. 1998; Ng et al. 2002; Arimbasseri & Bhargava 2008).

5.5 Outlook

Concerning yeast Pol I transcription termination, it will be crucial to verify the results in a promoter-dependent *in vitro* transcription assay using immobilized templates. This will provide information about the release activity of Reb1 and Nsi1. Furthermore, our knowledge of the actual termination mechanism will remain limited unless the mode of interaction between Reb1, Nsi1 and Fob1 including the spatial organization is not elucidated. For unification or refusal of the current termination models, it will be important to unravel whether Rat1-mediated transcript degradation is a prerequisite for termination *in vivo*. Additionally, further in vivo experiments have to validate the physiological relevance of our observations, although our preliminary data support our *in vitro* results (J. Perez Fernandez, unpublished data).

Regarding the chromatin transcription abilities of Pol I, II and III, work with polymerase mutants will be important to draw mechanistic conclusions of the observed phenotypes. Furthermore,

incorporation of other known Pol II elongation factors and/or histone remodelers will possibly reveal one of more candidates that facilitate Pol II traversal on a nucleosomal template *in vitro*.

CHAPTER VI – REFERENCES

Albert, B. et al., 2011. RNA polymerase I-specific subunits promote polymerase clustering to enhance the rRNA gene transcription cycle. *The Journal of Cell Biology*, 192(2), pp.277–293.

Albert, I. et al., 2007. Translational and rotational settings of H2A.Z nucleosomes across the Saccharomyces cerevisiae genome. *Nature*, 446(7135), pp.572–576.

Alic, N. et al., 2007. Selectivity and proofreading both contribute significantly to the fidelity of RNA polymerase III transcription. *Proceedings of the National Academy of Sciences of the United States of America*, 104(25), pp.10400–10405.

Allen, F.W., 1941. The Biochemistry of the Nucleic Acids, Purines, and Pyrimidines. *Annual Review of Biochemistry*, 10(1), pp.221–244.

Allmang, C. & Tollervey, D., 1998. The role of the 3' external transcribed spacer in yeast pre-rRNA processing. *Journal of molecular biology*, 278(1), pp.67–78.

Anderson, S.J. et al., 2011. The transcription elongation factor Spt5 influences transcription by RNA polymerase I positively and negatively. *The Journal of biological chemistry*, 286(21), pp.18816–18824.

Andrews, A.J. et al., 2008. A Thermodynamic Model for Nap1-Histone Interactions. *Journal of Biological Chemistry*, 283(47), pp.32412–32418.

Andrulis, E.D. et al., 2000. High-resolution localization of Drosophila Spt5 and Spt6 at heat shock genes in vivo: roles in promoter proximal pausing and transcription elongation. *Genes & Development*, 14(20), pp.2635–2649.

Angelov, D. et al., 2006. Nucleolin is a histone chaperone with FACT-like activity and assists remodeling of nucleosomes. *The EMBO Journal*, 25(8), pp.1669–1679.

Aprikian, P., Moorefield, B. & Reeder, R.H., 2001. New model for the yeast RNA polymerase I transcription cycle. *Molecular and Cellular Biology*, 21(15), pp.4847–4855.

Ardehali, M.B. et al., 2009. Spt6 enhances the elongation rate of RNA polymerase II in vivo. *The EMBO Journal*, 28(8), pp.1067–1077.

Arimbasseri, A.G. & Bhargava, P., 2008. Chromatin structure and expression of a gene transcribed by RNA polymerase III are independent of H2A.Z deposition. *Molecular and cellular biology*, 28(8), pp.2598–2607.

Arimbasseri, A.G. & Maraia, R.J., 2013. Distinguishing core and holoenzyme mechanisms of transcription termination by RNA polymerase III. *Molecular and cellular biology*, 33(8), pp.1571–1581.

Armache, K.-J. et al., 2005. Structures of complete RNA polymerase II and its subcomplex, Rpb4/7. *The Journal of biological chemistry*, 280(8), pp.7131–7134.

Banerjee, S. et al., 2006. Rho-dependent Transcription Termination: More Questions than Answers. *Journal of microbiology (Seoul, Korea)*, 44(1), pp.11–22.

Bardwell, V.J. et al., 1991. Site-directed ribose methylation identifies 2'-OH groups in polyadenylation substrates critical for AAUAAA recognition and poly(A) addition. *Cell*, 65(1), pp.125–133.

Bartsch, I., Schoneberg, C. & Grummt, I., 1988. Purification and characterization of TTFI, a factor that mediates termination of mouse ribosomal DNA transcription. *Molecular and cellular biology*, 8(9), pp.3891–3897.

Basehoar, A.D., Zanton, S.J. & Pugh, B.F., 2004. Identification and distinct regulation of yeast TATA box-containing genes. *Cell*, 116(5), pp.699–709.

Beckouet, F. et al., 2008. Two RNA polymerase I subunits control the binding and release of Rrn3 during transcription. *Molecular and cellular biology*, 28(5), pp.1596–1605.

Bell, C.E. & Lewis, M., 2000. A closer view of the conformation of the Lac repressor bound to operator. *Nature structural biology*, 7(3), pp.209–214.

Bell, S.D. et al., 1999. Orientation of the transcription preinitiation complex in Archaea. *Proceedings of the National Academy of Sciences*, 96(24), pp.13662–13667.

Bell, S.D. et al., 1998. Temperature, template topology, and factor requirements of archaeal transcription. *Proceedings of the National Academy of Sciences of the United States of America*, 95(26), pp.15218–15222.

Bell, S.D. et al., 2001. The archaeal TFIIEα homologue facilitates transcription initiation by enhancing TATA-box recognition. *EMBO reports*, 2(2), pp.133–138.

Bell, S.P. et al., 1988. Functional cooperativity between transcription factors UBF1 and SL1 mediates human ribosomal RNA synthesis. *Science (New York, N.Y.)*, 241(4870), pp.1192–1197.

Belotserkovskaya, R. et al., 2000. Inhibition of TATA-Binding Protein Function by SAGA Subunits Spt3 and Spt8 at Gcn4-Activated Promoters. *Molecular and Cellular Biology*, 20(2), pp.634–647.

Bengal, E. et al., 1991. Role of the mammalian transcription factors IIF, IIS, and IIX during elongation by RNA polymerase II. *Molecular and Cellular Biology*, 11(3), pp.1195–1206.

Berger, A.B. et al., 2007. Hmo1 is required for TOR-dependent regulation of ribosomal protein gene transcription. *Molecular and Cellular Biology*, 27(22), pp.8015–8026.

Berger, I., Fitzgerald, D.J. & Richmond, T.J., 2004. Baculovirus expression system for heterologous multiprotein complexes. *Nature biotechnology*, 22(12), pp.1583–1587.

Bintu, L. et al., 2011. The elongation rate of RNA polymerase determines the fate of transcribed nucleosomes. *Nature structural & molecular biology*, 18(12), pp.1394–1399.

Birch, J.L. et al., 2009. FACT facilitates chromatin transcription by RNA polymerases I and III. *The EMBO Journal*, 28(7), pp.854–865.

Bischler, N. et al., 2002. Localization of the yeast RNA polymerase I-specific subunits. *The EMBO journal*, 21(15), pp.4136–4144.

Bogenhagen, D.F. & Brown, D.D., 1981. Nucleotide sequences in Xenopus 5S DNA required for transcription termination. *Cell*, 24(1), pp.261–270.

Böhm, V. et al., 2011. Nucleosome accessibility governed by the dimer/tetramer interface. *Nucleic Acids Research*, 39(8), pp.3093–3102.

Bondarenko, V.A. et al., 2006. Nucleosomes can form a polar barrier to transcript elongation by RNA polymerase II. *Molecular Cell*, 24(3), pp.469–479.

Bordi, L., Cioci, F. & Camilloni, G., 2001. In vivo binding and hierarchy of assembly of the yeast RNA polymerase I transcription factors. *Molecular Biology of the Cell*, 12(3), pp.753–760.

Borukhov, S. & Severinov, K., 2002. Role of the RNA polymerase sigma subunit in transcription initiation. *Research in Microbiology*, 153(9), pp.557–562.

Brachmann, C.B. et al., 1998. Designer deletion strains derived from Saccharomyces cerevisiae S288C: a useful set of strains and plasmids for PCR-mediated gene disruption and other applications. *Yeast (Chichester, England)*, 14(2), pp.115–132.

Bradford, M.M., 1976. A rapid and sensitive method for the quantitation of microgram quantities of protein utilizing the principle of protein-dye binding. *Analytical biochemistry*, 72, pp.248–254.

Braglia, P. et al., 2010. Role of the RNA/DNA kinase Grc3 in transcription termination by RNA polymerase I. *EMBO reports*, 11(10), pp.758–764.

Braglia, P., Kawauchi, J. & Proudfoot, N.J., 2011. Co-transcriptional RNA cleavage provides a failsafe termination mechanism for yeast RNA polymerase I. *Nucleic acids research*, 39(4), pp.1439–1448.

Brennan, C.A., Dombroski, A.J. & Platt, T., 1987. Transcription termination factor rho is an RNA-DNA helicase. *Cell*, 48(6), pp.945–952.

Brewer, B.J. & Fangman, W.L., 1988. A replication fork barrier at the 3' end of yeast ribosomal RNA genes. *Cell*, 55(4), pp.637–643.

Brewer, B.J., Lockshon, D. & Fangman, W.L., 1992. The arrest of replication forks in the rDNA of yeast occurs independently of transcription. *Cell*, 71(2), pp.267–276.

Brogaard, K. et al., 2012. A map of nucleosome positions in yeast at base-pair resolution. *Nature*, advance online publication. Available at: http://www.nature.com/nature/journal/vaop/ncurrent/full/nature11142.html?WT.ec_id=NATURE-20120607 [Accessed September 28, 2013].

Bruno, M. et al., 2003. Histone H2A/H2B Dimer Exchange by ATP-Dependent Chromatin Remodeling Activities. *Molecular Cell*, 12(6), pp.1599–1606.

Bryant, G.O. & Ptashne, M., 2003. Independent Recruitment In Vivo by Gal4 of Two Complexes Required for Transcription. *Molecular Cell*, 11(5), pp.1301–1309.

Bryk, M. et al., 1997. Transcriptional silencing of Ty1 elements in the RDN1 locus of yeast. *Genes & Development*, 11(2), pp.255–269.

Buhler, J.M. et al., 1980. Immunological studies of yeast nuclear RNA polymerases at the subunit level. *The Journal of biological chemistry*, 255(20), pp.9949–9954.

Burkhalter, M.D. & Sogo, J.M., 2004. rDNA enhancer affects replication initiation and mitotic recombination: Fob1 mediates nucleolytic processing independently of replication. *Molecular cell*, 15(3), pp.409–421.

Busby, S. & Ebright, R.H., 1994. Promoter structure, promoter recognition, and transcription activation in prokaryotes. *Cell*, 79(5), pp.743–746.

Butala, M. et al., 2007. Intradomain LexA rotation is a prerequisite for DNA binding specificity. *FEBS letters*, 581(25), pp.4816–4820.

Butala, M., Zgur-Bertok, D. & Busby, S.J.W., 2009. The bacterial LexA transcriptional repressor. *Cellular and molecular life sciences: CMLS*, 66(1), pp.82–93.

De Carlo, S. et al., 2003. Cryo-negative staining reveals conformational flexibility within yeast RNA polymerase I. *Journal of molecular biology*, 329(5), pp.891–902.

Carroll, K.L. et al., 2007. Interaction of yeast RNA-binding proteins Nrd1 and Nab3 with RNA polymerase II terminator elements. *RNA (New York, N.Y.)*, 13(3), pp.361–373.

Carter, R. & Drouin, G., 2010. The Increase in the Number of Subunits in Eukaryotic RNA Polymerase III Relative to RNA Polymerase II Is due to the Permanent Recruitment of General Transcription Factors. *Molecular Biology and Evolution*, 27(5), pp.1035–1043.

Cesarini, E. et al., 2010. RNA Polymerase I Transcription Silences Noncoding RNAs at the Ribosomal DNA Locus in Saccharomyces cerevisiae. *Eukaryotic Cell*, 9(2), pp.325–335.

Challice, J.M. & Segall, J., 1989. Transcription of the 5 S rRNA gene of Saccharomyces cerevisiae requires a promoter element at +1 and a 14-base pair internal control region. *The Journal of biological chemistry*, 264(33), pp.20060–20067.

Chamberlin, M., Mcgrath, J. & Waskell, L., 1970. New RNA Polymerase from Escherichia coli infected with Bacteriophage T7. *Nature*, 228(5268), pp.227–231.

Chasman, D.I. et al., 1990. A yeast protein that influences the chromatin structure of UASG and functions as a powerful auxiliary gene activator. *Genes & development*, 4(4), pp.503–514.

Chédin, S. et al., 1998. The RNA cleavage activity of RNA polymerase III is mediated by an essential TFIIS-like subunit and is important for transcription termination. *Genes & Development*, 12(24), pp.3857–3871.

Chen, Z.A. et al., 2010. Architecture of the RNA polymerase II-TFIIF complex revealed by cross-linking and mass spectrometry. *The EMBO journal*, 29(4), pp.717–726.

Clapier, C.R. & Cairns, B.R., 2009. The Biology of Chromatin Remodeling Complexes. *Annual Review of Biochemistry*, 78(1), pp.273–304.

Cmarko, D. et al., 2000. Ultrastructural analysis of nucleolar transcription in cells microinjected with 5-bromo-UTP. *Histochemistry and cell biology*, 113(3), pp.181–187.

Conaway, J.W. et al., 2000. Control of elongation by RNA polymerase II. *Trends in biochemical sciences*, 25(8), pp.375–380.

Conaway, R.C., Kong, S.E. & Conaway, J.W., 2003. TFIIS and GreB: Two Like-Minded Transcription Elongation Factors with Sticky Fingers. *Cell*, 114(3), pp.272–274.

Conconi, A. et al., 1989. Two different chromatin structures coexist in ribosomal RNA genes throughout the cell cycle. *Cell*, 57(5), pp.753–761.

Cosgrove, M.S. & Wolberger, C., 2005. How does the histone code work? *Biochemistry and cell biology = Biochimie et biologie cellulaire*, 83(4), pp.468–476.

Cramer, J.H. et al., 1977. Construction and restriction endonuclease mapping of hybrid plasmids containing Saccharomyces cerevisiae ribosomal DNA. *Molecular & General Genetics: MGG*, 151(3), pp.229–244.

Cramer, J.H. & Rownd, R.H., 1980. Denaturation mapping of the ribosomal DNA of Saccharomyces cerevisiae. *Molecular & General Genetics: MGG*, 177(2), pp.199–205.

Cramer, P. et al., 2000. Architecture of RNA Polymerase II and Implications for the Transcription Mechanism. *Science*, 288(5466), pp.640–649.

Cramer, P., Bushnell, D.A. & Kornberg, R.D., 2001. Structural Basis of Transcription: RNA Polymerase II at 2.8 Ångstrom Resolution. *Science*, 292(5523), pp.1863–1876.

Dammann, R. et al., 1993. Chromatin structures and transcription of rDNA in yeast Saccharomyces cerevisiae. *Nucleic Acids Research*, 21(10), pp.2331–2338.

Das, C., Tyler, J.K. & Churchill, M.E.A., 2010. The histone shuffle: histone chaperones in an energetic dance. *Trends in Biochemical Sciences*, 35(9), pp.476–489.

Davanloo, P. et al., 1984. Cloning and expression of the gene for bacteriophage T7 RNA polymerase. *Proceedings of the National Academy of Sciences*, 81(7), pp.2035–2039.

Dechassa, M.L. et al., 2010. SWI/SNF Has Intrinsic Nucleosome Disassembly Activity that Is Dependent on Adjacent Nucleosomes. *Molecular Cell*, 38(4), pp.590–602.

Dedrick, R.L. & Chamberlin, M.J., 1985. Studies on transcription of 3'-extended templates by mammalian RNA polymerase II. Parameters that affect the initiation and elongation reactions. *Biochemistry*, 24(9), pp.2245–2253.

Dengl, S. & Cramer, P., 2009. Torpedo nuclease Rat1 is insufficient to terminate RNA polymerase II in vitro. *The Journal of biological chemistry*, 284(32), pp.21270–21279.

Denissov, S. et al., 2011. A model for the topology of active ribosomal RNA genes. *EMBO reports*, 12(3), pp.231–237.

Dichtl, B. & Keller, W., 2001. Recognition of polyadenylation sites in yeast pre-mRNAs by cleavage and polyadenylation factor. *The EMBO Journal*, 20(12), pp.3197–3209.

Dieci, G. et al., 2006. Distinct modes of TATA box utilization by the RNA polymerase III transcription machineries from budding yeast and higher plants. *Gene*, 379, pp.12–25.

Dieci, G. et al., 2002. Intragenic Promoter Adaptation and Facilitated RNA Polymerase III Recycling in the Transcription of SCR1, the 7SL RNA Gene ofSaccharomyces cerevisiae. *Journal of Biological Chemistry*, 277(9), pp.6903–6914.

Dieci, G. et al., 2000. TFIIIC-independent in vitro transcription of yeast tRNA genes. *Journal of Molecular Biology*, 299(3), pp.601–613.

Diezel, W., Kopperschläger, G. & Hofmann, E., 1972. An improved procedure for protein staining in polyacrylamide gels with a new type of Coomassie Brilliant Blue. *Analytical biochemistry*, 48(2), pp.617–620.

Dragon, F. et al., 2002. A large nucleolar U3 ribonucleoprotein required for 18S ribosomal RNA biogenesis. *Nature*, 417(6892), pp.967–970.

Dunn, J.J. & Studier, F.W., 1983. Complete nucleotide sequence of bacteriophage T7 DNA and the locations of T7 genetic elements. *Journal of molecular biology*, 166(4), pp.477–535.

Dvir, A., Conaway, J.W. & Conaway, R.C., 2001. Mechanism of transcription initiation and promoter escape by RNA polymerase II. *Current Opinion in Genetics & Development*, 11(2), pp.209–214.

Ebright, R.H., 2000. RNA Polymerase: Structural Similarities Between Bacterial RNA Polymerase and Eukaryotic RNA Polymerase II. *Journal of Molecular Biology*, 304(5), pp.687–698.

El Hage, A. et al., 2008. Efficient termination of transcription by RNA polymerase I requires the 5' exonuclease Rat1 in yeast. *Genes & development*, 22(8), pp.1069–1081.

Elela, S.A., Igel, H. & Ares, M., Jr, 1996. RNase III cleaves eukaryotic preribosomal RNA at a U3 snoRNP-dependent site. *Cell*, 85(1), pp.115–124.

Elion, E.A. & Warner, J.R., 1986. An RNA polymerase I enhancer in Saccharomyces cerevisiae. *Molecular and Cellular Biology*, 6(6), pp.2089–2097.

Elmendorf, B.J. et al., 2001. Transcription Factors TFIIF, ELL, and Elongin Negatively Regulate SII-induced Nascent Transcript Cleavage by Non-arrested RNA Polymerase II Elongation Intermediates. *Journal of Biological Chemistry*, 276(25), pp.23109–23114.

Englander, E.W., Wolffe, A.P. & Howard, B.H., 1993. Nucleosome interactions with a human Alu element. Transcriptional repression and effects of template methylation. *The Journal of biological chemistry*, 268(26), pp.19565–19573.

Epshtein, V. et al., 2007. An Allosteric Path to Transcription Termination. *Molecular Cell*, 28(6), pp.991–1001.

Errede, B. et al., 1984. Identification of regulatory regions within the Ty1 transposable element that regulate iso-2-cytochrome c production in the CYC7-H2 yeast mutant. *Molecular and Cellular Biology*, 4(7), pp.1393–1401.

Evers, R. et al., 1995. Different domains of the murine RNA polymerase I-specific termination factor mTTF-I serve distinct functions in transcription termination. *The EMBO journal*, 14(6), pp.1248–1256.

Evers, R. & Grummt, I., 1995. Molecular coevolution of mammalian ribosomal gene terminator sequences and the transcription termination factor TTF-I. *Proceedings of the National Academy of Sciences of the United States of America*, 92(13), pp.5827–5831.

Fish, R.N. & Kane, C.M., 2002. Promoting elongation with transcript cleavage stimulatory factors. *Biochimica et biophysica acta*, 1577(2), pp.287–307.

Fitzgerald, D.J. et al., 2006. Protein complex expression by using multigene baculoviral vectors. *Nature methods*, 3(12), pp.1021–1032.

Fleischer, T.C. et al., 2006. Systematic identification and functional screens of uncharacterized proteins associated with eukaryotic ribosomal complexes. *Genes & development*, 20(10), pp.1294–1307.

Flores, O., Lu, H. & Reinberg, D., 1992. Factors involved in specific transcription by mammalian RNA polymerase II. Identification and characterization of factor IIH. *The Journal of biological chemistry*, 267(4), pp.2786–2793.

Flores, O., Maldonado, E. & Reinberg, D., 1989. Factors involved in specific transcription by mammalian RNA polymerase II. Factors IIE and IIF independently interact with RNA polymerase II. *Journal of Biological Chemistry*, 264(15), pp.8913–8921.

Fouqueau, T. et al., 2013. The RNA polymerase trigger loop functions in all three phases of the transcription cycle. *Nucleic acids research*, 41(14), pp.7048–7059.

French, S.L. et al., 2003. In exponentially growing Saccharomyces cerevisiae cells, rRNA synthesis is determined by the summed RNA polymerase I loading rate rather than by the number of active genes. *Molecular and Cellular Biology*, 23(5), pp.1558–1568.

French, S.L. et al., 2008. Visual analysis of the yeast 5S rRNA gene transcriptome: regulation and role of La protein. *Molecular and cellular biology*, 28(14), pp.4576–4587.

Fritze, C.E. et al., 1997. Direct evidence for SIR2 modulation of chromatin structure in yeast rDNA. *The EMBO Journal*, 16(21), pp.6495–6509.

Gadal, O. et al., 1997. A34.5, a nonessential component of yeast RNA polymerase I, cooperates with subunit A14 and DNA topoisomerase I to produce a functional rRNA synthesis machine. *Molecular and Cellular Biology*, 17(4), pp.1787–1795.

Gadal, O. et al., 2002. Hmo1, an HMG-box protein, belongs to the yeast ribosomal DNA transcription system. *The EMBO Journal*, 21(20), pp.5498–5507.

Gadski, R.A. & Chae, C.B., 1976. Mode of reconstitution of chicken erythrocyte and reticulocyte chromatin. *Biochemistry*, 15(17), pp.3812–3817.

Ganley, A.R.D. et al., 2005. Identifying gene-independent noncoding functional elements in the yeast ribosomal DNA by phylogenetic footprinting. *Proceedings of the National Academy of Sciences of the United States of America*, 102(33), pp.11787–11792.

Gansen, A. et al., 2009. Nucleosome disassembly intermediates characterized by single-molecule FRET. *Proceedings of the National Academy of Sciences*, 106(36), pp.15308–15313.

Gaykalova, D.A. et al., 2011. A polar barrier to transcription can be circumvented by remodeler-induced nucleosome translocation. *Nucleic Acids Research*, 39(9), pp.3520–3528.

Geiduschek, E.P. & Kassavetis, G.A., 2001. The RNA polymerase III transcription apparatus. *Journal of Molecular Biology*, 310(1), pp.1–26.

Geiduschek, E.P. & Ouhammouch, M., 2005. Archaeal transcription and its regulators. *Molecular microbiology*, 56(6), pp.1397–1407.

Geiger, S.R. et al., 2010. RNA polymerase I contains a TFIIF-related DNA-binding subcomplex. *Molecular cell*, 39(4), pp.583–594.

Gerber, J. et al., 2008. Site specific phosphorylation of yeast RNA polymerase I. *Nucleic Acids Research*, 36(3), pp.793–802.

Gerber, J.-K. et al., 1997. Termination of Mammalian rDNA Replication: Polar Arrest of Replication Fork Movement by Transcription Termination Factor TTF-I. *Cell*, 90(3), pp.559–567.

Ghaemmaghami, S. et al., 2003. Global analysis of protein expression in yeast. *Nature*, 425(6959), pp.737–741.

Ghazal, G. et al., 2009. Yeast RNase III triggers polyadenylation-independent transcription termination. *Molecular cell*, 36(1), pp.99–109.

Gkikopoulos, T. et al., 2011. A Role for Snf2-Related Nucleosome-Spacing Enzymes in Genome-Wide Nucleosome Organization. *Science*, 333(6050), pp.1758–1760.

Glover-Cutter, K. et al., 2008. RNA polymerase II pauses and associates with pre-mRNA processing factors at both ends of genes. *Nature Structural & Molecular Biology*, 15(1), pp.71–78.

Gnatt, A.L. et al., 2001. Structural basis of transcription: an RNA polymerase II elongation complex at 3.3 A resolution. *Science (New York, N.Y.)*, 292(5523), pp.1876–1882.

Goetze, H. et al., 2010. Alternative chromatin structures of the 35S rRNA genes in Saccharomyces cerevisiae provide a molecular basis for the selective recruitment of RNA polymerases I and II. *Molecular and cellular biology*, 30(8), pp.2028–2045.

Gordân, R., Narlikar, L. & Hartemink, A.J., 2010. Finding regulatory DNA motifs using alignment-free evolutionary conservation information. *Nucleic acids research*, 38(6), p.e90.

Gray, W.M. & Fassler, J.S., 1996. Isolation and analysis of the yeast TEA1 gene, which encodes a zinc cluster Ty enhancer-binding protein. *Molecular and Cellular Biology*, 16(1), pp.347–358.

Gruber, T.M. & Gross, C.A., 2003. Multiple sigma subunits and the partitioning of bacterial transcription space. *Annual review of microbiology*, 57, pp.441–466.

Grünberg, S. et al., 2010. Rearrangement of the RNA polymerase subunit H and the lower jaw in archaeal elongation complexes. *Nucleic acids research*, 38(6), pp.1950–1963.

Grünberg, S. et al., 2007. Transcription Factor E Is a Part of Transcription Elongation Complexes. *Journal of Biological Chemistry*, 282(49), pp.35482–35490.

Grummt, I., Rosenbauer, H., et al., 1986. A repeated 18 bp sequence motif in the mouse rDNA spacer mediates binding of a nuclear factor and transcription termination. *Cell*, 45(6), pp.837–846.

Grummt, I., Kuhn, A., et al., 1986. A transcription terminator located upstream of the mouse rDNA initiation site affects rRNA synthesis. *Cell*, 47(6), pp.901–911.

Grummt, I. et al., 1985. Transcription of mouse rDNA terminates downstream of the 3’ end of 28S RNA and involves interaction of factors with repeated sequences in the 3’ spacer. *Cell*, 43(3 Pt 2), pp.801–810.

Grummt, I. & Längst, G., 2013. Epigenetic control of RNA polymerase I transcription in mammalian cells. *Biochimica et biophysica acta*, 1829(3-4), pp.393–404.

GRUNBERG-MANAGO, M., ORITZ, P.J. & OCHOA, S., 1955. Enzymatic synthesis of nucleic acidlike polynucleotides. *Science (New York, N.Y.)*, 122(3176), pp.907–910.

Günzl, A. et al., 2003. RNA polymerase I transcribes procyclin genes and variant surface glycoprotein gene expression sites in Trypanosoma brucei. *Eukaryotic cell*, 2(3), pp.542–551.

Guo, Z. & Sherman, F., 1996. 3′-end-forming signals of yeast mRNA. *Trends in Biochemical Sciences*, 21(12), pp.477–481.

Gupta, S. & Reddy, R., 1991. Compilation of small RNA sequences. *Nucleic acids research*, 19 Suppl, pp.2073–2075.

Gurney, T., Jr, 1985. Characterization of mouse 45S ribosomal RNA subspecies suggests that the first processing cleavage occurs 600 +/- 100 nucleotides from the 5’ end and the second 500 +/- 100 nucleotides from the 3’ end of a 13.9 kb precursor. *Nucleic acids research*, 13(13), pp.4905–4919.

Ha, C.W., Sung, M.-K. & Huh, W.-K., 2012. Nsi1 plays a significant role in the silencing of ribosomal DNA in Saccharomyces cerevisiae. *Nucleic acids research*, 40(11), pp.4892–4903.

Haag, J.R. & Pikaard, C.S., 2011. Multisubunit RNA polymerases IV and V: purveyors of non-coding RNA for plant gene silencing. *Nature Reviews Molecular Cell Biology*, 12(8), pp.483–492.

Hahn, S., 2004. Structure and mechanism of the RNA polymerase II transcription machinery. *Nature Structural & Molecular Biology*, 11(5), pp.394–403.

Hahn, S. & Young, E.T., 2011. Transcriptional regulation in Saccharomyces cerevisiae: transcription factor regulation and function, mechanisms of initiation, and roles of activators and coactivators. *Genetics*, 189(3), pp.705–736.

Hamada, M. et al., 2001. Widespread Use of TATA Elements in the Core Promoters for RNA Polymerases III, II, and I in Fission Yeast. *Molecular and Cellular Biology*, 21(20), pp.6870–6881.

Hamperl, S., 2012. *Compositional and structural analysis of selected chromosomal domains from Saccharomyces cerevisiae*. phd. Available at: http://epub.uni-regensburg.de/26586/ [Accessed July 19, 2013].

Hanahan, D., 1983. Studies on transformation of Escherichia coli with plasmids. *Journal of Molecular Biology*, 166(4), pp.557–580.

Hausner, W. et al., 1996. Two transcription factors related with the eucaryal transcription factors TATA-binding protein and transcription factor IIB direct promoter recognition by an archaeal RNA polymerase. *The Journal of biological chemistry*, 271(47), pp.30144–30148.

Hausner, W., Frey, G. & Thomm, M., 1991. Control regions of an archaeal gene. A TATA box and an initiator element promote cell-free transcription of the tRNA(Val) gene of Methanococcus vannielii. *Journal of molecular biology*, 222(3), pp.495–508.

Hausner, W., Lange, U. & Musfeldt, M., 2000. Transcription factor S, a cleavage induction factor of the archaeal RNA polymerase. *The Journal of biological chemistry*, 275(17), pp.12393–12399.

Henras, A.K., Bertrand, E. & Chanfreau, G., 2004. A cotranscriptional model for 3'-end processing of the Saccharomyces cerevisiae pre-ribosomal RNA precursor. *RNA (New York, N.Y.)*, 10(10), pp.1572–1585.

Hernandez, N., 1993. TBP, a universal eukaryotic transcription factor? *Genes & Development*, 7(7b), pp.1291–1308.

Herr, A.J. et al., 2005. RNA polymerase IV directs silencing of endogenous DNA. *Science (New York, N.Y.)*, 308(5718), pp.118–120.

Hethke, C. et al., 1996. A cell-free transcription system for the hyperthermophilic archaeon Pyrococcus furiosus. *Nucleic acids research*, 24(12), pp.2369–2376.

Hierlmeier, T. et al., 2013. Rrp5p, Noc1p and Noc2p form a protein module which is part of early large ribosomal subunit precursors in S. cerevisiae. *Nucleic acids research*, 41(2), pp.1191–1210.

Higashinakagawa, T., Wahn, H. & Reeder, R.H., 1977. Isolation of ribosomal gene chromatin. *Developmental biology*, 55(2), pp.375–386.

Hirata, A., Klein, B.J. & Murakami, K.S., 2008. The X-ray Crystal Structure of RNA Polymerase from Archaea. *Nature*, 451(7180), pp.851–854.

Hodges, C. et al., 2009. Nucleosomal fluctuations govern the transcription dynamics of RNA polymerase II. *Science (New York, N.Y.)*, 325(5940), pp.626–628.

Høiby, T. et al., 2007. A facelift for the general transcription factor TFIIA. *Biochimica et biophysica acta*, 1769(7-8), pp.429–436.

Hontz, R.D. et al., 2008. Transcription of Multiple Yeast Ribosomal DNA Genes Requires Targeting of UAF to the Promoter by Uaf30. *Molecular and Cellular Biology*, 28(21), pp.6709–6719.

Hota, S.K. & Bartholomew, B., 2011. Diversity of operation in ATP-dependent chromatin remodelers. *Biochimica et Biophysica Acta (BBA) - Gene Regulatory Mechanisms*, 1809(9), pp.476–487.

Houseley, J. & Tollervey, D., 2009. The many pathways of RNA degradation. *Cell*, 136(4), pp.763–776.

Hu, P. et al., 2002. Characterization of Human RNA Polymerase III Identifies Orthologues for Saccharomyces cerevisiae RNA Polymerase III Subunits. *Molecular and Cellular Biology*, 22(22), pp.8044–8055.

Huang, R.C., Maheshwari, N. & Bonner, J., 1960. Enzymatic synthes is of RNA. *Biochemical and Biophysical Research Communications*, 3(6), pp.689–694.

Huet, J. et al., 1983. Archaebacteria and eukaryotes possess DNA-dependent RNA polymerases of a common type. *The EMBO journal*, 2(8), pp.1291–1294.

Huet, J. et al., 1975. Dissociation of two polypeptide chains from yeast RNA polymerase A. *Proceedings of the National Academy of Sciences*, 72(8), pp.3034–3038.

Huisinga, K.L. & Pugh, B.F., 2004. A Genome-Wide Housekeeping Role for TFIID and a Highly Regulated Stress-Related Role for SAGA in Saccharomyces cerevisiae. *Molecular Cell*, 13(4), pp.573–585.

Hurwitz, J., Bresler, A. & Diringer, R., 1960. The enzymatic incorporation of ribonucleotides into polyribonucleotides and the effect of DNA. *Biochemical and Biophysical Research Communications*, 3(1), pp.15–18.

Iben, J.R. et al., 2011. Point mutations in the Rpb9-homologous domain of Rpc11 that impair transcription termination by RNA polymerase III. *Nucleic acids research*, 39(14), pp.6100–6113.

Ivanovska, I. et al., 2011. Control of Chromatin Structure by Spt6: Different Consequences in Coding and Regulatory Regions. *Molecular and Cellular Biology*, 31(3), pp.531–541.

Izban, M.G. & Luse, D.S., 1992. Factor-stimulated RNA polymerase II transcribes at physiological elongation rates on naked DNA but very poorly on chromatin templates. *Journal of Biological Chemistry*, 267(19), pp.13647–13655.

Izban, M.G. & Luse, D.S., 1991. Transcription on nucleosomal templates by RNA polymerase II in vitro: inhibition of elongation with enhancement of sequence-specific pausing. *Genes & Development*, 5(4), pp.683–696.

JACOB, F. & MONOD, J., 1961. Genetic regulatory mechanisms in the synthesis of proteins. *Journal of molecular biology*, 3, pp.318–356.

Jansa, P. et al., 1998. Cloning and functional characterization of PTRF, a novel protein which induces dissociation of paused ternary transcription complexes. *The EMBO journal*, 17(10), pp.2855–2864.

Jansa, P. et al., 2001. The transcript release factor PTRF augments ribosomal gene transcription by facilitating reinitiation of RNA polymerase I. *Nucleic Acids Research*, 29(2), pp.423–429.

Jantzen, H.-M. et al., 1990. Nucleolar transcription factor hUBF contains a DNA-binding motif with homology to HMG proteins. *Nature*, 344(6269), pp.830–836.

Jasiak, A.J. et al., 2006. Structural Biology of RNA Polymerase III: Subcomplex C17/25 X-Ray Structure and 11 Subunit Enzyme Model. *Molecular Cell*, 23(1), pp.71–81.

Jeng, S.T., Gardner, J.F. & Gumport, R.I., 1990. Transcription termination by bacteriophage T7 RNA polymerase at rho-independent terminators. *The Journal of biological chemistry*, 265(7), pp.3823–3830.

Jeong, S.W., Lang, W.H. & Reeder, R.H., 1995. The release element of the yeast polymerase I transcription terminator can function independently of Reb1p. *Molecular and Cellular Biology*, 15(11), pp.5929–5936.

Joazeiro, C.A., Kassavetis, G.A. & Geiduschek, E.P., 1996. Alternative outcomes in assembly of promoter complexes: the roles of TBP and a flexible linker in placing TFIIIB on tRNA genes. *Genes & Development*, 10(6), pp.725–739.

Jones, H.S. et al., 2007. RNA polymerase I in yeast transcribes dynamic nucleosomal rDNA. *Nature structural & molecular biology*, 14(2), pp.123–130.

Ju, Q.D., Morrow, B.E. & Warner, J.R., 1990. REB1, a yeast DNA-binding protein with many targets, is essential for growth and bears some resemblance to the oncogene myb. *Molecular and cellular biology*, 10(10), pp.5226–5234.

Kadesch, T.R. & Chamberlin, M.J., 1982. Studies of in vitro transcription by calf thymus RNA polymerase II using a novel duplex DNA template. *The Journal of Biological Chemistry*, 257(9), pp.5286–5295.

Kane, C.M. & Chamberlin, M.J., 1985. Studies on transcription of 3'-extended DNA templates by mammalian RNA polymerase II. Partial purification and characterization of a factor from HeLa cells that facilitates renaturation of the DNA template. *Biochemistry*, 24(9), pp.2254–2262.

Kapanidis, A.N. et al., 2005. Retention of transcription initiation factor sigma70 in transcription elongation: single-molecule analysis. *Molecular cell*, 20(3), pp.347–356.

Kaplan, C.D., Laprade, L. & Winston, F., 2003. Transcription Elongation Factors Repress Transcription Initiation from Cryptic Sites. *Science*, 301(5636), pp.1096–1099.

Kassavetis, G.A. & Chamberlin, M.J., 1981. Pausing and termination of transcription within the early region of bacteriophage T7 DNA in vitro. *The Journal of biological chemistry*, 256(6), pp.2777–2786.

Kassavetis, G.A., Prakash, P. & Shim, E., 2010. The C53/C37 Subcomplex of RNA Polymerase III Lies Near the Active Site and Participates in Promoter Opening. *Journal of Biological Chemistry*, 285(4), pp.2695–2706.

Kawauchi, J. et al., 2008. Budding yeast RNA polymerases I and II employ parallel mechanisms of transcriptional termination. *Genes & development*, 22(8), pp.1082–1092.

Keener, J. et al., 1997. Histones H3 and H4 are components of upstream activation factor required for the high-level transcription of yeast rDNA by RNA polymerase I. *Proceedings of the National Academy of Sciences of the United States of America*, 94(25), pp.13458–13462.

Keener, J. et al., 1998. Reconstitution of yeast RNA polymerase I transcription in vitro from purified components. TATA-binding protein is not required for basal transcription. *The Journal of Biological Chemistry*, 273(50), pp.33795–33802.

Kelly, J.L., Greenleaf, A.L. & Lehman, I.R., 1986. Isolation of the nuclear gene encoding a subunit of the yeast mitochondrial RNA polymerase. *The Journal of biological chemistry*, 261(22), pp.10348–10351.

Kempers-Veenstra, A.E. et al., 1985. Deletion mapping of the yeast Pol I promoter. *Current genetics*, 10(4), pp.253–260.

Kermekchiev, M.B. & Grummt, I., 1987. Natural point mutations within rat rDNA transcription terminator elements reveal the functional importance of single bases for factor binding and termination. *Nucleic acids research*, 15(10), pp.4131–4143.

Kettenberger, H., Armache, K.-J. & Cramer, P., 2003. Architecture of the RNA Polymerase II-TFIIS Complex and Implications for mRNA Cleavage. *Cell*, 114(3), pp.347–357.

Keys, D.A. et al., 1996. Multiprotein transcription factor UAF interacts with the upstream element of the yeast RNA polymerase I promoter and forms a stable preinitiation complex. *Genes & Development*, 10(7), pp.887–903.

Keys, D.A. et al., 1994. RRN6 and RRN7 encode subunits of a multiprotein complex essential for the initiation of rDNA transcription by RNA polymerase I in Saccharomyces cerevisiae. *Genes & Development*, 8(19), pp.2349–2362.

Khorasanizadeh, S., 2004. The nucleosome: from genomic organization to genomic regulation. *Cell*, 116(2), pp.259–272.

Kihm, A.J. et al., 1998. Phosphorylation of the rRNA transcription factor upstream binding factor promotes its association with TATA binding protein. *Proceedings of the National Academy of Sciences of the United States of America*, 95(25), pp.14816–14820.

Kim, H.D., Choe, J. & Seo, Y.S., 1999. The sen1(+) gene of Schizosaccharomyces pombe, a homologue of budding yeast SEN1, encodes an RNA and DNA helicase. *Biochemistry*, 38(44), pp.14697–14710.

Kireeva, M.L. et al., 2005. Nature of the nucleosomal barrier to RNA polymerase II. *Molecular cell*, 18(1), pp.97–108.

Kireeva, M.L. et al., 2002. Nucleosome remodeling induced by RNA polymerase II: loss of the H2A/H2B dimer during transcription. *Molecular Cell*, 9(3), pp.541–552.

Kireeva, M.L., Komissarova, N. & Kashlev, M., 2000. Overextended RNA:DNA hybrid as a negative regulator of RNA polymerase II processivity. *Journal of Molecular Biology*, 299(2), pp.325–335.

Kleiman, L. & Huang, R.C., 1972. Reconstitution of chromatin. The sequential binding of histones to DNA in the presence of salt and urea. *Journal of molecular biology*, 64(1), pp.1–8.

Klinger, C. et al., 1996. Localization of yeast RNA polymerase I core subunits by immunoelectron microscopy. *The EMBO Journal*, 15(17), pp.4643–4653.

Knezetic, J.A. & Luse, D.S., 1986. The presence of nucleosomes on a DNA template prevents initiation by RNA polymerase II in vitro. *Cell*, 45(1), pp.95–104.

Knop, M. et al., 1999. Epitope tagging of yeast genes using a PCR-based strategy: more tags and improved practical routines. *Yeast (Chichester, England)*, 15(10B), pp.963–972.

Kobayashi, T. et al., 1998. Expansion and contraction of ribosomal DNA repeats in Saccharomyces cerevisiae: requirement of replication fork blocking (Fob1) protein and the role of RNA polymerase I. *Genes & development*, 12(24), pp.3821–3830.

Kobayashi, T. et al., 1992. Identification of a site required for DNA replication fork blocking activity in the rRNA gene cluster in Saccharomyces cerevisiae. *Molecular & general genetics: MGG*, 233(3), pp.355–362.

Kobayashi, T. et al., 2004. SIR2 regulates recombination between different rDNA repeats, but not recombination within individual rRNA genes in yeast. *Cell*, 117(4), pp.441–453.

Kobayashi, T., 2003. The replication fork barrier site forms a unique structure with Fob1p and inhibits the replication fork. *Molecular and Cellular Biology*, 23(24), pp.9178–9188.

Kobayashi, T. & Ganley, A.R.D., 2005. Recombination regulation by transcription-induced cohesin dissociation in rDNA repeats. *Science (New York, N.Y.)*, 309(5740), pp.1581–1584.

Kobayashi, T. & Horiuchi, T., 1996. A yeast gene product, Fob1 protein, required for both replication fork blocking and recombinational hotspot activities. *Genes to cells: devoted to molecular & cellular mechanisms*, 1(5), pp.465–474.

Kobayashi, T., Nomura, M. & Horiuchi, T., 2001. Identification of DNA cis elements essential for expansion of ribosomal DNA repeats in Saccharomyces cerevisiae. *Molecular and cellular biology*, 21(1), pp.136–147.

Komissarova, N. et al., 2003. Engineering of elongation complexes of bacterial and yeast RNA polymerases. *Methods in enzymology*, 371, pp.233–251.

Korkhin, Y. et al., 2009. Evolution of Complex RNA Polymerases: The Complete Archaeal RNA Polymerase Structure. *PLoS Biol*, 7(5), p.e1000102.

Kornberg, R.D., 1974. Chromatin structure: a repeating unit of histones and DNA. *Science (New York, N.Y.)*, 184(139), pp.868–871.

Kornberg, R.D. & Thomas, J.O., 1974. Chromatin structure; oligomers of the histones. *Science (New York, N.Y.)*, 184(139), pp.865–868.

Koš, M. & Tollervey, D., 2010. Yeast Pre-rRNA Processing and Modification Occur Cotranscriptionally. *Molecular Cell*, 37(6), pp.809–820.

Kosa, P.F. et al., 1997. The 2.1-A crystal structure of an archaeal preinitiation complex: TATA-box-binding protein/transcription factor (II)B core/TATA-box. *Proceedings of the National Academy of Sciences of the United States of America*, 94(12), pp.6042–6047.

Kostrewa, D. et al., 2009. RNA polymerase II–TFIIB structure and mechanism of transcription initiation. *Nature*, 462(7271), pp.323–330.

Kouzarides, T., 2007. Chromatin modifications and their function. *Cell*, 128(4), pp.693–705.

Kressler, D., Linder, P. & de La Cruz, J., 1999. Protein trans-acting factors involved in ribosome biogenesis in Saccharomyces cerevisiae. *Molecular and Cellular Biology*, 19(12), pp.7897–7912.

Krogan, N.J. et al., 2002. RNA Polymerase II Elongation Factors of Saccharomyces cerevisiae: a Targeted Proteomics Approach. *Molecular and Cellular Biology*, 22(20), pp.6979–6992.

Kuehner, J.N., Pearson, E.L. & Moore, C., 2011. Unravelling the means to an end: RNA polymerase II transcription termination. *Nature reviews. Molecular cell biology*, 12(5), pp.283–294.

Kufel, J., Dichtl, B. & Tollervey, D., 1999. Yeast Rnt1p is required for cleavage of the pre-ribosomal RNA in the 3' ETS but not the 5' ETS. *RNA (New York, N.Y.)*, 5(7), pp.909–917.

Kuhn, A. et al., 1988. The mouse ribosomal gene terminator consists of three functionally separable sequence elements. *The EMBO journal*, 7(5), pp.1497–1502.

Kuhn, A., Bartsch, I. & Grummt, I., 1990. Specific interaction of the murine transcription termination factor TTF I with class-I RNA polymerases. *Nature*, 344(6266), pp.559–562.

Kuhn, C.-D. et al., 2007. Functional architecture of RNA polymerase I. *Cell*, 131(7), pp.1260–1272.

Kulkens, T. et al., 1991. The yeast RNA polymerase I promoter: ribosomal DNA sequences involved in transcription initiation and complex formation in vitro. *Nucleic Acids Research*, 19(19), pp.5363–5370.

Kuras, L. et al., 2000. TAF-Containing and TAF-Independent Forms of Transcriptionally Active TBP in Vivo. *Science*, 288(5469), pp.1244–1248.

Kwon, H. & Green, M.R., 1994. The RNA polymerase I transcription factor, upstream binding factor, interacts directly with the TATA box-binding protein. *The Journal of biological chemistry*, 269(48), pp.30140–30146.

Laemmli, U.K., 1970. Cleavage of structural proteins during the assembly of the head of bacteriophage T4. *Nature*, 227(5259), pp.680–685.

Laird, C.D. & Chooi, W.Y., 1976. Morphology of transcription units in Drosophila melanogaster. *Chromosoma*, 58(2), pp.193–218.

Lalo, D. et al., 1996. RRN11 encodes the third subunit of the complex containing Rrn6p and Rrn7p that is essential for the initiation of rDNA transcription by yeast RNA polymerase I. *The Journal of biological chemistry*, 271(35), pp.21062–21067.

Landrieux, E. et al., 2006. A subcomplex of RNA polymerase III subunits involved in transcription termination and reinitiation. *The EMBO Journal*, 25(1), pp.118–128.

Lang, W.H. et al., 1994. A model for transcription termination by RNA polymerase I. *Cell*, 79(3), pp.527–534.

Lang, W.H., Platt, T. & Reeder, R.H., 1998. Escherichia coli rho factor induces release of yeast RNA polymerase II but not polymerase I or III. *Proceedings of the National Academy of Sciences of the United States of America*, 95(9), pp.4900–4905.

Lang, W.H. & Reeder, R.H., 1993. The REB1 site is an essential component of a terminator for RNA polymerase I in Saccharomyces cerevisiae. *Molecular and cellular biology*, 13(1), pp.649–658.

Lang, W.H. & Reeder, R.H., 1995. Transcription termination of RNA polymerase I due to a T-rich element interacting with Reb1p. *Proceedings of the National Academy of Sciences of the United States of America*, 92(21), pp.9781–9785.

Längst, G. et al., 1997. RNA polymerase I transcription on nucleosomal templates: the transcription termination factor TTF-I induces chromatin remodeling and relieves transcriptional repression. *The EMBO Journal*, 16(4), pp.760–768.

Längst, G., Becker, P.B. & Grummt, I., 1998. TTF-I determines the chromatin architecture of the active rDNA promoter. *The EMBO journal*, 17(11), pp.3135–3145.

Larson, M.H. et al., 2008. Applied Force Reveals Mechanistic and Energetic Details of Transcription Termination. *Cell*, 132(6), pp.971–982.

Lee, K.M. & Narlikar, G., 2001. Assembly of nucleosomal templates by salt dialysis. *Current protocols in molecular biology / edited by Frederick M. Ausubel ... [et al.]*, Chapter 21, p.Unit 21.6.

Lee, Y. et al., 2004. MicroRNA genes are transcribed by RNA polymerase II. *The EMBO journal*, 23(20), pp.4051–4060.

Léger-Silvestre, I. et al., 1999. Functional compartmentalization of the nucleus in the budding yeast Saccharomyces cerevisiae. *Chromosoma*, 108(2), pp.103–113.

Li, B., Carey, M. & Workman, J.L., 2007. The role of chromatin during transcription. *Cell*, 128(4), pp.707–719.

Li, G. et al., 2005. Rapid spontaneous accessibility of nucleosomal DNA. *Nature Structural & Molecular Biology*, 12(1), pp.46–53.

Li, X.-Y., Bhaumik, S.R. & Green, M.R., 2000. Distinct Classes of Yeast Promoters Revealed by Differential TAF Recruitment. *Science*, 288(5469), pp.1242–1244.

Liaw, P.C. & Brandl, C.J., 1994. Defining the sequence specificity of the Saccharomyces cerevisiae DNA binding protein REB1p by selecting binding sites from random-sequence oligonucleotides. *Yeast (Chichester, England)*, 10(6), pp.771–787.

Lieb, J.D. & Clarke, N.D., 2005. Control of transcription through intragenic patterns of nucleosome composition. *Cell*, 123(7), pp.1187–1190.

Liew, C.K. et al., 2008. NMR spectroscopy as a tool for the rapid assessment of the conformation of GST-fusion proteins. *Protein science: a publication of the Protein Society*, 17(9), pp.1630–1635.

Liljelund, P. et al., 1992. Characterization and mutagenesis of the gene encoding the A49 subunit of RNA polymerase A in Saccharomyces cerevisiae. *Proceedings of the National Academy of Sciences*, 89(19), pp.9302–9305.

Lindstrom, D.L. et al., 2003. Dual Roles for Spt5 in Pre-mRNA Processing and Transcription Elongation Revealed by Identification of Spt5-Associated Proteins. *Molecular and Cellular Biology*, 23(4), pp.1368–1378.

Linskens, M.H. & Huberman, J.A., 1988. Organization of replication of ribosomal DNA in Saccharomyces cerevisiae. *Molecular and cellular biology*, 8(11), pp.4927–4935.

Liu, C. & Martin, C.T., 2002. Promoter Clearance by T7 RNA Polymerase INITIAL BUBBLE COLLAPSE AND TRANSCRIPT DISSOCIATION MONITORED BY BASE ANALOG FLUORESCENCE. *Journal of Biological Chemistry*, 277(4), pp.2725–2731.

Logan, J. et al., 1987. A poly(A) addition site and a downstream termination region are required for efficient cessation of transcription by RNA polymerase II in the mouse beta maj-globin gene. *Proceedings of the National Academy of Sciences of the United States of America*, 84(23), pp.8306–8310.

López-Estraño, C. et al., 1998. Co-localization of polar replication fork barriers and rRNA transcription terminators in mouse rDNA. *Journal of Molecular Biology*, 277(2), pp.249–256.

Lorch, Y., LaPointe, J.W. & Kornberg, R.D., 1987. Nucleosomes inhibit the initiation of transcription but allow chain elongation with the displacement of histones. *Cell*, 49(2), pp.203–210.

Lorch, Y., Maier-Davis, B. & Kornberg, R.D., 2006. Chromatin remodeling by nucleosome disassembly in vitro. *Proceedings of the National Academy of Sciences of the United States of America*, 103(9), pp.3090–3093.

Lorch, Y., Zhang, M. & Kornberg, R.D., 1999. Histone Octamer Transfer by a Chromatin-Remodeling Complex. *Cell*, 96(3), pp.389–392.

Louis, B.G. & Fitt, P.S., 1971. Nucleic acid enzymology of extremely halophilic bacteria. Halobacterium cutirubrum deoxyribonucleic acid-dependent ribonucleic acid polymerase. *Biochemical Journal*, 121(4), pp.621–627.

Lowary, P.T. & Widom, J., 1998. New DNA sequence rules for high affinity binding to histone octamer and sequence-directed nucleosome positioning. *Journal of Molecular Biology*, 276(1), pp.19–42.

Luse, D.S., 2012. Rethinking the role of TFIIF in transcript initiation by RNA polymerase II. *Transcription*, 3(4), pp.156–159.

Lusser, A., Urwin, D.L. & Kadonaga, J.T., 2005. Distinct activities of CHD1 and ACF in ATP-dependent chromatin assembly. *Nature Structural & Molecular Biology*, 12(2), pp.160–166.

Malik, H.S. & Henikoff, S., 2003. Phylogenomics of the nucleosome. *Nature Structural & Molecular Biology*, 10(11), pp.882–891.

Mandel, C.R., Bai, Y. & Tong, L., 2008. Protein factors in pre-mRNA 3'-end processing. *Cellular and molecular life sciences: CMLS*, 65(7-8), pp.1099–1122.

Marck, C. et al., 2006. The RNA polymerase III-dependent family of genes in hemiascomycetes: comparative RNomics, decoding strategies, transcription and evolutionary implications. *Nucleic Acids Research*, 34(6), pp.1816–1835.

Marr, M.T. & Roberts, J.W., 2000. Function of Transcription Cleavage Factors GreA and GreB at a Regulatory Pause Site. *Molecular Cell*, 6(6), pp.1275–1285.

Mason, P.B. & Struhl, K., 2003. The FACT Complex Travels with Elongating RNA Polymerase II and Is Important for the Fidelity of Transcriptional Initiation In Vivo. *Molecular and Cellular Biology*, 23(22), pp.8323–8333.

Mason, S.W., Sander, E.E. & Grummt, I., 1997. Identification of a transcript release activity acting on ternary transcription complexes containing murine RNA polymerase I. *The EMBO journal*, 16(1), pp.163–172.

Matsui, S. & Busch, H., 1977. Isolation and characterization of rDNA-containing chromatin from nucleoli. *Experimental cell research*, 109(1), pp.151–161.

Matsuzaki, H., Kassavetis, G.A. & Geiduschek, E.P., 1994. Analysis of RNA Chain Elongation and Termination by Saccharomyces cerevisiae RNA Polymerase III. *Journal of Molecular Biology*, 235(4), pp.1173–1192.

Mavrich, T.N. et al., 2008. A barrier nucleosome model for statistical positioning of nucleosomes throughout the yeast genome. *Genome research*, 18(7), pp.1073–1083.

Mayer, C. et al., 2006. Intergenic transcripts regulate the epigenetic state of rRNA genes. *Molecular cell*, 22(3), pp.351–361.

McStay, B., Frazier, M.W. & Reeder, R.H., 1991. xUBF contains a novel dimerization domain essential for RNA polymerase I transcription. *Genes & development*, 5(11), pp.1957–1968.

Mead, D.A., Szczesna-Skorupa, E. & Kemper, B., 1986. Single-stranded DNA “blue” T7 promoter plasmids: a versatile tandem promoter system for cloning and protein engineering. *Protein engineering*, 1(1), pp.67–74.

Mellor, J., 2006. Dynamic nucleosomes and gene transcription. *Trends in Genetics: TIG*, 22(6), pp.320–329.

Merkl, P., 2009. *Establishment of an in vitro transcription system for comparative analysis of the elongation of RNA polymerases from Saccharomyces cerevisiae*,

Merz, K. et al., 2008. Actively transcribed rRNA genes in S. cerevisiae are organized in a specialized chromatin associated with the high-mobility group protein Hmo1 and are largely devoid of histone molecules. *Genes & Development*, 22(9), pp.1190–1204.

Meyer, T.S. & Lamberts, B.L., 1965. Use of coomassie brilliant blue R250 for the electrophoresis of microgram quantities of parotid saliva proteins on acrylamide-gel strips. *Biochimica et biophysica acta*, 107(1), pp.144–145.

Milkereit, P. & Tschochner, H., 1998. A specialized form of RNA polymerase I, essential for initiation and growth-dependent regulation of rRNA synthesis, is disrupted during transcription. *The EMBO Journal*, 17(13), pp.3692–3703.

Miller, G. & Hahn, S., 2006. A DNA-tethered cleavage probe reveals the path for promoter DNA in the yeast preinitiation complex. *Nature Structural & Molecular Biology*, 13(7), pp.603–610.

Miller, O.L. & Beatty, B.R., 1969. Visualization of nucleolar genes. *Science (New York, N.Y.)*, 164(882), pp.955–957.

Millevoi, S. & Vagner, S., 2010. Molecular mechanisms of eukaryotic pre-mRNA 3’ end processing regulation. *Nucleic acids research*, 38(9), pp.2757–2774.

Minakhin, L. et al., 2001. Bacterial RNA polymerase subunit ω and eukaryotic RNA polymerase subunit RPB6 are sequence, structural, and functional homologs and promote RNA polymerase assembly. *Proceedings of the National Academy of Sciences*, 98(3), pp.892–897.

Mischo, H.E. & Proudfoot, N.J., 2013. Disengaging polymerase: terminating RNA polymerase II transcription in budding yeast. *Biochimica et biophysica acta*, 1829(1), pp.174–185.

Miwa, T. et al., 1987. Transcription termination and RNA processing in the 3’-end spacer of mouse ribosomal RNA genes. *Nucleic acids research*, 15(5), pp.2043–2058.

Mohanty, B.K. & Bastia, D., 2004. Binding of the Replication Terminator Protein Fob1p to the Ter Sites of Yeast Causes Polar Fork Arrest. *Journal of Biological Chemistry*, 279(3), pp.1932–1941.

Moreira, J.M.A. & Holmberg, S., 1998. Nucleosome structure of the yeast CHA1 promoter: analysis of activation-dependent chromatin remodeling of an RNA-polymerase-II-transcribed gene in TBP and RNA pol II mutants defective in vivo in response to acidic activators. *The EMBO Journal*, 17(20), pp.6028–6038.

Morgan, W.D. et al., 1985. RNA sequence and secondary structure requirements for rho-dependent transcription termination. *Nucleic acids research*, 13(10), pp.3739–3754.

Morrow, B.E., Johnson, S.P. & Warner, J.R., 1989. Proteins that bind to the yeast rDNA enhancer. *The Journal of Biological Chemistry*, 264(15), pp.9061–9068.

Morrow, B.E., Ju, Q. & Warner, J.R., 1993. A bipartite DNA-binding domain in yeast Reb1p. *Molecular and Cellular Biology*, 13(2), pp.1173–1182.

Morrow, B.E., Ju, Q. & Warner, J.R., 1990. Purification and characterization of the yeast rDNA binding protein REB1. *The Journal of Biological Chemistry*, 265(34), pp.20778–20783.

Morse, R.H., Roth, S.Y. & Simpson, R.T., 1992. A transcriptionally active tRNA gene interferes with nucleosome positioning in vivo. *Molecular and cellular biology*, 12(9), pp.4015–4025.

Mueller, C.L. et al., 2004. The Paf1 Complex Has Functions Independent of Actively Transcribing RNA Polymerase II. *Molecular Cell*, 14(4), pp.447–456.

Mueller, C.L. & Jaehning, J.A., 2002. Ctr9, Rtf1, and Leo1 Are Components of the Paf1/RNA Polymerase II Complex. *Molecular and Cellular Biology*, 22(7), pp.1971–1980.

Müller-Hill, B., 1975. Lac repressor and lac operator. *Progress in biophysics and molecular biology*, 30(2-3), pp.227–252.

Mūller, B., Allmansberger, R. & Klein, A., 1985. Termination of a transcription unit comprising highly expressed genes in the archaebacteriumMethanococcus voltae. *Nucleic Acids Research*, 13(18), pp.6439–6445.

Murano, K. et al., 2008. Transcription Regulation of the rRNA Gene by a Multifunctional Nucleolar Protein, B23/Nucleophosmin, through Its Histone Chaperone Activity. *Molecular and Cellular Biology*, 28(10), pp.3114–3126.

Musters, W. et al., 1989. Linker scanning of the yeast RNA polymerase I promoter. *Nucleic Acids Research*, 17(23), pp.9661–9678.

Nabavi, S. & Nazar, R.N., 2010. Pac1 endonuclease and Dhp1p 5'-->3' exonuclease are required for U3 snoRNA termination in Schizosaccharomyces pombe. *FEBS letters*, 584(15), pp.3436–3441.

NEELIN, J.M. & BUTLER, G.C., 1959. The fractionation of the histones of calf thymus and chicken erythrocytes by cation-exchange chromatography with sodium salts. *Canadian journal of biochemistry and physiology*, 37(7), pp.843–859.

Németh, A. et al., 2008. Epigenetic regulation of TTF-I-mediated promoter–terminator interactions of rRNA genes. *The EMBO Journal*, 27(8), pp.1255–1265.

Németh, A. et al., 2013. RNA polymerase I termination: Where is the end? *Biochimica et biophysica acta*, 1829(3-4), pp.306–317.

Németh, A. et al., 2004. The chromatin remodeling complex NoRC and TTF-I cooperate in the regulation of the mammalian rRNA genes in vivo. *Nucleic Acids Research*, 32(14), pp.4091 – 4099.

Ng, H.H. et al., 2002. Genome-wide location and regulated recruitment of the RSC nucleosome-remodeling complex. *Genes & development*, 16(7), pp.806–819.

Nielsen, S., Yuzenkova, Y. & Zenkin, N., 2013. Mechanism of Eukaryotic RNA Polymerase III Transcription Termination. *Science*, 340(6140), pp.1577–1580.

O'Sullivan, A.C., Sullivan, G.J. & McStay, B., 2002. UBF binding in vivo is not restricted to regulatory sequences within the vertebrate ribosomal DNA repeat. *Molecular and cellular biology*, 22(2), pp.657–668.

Oeffinger, M. et al., 2007. Comprehensive analysis of diverse ribonucleoprotein complexes. *Nature methods*, 4(11), pp.951–956.

Okuwaki, M. et al., 2001. Function of nucleophosmin/B23, a nucleolar acidic protein, as a histone chaperone. *FEBS Letters*, 506(3), pp.272–276.

Onodera, Y. et al., 2005. Plant nuclear RNA polymerase IV mediates siRNA and DNA methylation-dependent heterochromatin formation. *Cell*, 120(5), pp.613–622.

Orlova, M. et al., 1995. Intrinsic transcript cleavage activity of RNA polymerase. *Proceedings of the National Academy of Sciences*, 92(10), pp.4596–4600.

Orphanides, G. et al., 1998. FACT, a Factor that Facilitates Transcript Elongation through Nucleosomes. *Cell*, 92(1), pp.105–116.

Osheim, Y.N. et al., 2004. Pre-18S Ribosomal RNA Is Structurally Compacted into the SSU Processome Prior to Being Cleaved from Nascent Transcripts in Saccharomyces cerevisiae. *Molecular Cell*, 16(6), pp.943–954.

Ouzounis, C. & Sander, C., 1992. TFIIB, an evolutionary link between the transcription machineries of archaebacteria and eukaryotes. *Cell*, 71(2), pp.189–190.

Pace, H.C., Lu, P. & Lewis, M., 1990. lac repressor: crystallization of intact tetramer and its complexes with inducer and operator DNA. *Proceedings of the National Academy of Sciences of the United States of America*, 87(5), pp.1870–1873.

Parker, K.A. & Bond, U., 1989. Analysis of pre-rRNAs in heat-shocked HeLa cells allows identification of the upstream termination site of human polymerase I transcription. *Molecular and cellular biology*, 9(6), pp.2500–2512.

Pavesi, A. et al., 1994. Identification of new eukaryotic tRNA genes in genomic DNA databases by a multistep weight matrix analysis of transcriptional control regions. *Nucleic acids research*, 22(7), pp.1247–1256.

Pavri, R. et al., 2006. Histone H2B Monoubiquitination Functions Cooperatively with FACT to Regulate Elongation by RNA Polymerase II. *Cell*, 125(4), pp.703–717.

Pérez-Rueda, E. & Collado-Vides, J., 2000. The repertoire of DNA-binding transcriptional regulators in Escherichia coli K-12. *Nucleic Acids Research*, 28(8), pp.1838–1847.

Peterson, C.L., 2008. Salt gradient dialysis reconstitution of nucleosomes. *CSH protocols*, 2008, p.pdb.prot5113.

Petes, T.D., 1979. Yeast ribosomal DNA genes are located on chromosome XII. *Proceedings of the National Academy of Sciences of the United States of America*, 76(1), pp.410–414.

Petesch, S.J. & Lis, J.T., 2012. Overcoming the nucleosome barrier during transcript elongation. *Trends in genetics: TIG*, 28(6), pp.285–294.

Peyroche, G. et al., 2002. The A14–A43 heterodimer subunit in yeast RNA pol I and their relationship to Rpb4–Rpb7 pol II subunits. *Proceedings of the National Academy of Sciences*, 99(23), pp.14670–14675.

Peyroche, G. et al., 2000. The recruitment of RNA polymerase I on rDNA is mediated by the interaction of the A43 subunit with Rrn3. *The EMBO Journal*, 19(20), pp.5473–5482.

Philippsen, P. et al., 1978. Unique arrangement of coding sequences for 5 S, 5.8 S, 18 S and 25 S ribosomal RNA in Saccharomyces cerevisiae as determined by R-loop and hybridization analysis. *Journal of molecular biology*, 123(3), pp.387–404.

Pinskaya, M., Gourvennec, S. & Morillon, A., 2009. H3 lysine 4 di- and tri-methylation deposited by cryptic transcription attenuates promoter activation. *The EMBO journal*, 28(12), pp.1697–1707.

Pokholok, D.K., Hannett, N.M. & Young, R.A., 2002. Exchange of RNA Polymerase II Initiation and Elongation Factors during Gene Expression In Vivo. *Molecular Cell*, 9(4), pp.799–809.

Prangishvilli, D. et al., 1982. DNA-dependent RNA polymerase of thermoacidophilic archaebacteria. *European journal of biochemistry / FEBS*, 122(3), pp.471–477.

Preiss, J., Dieckmann, M. & Berg, P., 1961. The Enzymic Synthesis of Amino Acyl Derivatives of Ribonucleic Acid IV. THE FORMATION OF THE 3'-HYDROXYL TERMINAL TRINUCLEOTIDE SEQUENCE OF AMINO ACID-ACCEPTOR RIBONUCLEIC ACID. *Journal of Biological Chemistry*, 236(6), pp.1748–1757.

Prescott, E.M. et al., 2004. Transcriptional termination by RNA polymerase I requires the small subunit Rpa12p. *Proceedings of the National Academy of Sciences of the United States of America*, 101(16), pp.6068–6073.

Price, D.H., Sluder, A.E. & Greenleaf, A.L., 1989. Dynamic interaction between a Drosophila transcription factor and RNA polymerase II. *Molecular and Cellular Biology*, 9(4), pp.1465–1475.

Puig, O. et al., 2001. The tandem affinity purification (TAP) method: a general procedure of protein complex purification. *Methods (San Diego, Calif.)*, 24(3), pp.218–229.

Qiu, H. et al., 2004. An Array of Coactivators Is Required for Optimal Recruitment of TATA Binding Protein and RNA Polymerase II by Promoter-Bound Gcn4p. *Molecular and Cellular Biology*, 24(10), pp.4104–4117.

Rappaport, J. et al., 1987. Purification and functional characterization of transcription factor SII from calf thymus. Role in RNA polymerase II elongation. *Journal of Biological Chemistry*, 262(11), pp.5227–5232.

Reeder, R.H., Guevara, P. & Roan, J.G., 1999. Saccharomyces cerevisiae RNA polymerase I terminates transcription at the Reb1 terminator in vivo. *Molecular and Cellular Biology*, 19(11), pp.7369–7376.

Reeder, R.H. & Lang, W., 1994. The mechanism of transcription termination by RNA polymerase I. *Molecular microbiology*, 12(1), pp.11–15.

Reeve, J.N., Sandman, K. & Daniels, C.J., 1997. Archaeal histones, nucleosomes, and transcription initiation. *Cell*, 89(7), pp.999–1002.

Reinberg, D. & Roeder, R.G., 1987. Factors involved in specific transcription by mammalian RNA polymerase II. Transcription factor IIS stimulates elongation of RNA chains. *Journal of Biological Chemistry*, 262(7), pp.3331–3337.

Reines, D. et al., 1993. Transcription elongation by RNA polymerase II: mechanism of SII activation. *Cellular & molecular biology research*, 39(4), pp.331–338.

Reiter, A. et al., 2012. The Reb1-homologue Ydr026c/Nsi1 is required for efficient RNA polymerase I termination in yeast. *The EMBO journal*, 31(16), pp.3480–3493.

Renart, J., Reiser, J. & Stark, G.R., 1979. Transfer of proteins from gels to diazobenzyloxymethyl-paper and detection with antisera: a method for studying antibody specificity and antigen structure. *Proceedings of the National Academy of Sciences of the United States of America*, 76(7), pp.3116–3120.

Revyakin, A., Ebright, R.H. & Strick, T.R., 2004. Promoter unwinding and promoter clearance by RNA polymerase: Detection by single-molecule DNA nanomanipulation. *Proceedings of the National Academy of Sciences of the United States of America*, 101(14), pp.4776–4780.

Richardson, J.P., 2003. Loading Rho to terminate transcription. *Cell*, 114(2), pp.157–159.

Richardson, J.P., 2002. Rho-dependent termination and ATPases in transcript termination. *Biochimica et biophysica acta*, 1577(2), pp.251–260.

Richardson, J.P., 1993. Transcription termination. *Critical reviews in biochemistry and molecular biology*, 28(1), pp.1–30.

Rickards, B. et al., 2007. Nucleolin Is Required for RNA Polymerase I Transcription In Vivo. *Molecular and Cellular Biology*, 27(3), pp.937–948.

Rijal, K. & Maraia, R.J., 2013. RNA polymerase III mutants in TFIIFα-like C37 that cause terminator readthrough with no decrease in transcription output. *Nucleic acids research*, 41(1), pp.139–155.

Roberts, J.W., 1969. Termination factor for RNA synthesis. *Nature*, 224(5225), pp.1168–1174.

Roeder, R.G. & Rutter, W.J., 1969. Multiple forms of DNA-dependent RNA polymerase in eukaryotic organisms. *Nature*, 224(5216), pp.234–237.

Roeder, R.G. & Rutter, W.J., 1970. Specific nucleolar and nucleoplasmic RNA polymerases. *Proceedings of the National Academy of Sciences of the United States of America*, 65(3), pp.675–682.

Rondón, A.G. et al., 2009. Fail-safe transcriptional termination for protein-coding genes in S. cerevisiae. *Molecular cell*, 36(1), pp.88–98.

Rondón, A.G. et al., 2004. Molecular evidence indicating that the yeast PAF complex is required for transcription elongation. *EMBO reports*, 5(1), pp.47–53.

Rosario, B.C.D. & Pemberton, L.F., 2008. Nap1 Links Transcription Elongation, Chromatin Assembly, and Messenger RNP Complex Biogenesis. *Molecular and Cellular Biology*, 28(7), pp.2113–2124.

Ross, P.L. et al., 2004. Multiplexed protein quantitation in Saccharomyces cerevisiae using amine-reactive isobaric tagging reagents. *Molecular & cellular proteomics: MCP*, 3(12), pp.1154–1169.

Rowlands, T., Baumann, P. & Jackson, S.P., 1994. The TATA-binding protein: a general transcription factor in eukaryotes and archaebacteria. *Science (New York, N.Y.)*, 264(5163), pp.1326–1329.

Ruan, W. et al., 2011. Evolution of two modes of intrinsic RNA polymerase transcript cleavage. *The Journal of Biological Chemistry*, 286(21), pp.18701–18707.

Rudd, M.D., Izban, M.G. & Luse, D.S., 1994. The active site of RNA polymerase II participates in transcript cleavage within arrested ternary complexes. *Proceedings of the National Academy of Sciences*, 91(17), pp.8057–8061.

Sambrook, J., Fritsch, E.F. & Maniatis, T., 1989. *Molecular cloning: a laboratory manual*, Cold Spring Harbor, N.Y.: Cold Spring Harbor Laboratory.

Sánchez-Gorostiaga, A. et al., 2004. Transcription Termination Factor reb1p Causes Two Replication Fork Barriers at Its Cognate Sites in Fission Yeast Ribosomal DNA In Vivo. *Molecular and Cellular Biology*, 24(1), pp.398–406.

Van der Sande, C.A. et al., 1989. Termination of transcription by yeast RNA polymerase I. *Nucleic acids research*, 17(22), pp.9127–9146.

Sander, E.E. & Grummt, I., 1997. Oligomerization of the transcription termination factor TTF-I: implications for the structural organization of ribosomal transcription units. *Nucleic acids research*, 25(6), pp.1142–1147.

Santangelo, T.J. & Roberts, J.W., 2004. Forward Translocation Is the Natural Pathway of RNA Release at an Intrinsic Terminator. *Molecular Cell*, 14(1), pp.117–126.

Santoro, R. et al., 2010. Intergenic transcripts originating from a subclass of ribosomal DNA repeats silence ribosomal RNA genes in trans. *EMBO reports*, 11(1), pp.52–58.

Santoro, R., Li, J. & Grummt, I., 2002. The nucleolar remodeling complex NoRC mediates heterochromatin formation and silencing of ribosomal gene transcription. *Nature Genetics*, 32(3), pp.393–396.

Saunders, A. et al., 2003. Tracking FACT and the RNA Polymerase II Elongation Complex Through Chromatin in Vivo. *Science*, 301(5636), pp.1094–1096.

Saunders, A., Core, L.J. & Lis, J.T., 2006. Breaking barriers to transcription elongation. *Nature Reviews Molecular Cell Biology*, 7(8), pp.557–567.

Saunders, M.J. et al., 1990. Nucleosome depletion alters the chromatin structure of Saccharomyces cerevisiae centromeres. *Molecular and Cellular Biology*, 10(11), pp.5721–5727.

Schaeffer, L. et al., 1993. DNA repair helicase: a component of BTF2 (TFIIH) basic transcription factor. *Science (New York, N.Y.)*, 260(5104), pp.58–63.

Schaeffer, L. et al., 1994. The ERCC2/DNA repair protein is associated with the class II BTF2/TFIIH transcription factor. *The EMBO journal*, 13(10), pp.2388–2392.

Schmid, M., Durussel, T. & Laemmli, U.K., 2004. ChIC and ChEC; genomic mapping of chromatin proteins. *Molecular cell*, 16(1), pp.147–157.

Schmitz, K.-M. et al., 2010. Interaction of noncoding RNA with the rDNA promoter mediates recruitment of DNMT3b and silencing of rRNA genes. *Genes & development*, 24(20), pp.2264–2269.

Schnapp, G., Graveley, B.R. & Grummt, I., 1996. TFIIS binds to mouse RNA polymerase I and stimulates transcript elongation and hydrolytic cleavage of nascent rRNA. *Molecular & General Genetics: MGG*, 252(4), pp.412–419.

Schneider, D.A., 2012. RNA polymerase I activity is regulated at multiple steps in the transcription cycle: Recent insights into factors that influence transcription elongation. *Gene*, 493(2), pp.176–184.

Schneider, D.A. et al., 2006. RNA polymerase II elongation factors Spt4p and Spt5p play roles in transcription elongation by RNA polymerase I and rRNA processing. *Proceedings of the National Academy of Sciences of the United States of America*, 103(34), pp.12707–12712.

Schneider, D.A. et al., 2007. Transcription elongation by RNA polymerase I is linked to efficient rRNA processing and ribosome assembly. *Molecular Cell*, 26(2), pp.217–229.

Schultz, P. et al., 1993. Three-dimensional model of yeast RNA polymerase I determined by electron microscopy of two-dimensional crystals. *The EMBO Journal*, 12(7), pp.2601–2607.

Schwabish, M.A. & Struhl, K., 2004. Evidence for Eviction and Rapid Deposition of Histones upon Transcriptional Elongation by RNA Polymerase II. *Molecular and Cellular Biology*, 24(23), pp.10111–10117.

Schwabish, M.A. & Struhl, K., 2007. The Swi/Snf Complex Is Important for Histone Eviction during Transcriptional Activation and RNA Polymerase II Elongation In Vivo. *Molecular and Cellular Biology*, 27(20), pp.6987–6995.

Schwarzacher, H.G. & Wachtler, F., 1993. The nucleolus. *Anatomy and embryology*, 188(6), pp.515–536.

Sharp, S.J. et al., 1985. Structure and transcription of eukaryotic tRNA genes. *CRC critical reviews in biochemistry*, 19(2), pp.107–144.

Shen, W.-C. et al., 2003. Systematic analysis of essential yeast TAFs in genome-wide transcription and preinitiation complex assembly. *The EMBO Journal*, 22(13), pp.3395–3402.

Shevchenko, A. et al., 2006. In-gel digestion for mass spectrometric characterization of proteins and proteomes. *Nature protocols*, 1(6), pp.2856–2860.

Shevchenko, A. et al., 1996. Mass spectrometric sequencing of proteins silver-stained polyacrylamide gels. *Analytical chemistry*, 68(5), pp.850–858.

Shi, X. et al., 1997. Cdc73p and Paf1p are found in a novel RNA polymerase II-containing complex distinct from the Srbp-containing holoenzyme. *Molecular and Cellular Biology*, 17(3), pp.1160–1169.

Shivaswamy, S. & Iyer, V.R., 2008. Stress-Dependent Dynamics of Global Chromatin Remodeling in Yeast: Dual Role for SWI/SNF in the Heat Shock Stress Response. *Molecular and Cellular Biology*, 28(7), pp.2221–2234.

Siddiqi, I.N. et al., 2001. Transcription of chromosomal rRNA genes by both RNA polymerase I and II in yeast uaf30 mutants lacking the 30 kDa subunit of transcription factor UAF. *The EMBO Journal*, 20(16), pp.4512–4521.

Simic, R. et al., 2003. Chromatin remodeling protein Chd1 interacts with transcription elongation factors and localizes to transcribed genes. *The EMBO Journal*, 22(8), pp.1846–1856.

Sims, R.J., Belotserkovskaya, R. & Reinberg, D., 2004. Elongation by RNA polymerase II: the short and long of it. *Genes & Development*, 18(20), pp.2437–2468.

Sluder, A.E., Greenleaf, A.L. & Price, D.H., 1989. Properties of a Drosophila RNA polymerase II elongation factor. *Journal of Biological Chemistry*, 264(15), pp.8963–8969.

Smale, S.T. & Kadonaga, J.T., 2003. The Rna Polymerase Ii Core Promoter. *Annual Review of Biochemistry*, 72(1), pp.449–479.

Smid, A., Finsterer, M. & Grummt, I., 1992. Limited proteolysis unmasks specific DNA-binding of the murine RNA polymerase I-specific transcription termination factor TTFI. *Journal of molecular biology*, 227(3), pp.635–647.

Smith, J.S. & Boeke, J.D., 1997. An unusual form of transcriptional silencing in yeast ribosomal DNA. *Genes & Development*, 11(2), pp.241–254.

Spitalny, P. & Thomm, M., 2008. A polymerase III-like reinitiation mechanism is operating in regulation of histone expression in archaea. *Molecular microbiology*, 67(5), pp.958–970.

Sprinzl, M. et al., 1991. Compilation of tRNA sequences and sequences of tRNA genes. *Nucleic acids research*, 19 Suppl, pp.2127–2171.

Squazzo, S.L. et al., 2002. The Paf1 complex physically and functionally associates with transcription elongation factors in vivo. *The EMBO Journal*, 21(7), pp.1764–1774.

Srinivasan, S. et al., 2005. The Drosophila trithorax group protein Kismet facilitates an early step in transcriptional elongation by RNA Polymerase II. *Development*, 132(7), pp.1623–1635.

Stano, N.M., Levin, M.K. & Patel, S.S., 2002. The +2 NTP Binding Drives Open Complex Formation in T7 RNA Polymerase. *Journal of Biological Chemistry*, 277(40), pp.37292–37300.

Stefanovsky, V. et al., 2006. Growth Factor Signaling Regulates Elongation of RNA Polymerase I Transcription in Mammals via UBF Phosphorylation and r-Chromatin Remodeling. *Molecular Cell*, 21(5), pp.629–639.

Stefanovsky, V.Y. et al., 2006. ERK Modulates DNA Bending and Enhancesome Structure by Phosphorylating HMG1-Boxes 1 and 2 of the RNA Polymerase I Transcription Factor UBF†. *Biochemistry*, 45(11), pp.3626–3634.

Steffan, J.S. et al., 1998. Interaction of TATA-binding protein with upstream activation factor is required for activated transcription of ribosomal DNA by RNA polymerase I in Saccharomyces cerevisiae in vivo. *Molecular and cellular biology*, 18(7), pp.3752–3761.

Steffan, J.S. et al., 1996. The role of TBP in rDNA transcription by RNA polymerase I in Saccharomyces cerevisiae: TBP is required for upstream activation factor-dependent recruitment of core factor. *Genes & Development*, 10(20), pp.2551–2563.

Steinmetz, E.J. et al., 2006. Genome-wide distribution of yeast RNA polymerase II and its control by Sen1 helicase. *Molecular cell*, 24(5), pp.735–746.

Steinmetz, E.J. et al., 2001. RNA-binding protein Nrd1 directs poly(A)-independent 3'-end formation of RNA polymerase II transcripts. *Nature*, 413(6853), pp.327–331.

Steinmetz, E.J. & Brow, D.A., 1996. Repression of gene expression by an exogenous sequence element acting in concert with a heterogeneous nuclear ribonucleoprotein-like protein, Nrd1, and the putative helicase Sen1. *Molecular and cellular biology*, 16(12), pp.6993–7003.

Steitz, T.A. et al., 1994. A unified polymerase mechanism for nonhomologous DNA and RNA polymerases. *Science (New York, N.Y.)*, 266(5193), pp.2022–2025.

Stevens, A., 1960. Incorporation of the adenine ribonucleotide into RNA by cell fractions from E. coli B. *Biochemical and Biophysical Research Communications*, 3(1), pp.92–96.

Studitsky, V.M. et al., 1997. Mechanism of transcription through the nucleosome by eukaryotic RNA polymerase. *Science (New York, N.Y.)*, 278(5345), pp.1960–1963.

Sugihara, F., Kasahara, K. & Kokubo, T., 2011. Highly redundant function of multiple AT-rich sequences as core promoter elements in the TATA-less RPS5 promoter of Saccharomyces cerevisiae. *Nucleic Acids Research*, 39(1), pp.59–75.

Swanson, M.S. & Winston, F., 1992. SPT4, SPT5 and SPT6 interactions: effects on transcription and viability in Saccharomyces cerevisiae. *Genetics*, 132(2), pp.325–336.

Switzer, R.C., 3rd, Merril, C.R. & Shifrin, S., 1979. A highly sensitive silver stain for detecting proteins and peptides in polyacrylamide gels. *Analytical biochemistry*, 98(1), pp.231–237.

Szymanski, M. et al., 1998. 5S rRNA Data Bank. *Nucleic acids research*, 26(1), pp.156–159.

Tan, S. et al., 1994. Roles for both the RAP30 and RAP74 subunits of transcription factor IIF in transcription initiation and elongation by RNA polymerase II. *Journal of Biological Chemistry*, 269(41), pp.25684–25691.

Teixeira, A. et al., 2004. Autocatalytic RNA cleavage in the human beta-globin pre-mRNA promotes transcription termination. *Nature*, 432(7016), pp.526–530.

Teixeira, M.C. et al., 2006. The YEASTRACT database: a tool for the analysis of transcription regulatory associations in Saccharomyces cerevisiae. *Nucleic Acids Research*, 34(suppl 1), pp.D446–D451.

Teng, Y., Yu, S. & Waters, R., 2001. The mapping of nucleosomes and regulatory protein binding sites at the Saccharomyces cerevisiae MFA2 gene: a high resolution approach. *Nucleic Acids Research*, 29(13), pp.e64–e64.

Thomas, M.C. & Chiang, C.-M., 2006. The general transcription machinery and general cofactors. *Critical reviews in biochemistry and molecular biology*, 41(3), pp.105–178.

Thomas, M.J., Platas, A.A. & Hawley, D.K., 1998. Transcriptional fidelity and proofreading by RNA polymerase II. *Cell*, 93(4), pp.627–637.

Thomm, M., Hausner, W. & Hethke, C., 1993. Transcription Factors and Termination of Transcription in Methanococcus. *Systematic and Applied Microbiology*, 16(4), pp.648–655.

Towbin, H., Staehelin, T. & Gordon, J., 1979. Electrophoretic transfer of proteins from polyacrylamide gels to nitrocellulose sheets: procedure and some applications. *Proceedings of the National Academy of Sciences of the United States of America*, 76(9), pp.4350–4354.

Tschochne, H. & Milkereit, P., 1997. RNA polymerase I from S. cerevisiae depends on an additional factor to release terminated transcripts from the template. *FEBS Letters*, 410(2-3), pp.461–466.

Tschochner, H., 1996. A novel RNA polymerase I-dependent RNase activity that shortens nascent transcripts from the 3′ end. *Proceedings of the National Academy of Sciences of the United States of America*, 93(23), pp.12914–12919.

Tse, C. et al., 1998. Disruption of higher-order folding by core histone acetylation dramatically enhances transcription of nucleosomal arrays by RNA polymerase III. *Molecular and cellular biology*, 18(8), pp.4629–4638.

Tuan, J.C., Zhai, W. & Comai, L., 1999. Recruitment of TATA-binding protein-TAFI complex SL1 to the human ribosomal DNA promoter is mediated by the carboxy-terminal activation domain of upstream binding factor (UBF) and is regulated by UBF phosphorylation. *Molecular and cellular biology*, 19(4), pp.2872–2879.

Uetz, P. et al., 2000. A comprehensive analysis of protein–protein interactions in Saccharomyces cerevisiae. *Nature*, 403(6770), pp.623–627.

Újvári, A. & Martin, C.T., 2000. Evidence for DNA bending at the T7 RNA polymerase promoter. *Journal of Molecular Biology*, 295(5), pp.1173–1184.

Uptain, S.M., Kane, C.M. & Chamberlin, M.J., 1997. Basic mechanisms of transcript elongation and its regulation. *Annual review of biochemistry*, 66, pp.117–172.

Ura, K. et al., 1997. Histone acetylation: influence on transcription, nucleosome mobility and positioning, and linker histone-dependent transcriptional repression. *The EMBO journal*, 16(8), pp.2096–2107.

Valentini, S.R., Weiss, V.H. & Silver, P.A., 1999. Arginine methylation and binding of Hrp1p to the efficiency element for mRNA 3'-end formation. *RNA (New York, N.Y.)*, 5(2), pp.272–280.

Vannini, A. et al., 2010. Molecular Basis of RNA Polymerase III Transcription Repression by Maf1. *Cell*, 143(1), pp.59–70.

Vannini, A. & Cramer, P., 2012. Conservation between the RNA Polymerase I, II, and III Transcription Initiation Machineries. *Molecular Cell*, 45(4), pp.439–446.

Viktorovskaya, O.V., Appling, F.D. & Schneider, D.A., 2011. Yeast transcription elongation factor Spt5 associates with RNA polymerase I and RNA polymerase II directly. *The Journal of biological chemistry*, 286(21), pp.18825–18833.

Vogelauer, M., Cioci, F. & Camilloni, G., 1998. DNA protein-interactions at the Saccharomyces cerevisiae 35 S rRNA promoter and in its surrounding region. *Journal of Molecular Biology*, 275(2), pp.197–209.

Voit, R. et al., 1992. The nucleolar transcription factor mUBF is phosphorylated by casein kinase II in the C-terminal hyperacidic tail which is essential for transactivation. *The EMBO journal*, 11(6), pp.2211–2218.

Vu, L. et al., 1999. RNA polymerase switch in transcription of yeast rDNA: role of transcription factor UAF (upstream activation factor) in silencing rDNA transcription by RNA polymerase II. *Proceedings of the National Academy of Sciences of the United States of America*, 96(8), pp.4390–4395.

Wada, T. et al., 1998. DSIF, a novel transcription elongation factor that regulates RNA polymerase II processivity, is composed of human Spt4 and Spt5 homologs. *Genes & Development*, 12(3), pp.343–356.

Wai, H. et al., 2001. Yeast RNA polymerase I enhancer is dispensable for transcription of the chromosomal rRNA gene and cell growth, and its apparent transcription enhancement from ectopic promoters requires Fob1 protein. *Molecular and Cellular Biology*, 21(16), pp.5541–5553.

Wai, H.H. et al., 2000. Complete deletion of yeast chromosomal rDNA repeats and integration of a new rDNA repeat: use of rDNA deletion strains for functional analysis of rDNA promoter elements in vivo. *Nucleic Acids Research*, 28(18), pp.3524–3534.

Walfridsson, J. et al., 2007. A genome-wide role for CHD remodelling factors and Nap1 in nucleosome disassembly. *The EMBO Journal*, 26(12), pp.2868–2879.

Wang, K.L. & Warner, J.R., 1998. Positive and negative autoregulation of REB1 transcription in Saccharomyces cerevisiae. *Molecular and Cellular Biology*, 18(7), pp.4368–4376.

Wang, Z. & Roeder, R.G., 1997. Three human RNA polymerase III-specific subunits form a subcomplex with a selective function in specific transcription initiation. *Genes & Development*, 11(10), pp.1315–1326.

Ward, T.R. et al., 2000. Ribosomal DNA replication fork barrier and HOT1 recombination hot spot: shared sequences but independent activities. *Molecular and cellular biology*, 20(13), pp.4948–4957.

Weintraub, H. & Groudine, M., 1976. Chromosomal subunits in active genes have an altered conformation. *Science (New York, N.Y.)*, 193(4256), pp.848–856.

Weiss, S.B. & Gladstone, L., 1959. A MAMMALIAN SYSTEM FOR THE INCORPORATION OF CYTIDINE TRIPHOSPHATE INTO RIBONUCLEIC ACID1. *Journal of the American Chemical Society*, 81(15), pp.4118–4119.

Wessel, D. & Flügge, U.I., 1984. A method for the quantitative recovery of protein in dilute solution in the presence of detergents and lipids. *Analytical Biochemistry*, 138(1), pp.141–143.

Whitehouse, I. et al., 2007. Chromatin remodelling at promoters suppresses antisense transcription. *Nature*, 450(7172), pp.1031–1035.

Whitelaw, E. & Proudfoot, N., 1986. Alpha-thalassaemia caused by a poly(A) site mutation reveals that transcriptional termination is linked to 3' end processing in the human alpha 2 globin gene. *The EMBO journal*, 5(11), pp.2915–2922.

Wierzbicki, A.T., Haag, J.R. & Pikaard, C.S., 2008. Noncoding transcription by RNA polymerase Pol IVb/Pol V mediates transcriptional silencing of overlapping and adjacent genes. *Cell*, 135(4), pp.635–648.

Wilhelm, F.X. et al., 1978. Reconstitution of chromatin: assembly of the nucleosome. *Nucleic acids research*, 5(2), pp.505–521.

Wittig, S. & Wittig, B., 1982. Function of a tRNA gene promoter depends on nucleosome position. *Nature*, 297(5861), pp.31–38.

Wittner, M. et al., 2011. Establishment and maintenance of alternative chromatin states at a multicopy gene locus. *Cell*, 145(4), pp.543–554.

Woodcock, C.L., 1977. Reconstitution of chromatin subunits. *Science (New York, N.Y.)*, 195(4284), pp.1350–1352.

Yager, T.D. & Von Hippel, P.H., 1991. A thermodynamic analysis of RNA transcript elongation and termination in Escherichia coli. *Biochemistry*, 30(4), pp.1097–1118.

Yamaguchi, Y. et al., 1999. NELF, a Multisubunit Complex Containing RD, Cooperates with DSIF to Repress RNA Polymerase II Elongation. *Cell*, 97(1), pp.41–51.

Yamamoto, R.T. et al., 1996. RRN3 gene of Saccharomyces cerevisiae encodes an essential RNA polymerase I transcription factor which interacts with the polymerase independently of DNA template. *The EMBO Journal*, 15(15), pp.3964–3973.

Yuan, G.-C. et al., 2005. Genome-Scale Identification of Nucleosome Positions in S. cerevisiae. *Science*, 309(5734), pp.626–630.

Yuan, X. et al., 2007. Activation of RNA polymerase I transcription by cockayne syndrome group B protein and histone methyltransferase G9a. *Molecular cell*, 27(4), pp.585–595.

Yukawa, Y. et al., 2000. The TATA motif, the CAA motif and the poly(T) transcription termination motif are all important for transcription re-initiation on plant tRNA genes. *The Plant Journal*, 22(5), pp.439–447.

Zaret, K.S. & Sherman, F., 1982. DNA sequence required for efficient transcription termination in yeast. *Cell*, 28(3), pp.563–573.

Zawel, L., Kumar, K.P. & Reinberg, D., 1995. Recycling of the general transcription factors during RNA polymerase II transcription. *Genes & Development*, 9(12), pp.1479–1490.

Zhang, A.P.P., Pigli, Y.Z. & Rice, P.A., 2010. Structure of the LexA-DNA complex and implications for SOS box measurement. *Nature*, 466(7308), pp.883–886.

Zhang, C., Yan, H. & Burton, Z.F., 2003. Combinatorial Control of Human RNA Polymerase II (RNAP II) Pausing and Transcript Cleavage by Transcription Factor IIF, Hepatitis δ Antigen, and Stimulatory Factor II. *Journal of Biological Chemistry*, 278(50), pp.50101–50111.

Zhang, G. et al., 1999. Crystal structure of Thermus aquaticus core RNA polymerase at 3.3 A resolution. *Cell*, 98(6), pp.811–824.

Zhang, Y. et al., 2009. The Paf1 complex is required for efficient transcription elongation by RNA polymerase I. *Proceedings of the National Academy of Sciences of the United States of America*, 106(7), pp.2153–2158.

Zhang, Y. et al., 2010. The RNA Polymerase-associated Factor 1 Complex (Paf1C) Directly Increases the Elongation Rate of RNA Polymerase I and Is Required for Efficient Regulation of rRNA Synthesis. *Journal of Biological Chemistry*, 285(19), pp.14152–14159.

Zhao, A. et al., 1997. Molecular cloning and analysis of Schizosaccharomyces pombe Reb1p: sequence-specific recognition of two sites in the far upstream rDNA intergenic spacer. *Nucleic Acids Research*, 25(4), pp.904–910.

Zhou, Y., Santoro, R. & Grummt, I., 2002. The chromatin remodeling complex NoRC targets HDAC1 to the ribosomal gene promoter and represses RNA polymerase I transcription. *The EMBO journal*, 21(17), pp.4632–4640.

CHAPTER VII – PUBLICATIONS

Working title: Requirements for Nsi1 to terminate Pol I-dependent transcription

Merkl P, Pérez-Fernández J, Reiter A, Williams L, Hamperl S, Pilsl M, Gerber J, Milkereit P, Griesenbeck J, Tschochner H
manuscript in preparation

RNA polymerase I termination: Where is the end?

Németh A, Perez-Fernandez J, **Merkl P**, Hamperl S, Gerber J, Griesenbeck J, Tschochner H
Biochim Biophys Acta. 2013 Mar-Apr; 1829(3-4):306-17. Review.

The Reb1-homologue Ydr026c/Nsi1 is required for efficient RNA polymerase I termination in yeast.

Reiter A, Hamperl S, Seitz H, **Merkl P**, Perez-Fernandez J, Williams L, Gerber J, Németh A, Léger I, Gadal O, Milkereit P, Griesenbeck J, Tschochner H
EMBO J. 2012 Aug 15; 31(16):3480-93.

CHAPTER VIII – ABBREVIATIONS

°C	temperature in degrees celcius
AA	acrylamide
Amp	Ampicillin
APS	ammonium persulfate
ATP	adenosine triphosphate
BisAA	bisacrylamide
BSA	bovine serum albumine
C-/N-terminal	carboxy/aminoterminal
CBP	Calmodulin binding protein
CE	core element
CF	core factor
CIP	calf intestinal phosphatase
CTP	cytosine triphosphate
DMSO	dimethylsulfoxide
DNA	deoxyribonucleic acid
dNTP	deoxynucleoside triphosphate
E. coli	*Escherichia coli*
EDTA	ethylene diamine tetra acetate
EtOH	ethanol
FCS	fetal calf serum
Fig.	figure
g	gram(s)
g	gravitational force
GTP	Guanosine triphosphate
HCl	hydrochloric acid
HEPES	4-(2-hydroxyethyl-)-piperazine-1-ethane sulfonic acid

HOAc	acetic acid
IPTG	isopropyl β-D-1-thiogalactopyranoside
kb, bp, nt	kilobase, basepair, nucleotide
kDa	kilo Dalton
kV	kilovolts
l	liter(s)
LB	lysogeny broth
M	molar
M. musculus	*Mus musculus*
MALDI	Matrix assisted laser desorption ionization
MeOH	methanol
MES	2-(*N*-morpholino)ethanesulfonic acid
miRNA	micro RNA
MOPS	3-(N-morpholino)propanesulfonic acid
mRNA	messenger RNA
MW	molecular weight
N_2(l)	liquid nitrogen
NaOAc	sodium acetate
NaOH	sodium hydroxide
Ni-NTA	Ni(II)-nitrilotriacetic acid
nm	nanometer(s)
NTP	nucleoside triphosphate
OD_{600}	optical density at 600nm wavelength
ORF	open reading frame
p.a.	*pro analysi*
PA600	a crude chromatographic fraction enriched in RNA Pol I
PAGE	polyacrylamide gel electrophoresis
PCR	polymerase chain reaction
pH	negative decadic logarithm of the H^+ ion concentration
PI(s)	protease inhibitors
PIP	RNA Pol I promoter
PMSF	phenylmethylsulfonylflouride
ProtA	Protein A

ProtK	Proteinase K
PVDF	polyvinylidene fluoride
rDNA	ribosomal DNA
RNA	ribonucleic acid
rRNA	ribosomal RNA
RT	room temperature
S	sedimentation coefficient
s, min, h	second, minute, hour
S. cerevisiae	*Saccharomyces cerevisiae*
SDS	sodium dodecyl sulfate
snoRNA	small nucleolar RNA
snRNA	small nuclear RNA
TAP	tandem affinity purification
Taq	thermostable DNA polymerase from *Thermus aquaticus*
TCA	trichloroacetic acid
TEMED	tetramethylethylenediamine
TEV	Tobacco etch virus protease
T_M	melting temperature
TOF	time of flight
U	enzymatic unit
UAF	upstream activating factor
UE	upstream factor
UTP	uridine triphosphate
WT	wildtype
X-GAL	5-bromo-4-chloro-3-indolyl-β-D-galactopyranoside
β-ME	β-mercaptoethanol

Danksagung

An dieser Stelle möchte ich mich bei allen Personen bedanken, die zum Gelingen dieser Arbeit beigetragen haben.

Mein herzlicher Dank gilt an erster Stelle meinem Doktorvater Herrn Prof. Dr. Herbert Tschochner für die Möglichkeit, diese Promotion in seinem Labor durchzuführen, die sehr interessante Themenstellung, die stete Bereitschaft zur Diskussion, die wertvollen Anregungen und sein großes Interesse am Fortgang der Arbeit.

Ferner gebührt mein Dank PD Dr. Joachim Griesenbeck für die immerwährende Möglichkeit zur Diskussion und viele produktive Anregungen. Für viele fruchtbare Diskussionen und Ratschläge möchte ich auch Dr. Philipp Milkereit danken.

Herzlich danken möchte ich auch meinem Mentor Prof. Dr. Thomas Moss von der Universié Laval, Québec, Kanada, der sich im Rahmen seiner Aufenthalte in Regensburg immer sehr für den Fortgang der Arbeit interessiert hat und wertvolle Anregungen gab. Darüberhinaus gebührt ihm Dank, dass er sich bereiterklärt hat, Zweitprüfer im Promotionsverfahren zu sein. Thank you Tom!

Weiterhin danke ich Herrn Prof. Dr. Gernot Längst für die Möglichkeit in seinem Labor *in vitro* Assemblierungen von Nukleosomen durchzuführen und seine Bereitschaft zur Diskussion der Ergebnisse.

Dr. Jorge Pérez-Fernández danke ich für seine Unterstützung des Projekts, viele Anregungen und die Bereitstellung von gereinigten RNA Polymerase I Mutanten.

Bei PD Dr. Attila Németh bedanke ich mich für die Überlassung von gereinigtem TTF-I ΔN348 und bei Dr. Sebastian Geiger für den Hefestamm zur Reinigung von TFIIF und für das Plasmid zur Expression von A49/A34.5.

Ich möchte mich auch bei Dr. Helfried Mallow, der die Fertigstellung dieser Arbeit leider nicht mehr erleben konnte, für seine Unterstützung in zahlreichen technischen Belangen, Verwaltungsangelegenheiten und die Einführung in das Medizinerpraktikum bedanken.

Weiterhin gilt mein Dank allen momentanen und ehemaligen Arbeitskollegen der Subgruppe „Transkription“ für Anregungen, Ratschläge und die gute Zusammenarbeit.

Den von mir betreuten Bachelorstudenten und Masterstudenten Sonja Blumenstock, Simone Lukas, Rebekka Pohl und Simon Obermeyer danke ich für ihre Hilfe bei dieser Arbeit.

Dem Graduiertenkolleg des SFB960 danke ich für die Bereitstellung von Mitteln zur Beschäftigung einer WHK.

Schließlich gebührt mein Dank allen Mitgliedern des „House of the Ribosome“ für jegliche Unterstützung und das gute Arbeitsklima. Insbesondere danke ich Dr. Stephan Hamperl, Dr. Robert Steinbauer, Dr. Alarich Reiter, Dr. Thomas Hierlmeier, Virginia Babl, Uli Ohmayer und Gisela Pöll für Unterstützung in Fragen des Laboralltags und Dr. Sarah Diermeier und Elisabeth Silberhorn für Hilfe bei der Assemblierung von Nukleosomen.

Für Ihre finanzielle aber vor allem ideelle Unterstützung während meines Promotionsstudiums danke ich der Studienstiftung des Deutschen Volkes sehr herzlich.

Abschließend möchte ich besonders meinen Eltern sowie meinem Bruder Rainer und seiner Familie für Ihre stetige Unterstützung während Studium und Promotion, für Ihren moralischen Beistand in schwierigen Zeiten und Ihre Liebe danken, ohne die mein Werdegang so nicht möglich gewesen wäre.